UNIVERSITY OF LIVERPOOL

Design of Lipid-Based Nanocarriers for the Treatment of Human Immunodeficiency Virus (HIV)

Heba Elkateb

April 2021

Thesis submitted in accordance with the requirements of the University of Liverpool for the degree of Doctor in Philosophy

Acknowledgement

Firstly, I would like to begin by thanking my family, my Mum and Dad, and my sisters Hend, Noha and Mona for their endless support and love throughout my PhD experience. I would not have got that far in life without you being by my side. I love you all so much.

Many thanks to my supervisor Dr Tom McDonald, who gave me this wonderful opportunity to come to the UK to get my PhD degree. I really appreciate that he believed in my abilities and supported my funding application, which was crucial for me to continue my studies. He has always encouraged me through all the ups and downs of my PhD journey. I improved my research and writing skills because of his support and guidance. I would like to thank him for his kindness, exceptional supervision, mentoring and patience.

I would like also to thank my secondary supervisor professor Steve Rannard, for the guidance, equipment access and all the resources he provided to me.

Additionally, I owe many thanks to Helen Cauldbeck for her support and help, especially with the radiometric analysis experiments, Lee Tatham for performing the cell work in my thesis, Edyta Niezabitowska for being such a nice co-worker and for the SEM imaging, Sean Flynn for helping with the NMR and GPC analysis, and Keith Arnold for the CryoSEM analysis.

I would like to thank both the McDonald and Rannard research groups for their help and support. Special thanks to the group members, Jess Taylor, Cameron Hogarth, Steph Edwards, Dominic Gray and Andrew McLauchlin. I would like also to thank previous members of the group, Adam Town, and Nancy Elbaz. It has been a pleasure working with you all.

My sincere thanks go to Schlumberger Foundation Faculty for The Future for the generous financial support throughout my PhD. I am grateful that I was awarded such an exceptional fellowship and had the opportunity to meet such strong and influential women.

Finally, I would like to thank my colleagues and the staff in the faculty of Pharmacy, Mansoura University, Egypt.

Abstract

Human immunodeficiency virus (HIV) is a global health problem that can lead to death if left untreated. For HIV treatment, darunavir (DRV), a protease inhibitor and a promising first line antiretroviral drug, is usually co-administered with ritonavir (RTV) in a daily dose of 800 mg DRV with 100 mg RTV. RTV is used as a pharmacokinetic booster for DRV to increase its oral bioavailability. Lipid nanocarriers are considered a possible approach to enhance the targeting of these two drugs to the HIV reservoir sites, decrease the required doses, and overcome the pharmacokinetic challenges. In this thesis, solid lipid nanoparticles (SLNs), nanostructured lipid carriers (NLCs), nanoemulsions (NEs) and lipid polymer hybrid nanoparticles (LPHNs) were investigated as lipid nanocarriers for the drug mixture DRV/RTV (8:1). Solvent injection was used as a synthesis technique for these formulations as it is fast, cheap, and reproducible method.

A comparison between SLNs, NLCs, and NEs was carried out to determine the optimum formulation for DRV/RTV (8:1) loading. Hot and cold solvent injection methods were used in the synthesis of these three formulations, in which the hydrophobic phase was heated or kept at room temperature, respectively, before injecting into a hydrophilic surfactant solution. The cold solvent injection method was used to overcome the residual solvent problem of the hot solvent injection, where the more volatile tetrahydrofuran (THF) was used as a solvent instead of ethanol. In the cold solvent injection, Brij 78 was used as the surfactant of choice, while Imwitor®900 K and soybean oil were used as solid and liquid lipids, respectively. For both methods, and the Z-average diameter decreased in the following in order SLNs> NLCs > NEs. For NLCs, the size depended on solid lipid/liquid lipid ratio (S/L), the higher the S/L ratio the bigger the Z-average. The entrapment efficiency (EE%) for these drug-loaded formulations was 92.5- 95.8%. Among all the tested formulations, NLCs (5:5) showed the most controlled drug release (52% drug release over 24 hours duration).

A main target of this research was to obtain high drug-loaded SLNs (HDL-SLNs). The targeted DRV loading was 50% w/w, with keeping the DRV/RTV ratio fixed at 8:1. For that purpose, the branched polymer DBiB-*p*(OEGMA$_{10}$-*co*-EGDMA$_{0.6}$) was tested as a potential surfactant for HDL-SLNs, as it would attach to the lipid cores at multiple points. The branched copolymer was synthesised by atom transfer radical polymerisation (ATRP), where dodecyl α-bromoisobutyrate (DBiB), oligo (ethylene glycol) methacrylates (OEGMA) and ethylene glycol

dimethacrylate (EGDMA) were used as initiator, monomer and brancher, respectively. The solvent injection method was optimised for the synthesis of HDL-SLNs. When DBiB-*p*(OEGMA$_{10}$-*co*-EGDMA$_{0.6}$) was used as a surfactant, the Z-average diameter for the single drug-loaded DRV-HDL-SLNs was 224 nm and was 290 nm for the dual drug-loaded DRV-RTV-HDL-SLNs. The HDL-SLNs were freeze-dried to remove both water and the water-miscible organic solvent (isopropanol). Unfortunately, without the use of cryoprotectants, the freeze-drying led to the aggregation of HDL-SLNs.

To limit the aggregation of HDL-SLNs during the freeze-drying process, several cryoprotectants were investigated. Polyethylene glycol (PEG 2050) was chosen over sugar cryoprotectants at a concentration of 0.5% w/v. The required PEG/HDL-SLNs weight ratio and the concentration of the freeze-drying mixture to provide cryoprotection were 38/1 w/w and 3 mg/mL, respectively. The freeze-dried cakes of PEG 2050 were re-dispersed in phosphate buffered saline (PBS) keeping a Z-average diameter of ~200 nm, however they aggregated upon re-dispersion in simulated gastric fluid (SGF). For drug release, 80% of DRV was released over 8 hours period, which was accompanied by initial burst release. The formulation of HDL-SLNs resulted in increased cellular uptake of DRV. However, there was no increase in the apparent oral absorption observed for the HDL-SLNs, which could be due to the use of the hydrophilic PEG 2050 which alters the lipophilic nature of SLNs.

The LPHNs were designed with a poly (D, L-lactide-co-glycolide) (PLGA) core, and soybean lecithin (SBL) and Brij 78 as stabilisers. The optimum weight percentage of stabiliser/polymer was 20% w/w. The minimum percentage of Brij 78 required to provide stability in phosphate buffered saline was 70% of the total stabiliser mass. LPHNs containing DRV/RTV (8:1) were prepared using 20% w/w DRV/PLGA. The use of PEG 2050 as a cryoprotectant during freeze-drying yielded LPHNs with a Z-average diameter of 150 nm when the particles were re-dispersed in water. The oral absorption behavior was assessed using an *in vitro* triple culture model. Whilst the use of cryoprotectant and freeze-drying led to no improvement of the transcellular permeability. The non-freeze-dried samples with the highest SBL led to increased transcellular permeability, revealing the potential of LPHNs for enhancing HIV treatment.

This thesis provides detailed insight into the formulation parameters that control the formation of novel lipid-based nanocarriers containing DRV and RTV. This understanding may allow the design of drug delivery systems that improve the oral dosing of HIV drugs in the future.

Preface

Publications

Elkateb, Heba et al. 2020. "Optimization of the Synthetic Parameters of Lipid Polymer Hybrid Nanoparticles Dual Loaded with Darunavir and Ritonavir for the Treatment of HIV." *International Journal of Pharmaceutics* 588(August): 119794. https://doi.org/10.1016/j.ijpharm.2020.119794.

Manuscripts in preparation

1. **Heba, Elkateb,** Helen Cauldbeck, Lee M. Tatham, Edyta Niezabitowska, Andrew Owen, Steve Rannard and Tom O. McDonald "A Comparative Study of Solid Lipid Nanoparticles, Nanostructured Lipid Carriers and Nanoemulsions for a Dual Drug Delivery of Darunavir and Ritonavir for the treatment of HIV"

2. **Heba, Elkateb,** Helen Cauldbeck, Lee M. Tatham, Edyta Niezabitowska, Andrew Owen, Steve Rannard and Tom O. McDonald "Optimisation of the Freeze-Drying Parameters of High Drug-Loaded SLNs (HDL-SLNs) Using Cryoprotectants"

Conferences Attended and Posters Presented

1. ACS National Meeting & Expo (Chemistry for New Frontiers) Orlando, FL, USA, March 31 - April 4, 2019

2. 6th International Conference on Multifunctional, Hybrid and Nanomaterials in Stiges, Spain, March 11-15, 2019

3. The RSC Biomaterials Chemistry Annual Conference in Liverpool UK, January (9-11, 2019

4. 5th Royal society of chemistry (RSC) Early Career Symposium, Liverpool, UK, August 30-31, 2018

5. Early Careers Researcher Meeting, University College London, UK, August 6-7, 2018

6. Materials research exchange 2018 (MRE 2018) London, UK, March 12-13, 2018

7. Early Careers Researcher Meeting, Queens University Belfast, UK, August 10-11, 2017

8. MACRO Group, Young researchers' Meeting, University of Edinburg, UK, June 19-20, 2017

9. Syrris microfluidics workshop, Manchester, UK, May 25, 2017

10. European Nanomedicine Meeting 2017, London, UK, April 3-4, 2017

List of Abbreviations

μCi	Microcurie(s)
AIDS	Acquired Immune Deficiency Syndrome
ATRP	Atom Transfer Radical Polymerisation
B.P	Boiling Point
BBB	Blood Brain Barrier
Bpy	2,2-bipyridyl
CCR5	C-C Chemokine Receptor
CD4	Cluster Differentiation 4
CI-MS	Chemical Ionisation Mass Spectroscopy
CMC	Critical Micelle Concentration
CNS	Central Nervous System
CryoSEM	Scanning Electron Cryomicroscopy
CXCR4	Chemokine Receptor Type 4
CYP450	Cytochrome P450
DBiB	Dodecyl α-bromoisobutyrate
DCM	Dichloromethane
DI water	Deionised water
DLS	Dynamic Light Scattering
DMF	Dimethyl Formamide
DNA	Deoxyribonucleic Acid
DP_n	Number-Average Degree of Polymerisation
DRV	Darunavir
DSC	Differential Scanning Calorimetry
EE%	Encapsulation Efficiency
EGDMA	Ethylene Glycol Dimethacrylate
GALT	Gut Associated Lymphoid Tissue
GIT	Gastrointestinal Tract
gp	Glycoprotein
GPC	Gel Permeation Chromatography
HAART	Highly Active Antiretroviral Therapy
HDL-SLNs	High Drug-Loaded SLNs
HIV	Human Immunodeficiency Virus
HPLC	High Pressure Liquid Chromatography
IPA	Isopropanol
LPHNs	Lipid Polymer Hybrid Nanoparticles
M cells	Microfold Cells
M.P	Melting Point
M_n	Number Average Molecular Weight
Mo/Mac	Monocytes/Macrophages
M_w	Average Molecular Weight

MWCO	Molecular Weight Cut Off
NEs	Nanoemulsions
NLCs	Nanostructured Lipid Carriers
NMR	Nuclear Magnetic Resonance
NNRTIs	Non-Nucleoside Reverse Transcriptase Inhibitors
NPs	Nanoparticles
NRTIs	Nucleoside/Nucleotide Reverse Transcriptase Inhibitors
OEGMA	Oligo (ethylene glycol) Methacrylates
PBS	Phosphate-buffered saline
PDI	Polydispersity
PEG	Polyethylene Glycol
PLGA	Poly (Lactide-*co*-Glycolides)
PNPs	Polymeric Nanoparticles
RALS	Right-Angle Light Scattering
RBF	Round Bottom Flask
RI	Refractive Index
RNA	Ribonucleic Acid
RTV	Ritonavir
S/L	Solid lipid/Liquid lipid
SBL	Soybean Lecithin
SDNs	Solid Drug Nanoparticles
SEM	Scanning Electron Microscope
SGF	Simulated Gastric Fluid
SLNs	Solid Lipid Nanoparticles
TD-SEC	Triple Detection Size Exclusion Chromatography
TEA	Triethyl Amine
TEM	Transmission Electron Microscopy
T_g	Glass Transition Temperature
THF	Tetrahydrofuran
WHO	World Health Organisation

Table of contents

CHAPTER 1 Literature Background 13

1.1 HUMAN IMMUNODEFICIENCY VIRUS (HIV) 14
1.2 THE LIFECYCLE OF HIV/AIDS AND MAIN CLASSES OF TREATMENT 14
1.3 HIGHLY ACTIVE ANTIRETROVIRAL THERAPY CHALLENGES 17
1.4 DARUNAVIR AND RITONAVIR COMBINATION 18
1.5 HIV-TARGETED ORAL DRUG DELIVERY APPROACHES 20
1.5.1 POLYMERIC NANOCARRIERS 22
1.5.1.1 Polymeric nanoparticles (PNPs) 22
1.5.1.2 Dendrimers 23
1.5.1.3 Polymeric micelles 24
1.5.1.4 Polymeric drug conjugates 25
1.5.2 LIPID NANOCARRIERS 26
1.5.2.1 Lipid-based nanocarriers and HIV drug targeting 26
1.5.2.2 Lipid-based nanocarriers types 28
1.5.2.2.1 Liposomes 30
1.5.2.2.2 Solid lipid nanoparticles (SLNs) 31
1.5.2.2.3 Nanoemulsions (NEs) 35
1.5.2.2.4 Nanostructured lipid carriers (NLCs) 39
1.5.2.2.5 Lipid polymer hybrid nanoparticles (LPHNs) 40
1.5.2.3 Methods of preparation of lipid-based nanoparticles 43
1.5.2.3.1 High pressure homogenisation method 44
1.5.2.3.2 Solvent injection/nanoprecipitation method 45
1.5.2.3.2.1 Challenges of the solvent injection technique 48
1.5.2.4 Drying of lipid nanodispersions 48
1.5.2.4.1 Spray drying 49
1.5.2.4.2 Freeze-drying 49
1.6 OBJECTIVE OF THE RESEARCH 54

CHAPTER 2 A Comparative Study Of Solid Lipid Nanoparticles, Nanostructured Lipid Carriers And Nanoemulsions For A Dual Drug Delivery Of Darunavir And Ritonavir For The Treatment Of HIV.. 56

2.1 INTRODUCTION 57
2.2 CHAPTER OBJECTIVES 57
2.3 MATERIALS AND METHODOLOGY 59
2.3.1 MATERIALS 59
2.3.2 METHODOLOGY 59
2.3.2.1 Synthesis of blank SLNs, NLCs and NEs by hot solvent injection method 59
2.3.2.2 Synthesis of blank and drug loaded SLNs, NLCs and NEs by cold solvent injection method. 60
2.3.2.3 Characterisation of the size and morphology of SLNs, NLCs and NEs 61
2.3.2.3.1 Size measurement by DLS 61
2.3.2.3.2 Determination of the size and morphology by scanning electron cryomicroscopy (CryoSEM) imaging 62
2.3.2.4 Differential scanning calorimetry (DSC) analysis 62
2.3.2.5 Measurement of drug release using radiometric analysis 63
2.4 RESULTS AND DISCUSSION 66
2.4.1 HOT SOLVENT INJECTION 66
2.4.1.1 The effect of varying the synthesis parameters on the DLS data of blank SLNs, NLCs and NEs synthesised by hot solvent injection method. 66
2.4.1.1.1 The effect of varying the lipid concentration in the hydrophobic phase on the DLS data of the produced lipid nanoformulation 68
2.4.1.1.1.1 The effect of increasing the concentration of a single lipid on the DLS data of SLNs and NEs 68
2.4.1.1.1.2 The effect of increasing the concentration of the total lipid with different S/L ratios on the DLS data of NLCs 71
2.4.1.1.2 The effect of the surfactant concentration on the DLS data of both SLNs and NEs 76
2.4.1.2 Investigation of size and morphology of blank SLNs, NLCs and NEs by CryoSEM 78
2.4.1.3 DSC investigations of blank SLNs, NLCs and NEs 80
2.4.2 COLD SOLVENT INJECTION 83
2.4.2.1 The effect of varying the synthesis parameters on the DLS data of SLNs, NLCs and NEs synthesised by cold solvent injection method. 83
2.4.2.1.1 Optimisation of blank SLNs, NLCs and NEs formulations 85
2.4.2.1.1.1 The effect of the type of the surfactant on the DLS data of SLNs and NEs 85
2.4.2.1.1.2 The effect of the type of the solid lipid on the DLS data of SLNs 88
2.4.2.1.1.3 The effect of increasing the concentration of the total lipid concentration with different S/L ratios on the DLS data of NLCs 91

2.4.2.1.2 Optimisation of drug loaded SLNs, NLCs and NEs formulations 93
2.4.2.1.2.1 The effect of drug loading on the DLS data of SLNs, NLCs and NEs 94
2.4.2.1.2.2 Measurement of colloidal stability of SLNs, NLCs and NEs in PBS and SGF by DLS 99
2.4.2.1.2.3 Encapsulation efficiency (EE%) and drug release 99
2.4.2.1.2.4 Investigation of size and morphology of drug loaded SLNs, NLCs (5:5) and NEs by CryoSEM 101
2.4.2.1.2.5 DSC investigations of drug loaded SLNs, NLCs and NEs 102
2.5 CONCLUSION 103

CHAPTER 3 Synthesis Of High Drug Loaded Solid Lipid Nanoparticles Stabilised By Branched Copolymers And Loaded With A Mixture Of Darunavir And Ritonavir For The Treatment Of HIV 105

3.1 INTRODUCTION 106
3.2 CHAPTER OBJECTIVE 108
3.3 MATERIALS AND METHODOLOGY 109
3.3.1 MATERIALS 109
3.3.1.1 Materials for the synthesis and characterisation of ATRP initiator and branched copolymer 109
3.3.1.2 Materials for the synthesis and characterisation of HDL-SLNs by solvent injection 109
3.3.2 METHODOLOGY 109
3.3.2.1 Synthesis of dodecyl α-bromoisobutyrate initiator 109
3.3.2.2 Synthesis of branched P(OEGMA) by ATRP 110
3.3.2.3 Characterisation of ATRP initiator and branched copolymer 111
3.3.2.3.1 Mass spectrometry 111
3.3.2.3.2 NMR spectrometry 111
3.3.2.3.3 Gel permeation chromatography (GPC) 111
3.3.2.4 Synthesis of HDL-SLNs by solvent injection method 112
3.3.2.5 Freeze-drying of HDL-SLNs 113
3.3.2.6 Characterisation of the size of HDL-SLNs by DLS 113
3.4 RESULTS AND DISCUSSION 114
3.4.1 CHARACTERISATION OF THE SYNTHESISED DBIB INITIATOR 114
3.4.2 CHARACTERISATION OF THE SYNTHESISED BRANCHED COPOLYMERS 116
3.4.3 OPTIMISATION OF THE SYNTHETIC PARAMETERS OF HDL-SLNS BY SOLVENT INJECTION 120
3.4.3.1 The effect of varying the heating temperature of the hydrophobic phase on the DLS data of blank-SLNs and HDL-SLNs dispersions. 122

3.4.3.2 The effect of varying the heating time of the hydrophobic phase on the DLS data of blank-SLNs and HDL-SLNs 124
3.4.3.3 Varying the stirring time of the blank-SLNs and HDL-SLNs dispersions after the solvent injection 125
3.4.3.4 The effect of varying the type of solid lipid on the DLS data of blank-SLNs and HDL-SLNs. 126
3.4.3.5 The effect of using mixture of surfactants on the DLS data of blank-SLNs and HDL-SLNs .. 127
3.4.4 FREEZE-DRYING OF BLANK-SLNS AND HDL-SLNS DISPERSIONS 129
3.5 CONCLUSION 130

CHAPTER 4 Optimisation Of The Freeze-Drying Parameters Of High Drug-Loaded Solid Lipid Nanoparticles Using Cryoprotectants 131

4.1 INTRODUCTION 132
4.2 CHAPTER OBJECTIVES 133
4.3 MATERIALS AND METHODOLOGY 135
4.3.1 MATERIALS 135
4.3.2 METHODOLOGY 135
4.3.2.1 Synthesis of HDL-SLNs by solvent injection 135
4.3.2.2 Synthesis of radiolabelled HDL-SLNs by solvent injection (scale-down) 136
4.3.2.3 Freeze-drying and re-dispersion of HDL-SLNs 136
4.3.2.4 Freeze-drying and re-dispersion of radiolabelled HDL-SLNs 137
4.3.2.5 Characterisation of the size and morphology of HDL-SLNs by DLS and scanning electron microscope (SEM) 137
4.3.2.6 Measurement of drug release using radiometric analysis 138
4.3.2.7 Cellular accumulation and transcellular permeability of DRV across Caco-2 cells and triple culture model respectively 138
4.3.2.7.1 Cell culture and maintenance 138
4.3.2.7.2 Cellular Accumulation 138
4.3.2.7.3 Transcellular Permeability 139
4.3.2.7.4 Statistical analysis 140
4.4 RESULTS AND DISCUSSION 141
4.4.1 OPTIMISATION OF FREEZE-DRYING CONDITIONS 142
4.4.1.1 Duration of freeze-drying 142
4.4.1.2 Storage of the freeze-dried HDL-SLNs 143
4.4.2 THE EFFECT OF VARYING FREEZE-DRYING PARAMETERS ON THE DLS DATA OF HDL-SLNS 144

4.4.2.1 Influence of different sugar cryoprotectants on the DLS data of HDL-DRV-SLNs 145
4.4.2.1.1 The effect of using dextrose, mannitol, and maltodextrin as cryoprotectants on the size properties of re-dispersed HDL-DRV-SLNs 145
4.4.2.1.2 The effect of using trehalose and sucrose as cryoprotectants on the DLS data of re-dispersed HDL-DRV-SLNs 147
4.4.2.2 Influence of PEG as a polymeric cryoprotectant on the re-dispersion of HDL-SLNs 157
4.4.2.2.1 The effect of PEG/HDL-SLNs weight ratio and the concentration of the freeze-drying mixture on the DLS data of HDL-SLNs 157
4.4.2.2.2 Scale up of the freeze-drying of HDL-SLNs using PEG as a cryoprotectant 164
4.4.2.2.3 Testing of colloidal stability of freeze-dried HDL-SLNs by reconstitution in PBS and SGF 167
4.4.3 MORPHOLOGY AND SIZE ANALYSIS OF THE FREEZE-DRIED HDL-SLNS BY SEM 168
4.4.4 SCALE-DOWN OF THE SYNTHESIS OF HDL-SLNS BY SOLVENT INJECTION 169
4.4.5 RELEASE STUDIES 170
4.4.6 THE BEHAVIOUR OF FREEZE-DRIED HDL-SLNS AND THE ABSORPTION OF DRV ACROSS CACO-2 AND TRIPLE CULTURE MODEL 171
4.4.6.1 Cellular Accumulation 171
4.4.6.2 Transcellular Permeability 172
4.5 CONCLUSION 176

CHAPTER 5 Optimisation Of The Synthetic Parameters Of Lipid Polymer Hybrid Nanoparticles Dual Loaded With Darunavir And Ritonavir For The Treatment Of HIV 179

5.1 INTRODUCTION 180
5.2 CHAPTER OBJECTIVE 181
5.3 MATERIALS AND METHODOLOGY 182
5.3.1 MATERIALS 182
5.3.2 METHODOLOGY 182
5.3.2.1 Synthesis of LPHNs 182
5.3.2.2 Freeze-drying 183
5.3.2.3 Characterisation of the size and morphology of LPHNs 183
5.3.2.4 Measurement of entrapment efficiency and drug release using radiometric analysis 184
5.3.2.5 Transcellular permeability of Darunavir across a triple culture model 185
5.3.2.5.1 Cell culture and maintenance 185
5.3.2.6 Statistical analysis 186
5.4 RESULTS AND DISCUSSION 187

5.4.1 OPTIMISATION OF THE SYNTHESIS OF LPHNS 187
5.4.1.1 The effect of varying the mass percentage of total stabiliser to the polymer core 188
5.4.1.1.1 Soybean lecithin as a stabiliser for LPHNs 188
5.4.1.1.2 Brij 78 as a stabiliser for LPHNs 189
5.4.1.2 Using a combination of Brij 78 and soybean lecithin as stabilisers for LPHNs 190
5.4.1.3 Effect of drug/PLGA mass percentage on particle properties and formation of dispersible formulation 191
5.4.2 ANALYSIS OF THE MORPHOLOGY AND SIZE OF THE LPHNS BY SEM AND TEM 195
5.4.3 ENCAPSULATION EFFICIENCY AND DRUG RELEASE 196
5.4.4 THE EFFECT OF LPHNS SURFACTANT COMPOSITION ON THE ABSORPTION OF DRV ACROSS A TRIPLE CULTURE MODEL 199
5.5 CONCLUSION 205

CHAPTER 6 Conclusions And Future Work 206

6.1 CONCLUSIONS 207
6.2 FUTURE WORK 211
REFERENCES 214

Chapter 1

Literature Background

1.1 Human immunodeficiency virus (HIV)

Human immunodeficiency virus (HIV) is a virus that is transmitted *via* body fluid contact through contaminated needles, unprotected sex, or during pregnancy from mother to her infant.[1] The infection affects the body's immune system by damaging the cells responsible for its defence. According to the World Health Organisation (WHO),[2] in 2019, the estimated number of people infected with HIV worldwide exceeded 38 million and more than half of these people did not receive any treatment. Most of the infections are in the third world countries and in Sub-Saharan Africa due to poor hygiene and lack of financial resources to provide treatment to high number of patients.[2] HIV results in a syndrome known as acquired immunodeficiency syndrome (AIDS) if left untreated, which causes a severe damage to the immune system and makes the body susceptible to other infections and diseases including cancer, that is why HIV is life threatening.[1,3]

1.2 The lifecycle of HIV/AIDS and main classes of treatment

HIV is a lentivirus which is a subgroup of retrovirus. Retroviruses have the ability of integrating their genome into the host cell genome causing chronic and fatal diseases and characterised by long incubation period.[4] HIV is spherical in shape, with a diameter of 80-120 nm and it is composed of an outer envelope and an inner capsid. Its outer surface envelope is double layered and functionalised with glycoproteins, known as gp120 and gp41. The inner capsid is a protein coat that surrounds a core containing two identical strands of ribonucleic acid (RNA) and three enzymes (integrase, reverse transcriptase and protease).[3,5] The virus uses human immune cells as host cells to proliferate and these include T cells which are also called cluster differentiation 4 (CD4 cells), monocytes/macrophages (Mo/Mac) and the dendritic cells.[5] The continuous depletion of T cells leads to the development of AIDS in patients not receiving antiretroviral treatment. The HIV complete life cycle is shown in Figure 1.1 and is classified into seven stages by the U.S. Department of Health & Human Services:[6] **Stage 1. (Docking stage):** The glycoproteins on the surface of the virus bind to the receptor CD4, C-C chemokine receptor (CCR5) or C-X-C chemokine receptor type 4 (CXCR4) on the surface of the host cell.[5,7] **Stage 2. (Fusion stage):** The HIV envelop fuses with CD4 cell membrane allowing viral cell entry via endocytosis to the host cell.[8] **Stage 3. (Reverse transcription):**

HIV releases transcriptase enzyme to convert HIV RNA into HIV DNA and allow the HIV to enter CD4 nucleus.[9,10] **Stage 4. (Integration):** The HIV DNA is integrated in the CD4 cell DNA using HIV integrase enzyme which is secreted inside the CD4 cell nucleus.[11,12] **Stage 5. (Replication and translation):** The HIV produces long chain proteins after integration into CD4 cell which are considered as building blocks for more HIV production.[12,13] **Stage 6. (Assembly):** The HIV protein and RNA assemble at the surface of CD4 cells to produce immature non-infectious virions.[5] **Stage 7. (Budding):** The immature virions push themselves to the outer surface of CD4 cell and the release of HIV protease which breaks long protein chains into smaller blocks which combine to form mature HIV cells that can spread and infect other host cells.[5,14–16]

Given the lifecycle of the virus, the antiretroviral drugs target specific stages in the HIV lifecycle to limit HIV replication without affecting human cells, see Figure 1.1. There are six main classes for HIV/AIDS treatment that interrupt the viral replication cycle as follows:

1. **Entry inhibitors (CCR5 antagonist):** interfere with binding and entry of HIV-1 to the host cell by blocking one of several receptors. Maraviroc is an agent of this class and works by targeting CCR5 receptors. Individuals who have mutation in CCR5 may develop resistance to Maraviroc.[7]
2. **Fusion inhibitors:** work on the outside of the host CD4 cell to prevent HIV from fusing with it. They act by binding to the envelop of HIV and block the subsequent structural changes that cause the virus to fuse with the host CD4 cell. Enfuvirtide is an example from this class and acts by interacting with the gp41 of HIV to form an inactive hetero six-helix bundle, therefore preventing infection of host cells.[8]
3. **Nucleoside/nucleotide reverse transcriptase inhibitors (NRTIs):** are classified as competitive substrate inhibitors. They are analogues of the naturally occurring deoxynucleotides that causes the viral DNA synthesis to be halted by chain termination as they compete with the natural deoxynucleotides to be incorporated in viral DNA chain. Examples include: zidovudine, emtricitabine, lamivudine, abacavir, and tenofovir.[9]
4. **Non-Nucleoside reverse transcriptase inhibitors (NNRTIs):** are classified as non-competitive inhibitors of reverse transcriptase, as they bind directly to reverse transcriptase enzyme which leads to the inhibition of the movement of its protein domains that are necessary in DNA synthesis. Examples include: nevirapine, efavirenz, etravirine and rilpivirine.[10]

5. **Integrase inhibitors:** are known as integrase strand transfer inhibitors which prevents HIV from integrating its DNA into the DNA of the host cell. It works by blocking HIV integrase enzyme and prevents HIV replication. Dolutegravir, elvitegravir and raltegravir are agents within this group.[12,13]
6. **Protease inhibitors:** bind to viral proteases and block the proteolytic cleavage of protein precursors into smaller protein pieces which are important in the production of mature infectious viral particles, thus prevent HIV replication. Drugs in this group include: amprenavir, atazanavir, darunavir, fosamprenavir, indinavir, ritonavir, nelfinavir, saquinavir and tipranavir.[1,5,14–19]

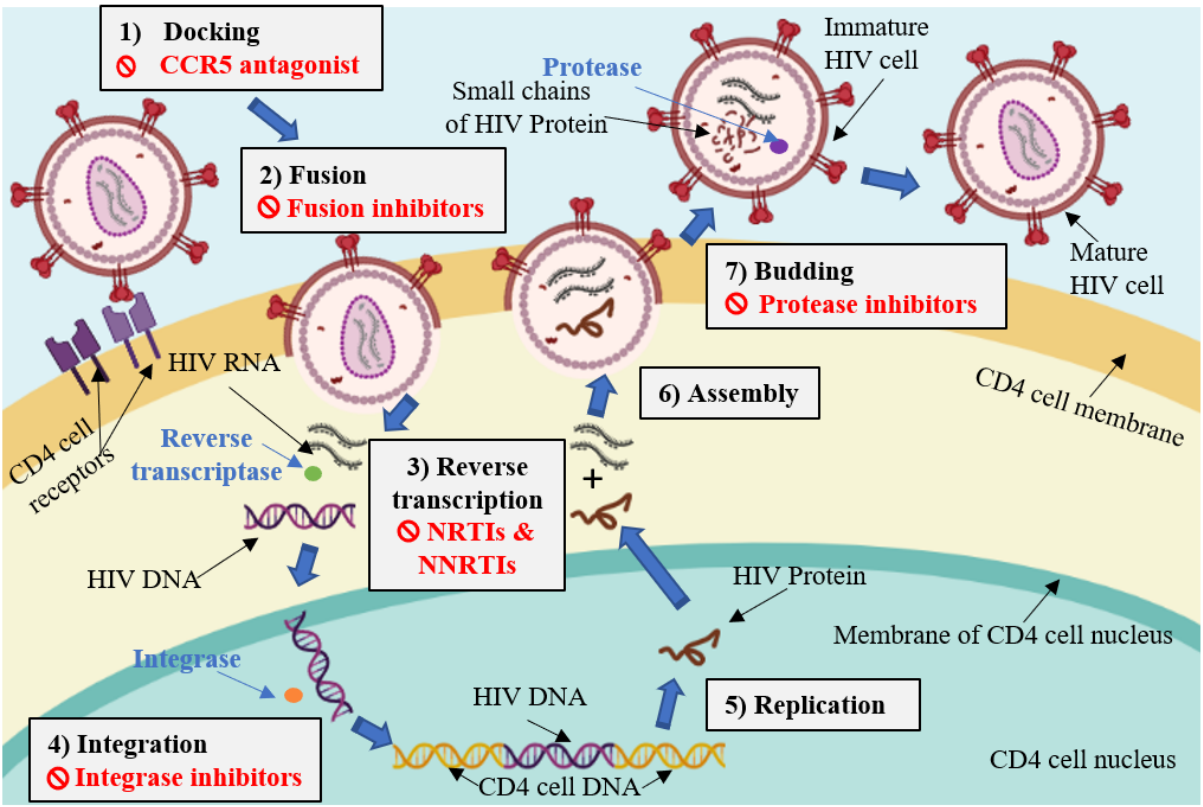

Figure 1.1 Different stages of the lifecycle of HIV and classes of antiretroviral agents used to disrupt them. Stage 1. (Docking stage): The glycoproteins on the surface of the virus bind to the receptor CD4 on the surface of the host cell, this stage is antagonised by CCR5 antagonist. Stage 2. (Fusion stage): The HIV envelop fuses with CD4 cell membrane allowing viral cell entry, this stage is antagonised by fusion inhibitors. Stage 3. (Reverse transcription): HIV releases transcriptase enzyme to convert HIV RNA into HIV DNA, this stage is antagonised by NRTIs and NNRTIs. Stage 4. (Integration): The HIV DNA is integrated in the CD4 cell DNA, this stage is antagonised by integrase inhibitors. Stage 5. (Replication and translation): The HIV produce long chain proteins after integration into CD4 cell. Stage 6. (Assembly): The HIV protein and RNA assemble at the surface of CD4 cells to produce immature non-infectious virions. Stage 7. (Budding): The immature virions push themselves to the outer surface of CD4 cell and formation of mature HIV cells that can spread and infect other host cells, this stage is antagonised by protease inhibitors.

1.3 Highly active antiretroviral therapy challenges

The treatment of HIV aims at reducing the viral load in the plasma to undetectable levels to help the recovery of CD4 cells. The treatment is usually done in the form of a combinational therapy including drugs from various categories,[5] as the use of a single drug is always inefficient and results in the development of HIV resistance to the treatment. The combination of drugs usually referred to as highly active antiretroviral therapy (HAART) and this concept was first introduced in 1996.[5,18,20,21] The combination of tenofovir (NRTI) and efavirenz (NNRTI) with either lamivudine (NRTI) or emtricitabine (NRTI) is an example of well-established HAART regimen recommended by the WHO.[22] Despite having a lot of advantages, HAART therapy has some limitations that affect its therapeutic effectiveness and decrease patient's compliance due to the following factors: 1) Toxicity and side effects which results from high and frequent dosing of HIV drugs due to their high hydrophobicity and low bioavailability. 2) HIV has many strains that are able to develop resistance to drug categories. 3) Activation of dormant HIV-infected cells during later stage of treatment. 4) The difficulty for therapies to access HIV reservoir sites which includes lymphatic system, central nervous system (CNS), lungs, cells of the monocyte-macrophage lineage which constitutes reticulo-endothelial system, reproductive organs and other body organs (as shown in Figure 1.2).[3,15,23] Gut associated lymphoid tissue (GALT) is considered as a main HIV reservoir site, therefore targeting of the antiretrovirals to it, is considered as a key strategy in tackling the high viral load in the body.[24] Drug delivery systems of antiretrovirals especially lipid based carriers have shown to overcome some of the challenges of HAART by decreasing the required does of the drugs, improving their bioavailability, reducing toxicity and have proved to be of great importance in targeting the HIV reservoir sites especially GALT.[20,23,25]

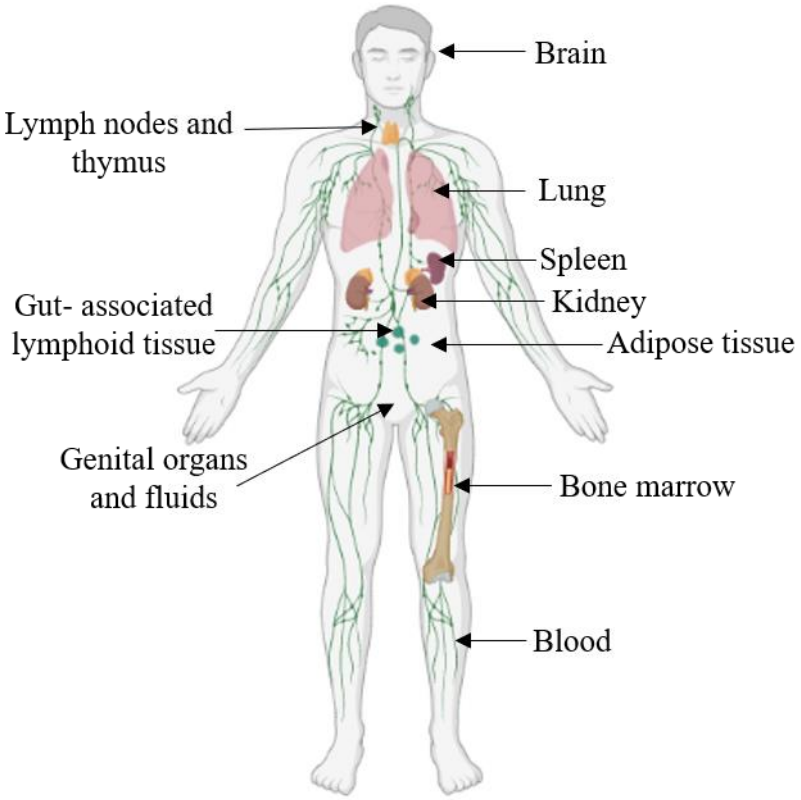

Figure 1.2 Diagram shows HIV reservoir sites in the body.

1.4 Darunavir and ritonavir combination

Among the 26 anti-HIV compounds that have been approved by the US Food and Drug Administration (FDA) since the discovery of HIV, there are 10 HIV protease inhibitors. Protease inhibitors are considered one of the most principal elements of HAART as they show lower resistance compared to other categories like NNRTI.[14] As mentioned before in the HIV life cycle (Figure 1.1), the protease is an essential enzyme for HIV maturation.[6] HIV-1 protease cleaves Gag and Gag-Pol polyprotein precursor at nine processing sites to produce six mature active proteins (matrix, capsid, P2, nucleocapsid, P1 and P6) and three enzymes (protease, reverse transcriptase and integrase).[14] The activity of HIV-1 protease enzyme activity can be inhibited by blocking its active site. In 1995, saquinavir was the first FDA approved HIV protease inhibitor to be used, however due to its low bioavailability and high resistance it was not preferred and more protease inhibitors were developed.[14] Darunavir (DRV) (brand name: Prezista), see Figure 1.3.A, is the latest HIV protease inhibitor to be introduced to the market and was approved in 2006.[5] Darunavir is a first line antiretroviral agent that shows high genetic barrier and has exceptional resistance profile against both wild type and mutant HIV strains. The high efficacy of DRV is attributed to its drug design which enables it to form more

hydrogen bonds with the backbone of the HIV protease than other protease inhibitors.[5,18,26] According to the backbone binding theory, the conformation of the active site backbone of mutant proteases is only slightly different from the wild type. Therefore, an inhibitor with high number of interactions within the active site of HIV protease can also keep these interactions in the presence of a mutant enzyme.[18] DRV has a high to affinity to the HIV-1 protease, which is estimated to be 100 times higher than amprenavir, which is another protease inhibitor known for its specificity for the HIV protease enzyme and was approved in 1999.[27] DRV's affinity to protease was also proved to be 1,000 times higher than older protease inhibitors like saquinavir, nelfinavir, indinavir and ritonavir which explains DRV potency against mutant types HIV more than other members of the protease inhibitor group.[18]

On the other hand, DRV has some limitations as reported by Desail and Thakkar,[28] including low oral bioavailability (37%) due to numerous factors such as its low water solubility, high lipophilicity, it is subjected to first pass metabolism by cytochrome P450 (CYP450) enzymes (hepatic and intestinal), it is a substrate of P-glycoprotein (P-gp) leading to P-gp efflux which causes efflux of the absorbed drug back into the intestinal lumen. Additionally, food with high lipid content increases DRV bioavailability, which means that its absorption is food dependant, also liver diseases and rashes are considered as common side effects to DRV especially in high doses.[28–30] DRV is usually co-administered with ritonavir (RTV), see Figure 1.3.B. RTV is as a booster for DRV and considered as a preferred protease inhibitor-based approach for the treatment of naïve HIV patients by the United States Department of Health and Human Services (DHHS) guidelines.[1] RTV is a protease inhibitor that inhibits the activity of both P-gp and CYP3A (a major CYP450 isoform), therefore increases the bioavailability of DRV from 37% to 82%, as it decrease the first pass metabolism of DRV and it also decrease the incidence of mutations.[31] DRV is usually co-administered with RTV at an adult dose of 600 mg with 100 mg RTV twice a day or 800 mg with 100 mg RTV once daily.[18,32] Due to the pharmacokinetic limitations of DRV and the side effects of both DRV and RTV which include allergic reaction liver diseases and pancreastitis,[28] drug delivery systems provide an opportunity to decrease the required dose of both drugs and enhance targeting to HIV reservoir sites.[15,28]

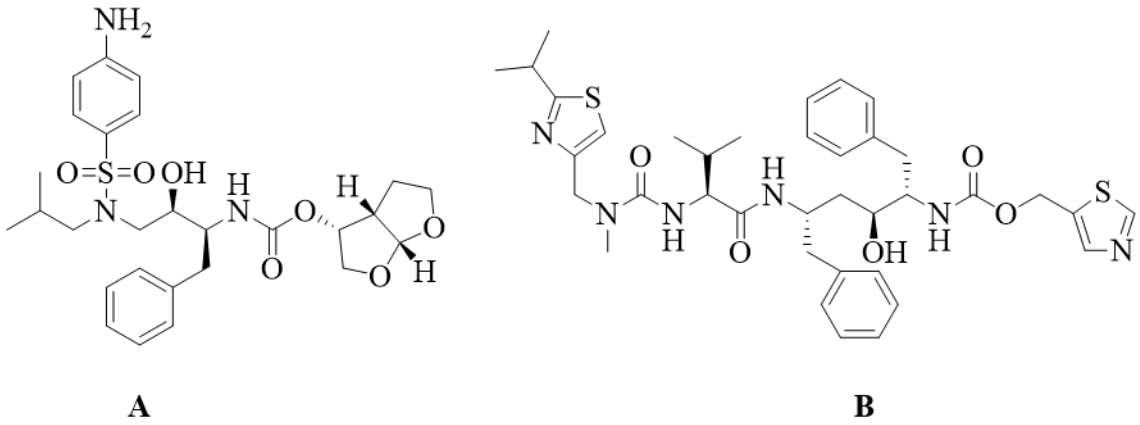

Figure 1.3 Chemical structure of: A) Darunavir (DRV) and B) Ritonavir (RTV)

In the past several years, research in the field of drug delivery had witnessed a revolutionary growth due to the wide use of nanocarriers for the targeted delivery of drugs to combat many diseases including serious diseases [33] like cancer,[34,35] tuberculosis,[36] HIV/AIDS [28,29,37] and heart diseases [36] among many others. Nanotechnology offers the advantages of tuning the formulation characteristics in such a way to make the drug targets specific areas in the GIT, like the stomach, different segments of the small intestine or the colon, and protect the drug from the extreme conditions of the GIT.[38]

1.5 HIV-targeted oral drug delivery approaches

The oral route is most convenient drug administration route for patients due to its numerous advantages: it is non-invasive unlike parenteral drug administration, pain-free, and suitable for most age groups. These advantages make the patients more likely adhere to the treatment which is crucial for chronic diseases like diabetes, arthritis, heart diseases, hypertension and HIV/AIDS.[39] On the other hand, successful oral delivery drugs must address some challenges, like gastrointestinal tract (GIT) mucus barrier, which can hinder the drug penetration and absorption, and the harsh conditions of the GIT (presence of acidic conditions and various digestive enzymes). This is in addition to the problem of first pass metabolism upon intestinal absorption, which causes the majority of drugs being metabolised before it reaches the systemic circulation which in turn means low bioavailability of the administered drug.[40] Another limitation for the oral route is the poor drug aqueous solubility. For any drug to absorbed through the GIT membranes, it must be soluble in the GIT fluids. For hydrophobic drugs, their

low dissolution rates are the main reason for their limited intestinal absorption upon oral administration. This represents a big challenge for the antiretroviral chronic therapy; a combination of 3-4 hydrophobic antiretroviral drugs in high doses, given daily for lifetime in the case of HIV/AIDS. The low bioavailability problem of the antiretroviral drugs was traditionally addressed by increasing the doses, an approach which usually increase the side effects and the cost of treatment, which is a main obstacle in the lack of treatment in the developing countries which have the largest number of patients.[40] Regardless to the limitations of the oral route, the overall advantages outweigh the drawbacks, which makes the oral route an attractive route for drug administration.

Upon HIV-1 infection there is a difference in the viral infection between CD4 cells and monocyte/macrophage (Mo/Mac cells). The activated CD4 lymphocytes experience a rapid viral reproduction followed by a significant cell death. However, Mo/Mac cells are known to be the secondary cellular target of HIV-1 that is responsible for the latent HIV infection which occurs over a prolonged period.[41] CD4 cells are present in large numbers in the gut associated lymphoid tissue (GALT) and can be targeted by lipid nanoparticles that are taken up by lymph vessels following oral administration. While polymeric nanoparticles have been well-reported in the literature in targeting Mo/Mac cells.[41–44] When the polymeric particles reach the blood following an intravenous or oral administration, the body identifies them as foreign bodies and they are cleared from the blood by the Mo/Mac cells as part of the mononuclear phagocyte system (MPS). The MPS in immunology are also referred to as reticuloendothelial system or macrophage system, it mainly consists of phagocytes, usually monocytes and macrophages. Their main function is the engulfment and destruction of microbes like bacteria and viruses, and foreign substances that includes nanoparticles.[45] Once inside the Mo/Mac cells, the polymeric nanoparticles release the loaded antiretroviral drugs killing the virus.[42]

Versatile types of polymeric[46–54] and lipid[55] nanoparticles (see Figure 1.4), have been developed over the years to enhance the behaviours of drugs in the body and to decrease side effects.[20] They are considered two widely used classes of nanocarriers for the drug delivery of poorly soluble drugs. The following subsections (1.5.1 and 1.5.2) introduce the different nanocarriers and discuss specific examples of nanocarriers for the delivery of HIV drugs, with a focus on lipid nanoparticles in this research. Polymeric nanoparticles include: nanocapsules, nanospheres, dendrimers, polymer conjugates and polymeric micelles. Lipid-based carriers

includes liposomes and solid lipid nanoparticles, nanostructured lipid carriers, nanoemulsions and lipid polymer hybrid nanoparticles. However, many of these nanocarriers have limitations like poor physical stability and aggregation, drug leakage during storage, presence of residual organic solvents in the final product and toxicity. Therefore, these formulations must be optimised to suit the used active ingredients and excipients.[56–58]

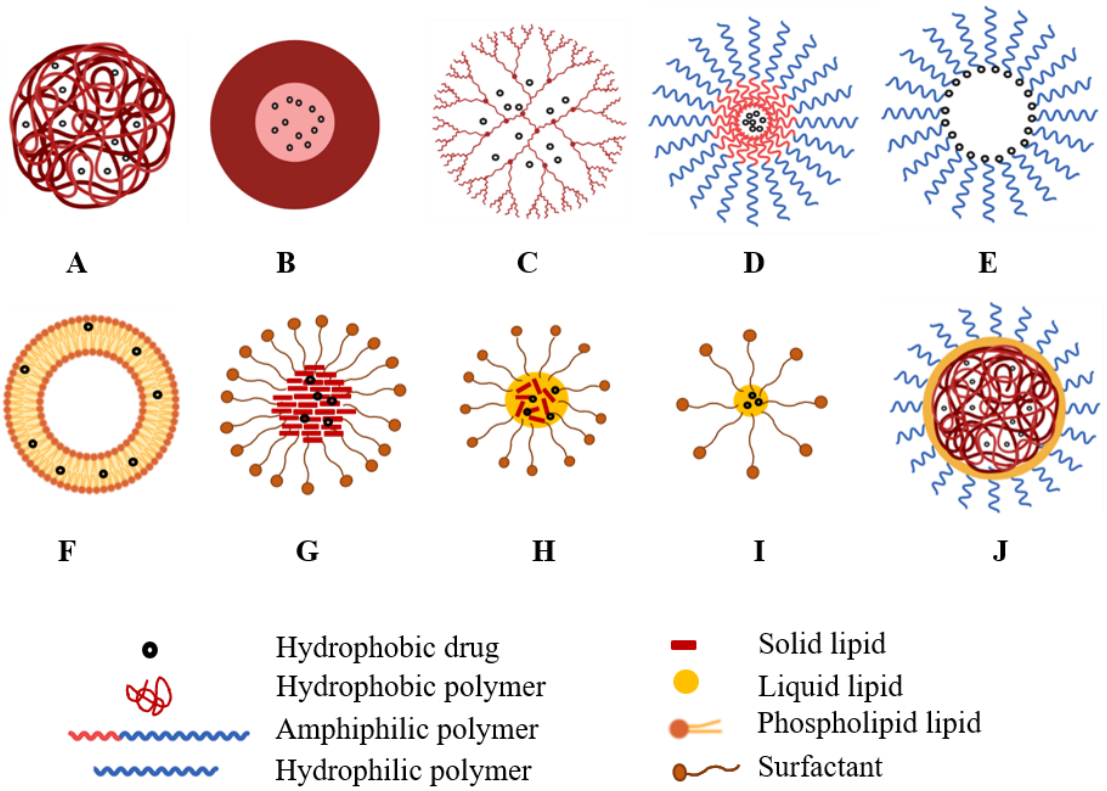

Figure 1.4 Overview of different types of drug loaded nanocarriers: A) polymeric nanospheres, B) polymeric nanocapsules, C) dendrimers, D) polymeric micelles, E) polymeric drug conjugates, F) liposomes. G) solid lipid nanoparticles (SLNs), H) nanostructured lipid carriers (NLCs), I) nanoemulsions (NEs) and J) lipid polymer hybrid nanoparticles (LPHNs).

1.5.1 Polymeric nanocarriers

1.5.1.1 Polymeric nanoparticles (PNPs)

Polymeric nanoparticles (PNPs) are defined as colloidal systems with size in the submicron range (1−1000 nm),[13] that are made of polymers of natural and/or synthetic origins. The most frequently used natural polymers include chitosan, sodium alginate and gelatine.[39,59,60] A wide range of synthetic polymers have also been used in polymeric nanoparticles like polylactides (PLA),[61] poly (lactide-*co*-glycolides) (PLGA),[46–54] polyglycolides (PGA),[62] polyanhydrides,[63] polyorthoesters (POE),[64] polycyanoacrylates,[60,65] poly-caprolactone (PCL),[59,66] poly(malic

acid) (PMLA)[67] and poly(methacrylic acid) (PMAA).[68] PNPs have a lot of advantages: they are easy to formulate, many are made of biodegradable polymers that have the advantage of being biocompatible, and a wide variety of materials can be used to make PNPs giving a great flexibility/diversity in the particles. In terms of efficacy and bioavailability, they have been shown to transport active ingredients to a targeted site with the specified concentration.[46] PNPs usually show high stability compared to liposomes and shows controlled release profiles.[21] They have been extensively used in different areas like cancer,[34,69–71] fungal infections,[72] targeted drug delivery,[73] vaccines delivery [74] and HIV/AIDS.[25]

PNPs can be classified into two main types: nanocapsules and nanospheres. Nanocapsules have a vesicular structure, in which the active ingredients are retained in a core surrounded by a solidified polymeric shell, while nanospheres is described as a polymeric mass in which the drug molecules are uniformly distrbuted.[39,60]

There have been numerous examples of PNPs targeting HIV cells. A study by Shah and Amiji showed an enhanced uptake of saquinavir into the THP-1 cells of monocyte/macrophage by 10 times when loaded in polymeric nanoparticles made of poly (ethylene oxide)-modified poly(epsilon-caprolactone) (PEO-PCL) compared to saquinavir aqueous solution. As stated earlier, monocyte/macrophage are main reservoirs of HIV and targeting them is one approach of potentially eradicating HIV/AIDS.[44] In a different study by Hillaireau *et al*, azidothymidine-triphosphate also known as zidovudine was encapsulated in polymeric hybrid nanocapsules made of poly(isobutylcyanoacrylate) (PIBCA) and poly(ethylene imine). This formulation showed enhanced intracellular uptake by J774.A1 cells which are mouse macrophages, which was 10-30 folds more than the uptake of the pure drug.[43] The general limitation for PNPs is that they might undesirably accumulate in body organs like spleen and liver, unlike SLNs for example which has the advantage of site-specific delivery.[75] Other limitations include biocompatibility problems especially for non-biodegradable polymers, nanotoxicity issues and safety considerations,[13] and till now, only a small number of the available polymers are approved drug delivery systems.[21]

1.5.1.2 Dendrimers

Dendrimers are highly branched synthetic three-dimensional molecules in the nanoscale that were first synthesised in the 1980's by Tomalia Donald and his group. The term dendrimer is

derived from the Greek word “dendron” which means tree and from the Greek suffix “mer” (segment). The tree-like branching architecture provides a lot of surface functional groups which can be modified by chemical conjugation, and also provide void space in the core suitable for encapsulation of drugs.[76] Dendrimers have a lot of attractive features which include: monodispersity, multivalency and high physical stability. They can be designed to have amphiphilic characters with hydrophilic groups on the surface and hydrophobic groups in the core, which enables them to encapsulate hydrophobic active moieties. Dendrimers have been widely investigated since their discovery for use in therapeutic and diagnostic applications and the most used polymers are: polyamidoamines, polypeptides, polypropyleneimines (PPI), polyglycerols, and polyesters.

As example from the literature for the use of dendrimers in the treatment of HIV, Dutta *et al.*[77] conducted a study for targeting of efavirenz to human Mo/Mac. They showed that generation 5 poly propyleneimine (PPI) dendrimers with mannose conjugated offered an improved uptake of efavirenz by Mo/Mac 12 folds more than the free drug, with low cytotoxicity to normal cells due to mannose conjugation.[77] Despite the promise of dendrimer-based systems, their clinical applications have been a challenge due to toxicity and biocompatibility concerns, which are usually affected by the surface functionalisation and generation number. In addition to the problems associated with complicated synthesis and production costs.[78,79]

1.5.1.3 Polymeric micelles

Polymeric micelles are supramolecular nanoparticles with typical sizes of 10-200 nm produced using amphiphilic polymers. Micelles have the ability to self-assemble at concentrations exceeding their critical micellar concentrations (CMC), which can be defined as the concentration of the surfactant above which micelle formation occurs.[80] In polymeric micelles used in the drug delivery of hydrophobic drugs, the hydrophobic components of the polymers are directed inwards to form hydrophobic core, and the hydrophilic components of the polymers are directed outwards to form hydrophilic shell.[79,80] The hydrophilic shells of the micelles can protect the micelle from detection and clearance by the immune system of the body, while the hydrophobic core acts as a reservoir which encapsulate hydrophobic drugs. Different amphiphilic copolymers have been used to synthesise micelles, with PEG being the most used polymer for hydrophilic moieties. PEG has been shown to prevent particles aggregation as they act as steric stabilisers. Particles surface modification by PEGylation also

limit bounding of the serum proteins to the surface of the particles, which minimise clearance by reticuloendothelial system (RES) and the uptake by Mo/Mac, as the phagocytic cells will not be able to recognise the nanoparticles as foreign materials,[81] therefore prolong circulation half-life in the body.[82] The application of polymeric micelles in nanomedicine include ocular[83], HIV/AIDS[21,84] and cancer.[79]

Chiappetta *et al.* studied polymeric micelle as a drug delivery approach to paediatric drug delivery for the hydrophobic drug efavirenz.[85] Their results showed that poloxamine micelles provided enhanced solubility of efavirenz by 8,400 times, improved drug encapsulation and significantly increased its bioavailability compared to extemporaneous suspension, showing a promising drug delivery system. The premature disintegration in the systemic circulation is a considerable limitation for polymeric micelles, which is a result from the dilution in the blood stream as well as interactions with the components of the blood including plasma proteins.[80] Another drawback is the low drug loading.[40]

1.5.1.4 Polymeric drug conjugates

Polymeric drug conjugates are considered as form of prodrugs where a drug is chemically conjugated to a polymer.[86] Usually hydrophilic polymers as polyethylene glycol (PEG) and poly(N-(2-hydroxypropyl) methacrylamide) (P-HPMA) are used to increase the water solubility of poorly water soluble drugs and to increase the residence time in the systemic circulation.[86,87] This approach has many advantages which include the enhancement of the bioavailability of hydrophobic drugs by increasing their water solubility and protection of the active drug moiety from deactivation and enzymatic degradation. Additional benefit of polymeric drug conjugates is the enhancement of drug targeting to the site of action and reducing the immunological body response by improving the pharmacokinetic properties.[88,79]

An example for polymeric drug conjugates for HIV drug delivery, was the coupling of zidovudine which is a NRTIs with the polymer a,b-poly(N-2-hydroxyethyl)-DL-aspartamide (PHEA). The Zidovudine polymer conjugate was stable in the gastric fluid and led to increasing of zidovudine short half-life and prolonged its drug release.[89]

Despite their benefits, polymeric drug conjugates have some challenges which affect their approval for clinical applications.[86] Firstly, the polymer-drug conjugates is considered as a new

chemical entity rather than a new formulation, such a new entity will have different pharmacokinetic and pharmacodynamic parameters such bioavailability, toxicity and biodistribution. This different biological behaviour poses an added barrier to regulatory approval. Additionally, unlike drug molecules which have a defined structure, polymer conjugates have heterogenous structures which needs further study and clarifications. Also polymer drug conjugates are considered as sophisticated structures that require complex synthesis and characterisation methods which hinder scale up to meet regulatory requirements.[86] Finally, another drawback is that polymeric drug conjugates have low drug loading due to the polymer to drug ratio, this is in addition to problems related to the polymers themselves which include toxicity and biodegradability issues.[79] All the above mentioned drawbacks make the development of drug polymer conjugates a challenge, although a number of compounds have received approval for non-oral administration.

1.5.2 Lipid nanocarriers

Lipid nanocarriers have emerged as a promising drug delivery route to overcome the problems of other drug delivery systems e.g. polymeric nanocarriers.[90] They are of special interest as carriers for hydrophobic drugs, with poor water solubility. They have the advantages of being low in toxicity as they are usually made of physiological lipids, highly compatible and offer improved bioavailability for encapsulated drugs. They also provide protection for the loaded drugs from the harsh conditions of the GIT, can be designed to produce controlled release formulations, they are usually less expensive than other drug delivery systems and easy to scale-up.[90]

1.5.2.1 Lipid-based nanocarriers and HIV drug targeting

As mentioned before in section 1.3, HIV has reservoir sites in the body that are difficult to access by the conventional drug administration methods, which means that the drugs cannot be kept in suitable effective concentrations for minimum required durations.[91] These anatomical sites include lymphatic system and especially the GALT. Approximately 99% of the HIV replication occurs in CD4+ receptors containing T cells.[20] Therefore, targeting of HIV drugs to the lymphatic system which is a HIV reservoir site has a significant importance.

Networks of both blood and lymphatic vessels supply the whole gastrointestinal tract, most of the dietary compounds are transported to portal blood vessels, as they have fluid flow 500 times higher than intestinal lymph vessels, where they are subjected to first pass metabolism, see Figure 1.5.[92–95] Therefore, many lipid based drug delivery systems were developed to enhance uptake of the drugs by the lymphatic route, such systems include liposomes, SLNs[24] and NEs.[96] Lipid-based formulations are selectively up taken by the lymphatic route.[79,97]

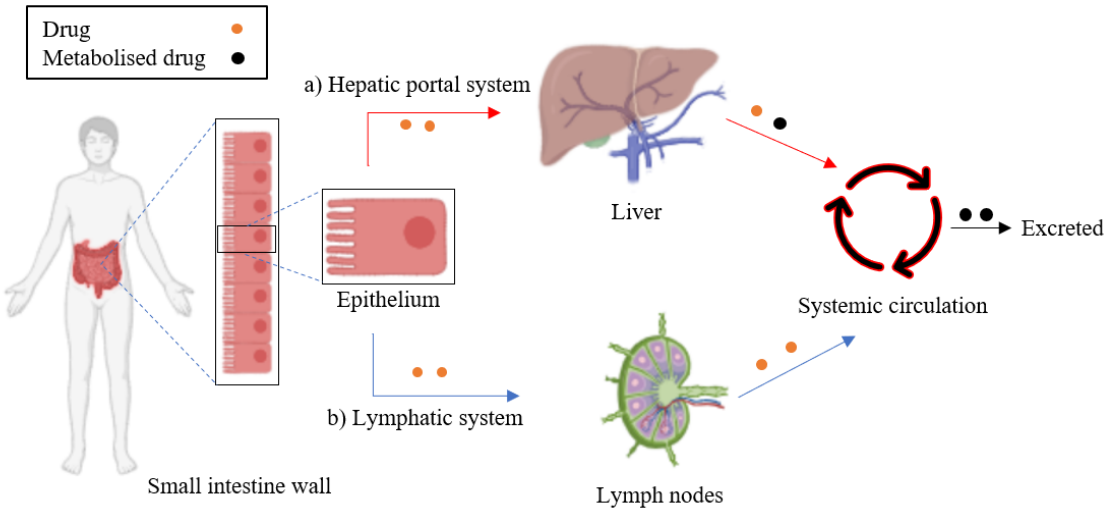

Figure 1.5 Diagram showing examples of the two oral delivery routes; a) hepatic portal system where the drug is subjected to first pass metabolism and b) lymphatic system.

The transport of lipid-based carriers to intestinal lymphatics could be achieved by different mechanisms as shown in Figure 1.6. The three proposed mechanisms are: 1) Transcellular mechanism which regulates the absorption of dietary lipids. The administration of lipid-based drug delivery systems stimulates the formation of chylomicron which are natural lipoprotein particles that help in the transportation of lipids from the GIT to different body parts. Chylomicron in turn will promote the transportation of encapsulated hydrophobic drugs into intestinal lymphatics.[93,94] 2) Transport through membranous epithelial cells (M cells) of Peyer patches which are lymphoid follicles that are part of the GIT lining and composed of enterocytes interspersed with M cells that cover lymphoid aggregates. The transport of nanoparticles through payers patches occurs by a combination of endocytosis or transcytosis.[92] 3) Paracellular uptake is another mechanism which contributes to a lesser extent in lipid transport. It is a passive route which transport molecules according to the concentration gradient and does not need carriers. Paracellular uptake happens through opening of tight junctions.[93,98] Among the essential aspects of the lymphatic uptake of particles that they should

have a log P between 3–5.[91] Nanoparticles taken up by the M cells are more likely to be transported to the GALT, on the other hands nanoparticles or drugs taken up by the enterocytes will mainly be delivered to the blood.[99]

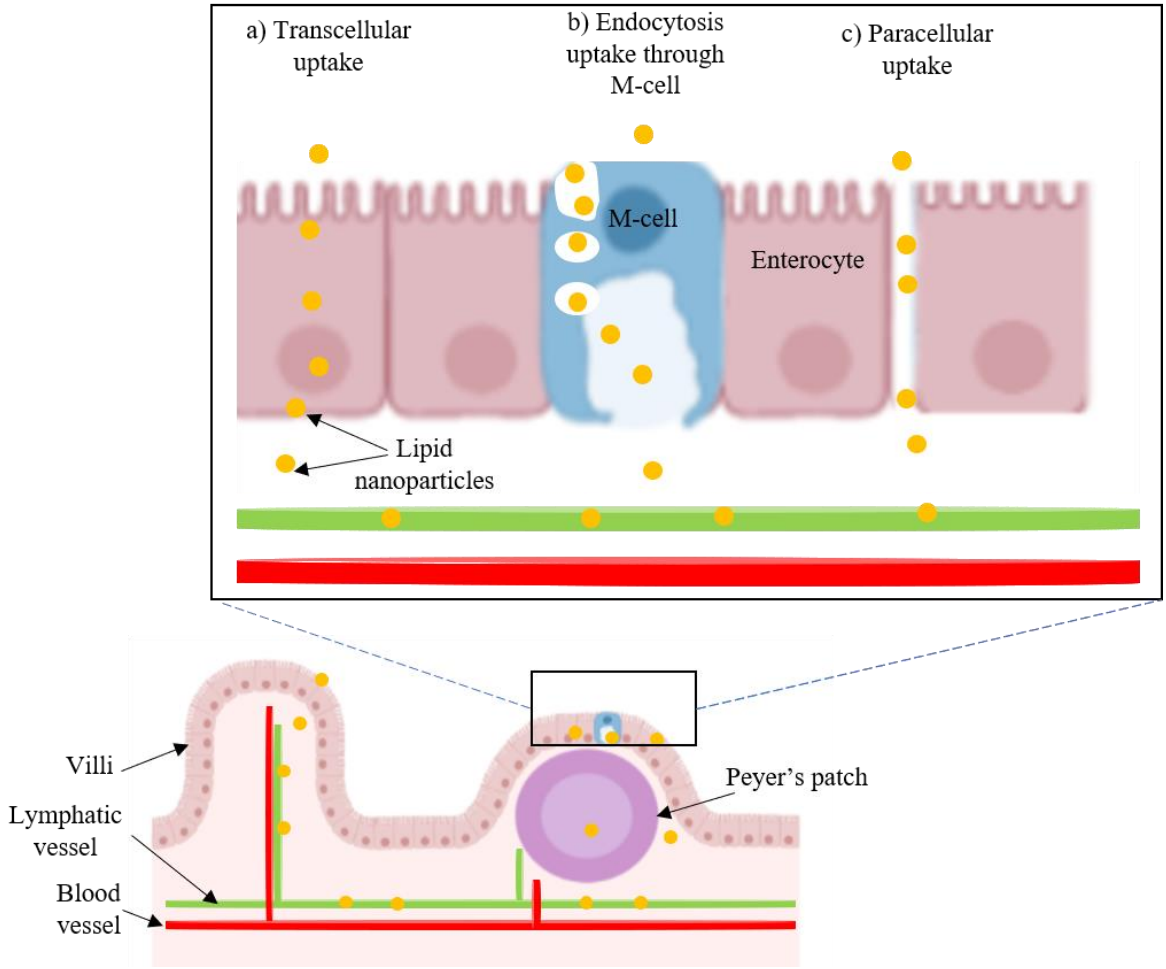

Figure 1.6 Mechanisms of uptake of lipid nanoparticles across the intestinal epithelial cells. Transport mechanisms include a) transcellular uptake, b) endocytosis uptake through M-cells and c) paracellular uptake.

1.5.2.2 Lipid-based nanocarriers types

There are different types of lipid-based nanocarriers depending on their structure and the nature of the used lipid as shown in the earlier Figure 1.4. Liposomes are distinct in that they are composed of aqueous cores that are surrounded by phospholipid layers. While for other types of lipid nanocarriers, the lipid generally forms the core of the particles, for example, solid lipid nanoparticles (SLNs) have a core made of solid lipids, while nanoemulsions (NEs) have liquid lipid cores and nanostructured lipid carriers (NLCs) have cores made of a combination of solid and liquid lipids. Although these different types of nanoparticles are made of lipids, however, they vary in the their size and shape, see Figure 1.7.[100] Another distinct structure for lipid-based

nanoparticles is that of lipid polymer hybrid nanoparticles (LPHNs), which have cores made of polymer that are surrounded by a layer of phospholipids.[57,58,90,101]

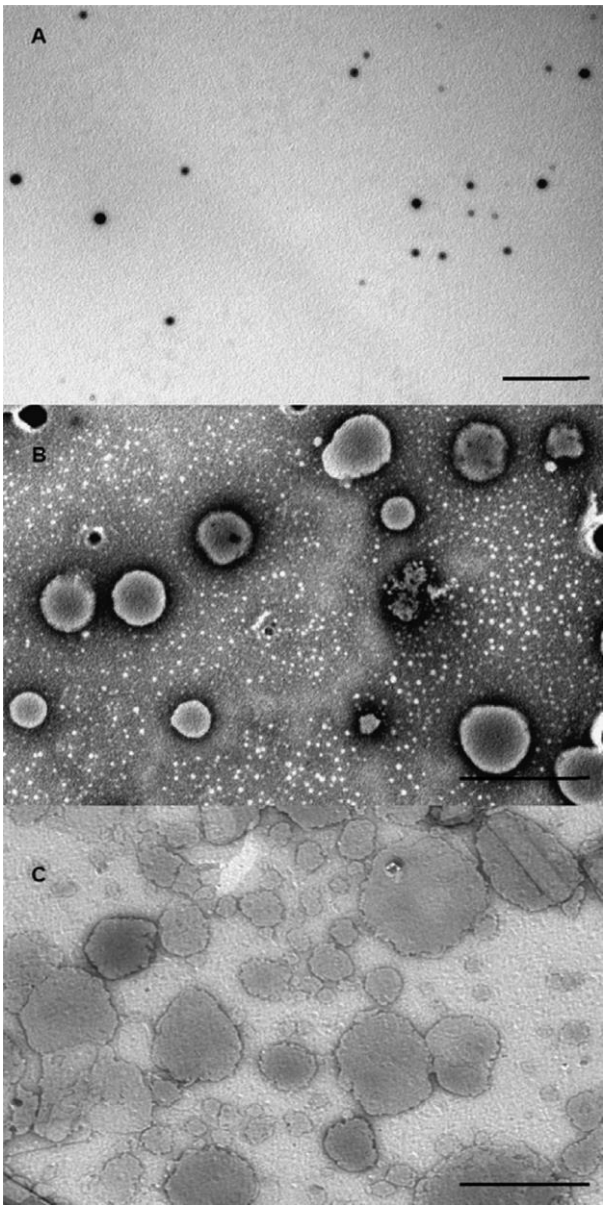

Figure 1.7 Transmission electron micrographs of retinyl palmitate loaded in (A) nanoemulsions, bar length 100 nm (B), SLNs, bar length 500 nm and (C) liposomes, bar length 500 nm. The figure was adopted from a study by Clares et al., with permission.[100]

Surfactants are essential components of the lipid-based nanocarriers which help to colloidally stabilise the lipid core and decrease particles agglomeration. Surfactants act by decreasing the interfacial tension between the interface of the particles causing particles to partition.[102] The choice of the surfactants and optimising their concentration greatly affects the quality of the produced nanoparticles. High concentrations of the surfactants reduce the interfacial tension

and facilitate the particle partition during preparation. The decrease in particle size is due to the increase in the interfacial area. The concentration of a surfactant should be high enough to ensure complete coverage of the new formed interfaces to prevent the agglomeration of particles. However, in some cases the increase of the surfactant concentration might lead to increase in the particles size. Liu *et al.* reported an increase in the particle size and the entrapment efficiency as a result of increasing the concentration of poly vinyl alcohol (PVA), where hydrogen bonds between the hydroxyl groups of PVA and the surrounding molecules and particles are formed, which led to particle aggregation. The type of surfactant can also change the properties of the produced nanocarriers. For example, RTV loaded-SLNs synthesised using Tween 80, had smaller particles size than those produced with the poloxamer.[103] This finding could be due the inability of poloxamer to cover all the surface of SLNs leading to the increase of Z-average diameter. On the other hand, the smaller particles size in the case of Tween 80 could be due to the higher interaction of the lipophilic portion of Tween 80 with the lipid core of SLNs as explained by Javan *et al*.[103]

1.5.2.2.1 Liposomes

The name liposome is derived from two Greek words: lipo ("fat") and soma ("body"). liposomes are microscopic vesicles with a size between 25 nm and several microns. They consist of one or more phospholipid bilayers, which usually surround an aqueous discrete core.[15,20,21,104] liposomes are mainly composed of natural or synthetic phospholipids, cholesterol and nontoxic surfactants.[104,105] They have advantages over other drug delivery systems which include the ability of encapsulating both hydrophilic and hydrophobic drugs. The hydrophilic drugs are entrapped in the aqueous core, while hydrophobic drugs can be incorporated in the lipid bilayers. In addition to that, they are biocompatible, have the ability for self-assembly, protect the drugs from degradation, reduce the toxicity of the encapsulated drugs by their ability to site specific targeting.[14,16,21,102] liposomes have an additional advantage in the treatment of HIV as they are recognized as foreign particles and easily taken up by mononuclear phagocytic cells, where HIV is mainly present in the case of infected patients. As such, liposomes represent a method for selective uptake which decrease the side effects of HIV drugs, as it target the mononuclear phagocytes. [15]

The use of liposomes for HIV targeting has been well-reported in the literature. Azidothymidine (AZT)-loaded liposomes, with surface modification was synthesised by Kaur

et al.[106] In this study, they engineered the surface of liposomes to have positive charge using stearyl amine or negative charge using dicetyl phosphate or modified it with a ligand to enhance HIV targeting to the lymphatics, including the spleen and lymph nodes. Images of the fluorescent microscopy suggested enhanced localisation of the modified liposomes in both the lymph nodes and spleen, where mannose modified liposomes showed the highest uptake.[106] liposomes may enhance the pharmacokinetics of encapsulated drugs; the loading of zidovudine myristate into liposomes led to the reduction in its clearance, increased its half-life and increased its distribution in mononuclear phagocyte system bearing organs compared to zidovudine solution according to Jin *et al.*[107] On the other hand liposomes suffer from some problems like drug leakage, low drug loading capacity, poor physical and chemical stability during storage. This is in addition to the difficulty of large scale production which is very expensive and require many sophisticated steps.[12,16,21,102]

1.5.2.2.2 Solid lipid nanoparticles (SLNs)

Solid lipid nanoparticles (SLNs) were first introduced in the early 1990s as an alternative colloidal drug delivery system to polymeric nanoparticles, emulsions and liposomes.[55] They are nanoparticles consisting of solid lipid core that are surrounded by suitable surfactants to give colloidal stability, with size ranges within the range 50-1000 nm.[55,108–110] The lipid core can be made from variable materials that are solid at both room temperature and human body temperature, thus protecting encapsulated drug moieties from degradation by harsh conditions in the body. The poor bioavailability of hydrophobic drugs like: rizatriptan, terbinafine and darunavir (see Table 1.1) can be enhanced by encapsulation in the lipid core of SLNs to be delivered to different sites in the body. Research in the SLNs included many diseases including fungal infections, lymphoma, HIV/AIDs, sclerosis and others, a list of some of the reported formulations are inculded in Table 1.1.

SLNs are considered as an efficient drug delivery system as they are composed of physiological biocompatible and biodegradable ingredients like cholesterol. Their methods of preparations do not usually require the use of organic solvents as in the case of high pressure homogenisation method, and also they can be scaled up.[111] SLNs can also be dried to be in a powder form which can be then easily incorporated in tablets, capsules or other convenient dosage form.[112] Furthermore, SLNs also overcome several disadvantages of other nanocarriers like NEs, where the solid lipid cores of SLNs has much less drug mobility in comparison the oily phases as in

the case of NEs, which in turn decrease drug leaking.[108,110] SLNs offer the potential to provide tuneable drug release: the drug release from SLNs is affected by melting point of lipids, after their administration in the body, the solid lipid degrades slowly which leads to sustained release of the drug. Drug release from SLNs typically shows biphasic pattern with an initial burst release from drug adsorbed on the particles surface followed by sustained release from the core.[15]

The core of the SLNs is composed of solid lipids which could be from a single type or a mixture of different lipid classes. Classes of lipids used for the synthesis of SLNs include acyl glycerols, waxes, hard fats, triglycerides and fatty acids.[111] Various solid lipids were used in the synthesis for SLNs as we can see in Table 1.1 such as glyceryl monostearate, Precirol ATO 5, stearic acid, tripalmitin, and Compritol ATO 888®, which is one of the most reported solid lipids.[30,84,91,95] Compritol ATO 888® is a lipid with a melting point of 70 °C,[113] and is also known as glyceryl behenate and it is composed of a mixture of mono-, di- and tribehenate.[114] It is safe and generally considered to be superior to other lipids in terms of drug entrapment ability. These drug loading properties are due to the complexity of its structure and imperfect orientation which gives more space for drug loading, also the long chain length of behenic acid in Compritol 888 ATO® enhances interchain intercalation thus enables the intermolecular entrapment of the drug.[114]

A big limitation for the SLNs is the lipid crystallisation, which affect the stability of the produced SLNs and have to be taken into consideration.[115] Usually crystallised lipids can be present in several configuration states in a certain crystal lattice, and in thermodynamically unstable configurations. Upon storage, lipids tend to return to the thermodynamically stable conditions and rearrangement of the crystals usually occurs leading to expulsion of the encapsulated drugs.[55,116] This instability problem has to be addressed to ensure the effectiveness of SLNs as a drug delivery system.[102,116,117] Drug loading can limit polymorphism, see Figure 1.8. The effect of drug loading on limiting the polymorphism was investigated by RH *et al*. [118] In their study they used Imwitor®900 K as a solid lipid, they showed that loading the SLNs with the drug cyclosporin helped in preventing the polymorphic changes from the alpha to the beta crystal, as the drug enhance the distortion of the crystal lattice structure of the Imwitor® 900 K, increasing the cyclosporin loading helped in further limiting the crystallinity, which further confirm the hypothesis.[118]

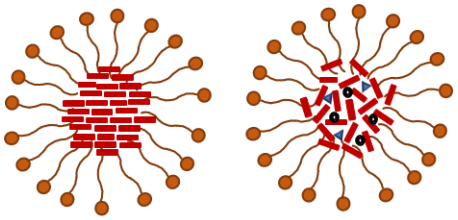

Figure 1.8 Diagram showing the structure of (A) Blank SLNs showing a core of perfect crystal structure. (B) Drug loaded SLNs showing cores with amorphous structure, where the drugs disrupted the crystal structure of the solid lipids.

Table 1.1 List of different solid lipids, surfactants, active ingredients, and methods of preparations of SLNs reported in the literature.

Solid Lipid	Surfactant	Active ingredient	Method of Preparation	Targeted disease	Reference
Glyceryl monostearate, Compritol 888 ATO® and Precirol ATO 5	Tween and Cremophor	Terbinafine	Microemulsion technique	Fungal infection	[119]
Compritol 888 ATO®	Taurocholate sodium salt and Epikuron 200	Riluzole	Microemulsion technique	Lateral sclerosis	[120]
Glyceryl monostearate, Compritol 888 ATO®, stearic acid and tristearin	Soya lecithin	Methotrexate	Solvent diffusion	Lymphoma	[93]
Glyceryl monostearate, Compritol 888 ATO® and Precirol ATO 5	Span 80, Soya lecithin, poloxamer and Tween 80	Darunavir	High-pressure homogenisation	HIV/AIDS	[121]
Palmitic acid and stearic acid	Poloxamer 407 and pluronic® F-127	Fenofibrate and nabumetone	Ultrasonication	Hypercholester-olemia and rheumatoid arthritis	[122]
Tristearin	Phospholipon 80	Rizatriptan	Solvent injection	Migraine	[123]

SLNs have been extensively studied as a drug delivery system for antiretrovirals for the treatment of HIV. The first study for SLNs as a potential carrier for antiretroviral drugs was conducted in 1998 by Heiati *et al.*[124] In this study, azidothymidine-palmitate (AZT-P) was loaded into SLNs made of trilaurin as a solid lipid, while dipalmitoyl phosphatidylcholine (DPPC) or a mixture of DPPC and dimyristoyl phosphatidylglycerol (DMPG) as phospholipids were used to render SLNs neutral and negative charge, respectively. It was found that the drug encapsulation increased with increasing the phospholipid content and that the drug release could be controlled when the SLNs surface was coated with PEG groups.[124] Further research

into SLNs managed to target SLNs to different body organs to reach different HIV reservoirs. A study by Negi *et al*. was designed to target the lopinavir-loaded-SLNs to the intestinal lymphatic system.[125] They found that the cumulative amount of lopinavir (LOP) in the lymph was 4.91-fold more than when the drug solution in methyl cellulose (MC) was used, see Figure 1.9.[125]

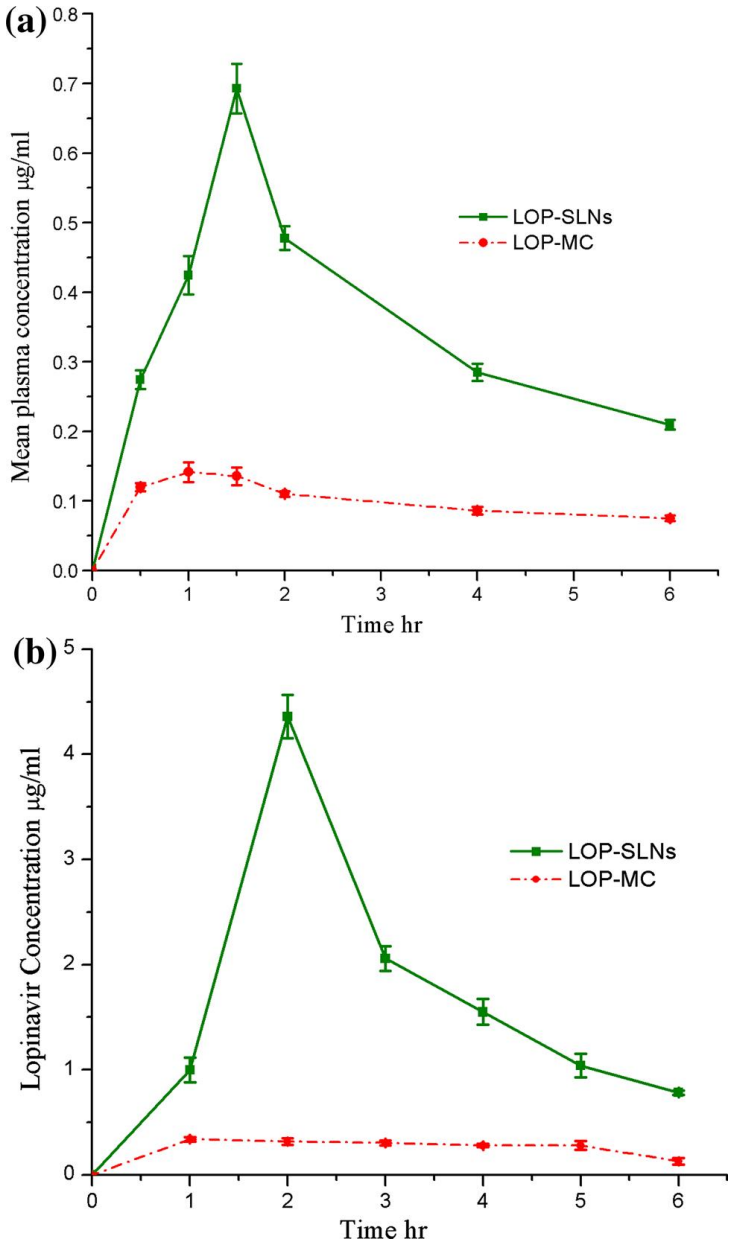

Figure 1.9 (a) Plasma profile of pure LOP-MC and LOP-SLNs (b) Lymphatic uptake rate of pure LOP-MC and LOP-SLNs. Statistical significances of LOP-SLNs compared with LOP-MC are p(0.05) (n = 5). This figure was adopted from a study by Negi et al., with permission.[125]

The brain is another key reservoir for HIV, Chattopadhyay *et al*. showed that loading of the protease inhibitors atazanavir into SLNs resulted in enhanced permeation across the human brain microvessel endothelial cell line (hCMEC/D3), as a simulation of the BBB in comparison

to the drug aqueous solution.[126] Ansari and Singh tested the transdermal drug delivery of lopinavir-loaded-SLNs to overcome the problems of the oral drug delivery like first metabolism. Their optimised formulation which was made of Compritol 888 ATO® as a lipid and poloxamer as a surfactant and labrasol as a co-surfactant resulted in an entrapment efficiency of 69.7% and small mean particles size of 48 nm. That formulation resulted in significant prolongation of drug release, where 71% of the drug was released over a duration of 12 hours in case of SLNs loading, in contrast to 98% drug release over 4 hours period in case of the pure drug.[127]

There have been some studies that involved darunavir-SLNs (DRV-SLNs), for example Desai and Thakkar studied the effect of the particle size of DRV- SLNs on the bioavailability. They concluded that SLNs with a size of ~ 200 nm, synthesised with high pressure homogenisation had increased oral bioavailability compared to SLNs with a size of 100 or 500 nm.[31] In another study by them, they suggested that DRV-SLNs with peptide grafting have better affinity for CD4 receptors and showed 569% increase in the bioavailability compared to plain drug suspension in an *in vivo* study carried out on rats.[128] A study by Bhalekar *et al*.,[129] showed successful synthesis of DRV-SLNs by high pressure homogenisation with a mean particle size of 270 nm and encapsulation efficiency of 69%. Their ex *vivo* studies suggested an uptake of the SLNs through the lymphatic route through endocytosis.[129] Although there have been a dual drug delivery of RTV with other antiretrovirals like lopinavir,[130] there have not been any published papers including dual oral drug delivery of DRV, which is a first line protease inhibitor and its booster RTV, up to our knowledge.

1.5.2.2.3 Nanoemulsions (NEs)

Emulsions are composed of a mixture of two immiscible liquids, usually water and oil. In this system, one of the liquids is called the dispersed phase, where it is dispersed in the form of small droplets in the other liquid which is called the continuous phase. Emulsions are classified into simple emulsions; oil in water (O/W) and water in oil (W/O) emulsions, and multiple emulsions; oil in water in oil (O/W/O) and water in oil in water (W/O/W) emulsions.[131] In contrast to classical emulsions, in NEs the dispersed phase is usually in the nano size range between 20 and 200 nm. NEs are also referred to as submicron emulsions.[132] The small size droplets of NEs provide higher surface area due to increased contact between oil and water. NEs show enhanced stability due to their small size, which make them less affected by gravity

forces which causes sedimentation and creaming.[133] NEs are non-irritant, non-toxic and can be safely applied to the mucous membranes, therefore can be orally administered. NEs are considered as a promising drug delivery system for lipophilic and poorly soluble drugs like vitamin D and E, darunavir, and eugenol. Different formulations of NEs are enlisted in Table 1.2. In NEs, the drugs are usually loaded in the internal phase of O/W emulsions, therefore, overcome the solubility problem of those drugs which in turn enhance their bioavailability. In addition to that the small size of nanodroplets that offer improved absorption across the GIT membrane due increased points of contact in oppose to classical emulsions, they also provide sustained release and reduced toxicity.[96] The most commonly used methods of the preparation of NEs include high pressure homogenisation and spontaneous emulsification (see Table 1.2).

Table 1.2 List of different liquid lipids, surfactants, active ingredients, and methods of preparations of NEs reported in the literature.

Liquid Lipid	Surfactant/ Cosurfactant	Active ingredient	Method of Preparation	Targeted disease	Reference
Soybean oil	Egg lecithin and Tween 80	Darunavir	High pressure homogenisation	HIV	[96]
Sunflower oil	Lecithin, pea proteins, sugar ester and a combination of Tween 20 and glycerol monooleate	Carvacrol, limonene and cinnamaldehyde	High pressure homogenisation	Bacterial infection	[134]
MCT	Tween 20, 40, 60, 80 and 85/ sodium dodecyl sulphate	Vitamin D	Spontaneous emulsification	Vitamin D deficiency	[135]
MCT	Tween 20, 40, 60, 80, and 85	Vitamin E acetate	Spontaneous emulsification	Antioxidant for cardiac diseases	[136]
Soybean oil	Soybean lecithin, Tween 80 and poloxamer 407/ propylene glycol	Camphor, menthol and methyl salicylate	High pressure Homogenisation	Topical therapy of arthritis	[137]
MCT	Starch	Eugenol	High pressure Homogenisation / micro fluidization	Cancer and inflammatory diseases	[138]

Vegetable oils which are mainly composed of medium or long chain triglycerides have been widely used in the pharmaceutical industry as they are biodegradable, come from renewable sources and nontoxic.[139,140] Many oils have already been used as liquid oils in the synthesis of emulsions such as sunflower oil, castor oil, coconut oil, olive oil, jojoba oil and soybean oil, however the main disadvantages of vegetable oil is their instability.[140] Most commonly used oils for nanoemulsions include; medium-chain triglycerides (MCTs) and soybean oil, see Table 1.2. Soybean oil is a vegetable oil that have been widely used in the pharmaceutical industry

as it has the advantage of being biodegradable, obtained from renewable natural sources and nontoxic.[139,140]

NEs suffer preparation problems and stability issues as they are highly influenced by the surrounding media and affected by pH and temperature.[100,141] Also, NEs requires high concentrations of emulsifiers to ensure the stability of the nanodroplets, and have a limited solubilisation for high melting point ingredients.[131] Another disadvantage for NEs is that the most commonly used methods for their preparation are high energy techniques like high pressure homogenisation and ultrasonication.[142]

In the context of HIV treatment, there have been few studies regarding the oral drug delivery of antiretrovirals using NEs. Vyas *et al.* studied O/W NEs as a potential carrier for saquinavir to enhance brain targeting following oral adminstration.[143] They concluded that the rate of oral absorption and subsequent brain localisation of saquinavir were greater in case of NEs compared to the aqueous suspension of the drug.[143] Another study included atazanavir as a protease inhibitor, where it suffers from poor water solubility, pH dependant dissolution and extensive first pass metabolism.[144] Singh and Pai prepared NEs of atazanavir using Maisine 35-1 as a liquid lipid, while Transcutol P and Span 20 were used as emulsifiers. They concluded that NEs resulted in the enhancement of the oral bioavailability of atazanavir, where the area under the curve (AUC) increased by 2.57-fold compared to the aqueous solution of the drug in experiments performed on rats.[144] In another example for HIV targeting, in comparing the drug absorption of saquinavir loaded into NEs using flax-seed oil to saquinavir aqueous suspension.[143] It was found that in the case of NEs, the drug concentration in both the plasma and the brain increased compared to when the drug aqueous suspension was used, see Figure 1.10. Both the maximum concentration (C_{max}) and the area-under-the curve (AUC) increased by 5-fold and 3-fold times in the brain, respectively, suggesting enhanced oral bioavailability in case of NEs.[143]

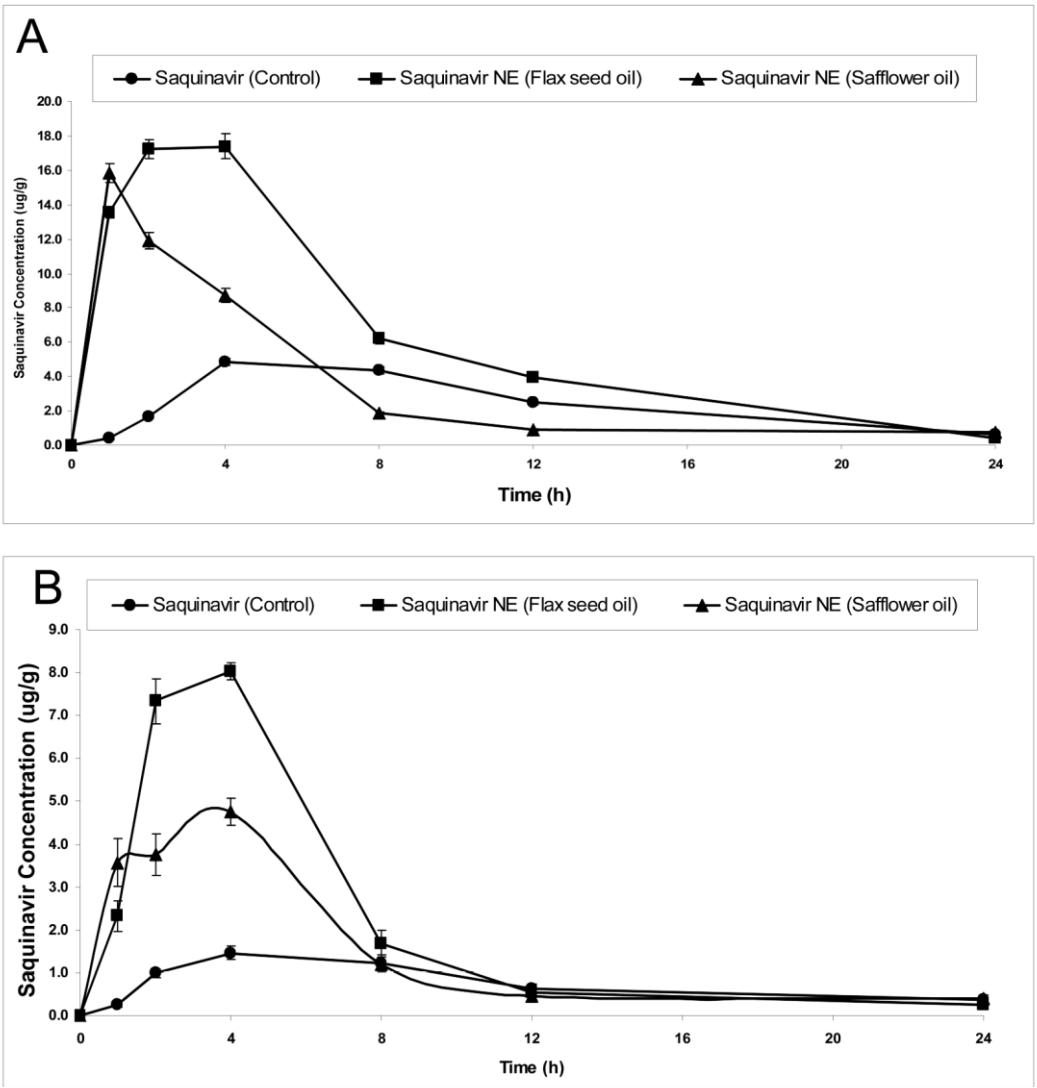

Figure 1.10 Plasma and brain saquinavir concentration versus time profiles following oral administration of the drug in aqueous suspension or nanoemulsion formulations to Balb/c mice. (A) The plots represent plasma concentrations versus time following oral administration (B) and brain concentrations versus time following oral administration. The Balb/c mice was dosed with 0.50 mL of the control aqueous suspension or nanoemulsion formulations by oral gavage. The administered dose contained 1 μCi radioactivity as tritiated [^{3}H] saquinavir. The is image is adopted from a study by Vyas et al, with permission. [143]

DRV-NEs has been reported in the literature, an example is a study by Desai and Thakkar.[96] They formulated DRV-NEs using soybean oil as the liquid lipid, and egg lecithin and Tween 80 as surfactants. The resultant NEs had mean droplet size of 109 nm, 93% entrapment efficiency and 223% enhancement of oral bioavailability compared to the drug suspension.[96] As in the case of SLNs, there have not been any published studies including the dual delivery of DRV and RTV up to our knowledge.

1.5.2.2.4 Nanostructured lipid carriers (NLCs)

NLCs were introduced as an alternative nanocarrier, to overcome the drawbacks of both SLNs and NEs. They are usually considered as a second generation of SLNs.[110] The concept behind their design was based on the incorporation of liquid oils to the solid lipid cores. The incorporation of the liquid oil disrupts the perfect crystal lattice of the solid lipid leading to enhancement of the stability of the system.[145] The decrease in the crystallinity of NLCs in comparison with SLNs was discussed in a differential scanning calorimetry (DSC) study conducted by Anantaworasakul *et al.*[146] They showed broadening of the melting peak of the lipid in case of NLCs either blank or chilli loaded,[146] in comparison with the pure lipid and SLNs. That finding suggests NLCs are more amorphous, see Figure 1.11.[146] Another advantage of NLCs is the increased drug loading of the hydrophobic drugs, as those drugs are more soluble in oils than in solid lipids. The design of NLCs help controlling drug release from the cores, as the drug will be encapsulated in the oil compartments, which are embedded in a solid lipid matrix.[147–149]

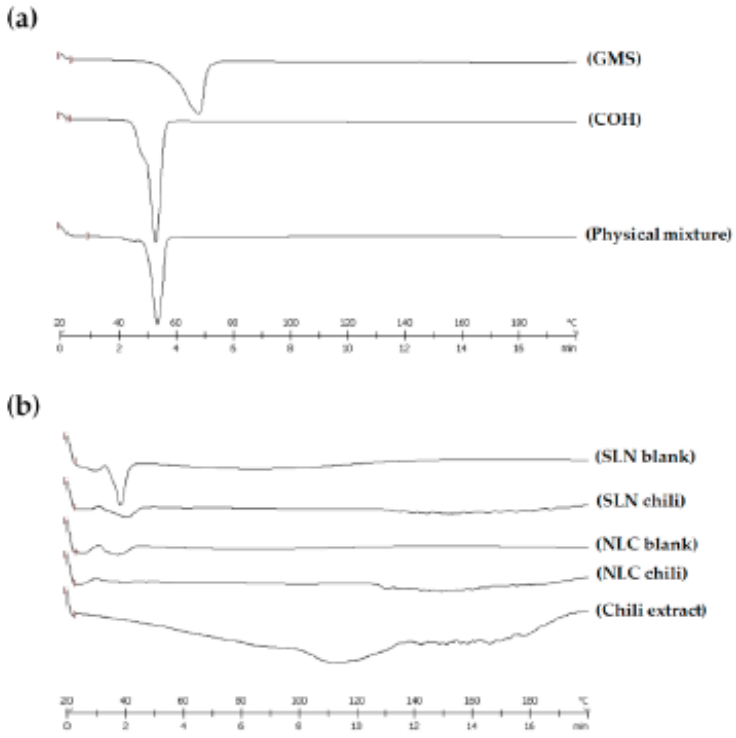

Figure 1.11 DSC thermograms of (a) the pure solid lipid and physical mixture, and (b) freeze-dried formulations. Abbreviations: SLN, solid lipid nanoparticles; NLC, nanostructured lipid carriers; GMS, glyceryl monostearate; COH, cetyl alcohol. This figure has been adopted from journal article by Anantaworasakul et al, with permission.[146]

NLCs have been well reported in the literature in the treatment of many diseases like different types of cancer, high blood pressure, HIV/AIDS, see Table 1.3. For the synthesis methods, high pressure homogenisation and microemulsification are commonly used. Precirol ATO 5 and Compritol 888 ATO® are among commonly used solid lipids in the synthesis of NLCs, while oleic acid, MCT Campul are among the most used oils, see Table 1.3.

Table 1.3 List of different solid and liquid lipids, surfactants, active ingredients, and methods of preparations of NLCs reported in the literature.

Solid Lipid	Liquid lipid	Surfactant	Active ingredient	Method of Preparation	Targeted disease	Reference
Precirol ATO 5	MCT and Captex 500	Pluronic® F-127 and sodium taurocholate	Bicalutamide	Hot high-pressure homogenisation	Prostate cancer	[150]
Stearic acid	Oleic acid	Poloxamer 188	Resveratrol	Solvent injection	Breast cancer	[151]
Cetyl palmitate	Isopropyl myristate, caprylic acid and oleic acid	Tween 80	Mefenamic acid	Microemulsion template strategy	Non- steroidal anti-inflammatory (NSAIDs)	[152]
Precirol ATO 5	Capmul MCM EP	Solutol®HS-15, Poloxamer-407 and Poloxamer-188	Olmesartan medoxomil	Hot high-pressure homogenisation	High blood pressure	[153]
Compritol 888 ATO®	Oleic acid	Tween 80	Lopinavir	Hot-melt microemulsification	HIV	[154]

Like other lipid nanocarriers, NLCs have been reported in the literature for the targeting of HIV. Pokharkar *et al.* studied NLCs for the intranasal drug delivery of efavirenz (EFV) as a route for brain targeting. EFV-NLCs with a mean particle size of 162 nm and 95.7% entrapment efficiency was successfully synthesised. This optimised formulation showed a 95% drug release over a 24 hours duration with 4.5% increase in the drug targeting potential to the CNS.[150] Another study involved the oral absorption of RTV by loading into NLCs (RTV-NLCs), the NLCs were synthesised using emulsification probe sonication method using myristic acid, capmul MCM EP as lipids and poloxamer 188 as a surfactant. The produced NLCs showed high permeability during membrane studies.[155]

1.5.2.2.5 Lipid polymer hybrid nanoparticles (LPHNs)

LPHNs are core-shell nanoscale particles, composed of a core of a biodegradable non-toxic polymer, coated by a lipid monolayer and often a lipid-polyethylene glycol (PEG) shell.[156,157] These components provide different properties: the polymer core encapsulates the hydrophobic

drug moieties, while the lipid coating which is usually composed of a layer of phospholipids, helps to stabilise the cores by electrostatic stabilisation.[158,159] This lipid shell has also been shown to enhance the entrapment efficiency of the drug,[160] and increase oral bioavailability of hydrophobic drugs.[161–164] A lipid-PEG conjugate is often included in the LPHNs shell as this has been shown to improve the physical stability of the particles especially in electrolyte solutions present in the body. In experiments by Chan *et al*. to determine the role of the PEG shell in LPHNs stabilisation, it was reported that large aggregates formed when LPHNs were dispersed in phosphate buffered saline (PBS) at a pH of 7.4 (a common model for biological ionic strength matrices) in the absence of the PEG shell despite the presence of high lipid coverage of the cores. While, LPHNs coated with lipid-PEG showed high stability in PBS, this was attributed to the steric stabilisation provided by the PEG.[165] The lipid-PEG conjugates also offer LPHNs increased residence time in blood circulation due to the avoidance of nanoparticle removal by the RES, this is an important consideration in parenteral formulations.[156,160]

LPHNs combine many of the advantages of lipid-based nanomedicines such as enhanced cellular uptake and the inherent benefits of polymeric nanocarriers including: architectural integrity, high stability over prolonged times and a controllable drug release profile.[166–168] The stabilising physicochemical properties of LPHNs make them a promising drug delivery system to target HIV reservoir sites in the lymphatic system where, currently, the drug cannot be maintained at therapeutic concentrations.[91] PLGA and [169, 170] PCL[171] are among the commonly used polymers in the synthesis of LPHNs. While soybean lecithin is one of the commonly used phospholipids in the synthesis of LPHNs. LPHNs has been extensively discussed in the literature for the treatment of various diseases especially different types of cancer (see Table 1.4), however there is very limited data about the use of LPHNs in the treatment of HIV, which would be an interesting area for future exploration. The only reported study involving LPHNs loaded with a combination of DRV and RTV is work from this thesis and will be discussed in detail in chapter 5.

Table 1.4 List of different polymers, phospholipids, surfactants, active ingredients, and methods of preparations of LPHNs reported in the literature.

Polymer	Lipid	Bulk stabiliser	Active ingredient	Method of Preparation	Targeted disease	Reference
PLGA	DSPE-PEG2000- NH2	Lutrol® F 127	Docetaxel	Self-assembled nanoprecipitation	Breast cancer	[169]
PLGA	Phosphatidyl-choline	d-α-tocopheryl polyethylene glycol 1000 succinate	Levofloxacin, ciprofloxacin, and ofloxacin	Modified emulsification solvent-evaporation	Lung biofilm infection therapy	[170]
PCL	Soybean lecithin	Polyvinyl alcohol	Itraconazole	Emulsification solvent evaporation method	Fungal infection	[171]
PLGA	Soybean lecithin	DSPE-PEG	Anti-carcinoembryonic antigen (CEA) half antibody	Self-assembled nanoprecipitation	Pancreatic cancer	[172]
Chitosan	Glyceryl monooleate	Pluronic F127	Enoxaparin	Modified self-assembled nanoprecipitation	Deep vein thrombosis, and pulmonary embolism	[173]
PLGA	Soya phosphatidylcholine	DSPE-PEG	Gemcitabine hydrochloride	Modified double emulsion solvent evaporation	Various cancer types	[174]
PLGA	Cationic lipid dioleyltrimethylammonium propane	Polyvinyl alcohol	Budesonide	Double emulsion solvent evaporation	Chronic obstructive pulmonary disease	[175]

The core shell structure of LPHNs (Figure 1.12.A) can be confirmed by TEM analysis, using uranyl acetate which stain the lecithin, which then appear as dark rings surrounding the polymeric cores, see Figure 1.12.B. On the other hand, there are several factors that determine the size of the produced LPHNs, among them is the lipid/polymer weight percentage. The optimum percentage according to Zhang *et al.* is 10-20% w/w, above it, the LPHNs size will increase as the excess lipid (above the CMC) will self-assemble to form liposomes, with a size of 100-1000 nm. However, below this weight percentage the lipid amount would not be sufficient to cover the cores surface leading to particles aggregation, see Figure 1.12.C.[160] Another factor that might influence the size of the LPHNs, is the viscosity of the used polymer, which is usually a reflection to its molecular weight. High molecular weight polymers would have high viscosity and would result in smaller particles, see Figure 1.12.D. One explanation, could be due to the more compact nuclei formed upon using high molecular weight polymer, which would lead to the formation of smaller nanoparticles.[160]

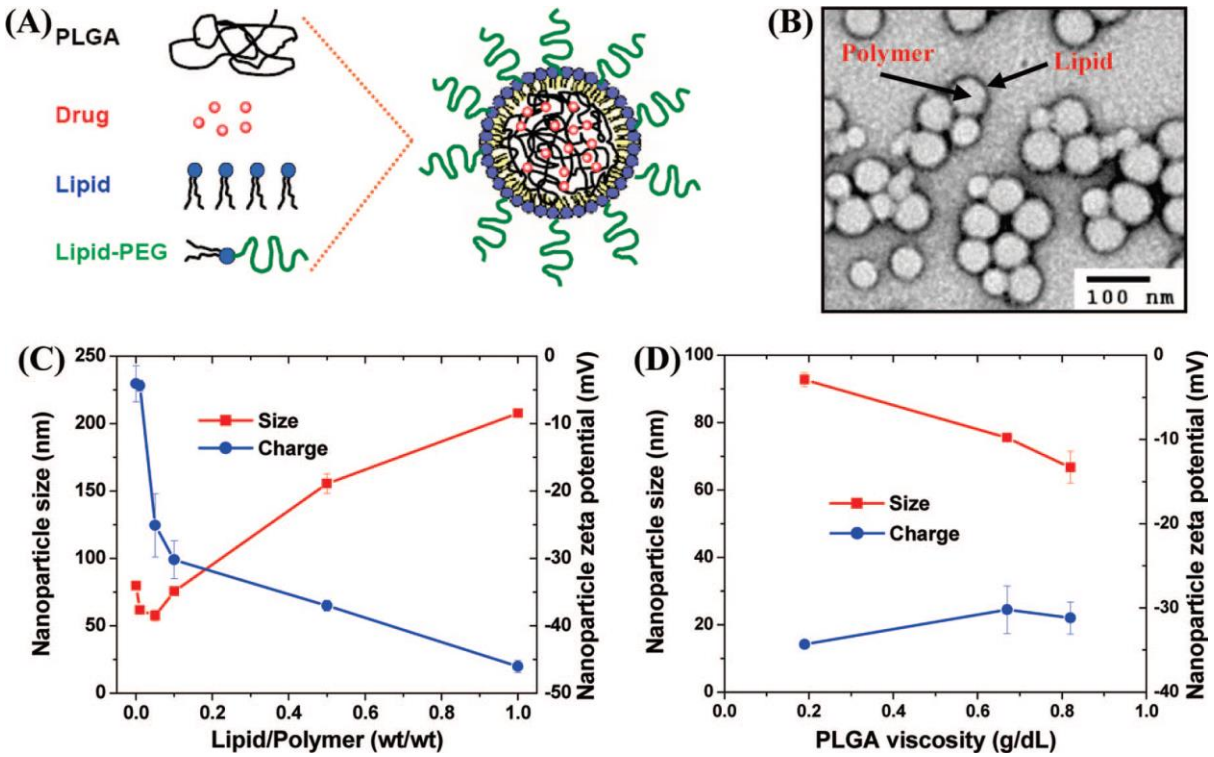

Figure 1.12 Development of LPHNs (A) Schematic illustration shows the formulation of LPHNs. The LPHNs comprise a hydrophobic PLGA core, a hydrophilic PEG shell, and a lipid (lecithin) monolayer at the interface of the hydrophobic core and the hydrophilic shell. (B) TEM image demonstrated the structure of the LPHNs proposed in (A). Uranyl acetate was used to stain lipids to enhance their electron contrast. (C) Effect of lipid/polymer weight ratio on LPHNs size and surface zeta potential. (D) Effect of PLGA polymer molecular weight indicated as inherent viscosity on LPHNs size and surface zeta potential. The figure was adopted from a study by Zhang et al., with permission.[160]

1.5.2.3 Methods of preparation of lipid-based nanoparticles

The majority of lipid-based nanocarriers have been synthesised using the traditional techniques for nanoparticles preparation which include: high pressure homogenisation,[143] emulsification/solvent evaporation,[176,102,109] microemulsion based method,[177] double emulsion-based method,[178] and solvent injection method.[179,8] The only exception is LPHNs, regardless to the method of synthesis, there are two general routes for their preparation: two-step method and one-step method.[156] In the two-step method, both the polymeric nanoparticles and lipid vesicles are synthesised separately and then the two nanoparticle systems are later mixed to form the LPHNs, see Figure 1.13. In the non-conventional two-step method, the preformed polymeric nanoparticles were dispersed into lipid solution, the resultant mixture are then spray dried to produce the LPHNs, see Figure 1.13.A. Another way of formation of LPHNs could be due to electrostatic adsorption of the lipid vesicles on the surface of the polymeric cores which is considered the conventional two-step method, see Figure 1.13.B. However, in the one-step

synthesis method, the formation of the polymeric cores and the assembly of the lipid around these cores happen simultaneously.[180]

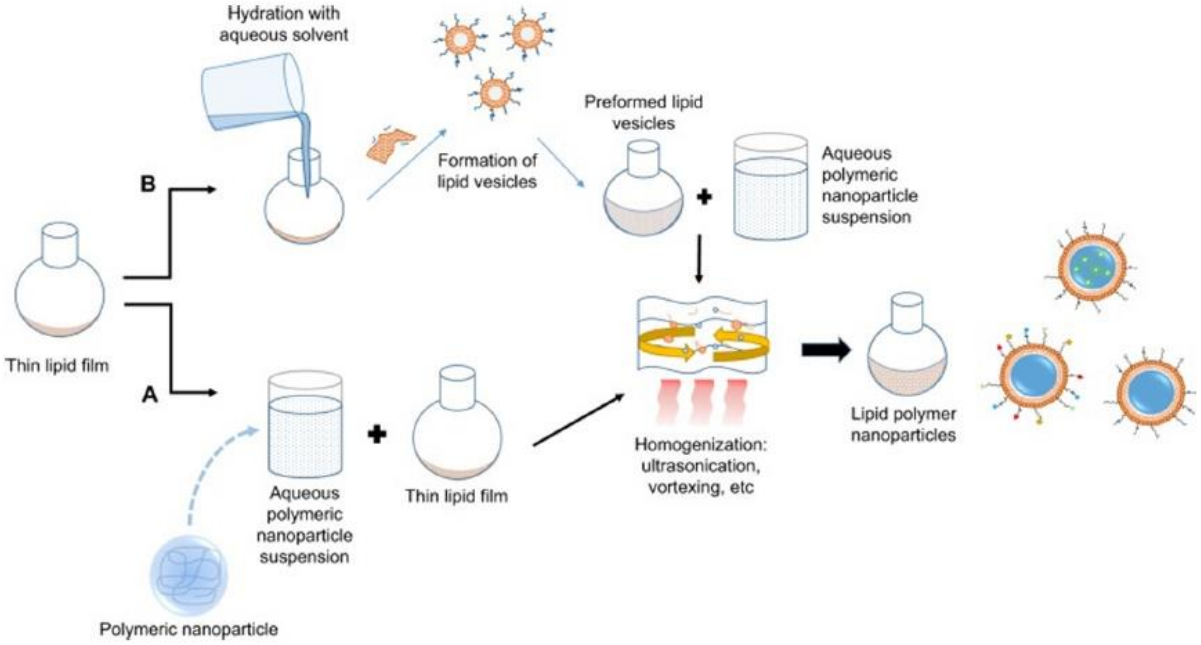

Figure 1.13 Different approaches to prepare LPHNs through the two-step method. In the method (A) an aqueous suspension of polymeric nanoparticles is added to the pre-formed thin lipidic film. On the other hand, in the method (B), pre-formed lipid vesicles are added to the polymeric nanoparticles. Figure was adopted from a review article by Soares et al, with permission.[181]

High pressure homogenisation is one of the most used techniques in the synthesis of nanocarriers and solvent injection method is one of the simplest and fastest method of preparations and therefore these two methods have been selected for more detailed discussion in the subsequent sections (1.5.2.3.1 and 1.5.2.3.2).

1.5.2.3.1 High pressure homogenisation method

In both hot and cold homogenisation, the drug is dispersed or dissolved in the melted lipid. For the hot method, the drug/lipid mixture is dispersed in a hot surfactant solution followed by mixing to produce a coarse pre-emulsion. This pre-emulsion is then subjected to high energy by using the high-pressure homogeniser at temperatures above the melting points of lipids. The hot nanoemulsions are solidified by cooling at room temperature. On the other hand, for the cold method, the lipid/drug mixture first is solidified by cooling using liquid nitrogen, followed by grinding of this solidified powder to reach the size range of 50-100 µm. The obtained powder is dispersed in a surfactant mixture and homogenised by high pressure temperature at

room temperature. This method has the advantage of scalability. The main disadvantages of high-pressure homogenisation for both hot and cold methods are associated with the use of high energy dispersion process. For the hot homogenisation heat-induced drug degradation and drug distribution in the aqueous phase during homogenisation are common drawbacks. While disadvantages of cold homogenisation are usually due to larger particles size with broad distributions.[102,115,182]

1.5.2.3.2 Solvent injection/nanoprecipitation method

The solvent injection method was first reported by Schubert *et al.* in 2003.[179] In this method, the lipid, and the hydrophobic drug are dissolved in a water miscible solvent (e.g. acetone, isopropanol, methanol or ethanol). The organic phase is then injected into a stirring aqueous phase made of a surfactant solution. The nanoprecipitation is based on the concept of reducing the quality of the solvent that the lipid and/or drug are soluble in. Such change in the quality of the media can be produced by altering the pH, salt addition, or addition to a non-solvent. The precipitation includes 5 steps, 1) injection of the hydrophobic phase into the aqueous phase, 2) supersaturation, 3) precipitation and nucleation, 4) growth and nanoparticles formation and 5) stabilisation in the presence of a surfactant with appropriate concentration, or coagulation in case of the absence of the surfactant,[183] see Figure 1.14.

For SLNs, and NLCs, upon injection, the water miscible solvent diffuses from the droplets into the aqueous phase increasing the concentration of the lipid within the injected droplets. As a result, the droplets shrink and decrease in size, creating areas of localised supersaturation made of the lipid and/or drug, where more solutes are present above the equilibrium concentration. Following the supersaturation phase, nucleation step starts to regain the thermodynamic stability, it is initiated when the solutes reach critical concentration, the interfacial turbulence caused by supersaturation resulted in the formation of the initial nuclei, which increase in size until they reach a critical size, after which the nuclei are not susceptible to dissolution. The nucleation usually stops, when the concentration of the free solutes, which are the lipids/and or drugs in our case is below the critical supersaturation concentration. Following the nucleation step, the nanoparticles are formed by deposition of the free solutes from the bulk solution to the surface of the nuclei which are integrated into the matrix of the nuclei. In the absence of a proper stabiliser for the formed nanoparticles, those nanoparticles will be attracted towards each other leading coagulation.[179,8]

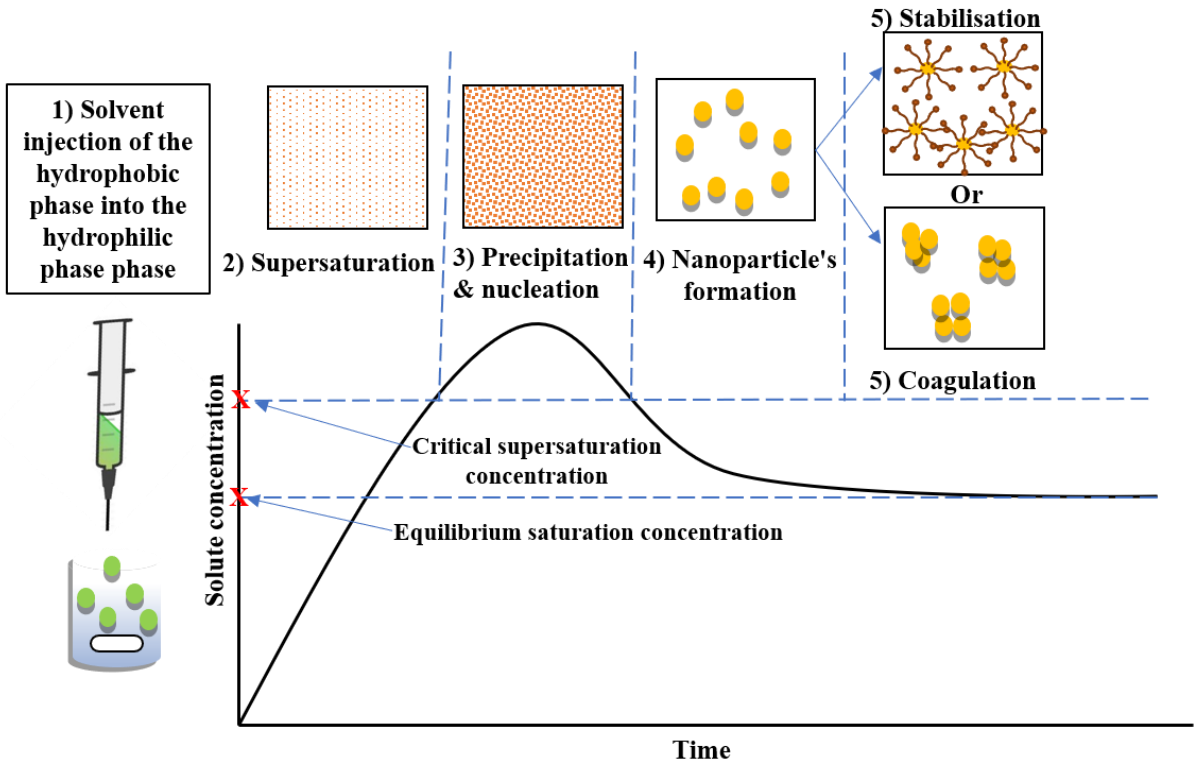

Figure 1.14 Schematic representation of the different steps of nanoprecipitation by solvent injection. These steps are: 1) injection of the hydrophobic phase into the aqueous phase, 2) supersaturation as the concentration of the lipid increase above the saturation concentration, 3) precipitation and nucleation as the concentration of the lipid increases beyond the critical supersaturation concentration, 4) growth and nanoparticles formation as the concentration of the lipid in the bulk solution decreases below the critical supersaturation concentration and 5) stabilisation in the presence of a surfactant with appropriate concentration, or coagulation in case of the absence of the surfactant.

The nanoprecipitation method for the synthesis of lipid nanoformulations has been reported in the literature. Dong *et al.* successfully synthesised SLNs loaded with fenofibrate as a model drug with average particle size below 200 nm. In this method, acetone was used as the water-miscible organic solvent, while Gelucire 44/14 was used as the solid lipid and d-alpha tocopheryl polyethylene glycol 1000 succinate was used a surfactant.[184] In a comparative study between SLNs and NLCs, Hu *et al.* studied the different preparation parameters for solvent injection method.[149] In that study stearic acid was used as a solid lipid in the case of SLNs or in combination with oleic acid in the case of NLCs. In both types of formulations, a combination of acetone and ethanol were used as the water miscible organic solvent which was heated to 70 °C, and sodium dodecyl sulphate was used as a surfactant. In case of NLCs, the incorporation of oleic acid led to a higher encapsulation efficiency of clobetasol propionate in comparison to SLNs, and the drug loading increased along with the increase of the oleic acid content. On the other hand, the size decreased upon increasing the oleic acid percentage.[149]

DSC results showed significant decrease in the crystallinity when oleic acid was incorporated.

For NEs, the solvent injection of the liquid oil in the hydrophilic phase is a considered a low-energy emulsification technique, where a spontaneous emulsification of the oil occurs upon addition of the oil/water-miscible organic solvent mixture into the surfactant solution. The liquid/liquid nucleation occurs as the organic solvent diffuses towards the hydrophilic phase, leading to oil supersaturation and a cloudy NEs are formed.[140]

NEs synthesised using solvent injection has been reported in the literature. For example, carbamazepine loaded NEs were synthesised using spontaneous emulsification for parenteral administration. In that method, castor oil or a mixture of castor and MCT, and lipophilic emulsifiers like soybean lecithin were dissolved in a water miscible organic solvent made of acetone and ethanol (1:1). The oily phase was added slowly to the stirring hydrophilic phase that contained polysorbate 80 as a hydrophilic stabiliser. The resultant NEs had a mean droplet size of 150 nm and a zeta potential of -40 mV. The drug encapsulation efficiency was around 95%, which was released over 11 hours period.[185]

The mechanism of the formation of LPHNs by single-step solvent injection method is slightly different form the solvent injection of the previously mentioned lipid nanocarriers like SLNs, NLCs and NEs. In this method, a solution of the polymer (such as PLGA) and/or drug is prepared with a water miscible organic solvent. This solvent is then added dropwise into the preheated stirred aqueous phase. This hydrophilic phase is made of a surfactant and phospholipid dissolved in 4% ethanol solution; the ethanol helps the dissolution of the phospholipid in water. The solvent injection leads to the precipitation of the polymer into nanoparticles, which is simultaneously covered by the phospholipid, where the hydrophobic moieties of the lipid are directed towards the polymeric cores and the hydrophilic heads are directed towards the aqueous phase, resulting in the formation of LPHNs.[156,166] The phospholipid molecules do not self-assemble to form vesicular structure prior the addition of the PLGA solution, as the hydrophilic phase containing the phospholipids is usually heated to 60 °C, which is above the gel-to-liquid transition temperature of most phospholipids. This condition ensures a homogenously dispersed liquid crystalline phase, so the phospholipids molecules are not close enough to each other to self-assemble into vesicular structure.[186]

The advantages of solvent injection method over other production methods is the simplicity of

the technique and fast production process without the need of complicated equipment,[102,103,187] ease of handling, fewer steps, low cost and no harsh synthesis conditions as high pressure. The solvent injection technique is considered as a convenient production technique for many nanocarrier systems including lipid and polymeric nanoparticles.

1.5.2.3.2.1 Challenges of the solvent injection technique

Solvent injection has been reported in the synthesis of SLNs,[179,188] NLCs, [188,189] NEs[133] and LPHNs.[190] Although solvent injection is generally considered a simplified and more gentle method compared to high energy methods like high pressure homogenisation, some of the solvent injection techniques reported in the literature require many further steps, such as adding of hydrochloric acid to help the precipitation of the NLCs, the requirement of a pre-emulsion formation or using of a homogeniser after the solvent injection step.[188,189,151] Jain *et al.*,[189] reported a solvent diffusion method that involved multiples steps as follows: a mixture of the tristearin and oleic acid were dissolved in acetone using a water bath at 40 °C. The hydrophobic mixture was then injected quickly into a preheated hydrophilic phase which is composed of Tween 80 and enoxaparin as the drug moiety dissolved in purified water. The resultant mixture was placed on a magnetic stirrer plate for 60 minutes. The mixing of the two phases led to the formation of a pre-emulsion, which was then cooled at room temperature to obtain the NLCs. The pH of the NLCs dispersion was adjusted to 1.2 by adding hydrochloric acid followed by centrifugation to initiate particles aggregation which were then centrifuged to help obtaining precipitated NLCs. The precipitate was washed few times. These complicated multiple steps usually make the synthesis method more time consuming and less potentially to introduce more variables to the process. Additionally, the production of NEs by solvent injection typically requires the use of two types of emulsifiers, a lipophilic emulsifier [185] and a hydrophilic emulsifier. Sometimes glycerol is added to the aqueous phase to adjust the isotonicity.[185] As such, the development of a simple solvent injection technique, with fewer steps and surfactants would be considered an advantage.

1.5.2.4 Drying of lipid nanodispersions

For many colloidal systems, liquid formulations present a challenge as they are thermodynamically unstable and particle aggregation and settling may occur over time.[191,192] Development of commercial nanoparticles requires the stability of the formulations during

storage and shipment, this can be achieved by the removal of water and other solvents from nanoparticles liquid dispersions.[193] However the removal of the liquids from the nanodispersions requires special techniques like spray-drying or freeze-drying which are time consuming, and may lead to particle aggregation, making the formulations difficult to re-disperse. Therefore, optimisation of the drying techniques of the nanoformulations must be considered to ensure the maintenance of the physicochemical properties of such formulations and avoid the leakage of the encapsulated drugs.[112,194]

1.5.2.4.1 Spray drying

Spray drying is a well-known drying technique that has been extensively used in the food and pharmaceutical industries since the early 20th century. In spray drying, the dry product is produced through several steps. In this process, a liquid feed is converted to fine droplets through atomisation by passing through a nozzle under pressure, the solvent is then evaporated by using hot drying gas.[195] In comparison to freeze drying, spray drying have the advantages of being fast, simple, less expensive, and suitable for mass production. On the other hand, for lab scale, the yield is far less, as there is a relatively high loss of the final dry product on the walls of the drying chambers.[196] Also the production of dry formulations in the nano-size range depends on the forces of atomisation, and usually spray drying produce particles with higher Z-average diameter and wider size distribution in comparison to freeze-drying.[196]

1.5.2.4.2 Freeze-drying

Freeze-drying or lyophilisation was introduced as a dehydration technique in the 1940s, and has been since widely used for the stabilisation of various pharmaceutical products.[197–199] Freeze-drying may enhance the stability of the liquid nanoparticles dispersions by the prevention of hydrolysis reactions, Ostwald ripening and settling. It also allows the incorporation of these nanoformulations into capsules and tablets. Unlike spray drying, freeze-drying have the capability of producing smaller particles, and the ability of drying the aqueous dispersions in the final container, which limit both contamination and loss, and it is therefore suitable for the production of sterile products.[200] That suggests that freeze-drying is more suitable for drying of lipid nanocarriers in a lab-scale.

Freeze-drying is based on the sublimation principle,[201] where water is converted from the solid state which is ice crystals to the gaseous state in form of vapor under vacuum, without passing through the liquid state.[202] Sublimation of water takes place at temperatures and pressures below the triple point, i.e. 0.001 °C and 0.006 atmospheres, respectively, see Figure 1.15. The aqueous material to be dried is frozen first and then heated under vacuum so that the frozen liquids are sublimed giving dried product.

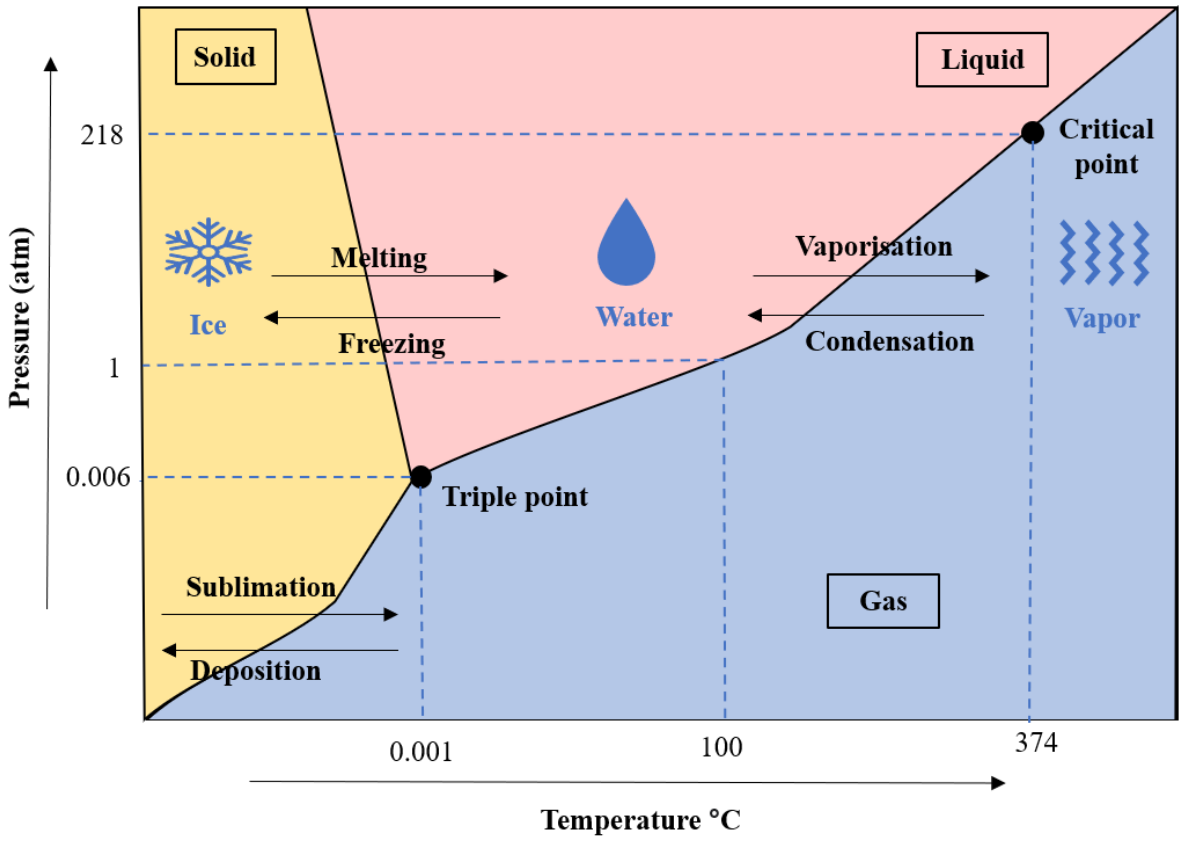

Figure 1.15 Typical phase diagram of water under pressure. Water present in three different states: 1) solid in the form of ice crystals, 2) liquid in the form of water droplets and 3) gas in the form of water vapor. For successful freeze drying, sublimation of water from the solid state directly to the gaseous state without converting to the liquid state is essential. The sublimation takes place at pressure and temperature below the triple point (i.e.,0.001 °C and 0.006 atmospheres).

The freeze-drying process includes several steps: freezing (solidification), primary drying (ice sublimation), and finally secondary drying (moisture desorption).[203,204,194] The freezing step is the most crucial step in the lyophilisation of nanoparticles. The freezing stage of a formulation starts with ice nucleation followed by ice growth, in this stage most of the water content of the formulation solidify into ice crystals through a matrix of crystalline solutes.[203,204] Multiple phases are formed during this step. The ice forms one phase, while the other phase consists of

the nanoparticles, free active ingredients, cryoprotectants and other additives.[205] The rate of freezing can determine the size of the final freeze-dried particles and their stability. Freezing can be done rapidly by dipping in liquid nitrogen or slowly in a freezer over few hours. Faster freezing rate help maintaining the original particle size of nanosuspensions as it leads to the formation of smaller crystals.[193] It has been shown that the size of the frozen crystals determines the size of the final freeze-dried particles. Fast freezing has also been shown to lead to an enhancement of the redispersion of the particles.[201] Therefore, dipping of the samples in liquid nitrogen is preferred as a freezing technique. In the second stage which is primary drying, heat is transferred to the frozen solution often from a heated shelf. Ice sublimes into water vapour which then passes through the dried segment of the sample and to the sublimation front. Water vapour is then collected to a chamber and condensed by the condenser. At the end of this stage a porous mass is formed, the porous spaces represents the ice crystals that have sublimed.[197] While in the secondary drying stage, which is the last stage, the bound water that did not form crystals during freezing is removed.[197]

Nanoparticles are fragile structures and may not withstand the stress caused by freeze-drying.[206] Therefore, cryoprotectants are usually used to limit nanoparticles aggregation and prevent structural damage caused by the harsh conditions of reduced temperature and pressure during freeze-drying,[206,207,193] see Figure 1.16. Sugar and polymeric cryoprotectants are considered the main categories of cryoprotectants used in the freeze-drying of nanoformulations. Sugars act as cryoprotectants for nanoformulations by three different mechanisms: 1) The formation of a protective capping layer around the nanoformulations, this layer is sustained by formation of hydrogen bonds between the polar functional groups at the surface of the SLNs and the hydroxyl groups of the sugar. 2) The ability to form glassy matrices when they are frozen below their glass transition temperatures (T_g).[206] Glass transition temperature can be defined as the temperature at which transition from a rigid to more a flexible state takes place. The glass coating on nanoparticles prevents their aggregation after water removal, as they protect them from mechanical stresses of ice crystals.[208] Ice sublimation has to be done at or below the T_g of the cryoprotectant, as higher temperatures will lead to ice melting and particle aggregation.[199] 3) Particle isolation hypothesis which suggests that during the freezing phase, carbohydrates especially disaccharides, due to their low surface tension, have the ability to keep individual nanoparticles separated.[193] Dextrose is an example of monosaccharide,[209] sucrose and trehalose are examples of disaccharides,[210] while maltodextrin

is an example of polysaccharides, and mannitol is an example of sugar alcohols, all used as cryoprotectants for nanoparticles.[197]

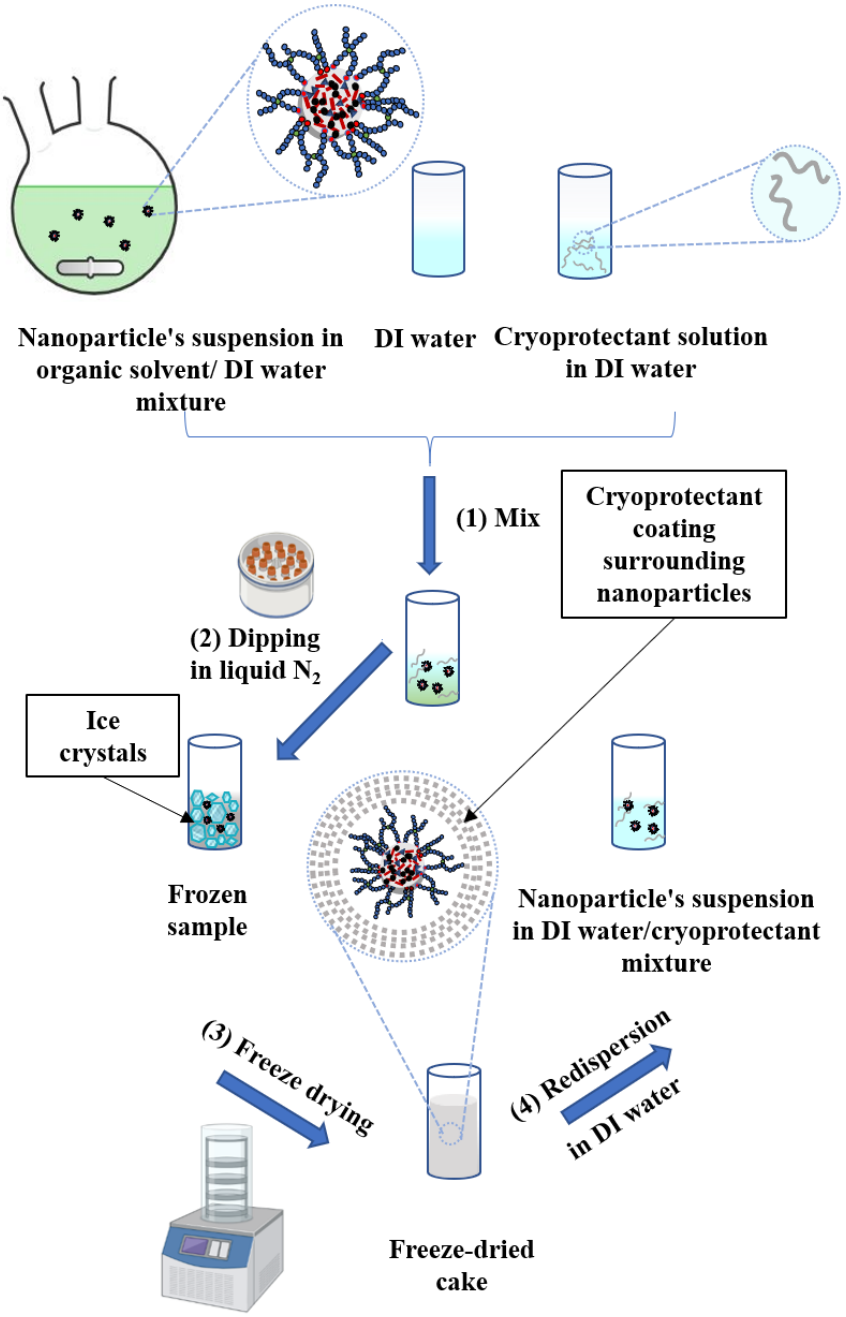

Figure 1.16 Schematic illustration of the freeze-drying steps of nanoparticles suspension using cryoprotectants. These steps are: 1) mixing of the nanoparticle's suspension, DI water and cryoprotectant solution in a single vial, 2) freezing of the samples by dipping in liquid nitrogen, 3) placing the frozen samples in the freeze dryer for few days until the complete removal of the water and/or organic solvent and 4) redispersion of the freeze-dried powdered material in DI water prior to administration using manual shaking or a vortex.

Polyethylene glycol (PEG) is one of the most commonly used polymeric cryoprotectants. PEG is a semicrystalline polymer and can show high degree of disorder.[211] PEG can act as a

cryoprotectant by three mechanisms: 1) Organising their chains in the form of lamellae in the crystal lattice.[192] 2) Acting as a collapse temperature modifier, where it increases the temperature required for the collapse of the final freeze-dried product.[197] 3) Stabilising the colloidal systems by surface adsorption and functioning as bulk stabilisers.[205]

The molecular weight of the used PEG is an important parameter, PEG with higher molecular weight (M_n 4000) have been shown to lead to the aggregation of NLCs with a significantly poor re-dispersity in water in a study by Varshosaz *et al.*[201] In their study, the size of NLCs increased to more than 3 microns and the zeta potential was as low as 3 mV which indicated poor re-dispersibility ability. Although other studies showed that increasing the molecular weight of PEG did not affect the size of nanoparticles and that the concentration was a more important factor. Varshosaz *et al.* recommended the use of PEG 2000 as it lead to lower viscosity of the system.[192] Umerska *et al.* concluded that increasing PEG 2000 concentration form 1% up to 5% resulted in the enhancement of the nanoparticles re-dispersibility after freeze-drying, and PEG 2000 was found to be more effective as a cryoprotectant than trehalose.[192] On the other hand, Moretton *et al*. attributed the inability of PEG at high molecular weight (i.e. M_n 3350, 6000 and 10000) to act as efficient cryoprotectants, to their increased viscosity compared to PEG 2000.[205] At high viscosity when high molecular weight PEG was used, the freezing rate will be limited causing particle aggregation before matrix formation.[205] Low molecular weight PEG would also lead to increasing of the drug loading as less excipients would be used.

Therefore, it is interesting to test freeze-drying as a technique that would provide stable powdered lipid nanocarriers. Successful freeze-drying of nanoparticles should maintain the primary physical and chemical properties of the nanoparticles dispersions, should yield fluffy cakes with acceptable appearance, should be reconstituted with water at a relatively short time and should not affect the particle size or particle size distribution of the original formulations.[197] Although the use of cryoprotectants has been reported to provide sufficient stability of lipid nanocarriers and other nanoparticle systems, the optimisation of the freeze-drying parameters of nanoformulations remains challenging. The process requires analysing wide range of cryoprotectants and varying the concentration of both cryoprotectants and nanoparticles.

1.6 Objective of the research

The overall aim of this project was to create an oral drug delivery system for darunavir (DRV)/ritonavir (RTV) (8:1) for the treatment of HIV. RTV is used as a booster for DRV to enhance its bioavailability, and is given as a daily dose of 800 mg DRV with 100 mg RTV.[18] In this work we aim to decrease the dose required of both drugs by loading them into various lipid nanocarriers with keeping the 8:1 ratio of DRV/RTV. The choice of lipid nanocarriers over other drug delivery systems was because they have the advantage of targeting HIV drugs to the lymphatic system, increase their bioavailability and decrease side effects.[15] This research project had four main goals: 1) Synthesis of various stable lipid nanocarriers including SLNs, NLCs, NEs and LPHNs using solvent injection method. 2) Optimisation of the formulations to obtain high drug loading of DRV/RTV (8:1). 3) Drying of the liquid nanodispersions using freeze-drying to obtain dry powdered formulations to enhance their stability. 4) Test the behaviour of the optimum formulations across triple cell culture module to test the effect of those formulations on the bioavailability of the loaded drugs.

This thesis is made of four experimental chapters, each with standalone experimental sections.

In chapter 2, a comparative study between SLNs, NLCs and NEs was carried out to examine the effect of the three different formulations on the Z-average diameter, morphology, crystallinity, stability, drug loading and drug release. The first focus was to optimise the solvent injection method to obtain lipid formulations in the submicron range, the optimisation parameters included varying the type of surfactants and lipids, and their concentrations, varying the temperature of the hydrophobic phase. Finally, the choice of the type of the water miscible organic solvent, where a solvent that have the capability of dissolving the drug/lipid mixture and at the same time evaporate at room temperature was required.

In chapter 3, the aim was to synthesise high drug-loaded SLNs (HDL-SLNs) with more than 50% w/w drug-loading using solvent injection method. For that purpose, an amphiphilic branched oligo(ethylene glycol) methyl ether methacrylate (OEGMA) polymer with dodecyl end group functionality was synthesised using atom transfer radical polymerisation (ATRP). The polymer was characterised and tested as stabiliser for HDL-SLNs. The rationale behind using this polymer as stabiliser for SLNs was based on the fact that branched polymers have

multiple points of contact with the lipid cores and thus offer better coverage and stabilisation for SLNs.

Chapter 4 focussed on the optimisation of the freeze-drying of the HDL-SLNs formulations. The aim of this work was to maintain the particles size and particles size distribution after freeze-drying, and for that target, various cryoprotectants were tested, both carbohydrate and polymeric with various concentrations. After establishing the freeze-drying parameters, the formulations were tested across triple cell culture to test bioavailability.

In contrary to the lipid formulations mentioned above where the cores of the particles were made of lipids, in chapter 5 the effect of having the lipid as a monolayer surrounding polymeric cores to form LPHNs was investigated. The optimum ratio between the phospholipid as electrostatic stabiliser and Brij 78 as a bulk stabiliser to have stable formulations with enhanced oral bioavailability was investigated. The effect of drug loaded LPHNs whether in the form of nanodispersions or freeze dried on the bioavailability was carried out across triple culture model.

Chapter 2

A Comparative Study of Solid Lipid Nanoparticles, Nanostructured Lipid Carriers and Nanoemulsions for a Dual Drug Delivery of Darunavir and Ritonavir for the Treatment of HIV

2.1 Introduction

In this chapter, a comparative study of the three lipid formulations SLNs, NLCs and NEs was carried out to determine the optimum lipid-based nanoformulation for DRV/RTV (8:1) loading. There have been a fewer comparative studies in the literature that included those three lipid nanocarriers.[212–214] However in most of these studies high pressure homogenisation was used as the synthesis technique. There have not been comparative studies that involved the three lipid nanoformulations loaded with antiretroviral drugs for the treatment HIV. Additionally, there have not been any reported comparative studies between the three nanocarriers that used solvent injection as a synthesis technique. The solvent injection method is based on the precipitation of the dissolved lipid and/or drugs from the hydrophobic phase rapidly into the aqueous phase.[179] The solvent injection method offers advantages for the synthesis of nanoparticles like the use of a simple low cost equipment, ease of handling, few steps, and no harsh synthesis conditions as high pressure, therefore it has been chosen as the synthesis method in this study.

2.2 Chapter objectives

The main objective of this chapter was focussed on a comparative study between SLNs, NLCs and NEs by solvent injection method, and understanding the different factors affecting particles size and stability. To optimise a reproducible method that produce stable formulations in the submicron range, and have the highest possible drug loading of DRV/RTV (8:1), different experiments were carried out as follows:

Investigation of lipid solubility- In the solvent injection method the lipid must be completely soluble in the water miscible organic solvent. As the solubility of the solid lipids in the organic solvent can be challenging, optimisation of several variables was carried out to ensure complete dissolution of the lipid in the hydrophobic phase. Among these variables were: type of both the solid lipid and the water miscible organic solvent, concentration of the lipid and the drug mixture in the hydrophobic phase, and the temperature of the hydrophobic phase. If the lipid e.g., Compritol 888 ATO® was not soluble in the water miscible organic solvent e.g., ethanol/acetone 1:1 v/v at room temperature, the hydrophobic phase was heated, and the method was called “hot solvent injection method”. On the other hand, when the solid lipids e.g., Imwitor® 900 K and Dynasan®114 and Dynasan®118 were soluble in tetrahydrofuran (THF) at room temperature, the hydrophobic phase was not heated, and the method was called

"cold solvent injection method". The solubility of the soybean oil as a liquid lipid was less of an issue, it was soluble in all the chosen solvents both at room temperature and heated.

Surfactant selection- Surfactants are key components in the formation of nanoformulations, they surround the lipid cores in the three formulations and provides the colloidal stability to the system. By maintaining the suitable hydrophilic lipophilic balance (HLB), and correct ratios between different excipients, the surfactant help keeping the particles in the nanosized range. For the hot solvent injection method, Tween 80 was used as a surfactant and the effect of the surfactant concentration on the particle size of both SLNs and NEs was investigated. On the other hand, in the cold solvent injection method, the concentration of the surfactant was kept constant and the effect of the type of surfactant on the particle size of both blank and drug-loaded SLNs, NLCs and NEs was investigated. The two surfactants used in the cold solvent injection study, were Tween 80 and Brij 78 at a concentration of 1% w/v. Both surfactants have similar HLB (~15), so the effect of HLB can be excluded, and the effect of the surfactant structure can rather be studied. Tween 80 has been used as a surfactant in this study, as it is a safe non-ionic surfactant that provides steric stabilisation of different colloidal drug delivery systems.[215] While, Brij 78 (polyoxyethylene 20 stearyl ether) was specifically used as surfactant for solid lipids such as Imwitor® 900 K (glycerol monostearate 40–50%), Dynasan®114 (glyceryl trimyristate), and Dynasan®118 (glyceryl tristearate) to study the compatibility concept between the surfactant and the solid lipid as both the surfactant and the mentioned lipids are derivatives of stearic acid.

Drug loading studies- After optimising the blank formulations, the drug loading studies were carried out to investigate the highest drug loading that could be achieved. Stability studies in simulated gastric fluid (SGF) at pH 1.2 and phosphate buffered saline (PBS) at pH 7.4 were carried out to determine suitability for oral dosing. The morphology of the optimised formulations was tested using scanning electron cryomicroscopy (CryoSEM). The encapsulation efficiency and drug release were measured using radiometric analysis, while the crystallinity of the formulations was tested using differential scanning calorimetry (DSC) analysis.

2.3 Materials and Methodology

2.3.1 Materials

HPLC grade acetone, ethanol (99% v/v), tetrahydrofuran (THF) (99% v/v), were purchased from Thermo Fischer Scientific, Leicestershire, UK. Imwitor® 900 K (≥99%), Dynasan®114 (≥99%), and Dynasan®118 (≥99%), were purchased from Cremer Oleo GmbH & Co. KG, Hamburg, Germany. Compritol 888 ATO® (glyceryl behenate) were kindly provided by Gattefossé, France. Soybean oil, Brij 78 (M.W. 1151 g/mol), Tween 80 (≥99%) (M.W. 1310 g/mol), DRV (≥98% (HPLC) and RTV (≥98% (HPLC) were all purchased from Sigma–Aldrich, Irvine, UK. All materials were used without further purification.

2.3.2 Methodology

2.3.2.1 Synthesis of blank SLNs, NLCs and NEs by hot solvent injection method

In the hot solvent injection method, the hydrophobic phase was composed of different lipids and 1 mL of water miscible organic solvent placed in a 4 mL vial, the mixture was heated in an oil bath at 70 °C for 2 minutes to ensure complete dissolution of the lipids in the solvent used, the final lipid concentration range was 2-10 mg/mL. On the other hand, the hydrophilic phase was made of Tween 80 solution in deionised (DI) water at room temperature with concentrations of 1, 2.5 or 5% w/v. The heated hydrophobic mixture was then injected rapidly using a hypodermic needle (21 g, 50 mm) into a 6 mL hydrophilic solution stirring at 200 rpm placed in a 14-mL vial. The lipid nanoparticles were formed instantaneously, as the water miscible organic solvent diffused towards the continuous aqueous phase leading to the precipitation of the lipids which were surrounded by the surfactant molecules to give colloidally stable nanodispersions. The nanodispersions were left to stir for 48 hours in a fume hood to allow the organic solvent evaporation. The lipids used in this experiment were Compritol 888 ATO® as a solid lipid, soybean oil as a liquid lipid to form SLNs and NEs, respectively. In case of NLCs a combination of the solid and liquid lipids was used at three different solid lipid/liquid lipid (S/L) ratios; 9:1, 7:3 and 5:5. The water miscible organic solvent used was made of a mixture of ethanol/acetone solution at 1:1 v/v.

2.3.2.2 Synthesis of blank and drug loaded SLNs, NLCs and NEs by cold solvent injection method

In the cold solvent injection method, the hydrophobic phase was prepared by dissolving different lipids in 1 mL of a water miscible organic solvent in a 4 mL vial, to give a final concentration of the lipid in the hydrophobic phase of 2-10 mg/mL. However, in this technique the hydrophobic phase was not heated, as the lipids were soluble in the water miscible organic solvent at room temperature. The hydrophilic phase was made of 6 mL of 1% w/v Tween 80 or Brij 78 solutions. The hydrophobic mixture was then injected rapidly using a hypodermic needle (21 g, 50 mm) into hydrophilic solution stirring at 200 rpm placed in a 14 mL vial. The long hypodermic needle was used, so that the tip of the needle would be above the surface of the solution we inject in. The lipid dispersions were left to stir for 48 hours to allow the evaporation of the water miscible organic solvent. The lipids used in this experiment were Imwitor® 900 K, Dynasan®114 or Dynasan®118 as solid lipids, soybean oil as a liquid lipid to form SLNs and NEs, respectively. In case of NLCs a combination of the solid and liquid lipids was used at three different S/L ratios; 9:1, 7:3 and 5:5. The water miscible organic solvent used was THF.

The drug-loaded formulations were prepared by cold solvent injection method as explained above, where the drug mixture DRV/RTV (8:1) was added to the hydrophobic phase with a lipid concentration in the hydrophobic phase of 4 mg/mL. Two batches of formulations were synthesised: one batch was synthesised using Tween 80 as a stabiliser, while in the other batch, Brij 78 was used. For each batch three different mass percentage of DRV/total lipid were tested 5, 10 and 20% w/w. Total lipid referred to the mass of all lipids present in the formulations whether solid or liquid.

The samples were named with the following approach:

SLNs-4 and NEs-4 referred to SLNs and NEs with using specific lipid concentration in the hydrophobic phase, in this case was 4 mg/mL, respectively (as denoted by the number after the abbreviation). The same naming method was applied to other concentrations like 10 mg/mL.

NLCs (9:1), NLCs (7:3) and NLCs (5:5) referred to NLCs with solid lipid to liquid lipid ratio (S/L) of 9:1, 7:3 and 5:5, respectively. For example, NLCs (9:1) would have 90% solid lipid and 10% liquid lipid.

NLCs (9:1)-4 refers to NLCs with S/L of 9:1 and using specific lipid concentration in the hydrophobic phase, in this case was 4 mg/mL (as denoted by the number after the abbreviation). The same naming method was applied to other concentrations and ratios.

SLNs-Tween 80 and SLNs-Brij 78 referred to SLNs synthesised using Tween 80 and Brij 78 as surfactants, respectively (as denoted by the name of the surfactant after the abbreviation). The same naming method was applied to other formulations like NEs.

SLNs-Imwitor® 900 K, SLNs-Dynasan®114 and SLNs-Dynasan®118, referred to SLNs synthesised using Imwitor® 900 K, Dynasan®114 and Dynasan®118 as solid lipids, respectively.

2.3.2.3 Characterisation of the size and morphology of SLNs, NLCs and NEs

2.3.2.3.1 Size measurement by DLS

Z-average diameter and PDI of SLNs, NLCs and NEs were determined by dynamic light scattering (DLS) using the Malvern Zetasizer Nano ZS (Malvern Instruments, Malvern, UK) with a detector positioned at 173°. The average particle size and PDI of all three-lipid formulations were determined without dilutions at 25 °C. Each size measurement was an average of three runs, with an equilibration period of 1 minute. The concentration range of the measured samples was 0.3- 1.6 mg/mL. The DLS measurements were carried out at two different time intervals for all formulations: day 1, which was the same day of the synthesis, within 1 hour of preparation to determine the initial size of the particles and determine the efficiency of the solvent injection technique in producing nanosized particles. Day 3, which was the third day after the synthesis to measure the DLS data of the particles after the organic solvent was allowed to evaporate, where samples were left to stir in a fume hood on a multipoint stirrer plate at 300 rpm. For drug-loaded formulations, in addition to the DLS measurements on day 1 and 3, measurements were also carried out on day 7, which was a week after the synthesis to determine the short-term stability of the particles.

2.3.2.3.2 Determination of the size and morphology by scanning electron cryomicroscopy (CryoSEM) imaging

Specimens prepared by freezing a small volume of sample between two brass rivets, which were plunged into slushed liquid nitrogen. Rivets transferred to a brass loading shuttle under liquid nitrogen and transferred under a nitrogen atmosphere to a preparation stage cooled to -120 °C. The anti-contaminator in the preparation stage was kept at -180 °C. A fracture surface was created in frozen specimen by pushing-off the upper rivet from the one held in the shuttle (using a liquid nitrogen cooled knife). The specimens were sublimed at -90 °C for 5 minutes to remove water, to a depth of a few microns, revealing the nanoparticles. The fracture surface was coated with Pt in the preparation chamber (PP3010 T Cryo-SEM Preparation System, Quorum Technologies, UK), to make it conductive, and specimen transferred to a cooled stage in the FIB/SEM (Tescan S8000G FIB/SEM with a Schottky emitter, Kohoutovice, Czech Republic) (at -130 °C, with an anti-contaminator held at -180 °C). The specimens were imaged using an in-chamber secondary electron detector (Everart Thornley) typically using 1.5keV or 5keV and a beam current of 10-30 pA. The samples tested were SLNs, NLCs (5:5) and NEs, prepared using a lipid concentration in the hydrophobic phase of 4 mg/mL. For samples prepared by hot solvent injection, Compritol 888 ATO® was used as the solid lipid, and Tween 80 with a concentration of 1% w/v was used as the surfactant solution. While samples prepared by cold solvent injection, Imwitor® 900 K was used as the solid lipid and Brij 78 with a concentration of 1% w/v was used as the surfactant solution. Soybean oil was used as the liquid lipid in both methods.

2.3.2.4 Differential scanning calorimetry (DSC) analysis

Prior to the DSC analysis, SLNs, NLCs and NEs dispersions were left to dry at room temperature for a week to remove all the water content. Bulk materials were tested as controls and that included: 1) Lipids: Compritol 888 ATO®, Imwitor® 900 K, and soybean oil, 2) Surfactants: Tween 80 and Brij 78 and 3) Drugs: DRV and RTV. The tested formulations were as follows: 1) blank SLNs, NLCs (9:1, 7:3 and 5:5) and NEs prepared by hot solvent injection at lipid concentration in the hydrophobic phase of 4 mg/mL using 1% w/v Tween 80 as a surfactant. 2) Drug-loaded SLNs, NLCs (9:1, 7:3 and 5:5) and NEs prepared by cold solvent injection at lipid concentration in the hydrophobic phase of 4 mg/mL using 1% w/v Brij 78 as a surfactant. The DSC analysis was carried out using model 25 DSC, (TA Instruments,

Wilmington, United States). Briefly, 4–5 mg of each sample was placed in Aluminium pans and sealed. Then the pans were placed under isothermal condition at 25 °C for 10 min. Linear heating rate was 10 °C/min from 10 to 150 °C under inert environment using the liquid nitrogen cooling accessory (TA Instruments, Wilmington, United States). An empty sealed pan was used as reference. The thermograms of the tested samples were recorded.

2.3.2.5 Measurement of drug release using radiometric analysis

Radiolabelled DRV containing formulations, analogous to the drug-loaded formulations as described in section 2.3.2.2 were formulated with the addition of tritiated [^{3}H]-DRV with a specific activity of 25 μCi/mg to the organic solvent phase, the DRV/RTV ratio was kept at 8:1. Formulations were prepared at a lipid concentration in the hydrophobic phase of 4 mg/mL, while 1% w/v Brij 78 was used as a surfactant. The mass percentage of DRV/total lipid was 10% w/w for SLNs and 20% w/w for NLCs (9:1, 7:3 and 5:5) and NEs. Entrapment efficiency (EE%) within the lipid nano-formulations were determined via liquid scintillation counting (LSC) analysis (Packard Tricarb 3100TR liquid scintillation counter). To determine the EE%, 0.4 mL of the lipid nano-dispersions with a concentration of 6-6.5 mg/mL was added to a centrifugal unit fitted with a 10,000 molecular weight cut-off (MWCO) filter and centrifuged at 14,000 revolutions per minute (rpm), for 60 minutes. Samples of the filtrate (3 × 100 μL) were taken to determine the free DRV which had crossed the filtration barrier. For the total DRV, samples of lipid nanosuspensions (3 × 100 μL) were taken without centrifugation, so they would have both the free and encapsulated DRV. The EE% was determined by the indirect method, according to Equation 2.1. While drug loading (DL%) was calculated according to Equation 2.2.

$$\mathbf{EE\%} = \frac{\mathbf{Total\ DRV\ mass - free\ DRV\ mass\ in\ the\ filtrate}}{\mathbf{Total\ DRV\ mass}} \times \mathbf{100}$$

Equation 2.1 Calculation of EE% of DRV, where the total DRV referred to the DRV present in the lipid nanoformulations without centrifugation, while free DRV referred to the DRV that passed through the filtration barrier after centrifugation using a spin filter.

$$\mathbf{DL\%} = \frac{\textbf{Total DRV mass} - \textbf{free DRV mass in the filtrate}}{\textbf{Total nanoparticles mass}} \times \mathbf{100}$$

Equation 2.2 Calculation of DL% of DRV, where the total DRV referred to the DRV present in the lipid nanoformulations without centrifugation, while free DRV referred to the DRV that passed through the filtration barrier after centrifugation using a spin filter. Total nanoparticles mass referred to the summation of the mass of the drug and the mass of the lipid.

To determine the mass of both the free and total radioactive DRV, the radioactivity of DRV had to be calculated first using the disintegrations per minute (DPM) data obtained by the LSC analysis according to Equation 2.3, where 10 mL of the scintillation cocktail were added to both the samples of the free and total DRV. The mass of radioactive DRV can then be calculated according to Equation 2.4.

$$\mathbf{DPM / 2.22\ x10^6 = Radioactivity\ (\mu Ci)}$$

Equation 2.3 Calculation of radioactivity of tritiated [^{3}H]-DRV using disintegrations per minute (DPM) data obtained by LSC analysis.

$$\mathbf{Radioactivity\ (\mu Ci) / Specific\ Activity\ (\mu Ci/mg) = Mass\ of\ DRV\ within\ the\ sample\ (mg)}$$

Equation 2.4 Calculation of the mass of radioactive DRV (mg) using the measured radioactivity.

Drug release behaviour from the lipid nanoformulations was quantified using a dialysis method as reported by Cauldbeck *et al.*[216] 1 mL of the lipid nano-dispersions at a concentration of 6-6.5 mg/mL was placed within a double-sided bio-dialyser fitted with 3.5 kDa MWCO membranes. Dialyses were conducted within sink conditions (1:100) in deionized water at 37 °C, 300 rpm. DRV release was monitored at set time points of 0.5, 1, 2, 3, 4, 5, 6, 7, 8 and 24 hours. Samples of the reservoirs (1 mL) were taken, and 10 mL of the scintillation cocktail were added. At each time point the bio-dialyser was removed from the reservoir and placed into fresh deionised water (100 mL). The radioactivity and masses of DRV released in 1 mL reservoir were calculated using Equation 2.3 and Equation 2.4, respectively. To calculate the mass of DRV released in 100 mL reservoir at any given time point, Equation 2.5 was applied. The cumulative mass of the DRV released at any given point will be equal to the summation of all the DRV masses released in 100 mL reservoir at that specific time point plus the DRV released at the previous time points. While the cumulative mass percentage of the DRV released was calculated according to the Equation 2.6. Samples of water (1 mL) were taken to

determine background of LSC, similarly to samples measuring drug release this was extrapolated to 100 mL.

$$\textbf{Mass of DRV within the 1 mL sample (mg) x 100 = Mass of DRV within the 100 mL reservoir (mg)}$$

Equation 2.5 Calculation of the mass of radioactive DRV (mg) in 100 mL reservoir.

$$\textbf{Cumulative drug release\%} = \frac{\textbf{Cumulative drug mass (mg)}}{\textbf{Mass of encapsulated drug (mg)}} \times \mathbf{100}$$

Equation 2.6 Calculation of the cumulative drug release% at any given time point, where the cumulative drug mass is the summation of all the DRV masses (mg) released in 100 mL reservoir at that specific time point plus the DRV released at the previous time points. While the encapsulated drug was calculated by the subtraction of the free drug mass (mg) from the total drug mass (mg).

Statistical analysis

One-way ANOVA was adopted as a statistical analysis tool for testing different lipid formulations in both EE% and drug release experiments using Microsoft Excel spreadsheet software, version 2105. The data difference was considered to be statistically significant when the p-value was less than 0.05. Number of samples (n) was 3.

2.4 Results and Discussion

Lipid nano-formulations were synthesised using hot and cold solvent injection methods. The purpose of this study was to determine how varying the synthesis parameters would affect the particle size, morphology, and crystallinity of the produced lipid formulations, see Figure 2.1. DLS was used as the main characterisation technique for the particle size. Measuring the particle size is crucial, as it is one of the main factors that affect the intestinal uptake and clearance of the nanoformulations, Faheim *et al.* have suggested that the appropriate particle size for intestinal transport is below 300 nm.[141] Additionally, characterising nanoparticle size provides insight into whether the process of nanoprecipitation has been successful. Optimised formulations were tested for drug loading and drug release.

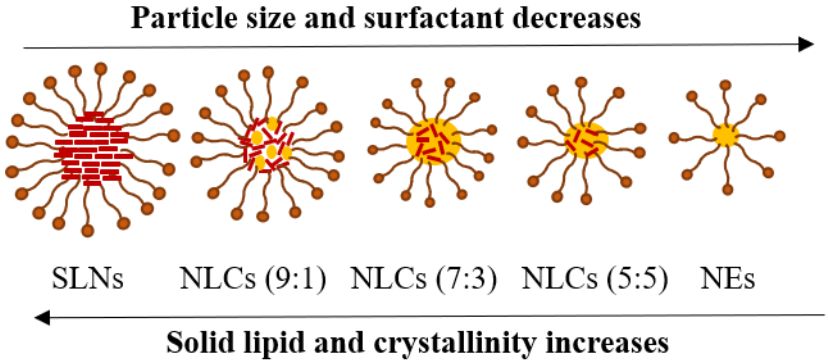

Figure 2.1 Diagram showing the composition of different lipid formulations; SLNs, NLCs (9:1, 7:3 and 5:5) and NEs. Increasing liquid oil content, resulted in smaller particles which required less surfactant. Increasing solid lipid content resulted in increasing the crystallinity and size of the particles.

2.4.1 Hot solvent injection

2.4.1.1 The effect of varying the synthesis parameters on the DLS data of blank SLNs, NLCs and NEs synthesised by hot solvent injection method.

Blank SLNs, NLCs (9:1, 7:3 and 5:5) and NEs were synthesised using hot solvent injection method, see Figure 2.2. The tested synthetic parameters included varying the lipid concentration in the hydrophobic phase, type, and physical state of lipid whether solid or liquid, different S/L ratios for NLCs and the concentration of the surfactant. All the parameters were kept constant, and one parameter was varied at a time to allow studying the effect of each variable on the size and the PDI of the particles.

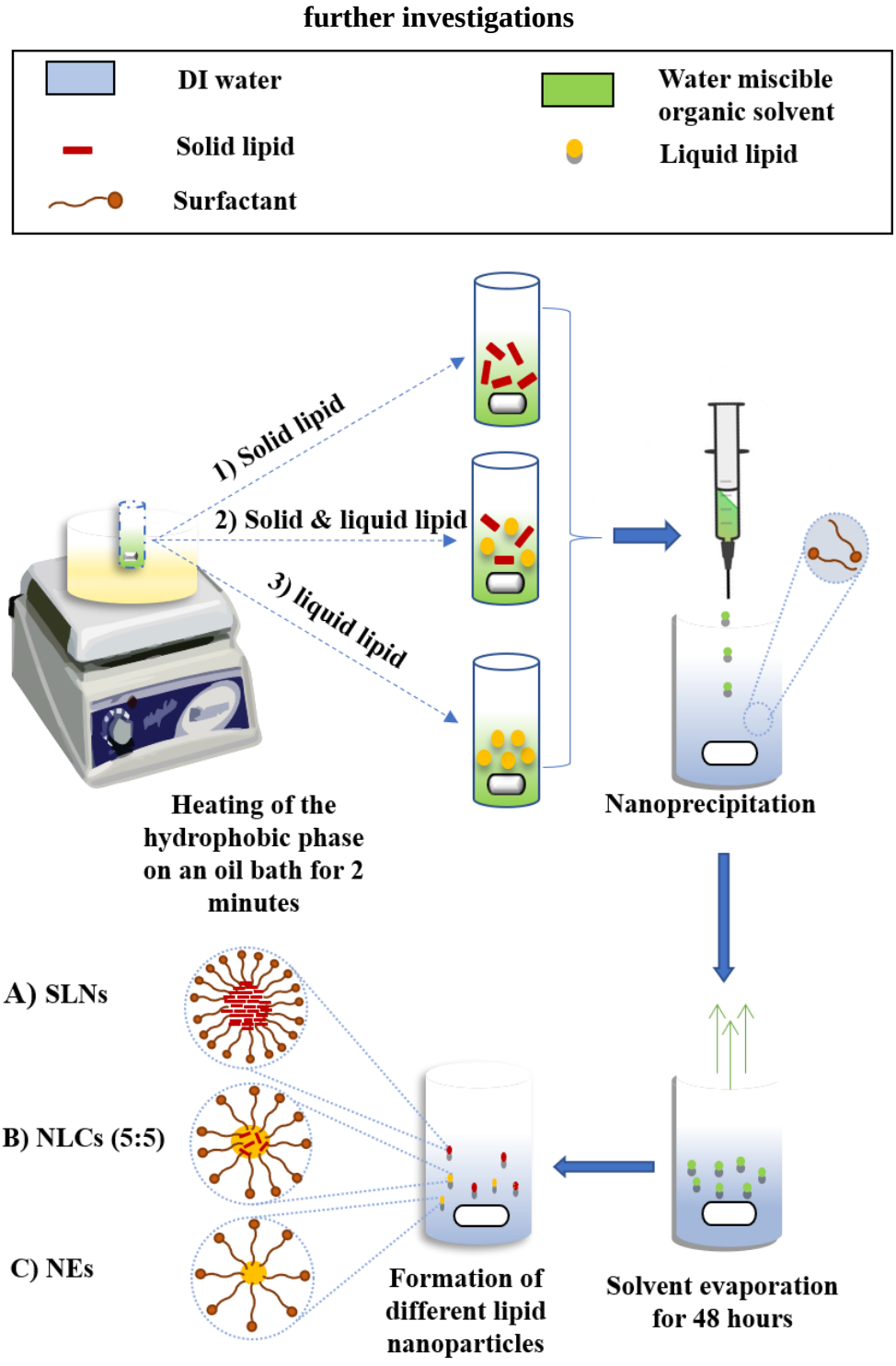

Figure 2.2 General scheme for the synthesis of different lipid formulations by hot solvent injection method. The hydrophobic phase was heated on an oil bath at 70 °C, stirring at 200 rpm for 2 minutes. The hydrophobic phase was then injected in Tween 80 solution in DI water stirring at 200 rpm at room temperature (25°C). Different lipid nanoformulations were synthesised: A) SLNs, B) NLCs or C) NEs depending on the type of lipid dissolved in the hydrophobic phase, whether it was solid lipid, a combination of solid and liquid lipid or liquid lipid, respectively. The lipid nanosuspensions were left to stir for 48 hours to allow the evaporation of the water miscible organic solvent.

2.4.1.1.1 The effect of varying the lipid concentration in the hydrophobic phase on the DLS data of the produced lipid nanoformulation

The effect of varying the lipid concentration in the hydrophobic phase on the final Z-average diameter of blank lipid nano-formulations synthesised by hot solvent injection method was studied. The purpose of that study was to determine the highest possible concentration of lipid that can be used and still preserve good quality DLS data in terms of Z-average diameter, PDI and size distribution. The volume of the hydrophobic phase (1 mL) was kept constant in all experiments, while a range of lipid concentrations (2-10 mg/mL) was tested using ethanol/acetone mixture (1:1) as the water miscible organic solvent. Compritol 888 ATO® was used as solid lipid for SLNs, soybean oil was used as liquid lipid for NEs and a combination of Compritol 888 ATO® and soybean oil was used as the lipid core for NLCs.

2.4.1.1.1.1 The effect of increasing the concentration of a single lipid on the DLS data of SLNs and NEs

Increasing the concentration of both Compritol 888 ATO® and soybean oil in the hydrophobic phase led to a subsequent increase of the Z-average diameter of SLNs and NEs, respectively, (see Figure 2.3). This general trend was found to be independent on the type of the formulations and the type of lipid. That trend was seen on both day 1 (same day of synthesis) and day 3 (third day after synthesis). For both SLNs and NEs, the Z-average diameter decreased on day 3 compared to day 1, which could be due to particles shrinkage as the solvent evaporates. Troncoso *et al.* reported a decrease in the droplet size of NEs after hexane evaporation from 125 to 97 nm.[217] In our experiment, the increase of the lipid concentration at ≥6 mg/mL led to deterioration of the DLS data quality (the sample was too polydisperse for good cumulant analysis fit) and visual aggregation of SLNs on day 1 (Figure 2.3.A) and an increase in the PDI ~ 0.5 which was an indication of an increase of the polydispersity and the Z-average diameter of SLNs.[145,218] Different behaviour was observed for the NEs, with the PDI decreasing along with an increase of the soybean oil concentration (Figure 2.3.B), the PDI range was 0.1-0.25. The PDI trend was in correlation with what Joseph *et al.*[219] have reported, where they found a decrease in the PDI accompanying the increase of the soybean oil concentration in the synthesis of NEs.

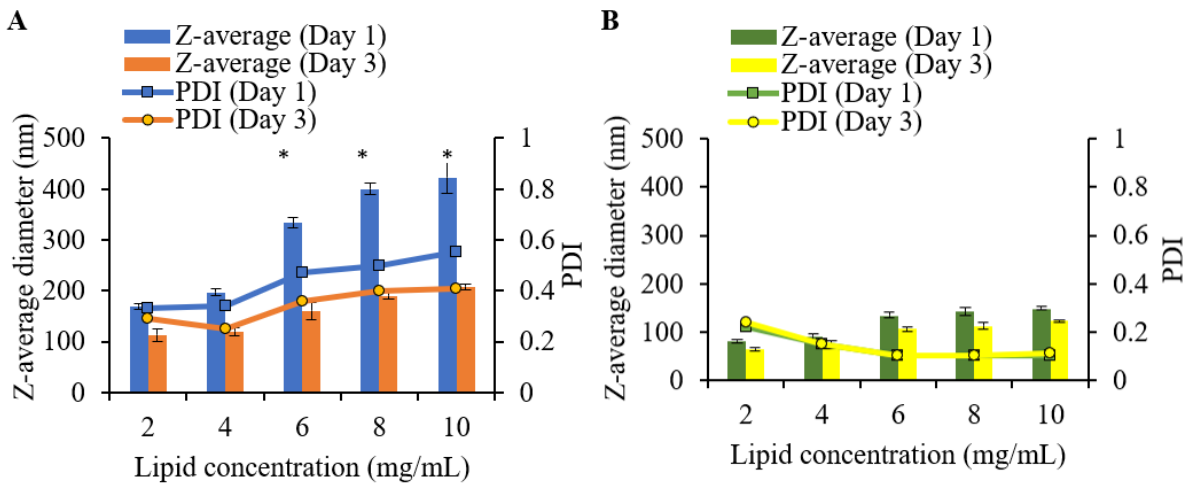

Figure 2.3 The effect of increasing the lipid concentration of the hydrophobic phase on the Z-average diameter and PDI of A) SLNs and B) NEs at a fixed surfactant concentration of 1% w/v. The asterisk (*) refers to poor quality DLS data. Data are represented as mean ± SD (n =3), where SD is the standard deviation and n is the number of samples measured.

The data of size distributions for SLNs and NEs (Figure 2.4) confirmed the Z-average diameter and PDI data in (Figure 2.3). The tested samples were SLNs and NEs samples with a lipid concentration in the hydrophobic phase of 4 and 10 mg/mL. SLNs-4 (Figure 2.4.A) and NEs-4 and NEs-10 (Figure 2.4.B) showed monomodal size distribution both day 1 and day 3. On the other hand, SLNs-10 (Figure 2.4.A) showed bimodal distribution and broad peaks indicating broad size distribution. The mode of SLNs-4 was around 100 nm, however the size distribution graph of SLNs-10 was very broad making the Z-average measurement less meaningful. Although the size distribution graphs of both NEs-4 and NEs-10 are both monomodal, but NEs-4 showed narrower size distribution graph with smaller size (<100 nm), while the size of NEs-10 was over 100 nm.

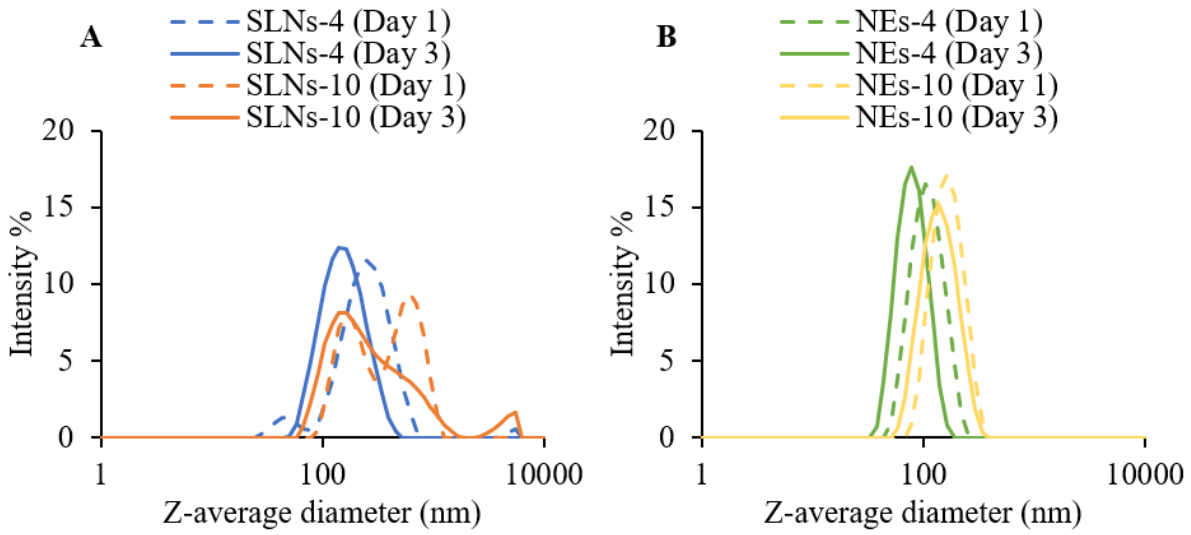

Figure 2.4 Size distribution obtained by DLS for two lipid formulations; (A) SLNs and (B) NEs, both formulations were prepared by hot solvent injection method using a lipid concentration in the hydrophobic phase of 4 and 10 mg/mL and measurements were done on day 1 and day 3.

The increase in the Z-average diameter in correlation to the increase of the lipid concentration is likely due to a combination of three factors: 1) The insufficient surfactant coverage of the lipid cores as the concentration of lipid increase.[218] 2) The increase in the viscosity of the hydrophobic phase associated with increasing the lipid concentration, which results in larger droplets upon solvent injection into the hydrophilic phase leading to the formation of larger nuclei, which in turn results in bigger particles and a broad size distribution. [218] 3) An increase in the interfacial tension between water and the lipid leading to particle size increase.[220] The study of Zhang *et al.* showed that there was a critical lipid concentration required for SLNs synthesis by solvent injection, above which, the increase in the particle size occurs.[165] For our study, the optimum concentration of the lipid in both SLNs and NEs was found to be 4 mg/mL, as above this concentration, an increase of Z-average and PDI was obvious in the case of SLNs. For NEs, the results were in line with the findings of Das *et al.*,[221] where they reported an increase in the particle size of the NEs when the lipid content of the system increased over 5-10%. In a different study, Adamczak *et al.*[140] found that oil concentration of 0.1% w/v produced NEs with the smallest particle size ~78 nm and a small PDI of 0.11, while increasing the oil concentration to over 10% w/v produced bigger particles with a size over 200 nm and a PDI up to 0.3.[140]

After establishing the effect of the lipid concentration in the hydrophobic phase on the Z-average of both SLNs and NEs (Figure 2.3), herein we discuss the effect of the physical state of the lipid, whether solid or liquid on the Z-average of SLNs and NEs, respectively. The Z-average of SLNs was compared to that of NEs at varied lipid concentrations on both day 1 and day 3. From data shown in Figure 2.3, it was obvious that the Z-average diameter of the SLNs was higher than that of NEs, at all lipid concentrations (2-10 mg/mL) on both day 1 and day 3. Two factors might have caused that variation of size between SLNs and NEs are discussed, these factors were the surfactant packing and the viscosity of the hydrophobic phase. For the surfactant packing explanation, the differences in the particle size between SLNs and NEs may be due to the variation of the stabilisation efficiency of the same surfactant as it packs differently depending on the nanoparticle type. Helgeson *et al*.,[222] attributed the variation in the size of the particles to the change of the surfactant packing or a reduced mobility of the surfactant upon solidification of the SLNs cores after cooling and solvent evaporation, which could lead to a reduction of the emulsifying ability of the same surfactant in SLNs compared to NEs.[222] The difference in affinity of Tween 80 to both soybean oil and Compritol 888 ATO® due to the difference in their chemical structure and hydrophobicity, could also explain the difference in size between NEs and SLNs. The lipophilic portion of the surfactant would arrange differently around the liquid or solid lipid cores. Low affinity between the surfactant to the lipid core could lead to incomplete surfactant coverage and particle aggregation.[223] The high viscosity of the solid particle matrix compared to oil/water emulsions could be another explanation for the smaller size of the NEs compared to SLNs.[118] The increased viscosity leads to an increase in the droplet size of SLNs compared to NEs during the solvent injection and therefore leading to an increase in the particle size. In conclusion, the combination of both factors explains why NEs have smaller particles size than SLNs, further investigations would be required to determine the precise mechanism. A possible investigation is to measure the viscosity of the injected droplet using a rheometer.

2.4.1.1.1.2 The effect of increasing the concentration of the total lipid with different S/L ratios on the DLS data of NLCs

In the previous section, the effect that each type of lipid, whether solid (Compritol 888 ATO®) or liquid (soybean oil) had on the particle size and PDI of both SLNs and NEs was discussed. In this section the effect of combining these two lipids into a single formulation to produce NLCs was investigated. The effect of two variables on the DLS data of the produced NLCs

was studied in this experiment: 1) Increasing the total lipid (solid and liquid lipids) concentration in the hydrophobic phase and 2) Varying the (S/L) ratio, (see Figure 2.5). The samples were analysed on day 1 and day 3 after solvent injection.

On day 1, (Figure 2.5.A) there were two observed general trends: 1) Increasing the lipid concentration in the hydrophobic phase from 4 to 10 mg/mL led to an increase of the Z-average diameter of the NLCs regardless to the S/L ratio. This trend was similar to that of SLNs and NEs, which could be due to the increase in the viscosity of the hydrophobic phase or insufficient coverage of the lipid cores as discussed in section (2.4.1.1.1.1). 2) Decreasing the S/L for all lipid concentrations, led to a decrease in the Z-average diameter and PDI on day 1 (Figure 2.5.A), where NLCs (9:1) showed the highest Z-average diameter and PDI, while NLCs (5:5) showed the lowest. These two trends were in line with the literature.[224,225] Gonzalez-Mira *et al.*, studied the effect of both the lipid concentration and the S/L ratio on the size of NLCs. Regarding the lipid concentration, they determined that 5% of the total formulation was the optimum concentration, above which, the viscosity of the NLCs dispersion increases leading to the disruption of the physicochemical properties of the system. For the S/L ratio, they found that increasing S/L ratio would also increase the total viscosity of the NLCs dispersion leading to increasing surface tension and accordingly particle size.[225]

On day 3 (Figure 2.5.B), both the Z-average diameter and PDI decreased compared to day 1, which could be due to cores shrinkage after solvent evaporation, while NLCs (9:1) still maintained the highest Z-average diameter and PDI.

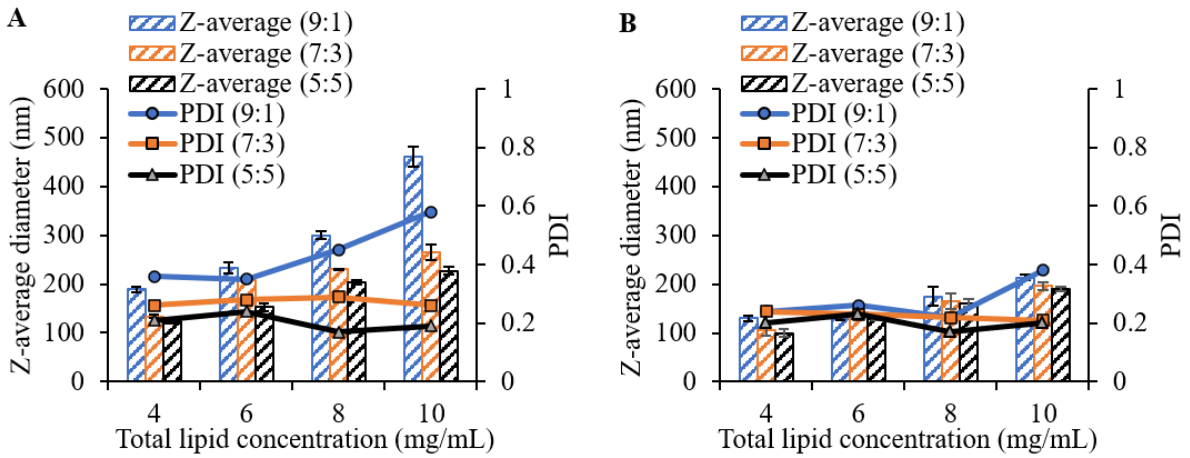

Figure 2.5 The effect of increasing total lipid concentration (solid and liquid lipids) in the hydrophobic phase on the Z-average diameter of: A) blank-NLCs on day 1 and B) blank-NLCs on day 3 at a fixed surfactant concentration of 1% w/v. The ratios 9:1, 7:3 and 5:5 referred to S/L mass ratio. Data are represented as mean ± SD (n =3), where SD is the standard deviation and n is the number of samples measured.

By direct comparison of the sizes and PDIs of the different formulations (SLNs, NLCs and NEs), it was possible to obtain an insight into the effect of the lipid composition on the particle properties. From the data shown in (Figure 2.5), we can conclude that NLCs would have similar particle size trends to either SLNs or NEs depending on the S/L ratio. Where NLCs (9:1) had Z-average diameters and PDI values similar to SLNs, as 10% w/w oil incorporation to the total lipid of NLCs, might not significantly change the viscosity of the hydrophobic phase, leading to the production of lipid nuclei of similar size to SLNs.[38] On the other hand, increasing the weight percentage of oil in the total lipid content of NLCs gradually to 30% and then to 50% w/w in NLCs (7:3) and NLCs (5:5), respectively, was accompanied by a decrease in the Z-average of the NLCs. However, the size of NLCs was still bigger than NEs which were composed of 100% w/w oil at varied concentrations (4-10 mg/mL). This is in agreement with the results from Jores *et al.*, which showed that SLNs and NLCs had larger size and high PDI than NEs.[224] The smaller size of NLCs compared to SLNs could be due the decrease in the density of the crystal lattice of the lipid crystal upon replacing solid lipid molecules by oily ones.[224,226] Muhamad *et al.* reported that NLCs size becomes similar to that of NEs at oil loading of 40% w/w or above.[227] Increasing the total lipid concentration of NLCs (5:5), which was the ratio with highest liquid lipid content, seemed to be accompanied with a decrease in the PDI on day 1, the same trend that was seen in NEs.

From the results shown in this section, the optimum NLCs formulas were that composed of a total lipid concentration (4 mg/mL) in the hydrophobic phase, and S/L of 5:5, the choice was based on the smallest Z-average diameter and PDI. A similar conclusion was made by Gonzalez-Mira *et al.*,[225] they studied the synthesis NLCs composed of stearic acid as a solid lipid, castor oil as liquid lipid and Tween 80 as surfactant by the ultrasound method, they found that a S/L of 6:4 and 5:5 gave the best DLS results and stability.

The size distributions of different NLCs formulations (Figure 2.6) changed in response to increasing the oil content and/or the concentration of the lipid in the hydrophobic phase on the particle size. The two lipid concentrations 4 and 10 mg/mL were studied as the lowest and highest lipid concentrations, respectively. For NLCs with the lowest oil content (9:1) (Figure 2.6.A), a broad size distribution can be seen for both lipid concentrations on both days indicating particles aggregation. This was with exception of NLCs (9:1)-4 (Day 3) which showed monomodal size distribution. For NLCs (7:3) (Figure 2.6.B), and NLCs (5:5) (Figure 2.6.C), both types of NLCs showed monomodal size distribution, indicating the effect of incorporating soybean oil into the solid lipid cores on the size distribution, and proved successful NLCs formation. Increasing the lipid concentration from 4 to 10 mg/mL in all three NLCs types led to an increase in the particles size as indicated by the shifted size distribution graphs.

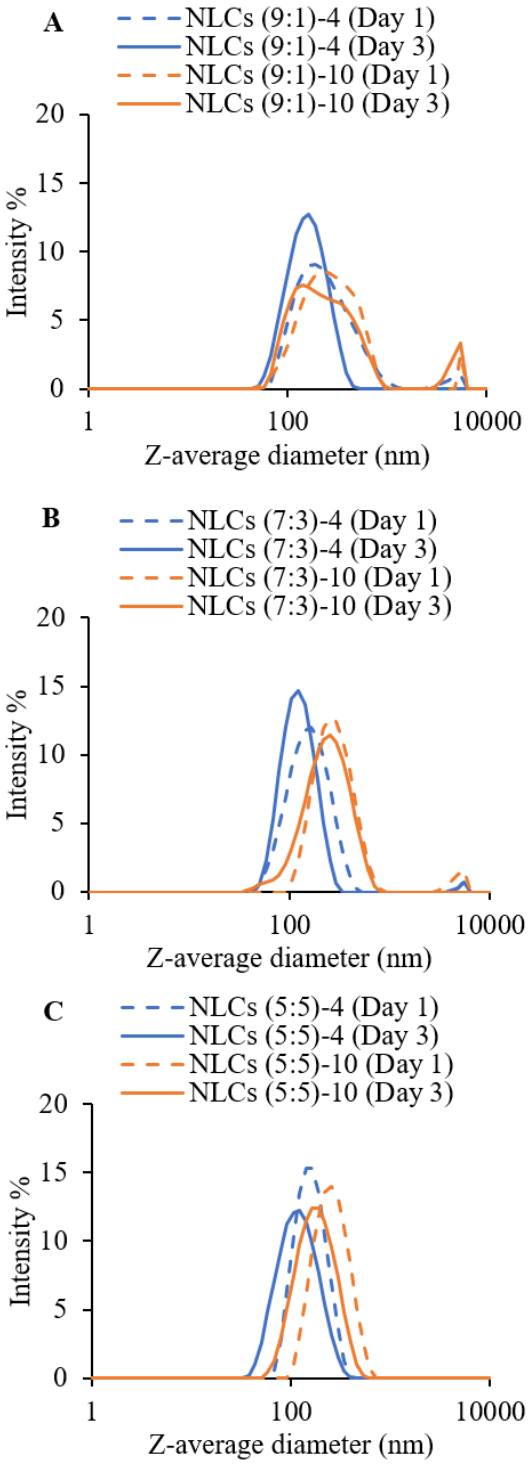

Figure 2.6 Size distribution obtained by DLS for different NLCs formulations; (A) NLCs (9:1), (B) NLCs (7:3) and (C) NLCs (5:5). All formulations were prepared by hot solvent injection method using a lipid concentration of 4 and 10 mg/mL and measurements were carried out on day 1 and day 3.

2.4.1.1.2 The effect of the surfactant concentration on the DLS data of both SLNs and NEs

In this experiment the effect of increasing the concentration of Tween 80 on the particle size was tested to determine the minimum surfactant concentration required to yield physically stable SLNs and NEs. Formulations with different concentrations of Compritol 888 ATO® or soybean oil in the hydrophobic phase (6, 8 and 10 mg/mL) were studied. The targeted particle size range was approximately 100-300 nm which is the size suitable for intestinal absorption of nanoparticles.[223] From Figure 2.7.A and B, it was evident that on day 1, the Z-average diameter and PDI of SLNs and NEs were affected by the concentration of both the surfactant and the lipid. Increasing the Tween 80 concentration from 1 to 5% w/v, led to an increase in the Z-average diameter and the PDI of both SLNs and NEs. The SLNs batch that showed the biggest size and PDI, was the one that had the highest concentration of Tween 80 (5% w/v) and the highest concentration of Compritol 888 ATO® (10 mg/mL).

The increase in the size correlated with the increase of the surfactant concentration, which was well above the critical micelle concentration (CMC) of the surfactant (0.0017% w/v for Tween 80). If the rate between particles collision was faster than the rate of adsorption of the surfactants on the particles surface,[222] then increasing the concentrations of surfactants well above their CMC, will result in the formation of a greater number of micelles, while the hydrophobic surfaces of the SLNs will colloid with each other before they have a chance to be covered with the surfactant molecules. Such situation will still mean that particle aggregation of SLNs can occur in spite of a high surfactant concentration.[222]

For the lipid concentration in the hydrophobic phase on day 1, at varied surfactant concentrations, the increase in the size of the SLNs in correlation with increase of the lipid concentration in the hydrophobic phase could be due to the increase in the viscosity of the hydrophobic phase as discussed before. The increase in size of the particles was also accompanied by an increase in the PDI due to the increase of heterogeneity of the sample with the increase in the surfactant molecules which can take many forms as micelles along with the formation of SLNs or NEs.[225] The PDI in the case of SLNs was around 0.3 at a Tween 80 concentration of 1% w/v and reached around 0.8 for SLNs samples synthesised using Tween 80 concentration of 5% w/v, which reflects high polydispersity and poor quality DLS data. The effect of increasing the soybean oil concentrations was less significant on the size of NEs at

Tween 80 concentrations of 2.5 and 5% w/v, and the size of NEs droplets was below 200 nm for all three Tween 80 concentrations. The PDI for NEs on day 1 (Figure 2.7.B) were all under 0.14 which indicated monodisperse distribution of the NEs droplets, the highest lipid concentration (10 mg/mL) showed lower PDI when compared to lower lipid concentration, which is consistent with our previous finding in section (2.4.1.1.1.1).

From the data in Figure 2.7.C and D that showed the effect of the Tween 80 concentration on SLNs and NEs, respectively on day 3 after solvent evaporation, it was obvious that after solvent evaporation the particle size decreased for both SLNs and NEs. The decrease in size was likely due the shrinkage of the particles after the solvent evaporation. On the other hand, we can see a different trend for SLNs with increasing the lipid concentration, at Tween 80 concentration of 2.5 and 5% w/v, the biggest SLNs Z-average diameters were seen at a Compritol 888 ATO® concentration of 6 mg/mL, while the smallest size was seen at a Compritol 888 ATO® concentration of 10 mg/mL. An explanation of this could be that at low Compritol 888 ATO® concentration (6 mg/mL) the concentration of Tween 80 of 2.5 and 5 % w/v was excessive in relation to this mass, so the excess surfactant might have led to a bridging between SLNs particles and causing their aggregation. While, at high Compritol 888 ATO® concentration, the high concentrations of Tween 80 could be used to cover the high amount of lipid used to cover their large hydrophobic surfaces.[228]

In the case of the NEs after solvent evaporation as in Figure 2.7.D, the NEs displayed the same trend of increasing the size average diameter in correlation with the increase if the soybean oil concentration. The PDI trends appeared the same before and after solvent evaporation for both SLNs and NEs. As increasing the concentration of Tween 80 did not decrease the Z-average diameter of either SLNs or NEs, the effect of the surfactant concentration on NLCs was not studied and a surfactant concentration of 1% w/v was kept constant for further studies.

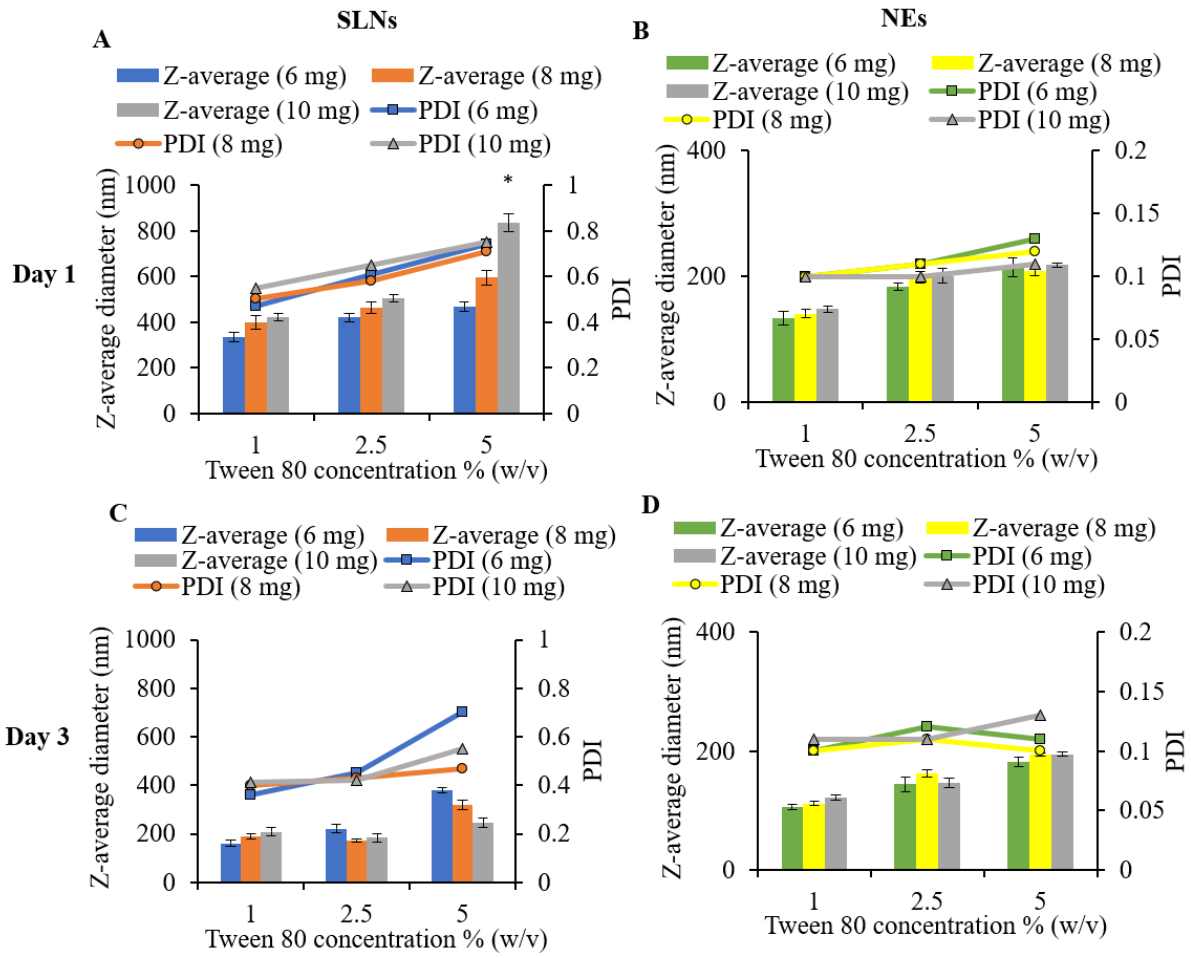

Figure 2.7 DLS measurements (Z-average diameter and PDI) for the effect of increasing the concentration of Tween 80 on varied lipid concentrations of A) Blank-SLNs on day 1, B) Blank-NEs on day 1, C) Blank-SLNs on day 3 and D) Blank-NEs on day 3. Day 1 was the same day of the synthesis and day 3 was the 3rd day after synthesis. The asterisk (*) referred to poor quality DLS data. Data are represented as mean ± SD (n =3), where SD is the standard deviation and n is the number of samples measured.

2.4.1.2 Investigation of size and morphology of blank SLNs, NLCs and NEs by CryoSEM

After examining how the lipid and surfactant concentration affected the particle size of the lipid nanoformulations using DLS. Further studies were carried out to examine the size and morphology of the lipid nanoformulations by CryoSEM. Samples' preparation was discussed in section 2.3.2.3.2. The images obtained by CryoSEM of SLNs, NLCs (5:5) and NEs (Figure 2.8) showed their morphology and size. CryoSEM was used for the size and morphology analysis here rather than the conventional SEM, as it is more suitable for soft nanomaterials, samples that have oil content i.e. nanoemulsions, or with samples prone to aggregation (i.e. SLNs).[229] Images obtained by SEM (data not shown) were of poor quality due to film formation

caused by the surfactant presence. Figure 2.8.A showed that SLNs had irregular shapes while both, NLCs (Figure 2.8.B) and NEs (Figure 2.8.C) were spherical in shape with smooth surfaces, with NLCs being more polydisperse than NEs. The non-spherical shape of the SLNs have been reported in the literature. Muhamad *et.al.* showed that SLNs made of Compritol 888 ATO® appeared as platelets when measured by SEM, while they found that NEs were spherical in shape and that NEs had smaller PDI than non-spherical particles like SLNs.[227] Our images also showed that the majority of particle sizes obtained by CryoSEM of NLCs and NEs were ~100-200 nm, few particles were above that size range. Also, the particle sizes obtained by CryoSEM were bigger than that obtained by the DLS (~100 nm), see Figure 2.8.D, which could be due to the relatively small samples sizes measured by microscopy not accurately reflecting the whole sample. Also particles aggregation might take place during the freezing step in CryoSEM sample preparation.

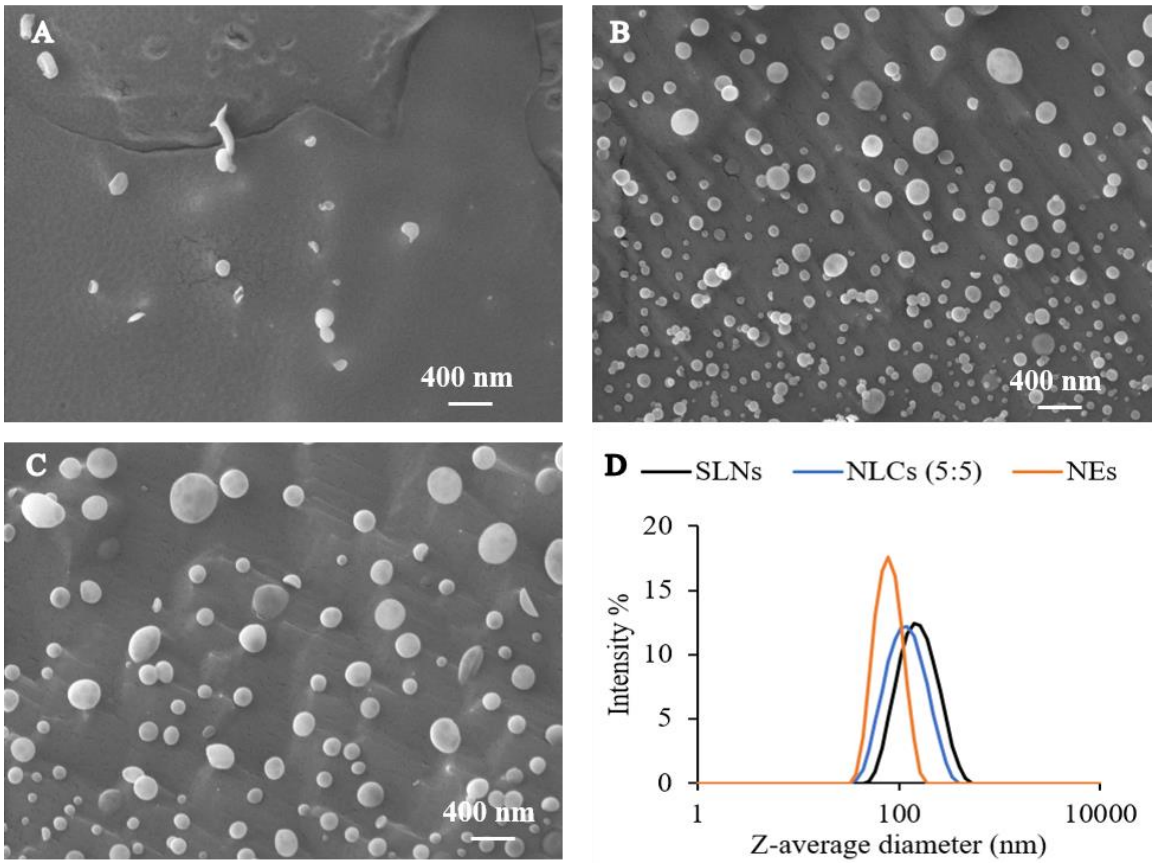

Figure 2.8 Particle characterisation of different lipid nanoformulations on day 3 prepared using hot solvent injection method and using a lipid concentration in the hydrophobic phase of 4 mg/mL and using 1% w/v Tween 80: (A) CryoSEM image of SLNs. (B) CryoSEM image of NLCs (5:5). (C) CryoSEM image of NEs. (D) Size distribution graphs obtained by DLS for the same 3 formulations on day 3 showing monomodal distribution of size with Z-average diameter of ~200 nm.

2.4.1.3 DSC investigations of blank SLNs, NLCs and NEs

DSC was used to investigate the crystallinity of unformulated bulk lipids and blank lipid formulations. Figure 2.9 showed an overlay of the melting peaks of the bulk materials: Compritol 888 ATO®, Tween 80 and soybean oil, and the dried blank formulations: SLNs, NLCs (9:1, 7:3 and 5:5) and NEs. For the bulk materials, only unformulated Compritol 888 ATO® showed a melting peak at 71.7 °C, while Tween 80 and soybean oil did not show melting peaks as they are both liquid at the temperature range tested. Above 100 °C, we can see endothermic peaks for all formulations (Figure 2.9), which might suggest the decomposition of the nanomaterials at such high temperature. Although the overlay graph of the thermograms (Figure 2.9), did not show obvious melting peaks of Compritol 888 ATO® for lipid nanoformulations around 70 °C, this was due to the low heat flow associated with the lipid formulations rather than the absence of the transitions. The melting peaks of the lipid formulations can still be seen when they are represented individually not in comparison with pure Compritol 888 ATO® (see Figure 2.10). This was except for NEs which had no Compritol 888 ATO® therefore showed no melting transitions. A comparison of the enthalpy and melting temperatures of different samples provides a way to determine the impact of the formulation's variables on the crystallinity of the solid lipid. The enthalpy is a property of a thermodynamic system and is defined as the sum of the system's internal energy and is the product of its pressure and volume.[230] From data shown in Table 2.1, we can see that unformulated Compritol 888 ATO® had the highest melting temperatures and enthalpy of (71.7 °C, 125.8 J/g), respectively, those values decreased when Compritol 888 ATO® was formulated into SLNs (71.0 °C, 4.47 J/g) which indicate successful nanoparticles formation. The decrease in the enthalpy of the lipid formulations compared to the unformulated bulk lipid could mean that the lipid nanoformulations are more amorphous, therefore required less energy (i.e., lower enthalpy) to disrupt their crystal structure to reach the melting point, unlike the unformulated lipid which has a perfect crystal structure and require more energy (i.e., higher enthalpy) to reach the melting point. This was in line with findings of Dong Zhi *et al*., where they reported a decrease in the enthalpy from 149.92 J/g for the solid lipid to 15.31 J/g when that lipid was formulated into SLNs.[231] Incorporation of soybean oil to form NLCs further decreased both the melting temperatures and enthalpy in a concentration dependant manner, where NLCs (5:5) with 50% oil content showed the lowest melting temperatures and enthalpy of 65.7 °C, 1.28 J/g of all formulations, which suggests that NLCs were less crystalline than SLNs, and that NLCs (5:5) was the least crystalline among all NLCs formulations. Another observation further

proved the successful nanoparticles formation was the shape of the peak, where pure materials like unformulated Compritol 888 ATO® showed a sharp peak (Figure 2.9), impure materials or less ordered crystals usually show broader peaks with a melting range such as NLCs (7:3), see Figure 2.10.[231]

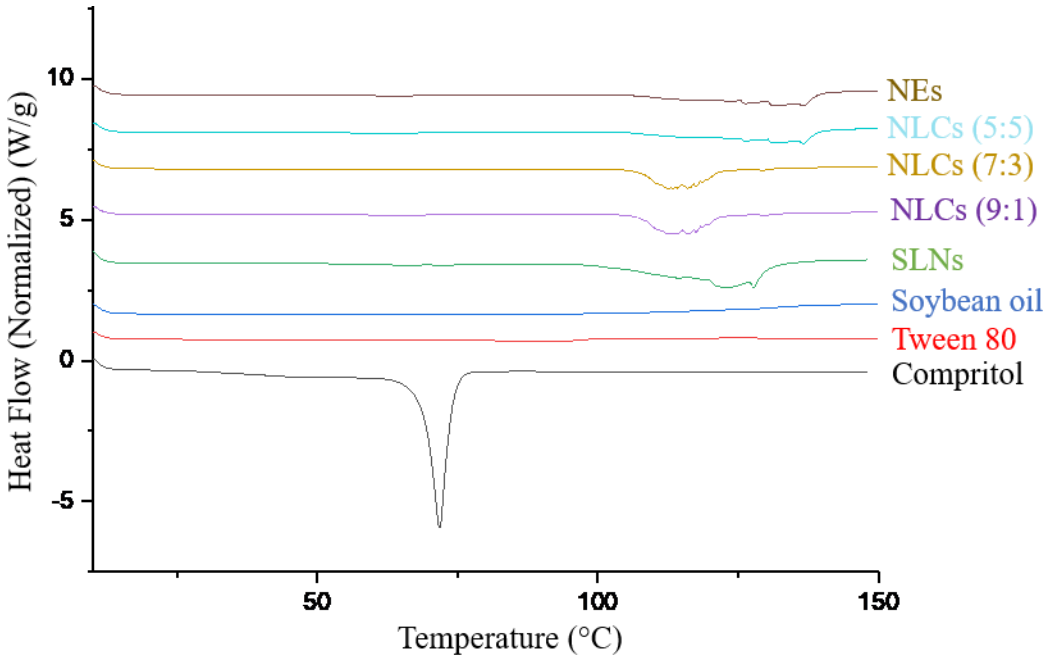

Figure 2.9 Overlay of the DSC thermograms of different lipid formulations prepared by hot solvent injection and the unformulated pure materials used for their synthesis.

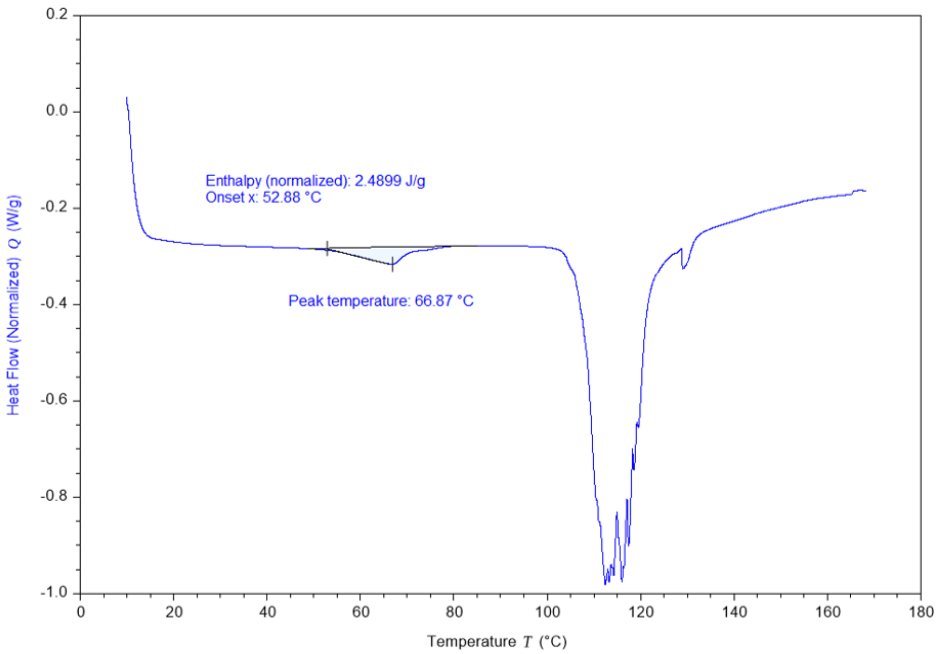

Figure 2.10 DSC thermograms for dried NLCs (7:3) prepared by hot solvent injection, showing lipid peak at a melting temperature of 66.87 °C and a melting enthalpy of 2.48 (J/g).

Table 2.1 Melting temperatures and Enthalpy obtained by DSC for Compritol 888 ATO® and several dried lipid formulations. The enthalpy was normalised to the total mass of the sample.

Sample	Melting Temperature (°C)	Enthalpy (normalised) (J/g)
Compritol 888 ATO®	71.7	125.8
SLNs	71.0	4.47
NLCs (9:1)	70.1	3.42
NLCs (7:3)	66.8	2.48
NLCs (5:5)	65.7	1.28

In all the previous experiments, 1:1 v/v ethanol/acetone solution was used as the water-miscible organic solvent. The choice of the solvent was based on the ability of the solvent mixture to dissolve both Compritol 888 ATO® and soybean oil at 70 °C. The solubility aspect is an important criterion to be considered when choosing a solvent for the preparation of the nanoparticles. However, another important consideration is the ability to remove the organic solvent after the formation of the nanoformulations. The solvent of choice must be volatile at room temperature within relatively short period of time (1-3 days), as it could affect the stability of the particles. No other techniques were used to remove the organic solvent to keep the method simple. The SLNs, NEs and NLCs dispersions were left to stir till day 3, to give the water-miscible organic solvent the chance to evaporate. However, after day 3, the ethanol was still present in the nanodispersions of the three lipid nanoformulations which was confirmed by the smell of ethanol and NMR analysis (data not shown). The lack of ethanol volatility limited its use as an appropriate solvent for the hot solvent injection preparation of these lipid nanoformulations, as the presence of traces of organic solvents will affect the stability of the formulation and might cause toxicity issues. The difficulty of ethanol evaporation could be due to the formation of hydrogen bond between ethanol and water in the hydrophilic phase, as ethanol/water is considered as an azeotropic solvent mixture.[232] Drug loading experiments were not carried out using hot solvent injection method as the presence of residual organic solvents

would cause drug leaching into the hydrophilic phase leading to a decreased encapsulation efficiency.

In conclusion, the hot solvent injection method was successful in producing blank SLNs, NEs and NLCs using: Compritol 888 ATO® and soybean oil at a concentration of 4 mg/mL in the hydrophobic phase whether on their own or combined, 1% w/v Tween 80 as a surfactant and 1:1 v/v ethanol/acetone solution as water-miscible organic solvent. The formulations were stable on day 3 as indicated by the DLS data, however the incomplete removal of ethanol by stirring at room temperature, was the only limitation. So, a different solvent/lipid mixture was to be investigated as will be discussed in the cold solvent injection section, where the no heat was required in the synthesis.

2.4.2 Cold solvent injection

2.4.2.1 The effect of varying the synthesis parameters on the DLS data of SLNs, NLCs and NEs synthesised by cold solvent injection method.

The aim of this study was to optimise the synthetic parameters of cold solvent injection method for the synthesis of drug loaded SLNs, NLCs and NEs, see Figure 2.11. In this method, a solvent with a relatively low boiling point was required, e.g., THF (B.P, 66 °C), to ensure its complete evaporation at room temperature and under atmospheric pressure. This requirement for the solvent was necessary to address the problem of residual solvent of the hot solvent injection method. That problem originated from the use of water miscible organic solvents of high boiling points e.g., ethanol (B.P, 78 °C), which allowed the dissolution of high melting point solid lipids e.g., Compritol ATO 888 (M.P, 70 °C), but was difficult to evaporate as it formed azeotropic mixtures with water. In addition to the low the boiling point, the solvent in the cold solvent injection method was also required to have the ability to solubilise the lipids at room temperature. Heating of low boiling point solvents at temperatures above their boiling point to solubilise lipids, would lead to the evaporation of the organic solvents and the precipitation of the lipid before its injection into the aqueous phase.

Imwitor® 900 K (M.P, 61 °C) is a solid lipid with a lower melting point and was the most used in this section as it is soluble in THF at room temperature. The effect of different variables on the DLS data of SLNs, NEs and NLCs were investigated. The variables studied included

varying: lipid concentration in the hydrophobic phase, type of surfactants, type of solid lipids, S/L ratios for NLCs and different drug loadings. Drug-loaded formulations were characterised using DLS, DSC, CryoSEM and radiometric analysis.

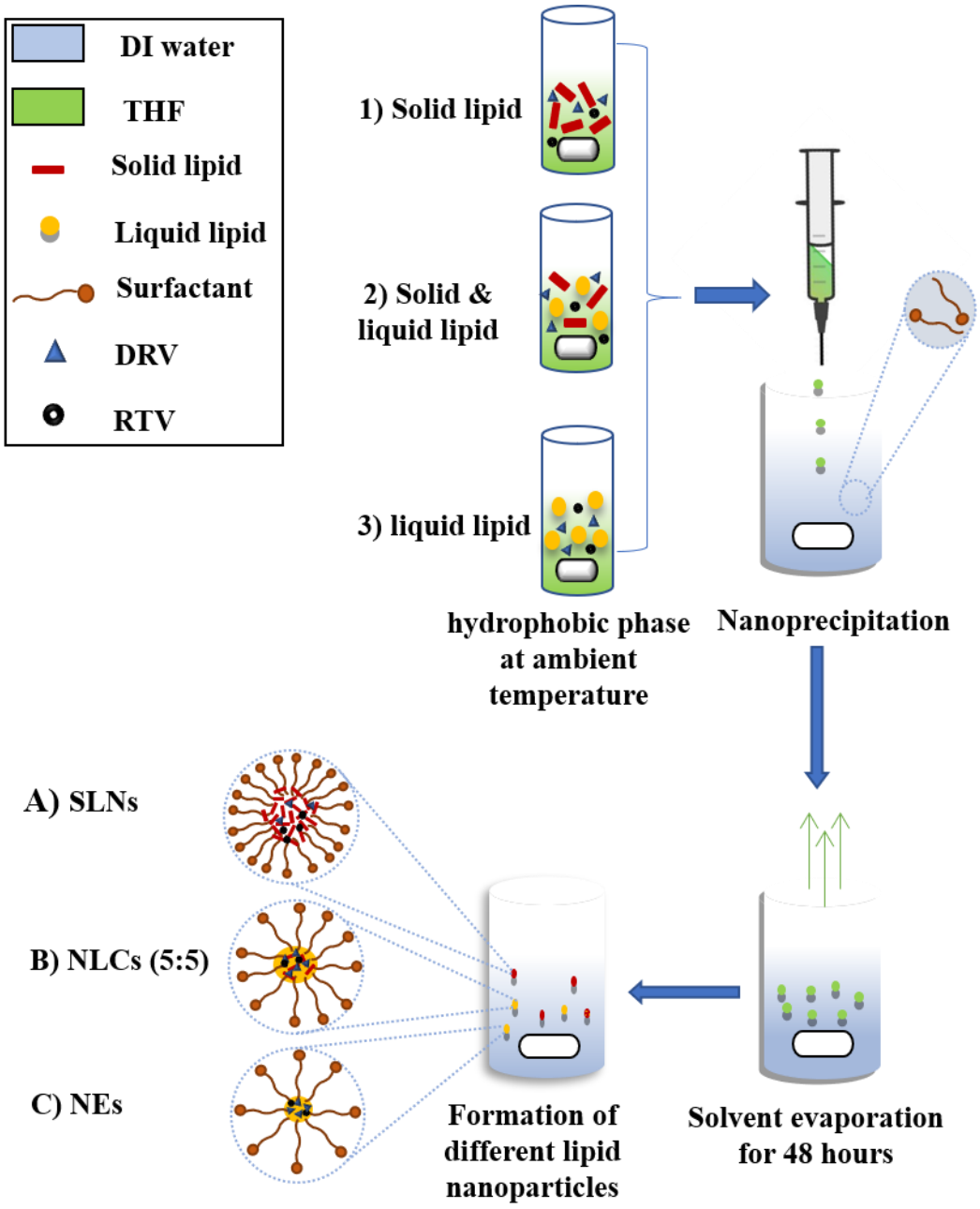

Figure 2.11 General scheme for the synthesis of different drug-loaded lipid nanoformulations by cold solvent injection method: A) SLNs, B) NLCs (5:5) or C) NEs depending on the type of lipid dissolved in the hydrophobic phase, whether it was solid lipid, a combination of solid and liquid lipid or liquid lipid, respectively.

2.4.2.1.1 Optimisation of blank SLNs, NLCs and NEs formulations

Blank lipid nanoformulations were optimised before the synthesis of the drug-loaded ones. In the following subsections (2.4.2.1.1.1, 2.4.2.1.1.2 and 2.4.2.1.1.3), the optimisation of blank lipid nanoformulations was discussed.

2.4.2.1.1.1 The effect of the type of the surfactant on the DLS data of SLNs and NEs

To understand the individual interaction of both Imwitor® 900 K as a solid lipid and soybean oil as a liquid lipid with different types of surfactants in the solvent injection process, two variables were studied: 1) Type of surfactant, Tween 80 (Figure 2.12.A) and Brij 78 (Figure 2.12.B) at a concentration of 1% w/v were used as surfactants for the synthesis of blank SLNs and NEs. 2) Different concentration of the lipids (2, 4, 6, 8 and 10 mg/mL) in the hydrophobic phase were used for the synthesis of SLNs and NEs using both surfactants. Although the effect of the lipid in the hydrophobic phase has been investigated before in the hot solvent injection section, but it will be reinvestigated in the cold solvent injection method due to the change in the solvent, lipid, surfactant, and temperature of the hydrophobic phase.

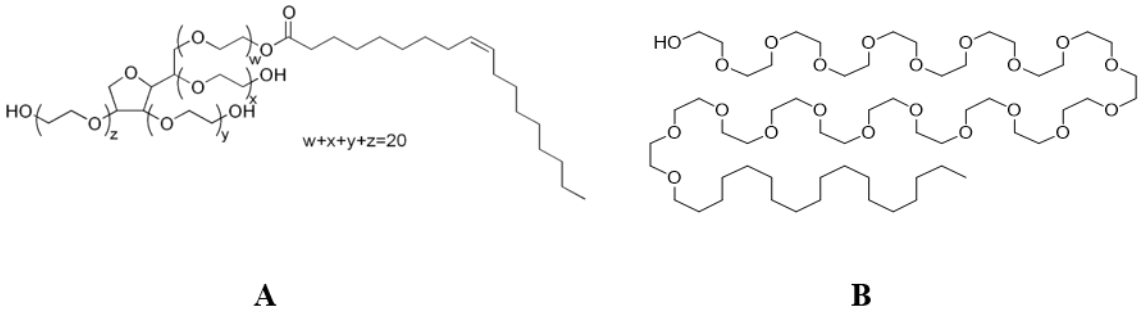

Figure 2.12 Chemical structure of: A) Tween 80 and B) Brij 78

For the first variable, changing the type of the surfactant had a significant impact on the Z-average diameter and stability of both SLNs and NEs (Figure 2.13). Using Tween 80 as a surfactant produced SLNs (SLNs-Tween 80) with an initial smaller particle size diameter (Figure 2.13A) compared to their equivalent SLNs formulations synthesised using Brij 78 (SLNs-Brij 78) (Figure 2.13B), on day 1. On the other hand, upon solvent evaporation on day 3, SLNs-Tween 80 (Figure 2.13A) showed a significant increase in size, which is a sign of the short-term instability of the SLNs leading to particle aggregation. Although the SLNs-Brij 78 (Figure 2.13B) were initially bigger than SLNs-Tween 80, they decreased in size on day 3,

which could be due to the particle's shrinkage after solvent evaporation. The highest Z-average diameter for SLNs-Tween 80 was below 400 nm on day 1 and increased to over 1000 nm on day 3, while the highest Z-average diameter for SLNs-Brij 78 was slightly above 400 nm on day 1 and decreased to below 400 nm on day 3. The decrease in size after solvent evaporation showed that the SLNs were stable over the 48 hours period and proved the efficiency of Brij 78 as a surfactant for SLNs. The most likely explanation of the initial relative small particle size of SLNs-Tween 80 (Figure 2.13A) compared to SLNs-Brij 78 (Figure 2.13B) could be related to a combination of two factors: 1) The rigidity of Tween 80 due to its unsaturated chain alkyl chain, unlike the saturated Brij 78 molecules. As the surfactant becomes more rigid, the density of surfactant packing around the core decreases, which might lead a smaller hydrodynamic diameter. On the other hand, the low surfactant density is considered as a drawback as it means that the cores are less shielded and some of the areas of solid lipid cores becomes uncovered, leading to SLNs particle aggregation over time (day 3). The same concept was discussed by Ribeiro *et al.*, they attributed the small particle size of micelles stabilised by Brij 98 which has unsaturated alkyl chain to the rigidity and reduced density of Brij 98 compared to bigger micelles size stabilised by Brij 78 which has saturated hydrophobic moiety.[233] Kovacevic *et al.* results suggested that rigid surfactants as Tween 80 may induce crystallisation of solid lipids such as tripalmitin.[234] 2) The compatibility between Imwitor® 900 K and Brij 78 might have been better than with Tween 80 as they are both derived from stearic acid. Imwitor® 900 K consists of 40-50% glyceryl monostearate and Brij 78 (polyoxyethylene 20 stearyl ether) which is derived from stearic acid molecules covalently attached to PEG 1000.[235] Indeed, Zhang *et al.* have shown that Brij 78 and stearic acid were a compatible surfactant and solid lipid mixture in the productions of SLNs.[235]

For NEs, both formulation sets synthesised using Tween 80 (NEs-Tween 80), see Figure 2.13C or Brij 78 (NEs-Brij 78) (see Figure 2.13D) showed smaller Z-average diameter on day 3 compared to the Z-average diameter on day 1, indicating the stability of the NEs with both surfactants. However, on day 1, NEs-Tween 80 were smaller than their equivalent NEs-Brij 78, the same trend as SLNs. Unlike SLNs, NEs also kept the smaller particle size on day 3, however the difference in size between the two surfactants was negligible, which suggests that Tween 80 and Brij 78 were both good surfactants for NEs. The NEs synthesised by both surfactants were bigger in size than SLNs, except SLNs synthesised using Tween 80 on day 3, due their instability. The reason behind this could be related to the self-emulsifying properties

of Imwitor® 900 K which provided extra stabilisation of the SLNs. Imwitor® 900 K has a HLB of 3, so it acted as an emulsifier besides its role as a lipid.[236]

For the second variable, the effect of the concentration of the hydrophobic phase, an increase of the concentration of both Imwitor® 900 K and soybean oil in the hydrophobic phase, led to an increase in the Z-average diameter of both SLNs and NEs, respectively (Figure 2.13). This trend was apparent on both day 1 and day 3, and with both types of surfactants. These results agreed with the results of the hot solvent injection method, which further proves that there is a direct proportion relationship between the concentration of the lipids in the hydrophobic phase and the size of the particles, regardless to the method of preparation (cold or hot), type of surfactant and regardless to the type of lipid (Imwitor® 900 K, Compritol ATO 888 or soybean oil). The explanation of the relationship between the size of the particles and the lipid concentration has already been explained in section (2.4.1.1.1.1). The quality of DLS of SLNs-Tween 80 was poor at all different lipid concentrations, and also for SLNs-Brij 78 except at a lipid concentration of 4 and 6 mg/mL. However, the quality of DLS data was poor for NEs-Brij 78 at lipid concentration of 8 mg/mL or above, and at 10 mg/mL for NEs-Tween 80. The optimum concentration of lipid in the hydrophobic phase that could be used for further studies was 4 mg/mL, as it was the highest lipid concentration the produced particles with a Z-average of ~200 nm for both NEs and SLNs, which is the size suitable for intestinal absorption.

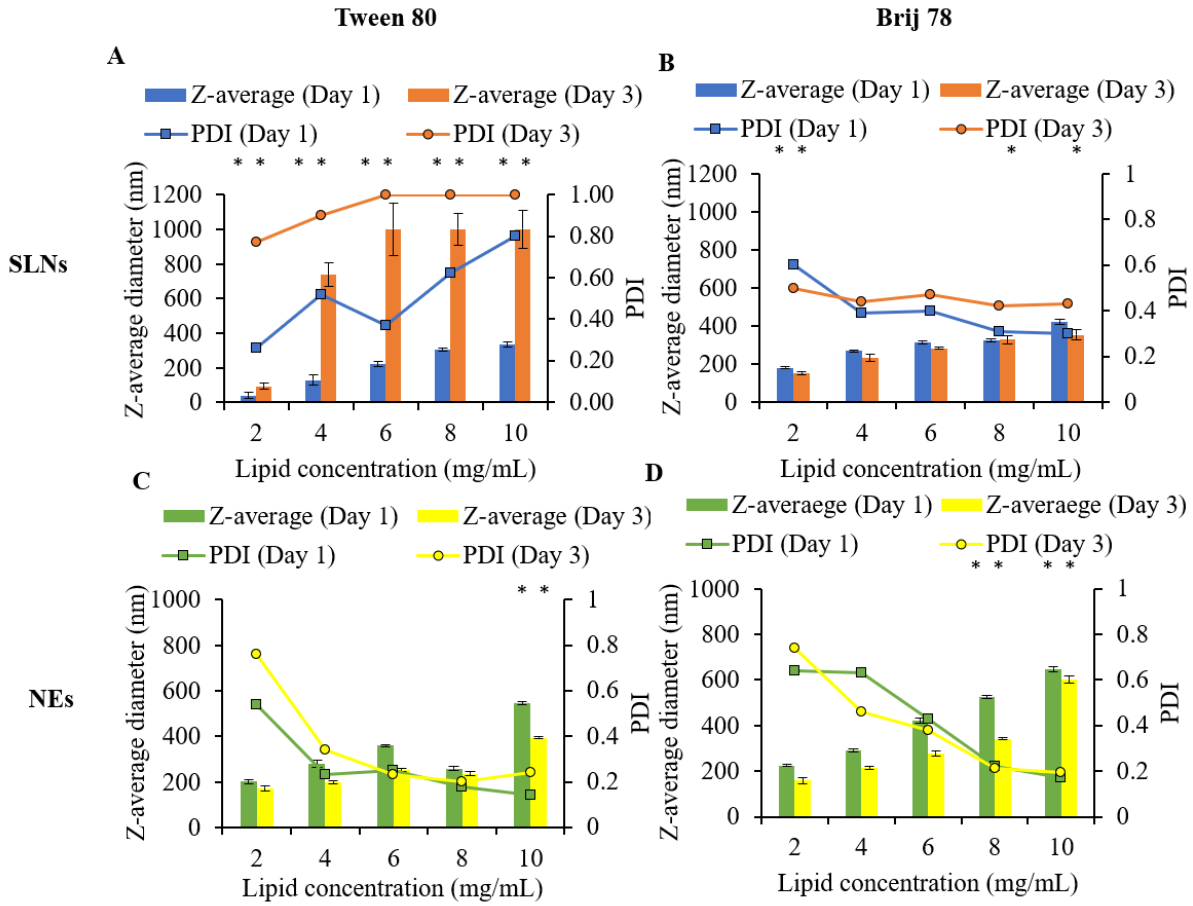

Figure 2.13 A comparison of the DLS data of blank lipid nanoformulations: A) SLNs-Tween 80, B) SLNs-Brij 78 C) NEs-Tween 80 and D) NEs-Brij 78, at day 1 and day 3 at varied lipid concentrations in the hydrophobic phase (2-10 mg/mL). The asterisk (*) referred to poor quality DLS data. Data was represented as mean ± SD (n =3), where SD is the standard deviation and n is the number of samples measured.

2.4.2.1.1.2 The effect of the type of the solid lipid on the DLS data of SLNs

A screening of different lipids was carried out to select the most appropriate solid lipid that would be used for the synthesis of both SLNs and NLCs in later studies. Herein, we discuss the effect of the type and concentration of the solid lipid on the DLS data of the produced SLNs. A high lipid content was usually targeted as it would provide more space for drug loading, however excessive lipid content should be avoided as it usually leads to particle aggregation and high PDI.[237] There were some assumptions in the literature that lipids that have amphiphilic characteristics as those with high content of monoglycerides e.g. Imwitor® 900 K, produce SLNs with a large hydrodynamic diameter and high PDI.[238] This hypothesis was based on the idea that an increase of the monoglycerides percentages in the lipid mixture gives a less lipophilic lipid which might limit its ability to nucleate upon solvent injection into the

hydrophilic phase. To investigate this hypothesis, and to determine if it explains the poor quality DLS data of SLNs synthesised using Imwitor® 900 K (SLNs-Imwitor® 900 K) in section 0), triglycerides like Dynasan®114 (trimyristin), see Figure 2.14.B and Dynasan®118 (tristearin), see Figure 2.14.C, were studied in comparison to Imwitor® 900 K which consists mainly of 40-50% glyceride monostearate (Figure 2.14.A). Triglycerides of single fatty acids type and long chain like Dynasans were reported to have high drug loading capacity between their lipid chains, therefore they might be good candidates as solid lipids for SLNs.[239] In this experiment, the SLNs were synthesised by cold solvent injection using THF as a water-miscible organic solvent and 1% w/v Brij 78 as a hydrophilic phase, as it was the surfactant that produced the most stable SLNs for Imwitor® 900 K.

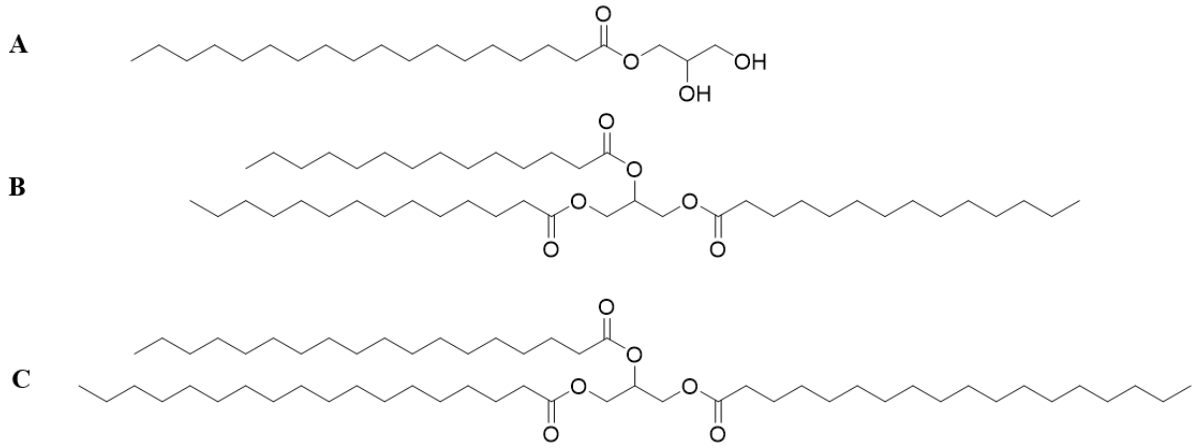

Figure 2.14 Chemical structure of: (A) Imwitor® 900 K, (B) Dynasan®114 and (C) Dynasan®118.

For both Dynasan®114 and Dynasan®118, increasing the solid lipid concentration was accompanied by an increase in the Z-average diameter of SLNs and PDI on day 1 (Figure 2.15). This behaviour could be due to an increase in the viscosity of the lipid with increasing the lipid concentration in the hydrophobic phase. After the solvent evaporation on day 3, the Z-average increased, which was an indication of the instability of the SLNs. Unlike other lipids that have only three polymorphic forms: unstable (α), metastable (B') and stable form (B), glycerides are reported to have extra intermediate stage between the B' form and the B form, which could explain the instability of the SLNs on day 3. The polymorphism issue should be considered in the stability of glycerides.[240]

The size of the SLNs synthesised using Dynasan®114 (SLNs-Dynasan®114) as shown in (Figure 2.15.A) were smaller than those synthesised using Dynasan®118 (SLNs-Dynasan®118) (Figure 2.15.B). An explanation for the difference in particle size could be due

the fact that Dynasan®114 has a lower molecular weight 723.2 (g.mol^{-1}), compared to 891.5 (g.mol^{-1}) for Dynasan®118, leading to a high viscosity of the hydrophobic phase in the case of Dynasan®118. These findings agreed with those of Dudhipala *et al*., who reported a smaller particle size of SLNs-Dynasan®114 compared to that of SLNs-Dynasan®118.[241]

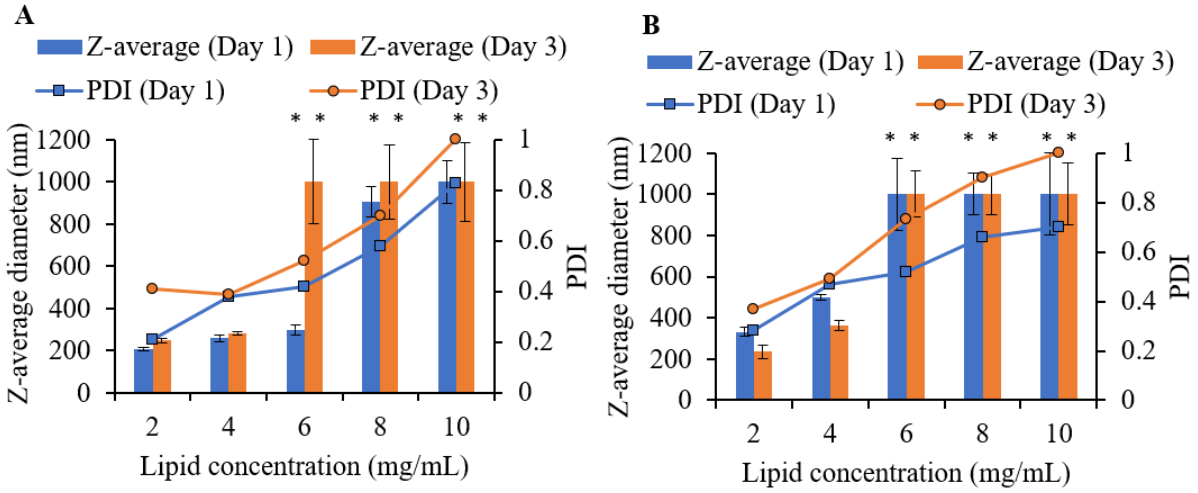

Figure 2.15 A comparison between the DLS data (Z-average diameter and PDI) of SLNs synthesised using cold solvent injection method on day 1 and day 3, solid lipids used A) Dynasan®114 and B) Dynasan®118. For both sets of SLNs, THF was used as a water-miscible organic solvent and 1% w/v Brij 78 was used as the hydrophilic phase. The asterisk (*) referred to poor quality DLS data. Data was represented as mean ± SD (n =3), where SD is the standard deviation and n is the number of samples measured.

The comparison of the size between the SLNs of the three solid lipids was carried out on day 1, to understand the effect of the lipid structure on the initial formation and nucleation of SLNs. On comparing SLNs synthesised with Imwitor® 900 K as a partial glyceride to both Dynasan®114 and Dynasan®118 as triglycerides on day 1 (Figure 2.16), it was obvious that Imwitor® 900 K produced the SLNs with the smallest particle size diameter and PDI, followed by Dynasan® 114 and then Dynasan®118. An explanation for the difference in size, could be due the self-emulsifying properties of Imwitor® 900 K, as it is considered non-ionic (o/w) emulsifier and stabiliser, which has an HLB of 3, which is hypothesised to limit Ostwald ripening, as it helped stabilise the SLNs system in addition to the used surfactant.[236] Mehnert and Mader discussed the effect of the lipid composition on the SLNs size, they reported a smaller size of SLNs synthesised using Witepsol W35, which is composed of short fatty acid chains of mono or diglycerides which has emulsifying properties, compared to Dynasan®118 which is composed of triglycerdes.[221] Additionally, Imwitor® 900 K has a lower melting point (~ 60 °C), [242] compared to (~ 80 °C) for Dynasan®114 and Dynasan®118, a high melting point

of a lipid is typically associated with a high viscosity leading to an increase in the size of SLNs particles.[221] Furthermore, differences in the affinity of Brij 78 to Imwitor® 900 K, Dynasan®114 and Dynasan®118 may also have influenced the final particle size.[223]

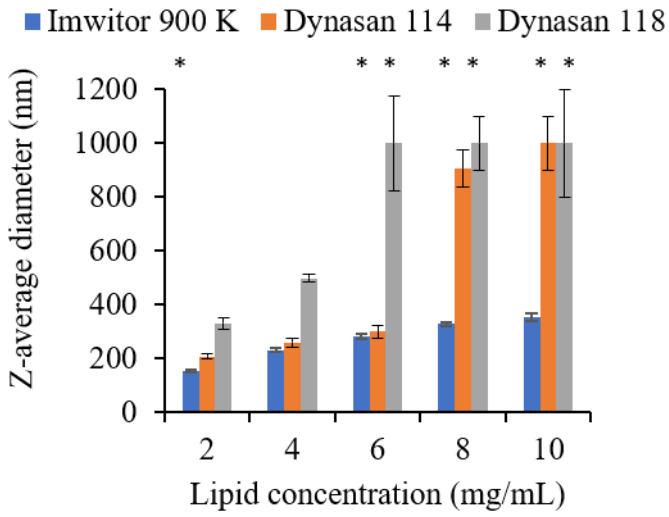

Figure 2.16 A comparison between the DLS data (Z-average diameter and PDI) of blank-SLNs synthesised using cold solvent injection method on day 1, solid lipids used Imwitor® 900 K, Dynasan®114 and Dynasan®118. THF was used as a water-miscible organic solvent and 1% w/v Brij 78 was used as the hydrophilic phase. The asterisk (*) referred to poor quality DLS data. Data was represented as mean ± SD (n =3), where SD is the standard deviation and n is the number of samples measured.

In conclusion, lipids with amphiphilic characters and high monoglyceride percentage e.g., Imwitor® 900 K showed a better DLS data in terms of smaller size and PDI, when compared to triglycerides. Therefore, Imwitor® 900 K was used as a solid lipid for further studies and in the synthesis of NLCs. As the synthesis of NEs, using soybean oil as a liquid lipid produced particles with good DLS data in terms of Z-average diameter and PDI (0), therefore there was no need to investigate additional liquid lipids.

2.4.2.1.1.3 The effect of increasing the concentration of the total lipid concentration with different S/L ratios on the DLS data of NLCs

In the previous sections (2.4.2.1.1.1 and 2.4.2.1.1.2), the effect of solid and liquid lipids on the particle size and PDI of both SLNs and NEs, respectively was investigated. In this section the effect of combining solid and liquid lipids into a single formulation to produce NLCs by cold solvent injection method was discussed. Three variables and their effect on the DLS data of the

produced NLCs were studied in this experiment: 1) Increasing the total lipid (Imwitor® 900 K and soybean oil) concentration in the hydrophobic phase, the concentrations used were 2, 4 and 6 mg/mL. 2) Varying the S/L ratio, S/L ratios used were 9:1, 7:3 and 5:5. 3) Changing the type of the used surfactant: Tween 80 or Brij 78.

Increasing the concentration of the total lipid in the hydrophobic phase was accompanied with an increase in the Z-average diameter of NLCs regardless to both the type of surfactant and the S/L ratio used (Figure 2.17), a behaviour that has been common throughout the experiments in this chapter. To understand the effect of the S/L ratio on the DLS data of NLCs, it was important to compare those data with the DLS data of SLNs and NEs in section (0). The same principles could be applied to the NLCs, where NLCs with high S/L ratio behaved like SLNs, and as the S/L ratio decreased, the NLCs tended to have similar trends like NEs. Increasing the S/L for the Tween 80 batch (Figure 2.17.A) led to a decrease in the particle size of NLCs on day 1, while on day 3 (Figure 2.17.B), the NLCs (9:1) showed the highest particle size which was an indication of instability and aggregation. While NLCs (7:3) and NLCs (5:5) showed a decrease in mean diameter on day 3 consistent with the shrinkage and solidification of the particles upon solvent evaporation. Reduction in the Z-average diameter over time can also be considered a sign of the formulation stability, so we conclude that a maximum S/L ratio that can be used, while maintaining good DLS data of the NLCs formulation was 7:3. Decreasing the S/L ratio to 5:5, resulted in the production of NLCs with a higher Z-average compared to NLCs with S/L ratio of 7:3. This finding was consistent with the previous findings that a higher amount of Imwitor® 900 K led to an decrease in the particle size as Imwitor® 900 K acts as an extra emulsifier due to its amphiphilic nature.[236]

In terms of the effect of different surfactants, when Brij 78 (Figure 2.17.C and D) was used as a surfactant, the Z-average diameter of all formulations was around 300 nm or below depending on the formulation (Figure 2.17.A and B) on day 1 and day 3. No formulation dramatically increased in size or aggregated unlike NLC (9:1)-Tween 80.

We could conclude that a total lipid concentration of 4 mg/mL was chosen for further analysis as it would allow higher drug encapsulation compared to a total lipid mass of 2 mg, it also produced a smaller particle size and PDI compared to the 6 mg. For the surfactant type, Tween 80 was a good surfactant for NLCs with lower S/L ratios (7:3 and 5:5) as they produced NLCs

with smaller particle size, while at S/L ratio of 9:1 the NLCs aggregated on day 3. Brij 78 could be considered a better surfactant for NLCs at all S/L ratios.

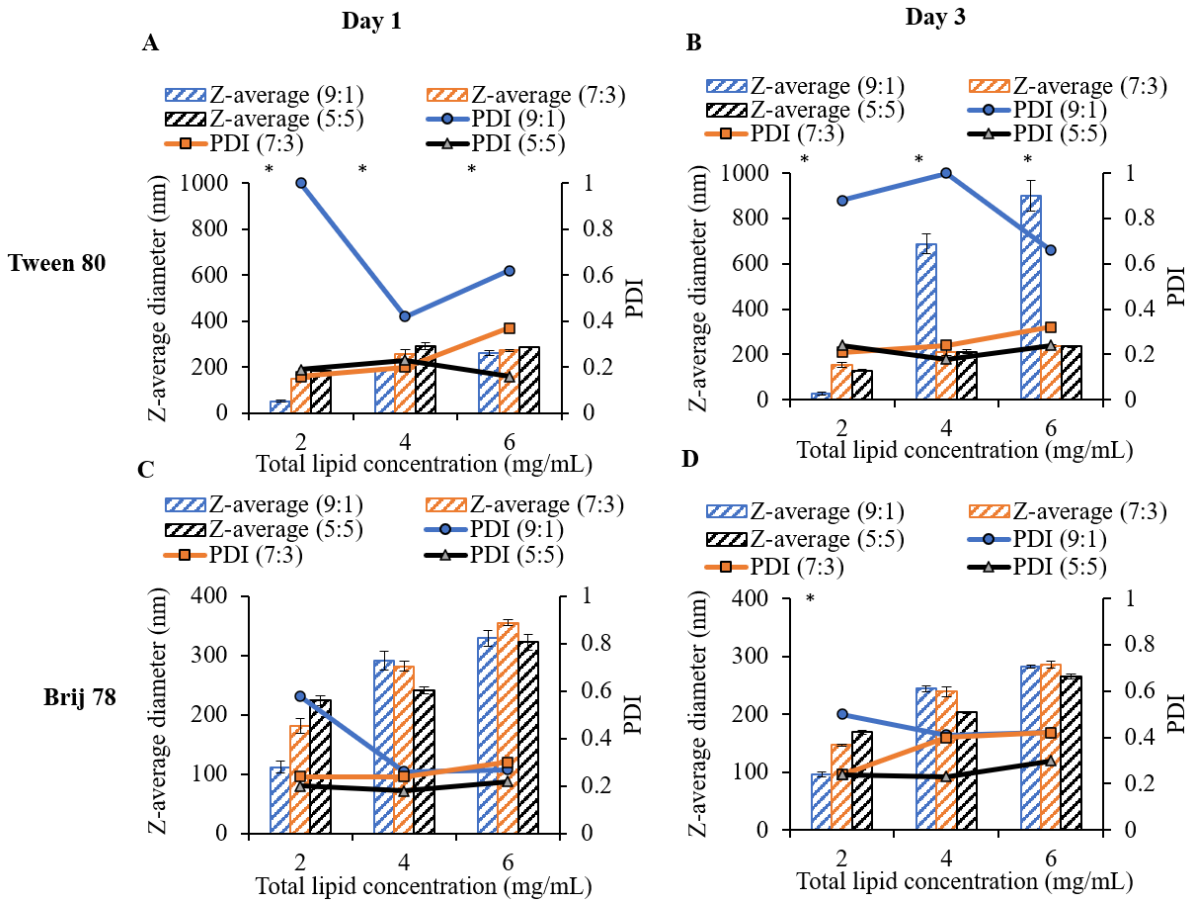

Figure 2.17 The effect of increasing total lipid concentration (solid and liquid lipids) on the Z-average diameter of A) Blank-NLCs-Tween 80 on day 1, B) Blank-NLCs-Tween 80 on day 3, C) Blank-NLCs-Brij 78 on day 1 and D) Blank-NLCs-Brij 78 on day 3, at a fixed surfactant concentration of 1% w/v. The ratios 9:1, 7:3 and 5:5 referred to the (S/L) mass ratio. The asterisk (*) refers to poor quality DLS data. Data was represented as mean ± SD (n =3), where SD is the standard deviation and n is the number of samples measured.

2.4.2.1.2 Optimisation of drug loaded SLNs, NLCs and NEs formulations

The effect of increasing the drug loading on the Z-average diameter and PDI of SLNs, NLCs and NEs was investigated using the DLS. The target of this study was to detect the highest possible DRV/total lipid mass percentage of the antiretroviral drug mixture DRV/RTV with a mass ratio of 8:1, respectively, that could be incorporated into the three different types of lipid nanoformulations. The drug encapsulation efficiency and drug release from the optimised formulations were detected using radiometric analysis. The morphology and size were investigated using CryoSEM technique and the crystallinity of the formulations were detected by DSC analysis.

2.4.2.1.2.1 The effect of drug loading on the DLS data of SLNs, NLCs and NEs

Two sets of the formulations: SLNs, NLCs (9:1, 7:3 and 5:5) and NEs were prepared, one set was stabilised with Tween 80 and the other stabilised with Brij 78. The tested DRV/total lipid mass percentages were 5, 10 and 20% w/w. The measurements were carried out at three-time intervals: day 1, day 3 and day 7. Loading the nanoformulations with the DRV/RTV mixture led to different trends and DLS results compared to their blank alternatives as explained in this section.

Increasing the DRV/ lipid mass percentage in the drug-loaded SLNs-Tween 80 (Figure 2.18.A), led to an increase in the Z-average diameter for SLNs-Tween 80 with increasing DRV/total lipid mass percentage. All the formulations showed Z-average diameter below 200 nm on day 1. Those Z-averages diameters decreased on day 3 after THF evaporation. The decrease in size could be due to the disruption of the crystal structure by the drug molecules which led to a slower rate of polymorphism and more stable particles compared to the blank particles which increased in size on day 3.[118] On the other hand, those Z-average diameters increased on day 7. However, given the DLS data quality (poor in terms of cumulant fit and high PDI) all the SLNs-Tween 80 at the three-time intervals the data was unreliable, and no further trends should be made. Based on these findings it was identified that Tween 80 was not the suitable surfactant for the drug loaded SLNs.

The drug-loaded SLNs-Brij 78 as in Figure 2.18.B showed an initially larger particle size (~200 nm) compared to their equivalent SLNs-Tween 80 on both day 1 and day 3. The Z-average diameter of the drug-loaded SLNs-Brij 78 on day 3 showed a decrease in particle size with solvent evaporation. SLNs-Brij 78 with DRV/lipid mass percentage of 10% w/w showed that the smallest size on both day 1 and day 3, this finding could be related to the fact that this is the optimum mass the gives a stable particle by inhibition of polymorphism. Below this percentage, the drug amount was likely too small to disrupt the crystal lattice and slow down polymorphism and above it, the drug loading could be above the encapsulation efficiency of the SLNs, and the free drug might cause particle aggregation. DLS data showed that by day 7, both the 5% w/w and 10% w/w showed a slight increase in the Z-average, but it remained at ~200 nm. On the other hand, for the 20% w/w the Z-average diameter jumped to 500 nm and the PDI increased to 1, which indicated the poor quality DLS data. We can therefore conclude that Brij 78 was a better surfactant for SLNs compared to Tween 80, where the DLS data for

SLNs-Tween 80 was poor in terms of poor in terms of cumulant fit and high PDI and the Z-average diameter was ~600 nm at day 7. We can also conclude that 10% w/w was the optimum DRV/lipid mass percentage for SLNs-Brij-78.

After examining SLNs, NLCs at different S/L ratios were studied. The DLS quality of drug-loaded NLCs (9:1)-Tween 80 (Figure 2.18.C) was poor (in terms of cumulant fit and high PDI), while the Z-average diameter on day 1 was ~200 nm, the PDI was high (0.42-.0.50) at different drug loadings. The quality of DLS data was also poor for day 3 and 7, and for DRV/lipid mass percentage of 20 % w/w, the Z-average diameter increased to 550 nm. From this data we can conclude that Tween 80 was not a suitable surfactant for NLCs (9:1) at all different drug loadings.

For NLCs (9:1)-Brij 78 (Figure 2.18.D), the Z-average diameter was ~300 nm for all three DRV/total lipid mass percentages on day 1 and then decreased to ~200 nm on day 3 and 7. The effect of the DRV/total lipid mass percentage on the stability and the quality of the DLS data was less obvious for NLCs (9:1)-Brij 78 (Figure 2.18.D), unlike drug-loaded NLCs (9:1)-Tween 80 (Figure 2.18.C).

In Figure 2.18.E, the Z-average diameter of the drug-loaded NLCs (7:3)-Tween 80 was ~270 nm on day 1 for all three DRV/total lipid mass percentages. Although Z-average diameter decreased to ~200 nm on day 3 and 7, but the DLS data was poor at higher drug loadings with visual aggregation of the particles.

The Z-average diameter of the drug-loaded NLCs (7:3)-Brij 78 as shown in Figure 2.18.F, the Z-average diameter increased with the increase of DRV/total lipid mass percentages on all three-time intervals, however there has been a small difference in Z-average diameter ± 20 nm between formulations with different loadings. The Z-average diameter was the highest on day 1 (~320 nm) and decreased on day 3 and 7 to ~260 nm. The DLS data was good for all formulations all time intervals.

When the liquid lipid content further was increased to 50% of the lipid mass as in NLCs (5:5)-Tween 80, the quality of the DLS data was good for all different loadings and at all time intervals (Figure 2.18.G). The decrease in the Z-average diameter on day 7 that accompanied the increase of the DRV/total lipid mass percentages, could be due to the reduction of the

amount of free lipid upon increasing the drug loading, reducing the chance of solid lipid crystallisation.[243]

For NLCs (5:5)-Brij 78, the Z-average diameter was 300 nm on day 1, while on day 3 and 7, the Z-average diameter decreased to be ~200 nm and with a good quality DLS data (Figure 2.18.H). The only exception was that noticed for DRV/total lipid mass percentage of 5% (w/w), where the Z-average diameter decreased to 158 nm on day 3 and then jumped to 500 nm on day 7. This was also accompanied with poor quality DLS data and PDI values of 0.44 and 1 for day 3 and day 7 respectively, a sign of the aggregation of the formulation.

For drug-loaded NLCs, we can conclude that because of its nature which are composed of mixtures of solid and liquid lipids, their compatibility with either Tween 80 or Brij 78 seemed to depend on the S/L ratio, where NLCs with a higher S/L ratio (9:1) or (7:3) seemed to behave similar to SLNs which were less compatible with Tween 80 and more compatible with Brij 78, while NLCs (5:5) seemed to be compatible with both surfactants as they have equal amounts of both solid and liquid lipids.

When Brij 78 was used as the surfactant, all NLCs formulations at all S/L ratios and DRV/total lipid mass percentages, showed Z-average diameters of 300 nm on day 1, while on day 3 and 7, the Z-average diameter decreased to be ~200 nm and with a good quality DLS data, the decrease in the size could be due to the solvent evaporation. Increasing the DRV/total lipid mass percentage did not seem to affect the Z-average diameter at different time intervals, as there has been small difference in Z-average diameter (± 20 nm).

In comparison with SLNs, NLCs proved to be more stable when Brij 78 was used as a surfactant, even when the minimal amount of soybean oil was used at S/L of 9:1. A higher drug loading was achieved (DRV/total lipid mass percentage 20% w/w), while keeping a Z-average diameter of ~200 nm over a one-week period. In contrast to SLNs-Brij 78, where the highest DRV/total lipid mass obtained was 10% w/w, above which particle aggregation occurred after a week. An explanation of the enhanced drug loading of NLCs compared to SLNs, could be attributed to the fact that NLCs were composed of a mixture of a liquid and solid lipids, the oil enhances the solubility of the hydrophobic drugs and therefore enhances drug entrapment.[225]

For drug-loaded NEs-Tween 80 (Figure 2.18.I), it was the obvious that the Z-average diameter of NEs droplets at all DRV/total lipid mass percentages were the highest on day 1 with a Z-average diameters ranging between (261-284 nm). On day 1, the increase of DRV/total lipid mass percentages led to a decrease in the Z-average diameter, however the difference between the different formulations was small (~20 nm) and insignificant. This was accompanied with a low PDI (0.13- 0.16). On day 3, as the THF evaporated, the NEs droplets shrank and decreased in size to ~200 nm at all DRV/total lipid mass percentages, however the highest Z-average diameter (215 nm) was that of the NEs with DRV/total lipid mass percentage of 10% w/w and the lowest (194 nm) was that of the 20 % w/w, while the PDI remained of a small value like that on day 1. On day 7, the NEs droplets kept almost the same diameter as on day 3. These results proved that the high stability of NEs over a one-week period where the Z-average diameter and PDI almost remained the same.

Finally, drug loaded-NEs-Brij 78 showed an increase in both the Z-average diameter and PDI on day 1 accompanying the increase of the DRV/total lipid mass percentage, see Figure 2.18.J. Also, the Z-average diameters on day 1 of NEs-Brij 78 were all around 300 nm and above, unlike those of NEs-Tween 80, which were all below 300 nm. On day 3 and 7 NEs-Brij 78 showed a similar trend to that of NEs-Tween 80, where the Z-average diameter decreased compared to that of day 1 for all drug loadings and the Z-average diameter was the highest for the DRV/total lipid mass percentage of 10% w/w on both days and the lowest for the 20% w/w, and the highest PDI was that of 10% w/w on both day 3 and day 7. The Z-average diameter did not vary significantly between day 3 and day 7, which might also indicate the stability of NEs synthesised by Brij 78. In conclusion for NEs, both surfactants were equally effective.

For further studies and characterisation of drug-loaded lipid nanoformulations, Brij 78 was used as a surfactant, where all the tested formulations synthesised using it was around 200 nm after solvent evaporation and maintained this size until day 7. A DRV/total lipid mass percentage of 20% w/w was used for all formulations, except for SLNs where a DRV/total lipid mass percentage of 10% w/w was used, above this percentage particles aggregated. Liquid lipids have been shown to have a greater ability of dissolving hydrophobic drugs compared to solid lipids,[225] which could explain why higher DRV/total lipid mass percentage was achieved in NEs and NLCs (20% w/w) on contrary to (10% w/w) of SLNs.

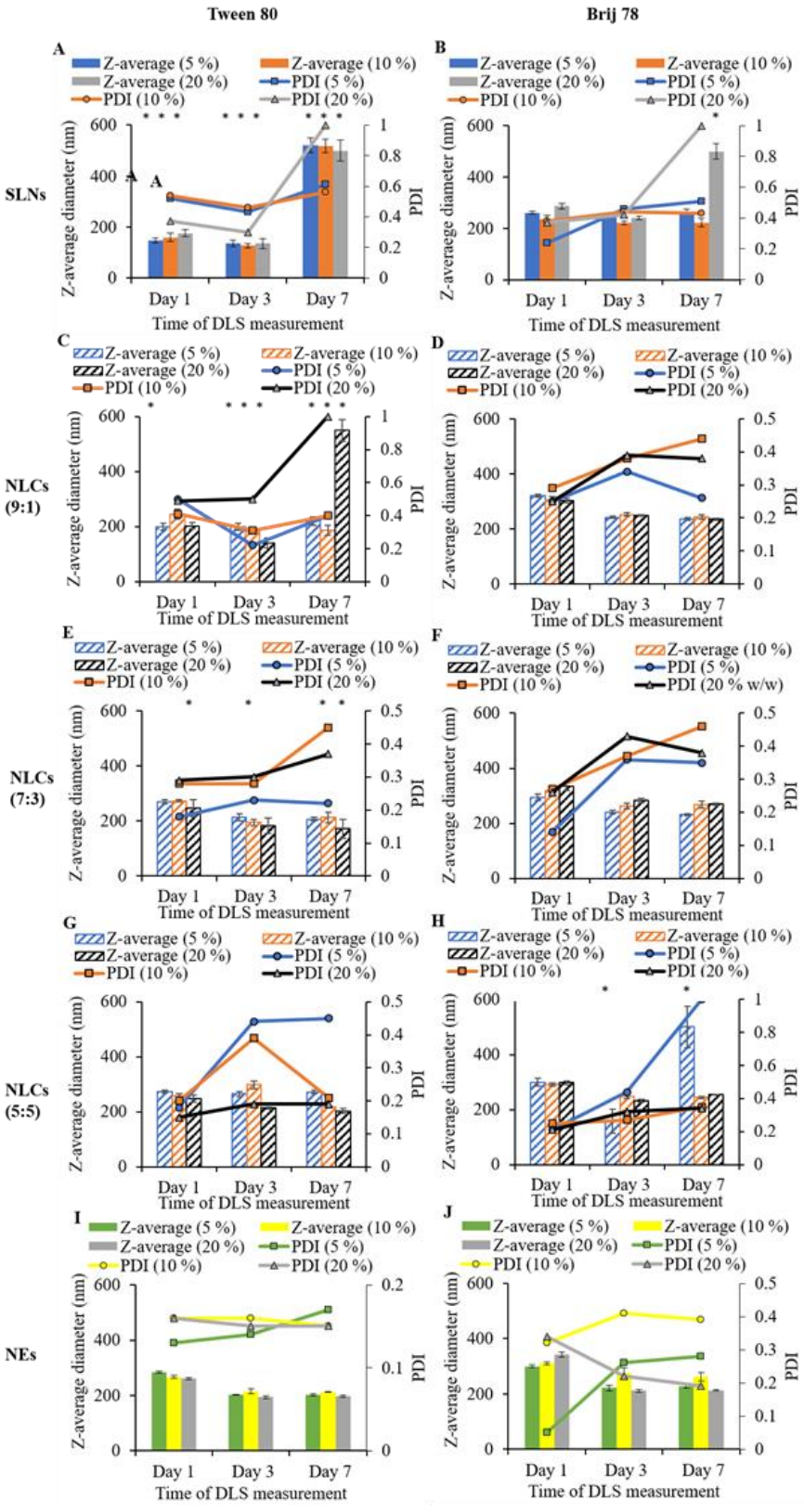

Figure 2.18 The effect of increasing DRV/lipid mass percentages (5, 10 and 20% w/w) on both the Z-average diameter and PDI of different drug loaded lipid nanoformulations on day 1, day 3 and day 7, using two types of surfactants: Tween 80 and Brij 78. The formulations were (A) SLNs-Tween 80, (B) SLNs-Brij 78, (C) NLCs (9:1)-Tween 80, (D) NLCs (9:1)-Brij 78, (E) NLCs (7:3)-Tween 80, (F) NLCs (7:3)-Brij 78, (G) NLCs (5:5)-Tween 80, (H) NLCs (5:5)-Brij 78, (I) NEs-Tween 80 and (J) NEs-Brij 78. The asterisk (*) referred to poor quality DLS data.

2.4.2.1.2.2 Measurement of colloidal stability of SLNs, NLCs and NEs in PBS and SGF by DLS

Colloidal stability of SLNs, NLCs (9:1, 7:3 and 5:5) and NEs were tested to determine the suitability of these formulations for oral administration. Samples were prepared by diluting the nanodispersions by half in PBS (pH 7.4), as this is the average pH of the intestine or SGF (pH 1.2), as examples for physiological solutions. The measurements were carried out on day 3 after the evaporation of THF. All 5 samples were stable at both pH values as indicated by DLS data in Table 2.2, where the Z-average of all samples were ~200s nm.

Table 2.2 DLS data (Z-average diameter and PDI) for SLNs, NLCs (9:1, 7:3 and 5:5) and NEs stabilised with 1% w/v Brij 78. For all formulations DRV/total lipid mass percentage of 20% w/w was used, except for SLNs where a DRV/total lipid mass percentage of 10% w/w was used instead. Measurements were carried out by diluting the nano-dispersions by half in PBS (pH 7.4) or SGF (pH 1.2). Data were represented as mean ± SD (n =3), where SD is the standard deviation and n is the number of samples measured.

Formula	In PBS		In SGF	
	Z-average diameter (nm) ± SD	PDI ± SD	Z-average diameter (nm) ± SD	PDI ± SD
SLNs	211 ± 8	0.43 ± 0.04	218 ± 12	0.54 ± 0.12
NLCs (9:1)	220 ± 11	0.39 ± 0.19	232 ± 6	0.49 ± 0.07
NLCs (7:3)	260 ± 18	0.26 ± 0.09	271 ± 9	0.31 ± 0.03
NLCs (5:5)	210 ± 5	0.17 ± 0.06	223 ± 12	0.20 ± 0.08
NEs	205 ± 3	0.12 ± 0.02	214 ± 7	0.24 ± 0.04

2.4.2.1.2.3 Encapsulation efficiency (EE%) and drug release

All five formulations showed high EE% (92.5- 95.8%), see Table 2.3. SLNs showed the highest EE% of 95.8%, as lower DRV/total lipid mass percentage (10% w/w) was used in the first place compared to other formulations. For the rest of the formulations, NLCs (7:3 and 5:5) showed slightly higher EE% of 92.8%, while that of NLCs (9:1) was 92.7%. NEs showed the lowest EE% of 92.5%. The EE% of both SLNs and NEs were significantly different ($P < 0.05$), and the EE% of both formulations were also significantly different from all types of NLCs (P

< 0.05). However, there was no statistical difference in the EE% of NLCs (9:1, 7:3 and 5:5), as P value was more than 0.05, according to the ANOVA test.

Table 2.3 Encapsulation efficiency (EE%) and drug loading (DL%) of SLNs, NLCs (9:1, 7:3 and 5:5) and NEs stabilised with 1% w/v Brij 78. For all the formulations, DRV/total lipid mass percentage of 20% w/w was used, except for SLNs where a DRV/total lipid mass percentage of 10% w/w was used instead.

Formulation type	EE (%)	DL (%)
SLNs	95.8	8.7
NLC (9:1)	92.7	15.6
NLC (7:3)	92.8	15.7
NLC (5:5)	92.8	15.7
NEs	92.5	15.6

In the drug release studies, all the five formulations showed little burst release (~2%) at the first time point (0.5 hour), which could be due to the small amount of the free unencapsulated drug adsorbed on the surface of the particles (Figure 2.19). All the formulations showed controlled drug release over 24 hours period, where ~60% occurred over 24 hours, except for NLCs (5:5), which showed 52% drug release over 24 hours duration. The slow release of NLCs (5:5) could be due to the encapsulation of DRV as a hydrophobic drug in the oil compartments, which are embedded in a solid lipid matrix.[57] Drug will need to more time to be released from both phases. On the hand, for SLNs, the potential for lipid crystallisation might expel the drug from the cores,[244] resulting is relatively faster drug release. According to the ANOVA test there was a significant difference in the accumulative drug release between the different lipid nanoformulations (P < 0.05).

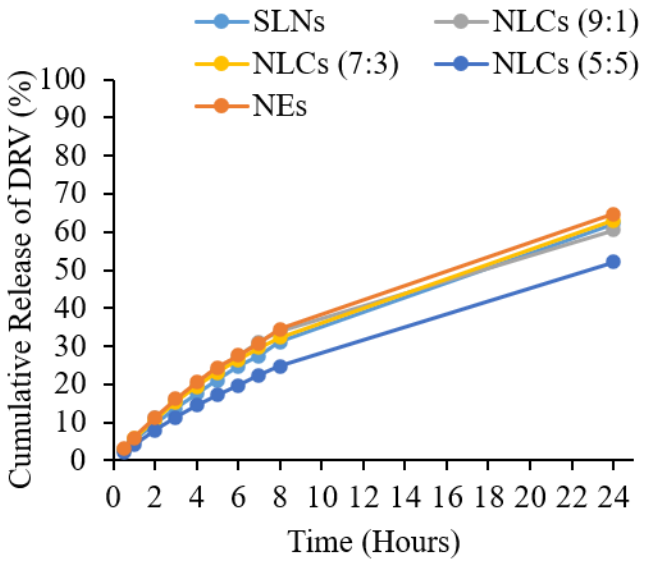

Figure 2.19 Drug release profile over 24 hours for SLNs, NLCs (9:1, 7:3 and 5:5) and NEs stabilised with 1% w/v Brij 78. For all formulations DRV/total lipid mass percentage of 20% w/w was used, except for SLNs where a DRV/total lipid mass percentage of 10% w/w was used instead.

2.4.2.1.2.4 Investigation of size and morphology of drug loaded SLNs, NLCs (5:5) and NEs by CryoSEM

Particles images obtained by CryoSEM for drug loaded SLNs, NLCs (5:5) and NEs showed their morphology and size. The choice of the samples was based that NLCs (5:5) showed the slowest drug release among all NLCs formulations, SLNs as it contained 100% solid lipid, while NEs contained 100% liquid lipid. SLNs (Figure 2.20.A), NLCs (5:5) (Figure 2.20.B) and NEs (Figure 2.20.C) were all spherical in shape with smooth surface. Analysis of the samples by DLS showed particles with a Z-average diameter ~250 nm, and the size distributions proved that SLNs had a broader size distribution than NLCs (5:5) and NEs (Figure 2.20.D).

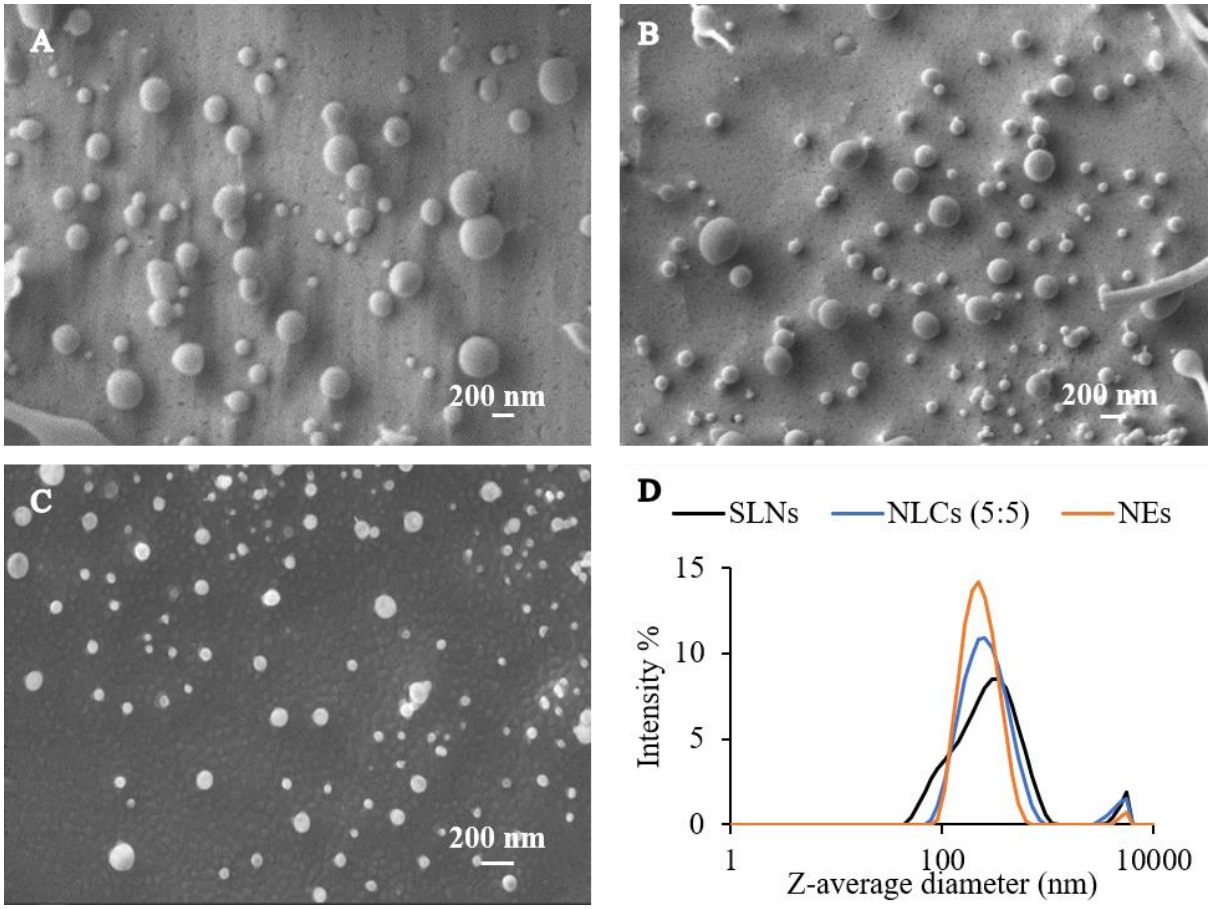

Figure 2.20 Particle characterisation of different lipid nanoformulations on day 3 prepared using cold solvent injection method and using a lipid concentration in the hydrophobic phase of 4 mg/mL and using 1% w/v Brij 78: (A) CryoSEM image of SLNs, (B) CryoSEM image of NLCs (5:5) and (C) CryoSEM image of NEs. (D) Size distribution graphs obtained by DLS for the same 3 formulations on day 3 showing monomodal distribution of size with Z-average diameter ~250 nm. DRV/lipid mass percentage for SLNs was 10% w/w, while for NLCs (5:5) and NEs was 20% w/w.

2.4.2.1.2.5 DSC investigations of drug loaded SLNs, NLCs and NEs

DSC was used to investigate the crystallinity of unformulated lipids and drug loaded lipid formulations. Figure 2.21 showed an overlay of the melting peaks of the bulk materials: Imwitor® 900 K, Brij 78, DRV and RTV and a mixture of all of these at the ratios used in the formulations, and the dried drug-loaded lipid nanoformulations: SLNs, NLCs (9:1, 7:3 and 5:5) and NEs. For the bulk materials, Imwitor® 900 K showed a melting peak at 59.7 °C, while Brij 78 showed melting peaks at 43.7 °C. DRV and RTV both showed peaks at 65 °C and 122.6 °C, respectively. The mixture showed only the peaks of Imwitor® 900 K and Brij 78, while the peaks of the drugs were not obvious which could be due to their small integration peaks, as much less amounts were used. For all the lipid nanoformulations, the Imwitor® 900 K melting peak disappeared, which could be a sign of nanoparticles formation. As discussed before in

section 2.4.1.3, the lipid melting peaks sharply drops or disappears when the lipid form nanoparticles. Unlike the blank formulations synthesised by hot solvent injection, the Imwitor® 900 K melting peak completely disappeared for the drug-loaded formulations, and the enthalpy could not be detected. This could be because the drug-loaded formulations are more amorphous than the blank ones, where the drug molecules disrupt the perfect crystal lattice of the lipid.[118] For the lipid formulations only a shifted Brij 78 melting peak was seen, the original melting peak of Brij 78 was seen at 43.7 °C but appeared between 37- 38 °C for the lipid nanoformulations indicating a disruption of the Brij 78 crystallisation due to possibly nanoparticle formation.

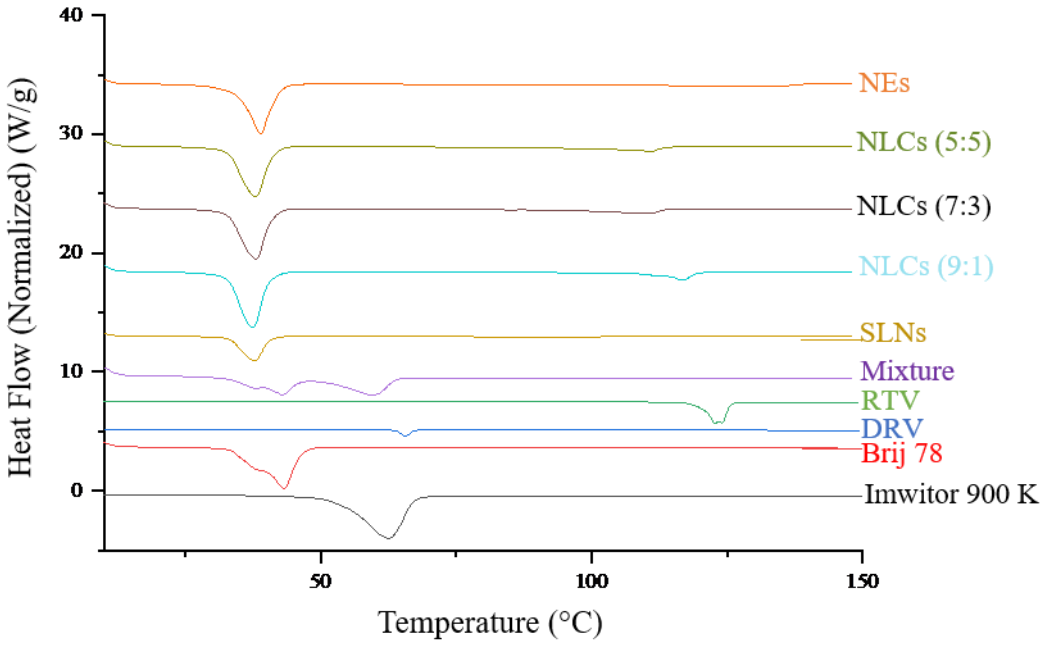

Figure 2.21 Overlay of the DSC thermograms of different lipid formulations prepared by cold solvent injection and the unformulated pure materials used for their synthesis. The mixture refers to the physical mixture of Imwitor® 900 k, Brij 78, DRV and RTV.

2.5 Conclusion

After investigating several parameters and variables in the comparative studies of SLNs, NEs and NLCs, we can conclude that both the hot and cold solvent injection methods enabled the successful synthesis of three different lipid nanocarriers in a simple and fast way that did not require complicated setups or equipment. The study allowed the understanding the relationship between the different excipients and their effect on the particle size and PDI. For the hot solvent injection method, we can conclude that increasing the lipid concentration in the hydrophobic

phase led to a subsequent increase in the particle size on both day 1 and day 3. This behaviour could be due to the increased viscosity of the hydrophobic phase or insufficient coverage of the cores with surfactants. The SLNs had bigger particle sizes compared to NEs, and NLCs have intermediate size depending on the S/L ratio. The size of all three types of lipid nanoformulations decreased on day 3 after solvent evaporation as the cores shrunk, and the optimum lipid concentration in the hydrophobic phase was 4 mg/mL. The optimum Tween 80 concentration was 1% w/v, above this concentration the particle size of both SLNs and NEs increased. The main disadvantage of this method was the residual solvent issue, where ethanol was not completely volatile after evaporation for 48 hours. The solvent removal problem was addressed in the cold solvent injection method where THF was used, that was volatile over the 48 hours period. In the cold solvent injection method, we can conclude that Brij 78 was more suitable for SLNs and NLCs (9:1), while Tween 80 was a better surfactant for NLCs (7:3) and (5:5). Imwitor® 900 K as a partial glyceride was a better solid lipid for SLNs over Dynasan®114 and Dynasan®118, as it produced particles with smaller Z-average diameter and PDI, which could be due its emulsification properties. The cold solvent injection techniques were used in the drug loading experiments, from which we can conclude that the 10% DRV/total lipid was the highest drug loading we can obtain while keeping the DLS properties within the accepted range for SLNs, while for the other lipid nanoformulations, 20% DRV/total lipid was the highest. Drug loading improved the size properties of the SLNs when compared to their blank alternatives as it limited polymorphism as it disrupted the perfect crystal structure of the solid lipids. Based on the DLS results, further studies like EE% and drug release were carried out where Brij 78 was used as a surfactant. The EE% range was 92.5- 95.8%, where drug-loaded SLNs showed the highest EE%, while NEs showed the lowest. Among all the tested formulations, NLCs (5:5) showed the most controlled drug release (52% drug release over 24 hours duration). For both hot and cold solvent injection methods, the investigation of the morphology of the synthesised formulations, were carried out using CryoSEM, which showed spherical particles with smooth surface. For the crystallinity studies by DSC, the disappearance, or the shifting of the melting peaks for the solid lipid and the shifted melting peaks of the surfactant proved the formation of lipid nanoparticles, which were more amorphous the pure solid lipid.

The significance of this comparative study was the synthesis all the three types of different lipid formulations were prepared the same way using solvent injection method, which has not been investigated before in a comparative study between these lipid formulations.

Chapter 3

Synthesis of High Drug loaded Solid Lipid Nanoparticles Stabilised by Branched Copolymers and Loaded with a Mixture of Darunavir and Ritonavir for the Treatment of HIV

3.1 Introduction

Surfactants are essential components of the SLNs which help stabilise the lipid core and decrease particles agglomeration. The choice of the type of surfactants can greatly affect the quality of the produced SLNs. Phospholipids,[93] ethylene oxide-propylene oxide copolymers,[33,102,245] sorbitan ethylene oxide copolymers,[207,246,247] and bile salts [120] are among the commercially available surfactant groups that have been commonly used in the stabilisation of SLNs. The surfactant for SLNs has to be amphiphilic i.e., containing a hydrophobic and hydrophilic components to lower the surface tension between the aqueous phase and the lipid cores.[102] In addition to the surfactants reported in the literature, amphiphilic polymers synthesised by different polymerisation reactions can be used as possible stabilisers for SLNs. Among many types of polymerisation techniques, atom transfer radical polymerisation (ATRP) is of special interest for the synthesis of polymeric stabilisers for SLNs. The benefit of using polymers synthesised by using a controlled polymerisation method such as ATRP, is that the architecture of the polymer can be controlled, where the chain length and degree of branching of the polymer can be tailored to suit different applications.[248] ATRP which is considered a reversible-deactivation radical polymerisation, was first introduced by Jin-Shan Wang and Krzysztof Matyjaszewski in 1995.[249] The naming of ATRP refers to the atom transfer step, which is a crucial element of the reaction responsible for the uniform growth of the polymer chains, where an equilibrium between the dormant (R-X) and actives species ($R^{\cdot}$) is established. $R^{\cdot}$ are kept at low concentration which helps the polymerisation process being maintained. The $R^{\cdot}$ in ATRP are produced as a result of reversible redox reaction with the use of transition metal complex (M^n-Y/Ligand) as a catalyst.[250] In this reaction, a halogen atom is abstracted from R-X and transferred to the transition metal complex which becomes oxidised. Cu(I)Br and bipyridyl (bpy) which complexes together, are among the most common catalytic systems that are used in ATRP. The initiator used is usually in the form of alkyl halide.[251] The reversible redox reaction takes place with an activation rate constant (K_{act}) and a deactivation rate constant of (K_{deact}) as shown in Scheme 3.1. To keep the polymerisation reaction going, the activation rate (K_{act}) is kept low in comparison with the deactivation rate (K_{deact}), which would limit the number of the active species and therefore limit the probability of termination reactions. As the equilibrium of the reaction is pushed to the left, the number of dormant species will be higher than the actives species. The rate of the addition of the monomer to the active species is called the propagation rate constant (K_p), on the other hand the termination reaction which is controlled due to the low concentration of the active species have rate constant of K_t.

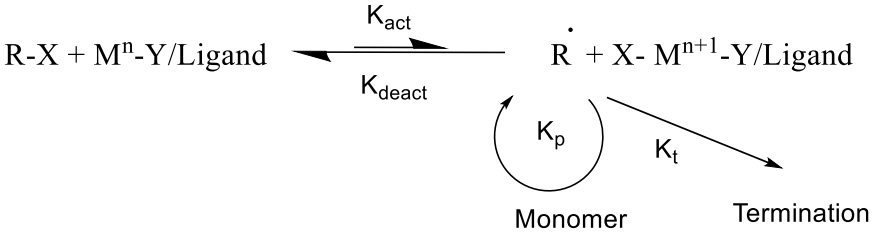

Scheme 3.1 General mechanism for ATRP, where the alkyl halide (R-X) is in equilibrium with the alkyl radical (R·) which can be propagated in the presence of a monomer at a rate of K_p or terminated at a rate of K_t.

ATRP allows the incorporation of hydrophobic and hydrophilic moieties to produce amphiphilic polymeric structures. In addition, ATRP allows the synthesis of polymers with high molecular weight and branched structures, which are hypothesised to act as better surfactants for nanoparticles compared to low molecular weight surfactants and linear polymers.[252] Branched polymers provide better coverage for the hydrophobic cores of the nanoparticles, where the branched nature of the polymer provides several amphiphilic polymeric chains on a single molecule. This structure allows multiple points of attachment between the hydrophobic moiety of the polymeric surfactant and the solid lipid cores of the SLNs.[252]

In Chapter 2, the results showed that hot solvent injection method, where Compritol 888 ATO® was used as a solid lipid and Tween 80 was used as a surfactant produced blank-SLNs with small Z-average diameter (~ 200 nm) on day 1. However, the main disadvantage of this method was the presence of ethanol as a residual solvent after stirring the SLNs dispersion for 48 hours. Herein, we aim to synthesise SLNs loaded with DRV and RTV with 8:1 weight ratio, respectively using hot solvent injection, followed by freeze-drying to remove both water and the water miscible organic solvent. Another aim of this study was to obtain high drug loaded SLNs (HDL-SLNs), with targeted DRV loading of 50% w/w. A poly-oligo (ethylene glycol) methacrylates (*p*(OEGMA)) based branched polymer was synthesised by ATRP and tested as a potential stabiliser for HDL-SLNs, as it might provide better stabilisation for SLNs especially with such high drug loading.

3.2 Chapter objective

This chapter was aimed at the formation of amphiphilic branched copolymer for the stabilisation of HDL-SLNs. For that purpose, DBiB initiator was synthesised by esterification reaction and was characterised by ^{1}H, ^{13}C nuclear magnetic resonance spectroscopy (NMR) and mass spectrometry. That initiator was then used to synthesise DBiB-*p*(OEGMA$_{10}$-*co*-EGDMA$_{0.6}$) by ATRP, which is a branched amphiphilic copolymer (Figure 3.1). The naming of the polymer indicated that DBiB was used as the initiator, the targeted degree of polymerisation was 10 and degree of branching was 0.6. This polymer was characterised by ^{1}H NMR and gel permeation chromatography (GPC). Another aim of this study was to optimise the solvent injection method to fit the use of branched copolymer as a stabiliser for HDL-SLNs, and to fit the high targeted drug loading made of combination of DRV and RTV. Therefore, several parameters were tested to optimise the hot solvent injection method for the synthesis of HDL-SLNs which included: 1) the heating temperature of the hydrophobic phase, 2) the heating time of the hydrophobic phase, 3) stirring time of the HDL-SLNs dispersions before freeze-drying, 4) the type of the solid lipid and 5) the type of surfactants, where DBiB-*p*(OEGMA$_{10}$-*co*-EGDMA$_{0.6}$) was tested as a potential stabiliser for HDL-SLNs in comparison with commercially available surfactants like soybean lecithin (SBL) and Tween 80. SLNs with three varied compositions were synthesised and tested for the different synthesis variables, these formulations were: blank-SLNs, HDL-DRV-SLNs, HDL-DRV-RTV-SLNs, with no drugs, DRV-loaded and DRV/RTV (8:1)-loaded, respectively. The abbreviation HDL-SLNs was used in this chapter to refer to both HDL-DRV-SLNs and HDL-DRV-RTV-SLNs to distinguish them from blank-SLNs.

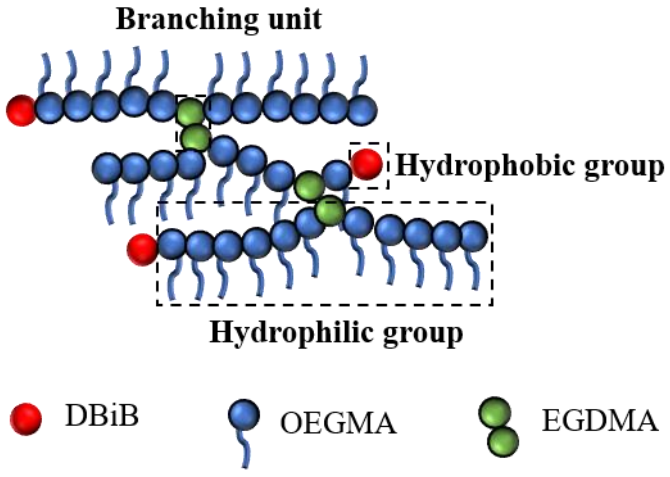

Figure 3.1 Structural representation of an amphiphilic branched copolymer with hydrophobic chain end (DBiB), hydrophilic monomer, oligo (ethylene glycol) methacrylate (OEGMA) and branching unit, ethylene glycol dimethacrylate (EGDMA).

3.3 Materials and methodology

3.3.1 Materials

3.3.1.1 Materials for the synthesis and characterisation of ATRP initiator and branched copolymer

Triethylamine (TEA, ≥99.5%), sodium hydrogen carbonate ($NaHCO_3$, 99.7%), magnesium sulphate ($MgSO_4$, ≥99.5%), petroleum ether (analytical grade), N, N-dimethylformamide (DMF, HPLC-grade) and tetrahydrofuran (THF, 99%) were purchased from Thermo Fischer Scientific, Leicestershire, UK. α-bromoisobutyryl bromide (98%), 1-dodecanol (99%), Oligo (ethylene glycol) methyl ether methacrylate (OEGMA, M_w = 300 $g.mol^{-1}$, 99%), ethylene glycol dimethacrylate (EGDMA, M_w = 198.2 $g.mol^{-1}$, 98%), 2,2'-bipyridine (bpy, 99%), copper (I) chloride (Cu(I) Cl, 99%), aluminium oxide (Al_2O_3, activated, basic, Brockmann I, 99.99%), aluminium oxide (Al_2O_3, activated, neutral, Brockmann I, 99%), silica gel (≥99%), dichloromethane (DCM, 99%), hexane (HPLC grade), ethyl acetate (HPLC grade), isopropyl alcohol (IPA, 99.7%), NMR solvents $CDCl_3$ (99.8 atom % D) were purchased from Sigma–Aldrich, Irvine, UK, and used as received.

3.3.1.2 Materials for the synthesis and characterisation of HDL-SLNs by solvent injection

Glycerol dibehenate (Compritol ATO 888®) was a generous gift from Gattefossé, France. Tween 80 (≥99%), DRV (≥98% (HPLC) and RTV (≥98% (HPLC) were supplied from Sigma–Aldrich, Irvine, UK. Glyceryl monostearate (GMS, ≥99%),) and soybean lecithin (SBL, 90%) were purchased from Alfa Aesar, Lancashire, UK.

3.3.2 Methodology

3.3.2.1 Synthesis of dodecyl α-bromoisobutyrate initiator

In this work, an ATRP initiator with dodecyl functionality (Figure 3.2) was synthesised by esterification reaction according to a method reported by Hou *et al.*[253]

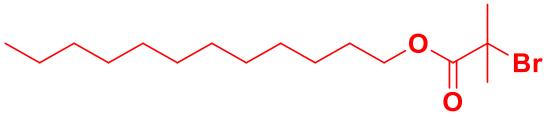

Figure 3.2 Chemical structure of dodecyl α-bromoisobutyrate

1-dodecanol (16 g, 86. mmol, 1.0 eq.) and TEA (17.37 g, 172 mmol, 1.2 eq.) were dissolved in DCM in a two-neck round bottom flask (RBF), the mixture was cooled in an ice bath to 0°C for 10 minutes. α-bromo-isobutyryl bromide (29.61 g, 128.80 mmol, 1.2 eq.) was then added dropwise using a dripping funnel to the stirring mixture under N_2. After complete addition, the reaction was left to stir at room temperature for 24 hours. The mixture was then filtered through Whatman filter paper, the solution was rotary evaporated and dissolved in 50 mL DCM and washed with distilled water (3 x 300 mL), $NaHCO_3$ (3 x 300 mL), and the organic layer was dried over anhydrous $MgSO_4$. After filtration, the solution was passed through basic alumina column and eluted with DCM. TLC experiments showed the presence of some impurities, so the product was passed through silica gel column and was eluted with hexane/ethyl acetate mixture (90:10). The solvent was evaporated in a vacuum oven to yield 14.5 g (99 %) pale yellow liquid.

DBiB was characterised by ^{1}H NMR, ^{13}C NMR, and mass Spectrometry and elemental analysis as shown the section 3.4.1. ^{1}H NMR (400 MHz, $CDCl_3$) δ (ppm) = 0.88 (t, 3H), 1.19 (m, 18H), 1.67 (m, 2H), 1.93 (s, 6H), 4.16 (t, 2H). ^{13}C NMR (100 MHz, $CDCl_3$) δ (ppm) = 77.33 (s), 77.01 (s), 76.70 (s), 66.17 (s), 55.99 (s), 31.91 (s), 30.80 (s), 29.72 – 29.02 (m), 28.35 (s), 25.79 (s), 22.68 (s), 14.10 (s). Elemental analysis: Calculated (%): ($C_{16}H_{31}O_2Br$) = C, (57.31%); H (9.32%). Experimental (%) = C (57.78%), H (9.35%). Mass Spectrometry: DBiB mass = 335 and the Chemical ionisation mass spectroscopy (CI-MS) experimentally determined $[M+NH_4]^+$ m/z = 352.

3.3.2.2 Synthesis of branched P(OEGMA) by ATRP

OEGMA (4 g, 13.3 mmol, 10 eq.), EGDMA (0.15 g, 0.8 mmol, 0.6 eq.), 2,2'-bipyridyl (0.41 g, 2.6 mmol, 2 eq.) and DBiB (0.44 g, 1.3 mmol, 1 eq.) were added to a mixture of isopropanol/water (IPA/H_2O; 92.5, 7.5 v/v, 6.06: 0.38 mL, 55% w/v (monomer/solvent). The reaction mixture was placed in one-neck RBF equipped with magnetic stirrer. The RBF was sealed and degassed with dry N_2 for 5 minutes. CuCl(I) (0.13 g, 1.3 mmol, 1 eq.) was added to the reaction mixture, which was further degassed with nitrogen for further 5 minutes. The RBF

was placed in oil bath at 40 °C and left for 24 hours for complete polymerisation and branching. The reaction was terminated by inactivation of the active copper by exposure to air and the addition of THF. To purify the polymer, the copper catalyst was removed by passing the crude polymer mixture through neutral Al_2O_3 column which was eluted with THF. THF was removed *in vacuo*, and the crude polymer was then twice precipitated by dropwise addition in petroleum ether placed in ice bath at 0 °C. The used solvents were decanted, and the polymer was collected using rotary evaporator to remove residual solvents. The polymer was left to dry in a vacuum oven for 24 hrs at 40 °C and was kept at room temperature in a glass vial to be used later. The reaction was monitored by ^{1}H NMR and worked up when >90 % conversion was obtained. The polymer was analysed by ^{1}H NMR and GPC.

3.3.2.3 Characterisation of ATRP initiator and branched copolymer

3.3.2.3.1 Mass spectrometry

Chemical ionisation mass spectrometry (CI-MS) data was obtained using Agilent GCQTOF 7200 (Agilent Technologies Inc., Wilmington, Delaware, USA) using ammonia gas.

3.3.2.3.2 NMR spectrometry

Nuclear magnetic resonance (NMR) data was recorded using Bruker DPX-400 spectrometer (Bruker Bioscience, Billerica, Massachusetts, USA) operating at a frequency of 400 MHz for ^{1}H NMR and 100 MHz for ^{13}C NMR. Solvent used for NMR spectroscopy analysis was $CDCl_3$.

3.3.2.3.3 Gel permeation chromatography (GPC)

Molecular weights and molecular weight distributions were detected *via* triple detection GPC using Malvern Viscotek instruments. In triple detection GPC refractive index, viscometry and light scattering detectors were used to calculate the absolute molecular weight of the polymer. The instrument was equipped with two Viscotek D6000 columns, guard column, GPCmax VE2001 auto sampler and triple detector array TDA305 (refractive index, light scattering and viscometer). The mobile phase used was DMF containing 0.01 M lithium bromide with a flow rate of 1 mL/minute at 60 °C.

3.3.2.4 Synthesis of HDL-SLNs by solvent injection method

HDL-SLNs were synthesised using solvent injection method as reported in the thesis of a previous member of the group M. Omir, with some modifications to make the method simpler and more reproducible.[254] Unlike M. Omir's method which required the injection of the hydrophobic phase into the hydrophilic phase at 45° angle placed in a two neck RBF, our preliminary studies showed that neither the angle of injection nor the shape of the RBF made a difference in the size of the produced SLNs. The injection had to be carried out in the formed vortex of the hydrophilic phase, this was the only requirement, according to our results. Another modification was the injection of the hydrophobic phase had to be carried out quickly at one time using a 6 mL syringe. This was in contrary to M. Omir method, which included injecting the hydrophobic phase using a 3 mL syringe in two times, therefore the two portions of the hydrophobic phase would have different temperatures, leading to the formation of two populations of the particles, therefore the method was not reproducible. Briefly our modified method was as follows: a hydrophobic phase was made of 3.6 mg Compritol 888 ATO® or GMS, 12.8 mg DRV and/or 1.6 mg RTV dissolved in 4 mL IPA, which was placed in a 14-mL vial. For blank-SLNs no drugs were added. The hydrophobic phase was heated to 70 or 80 °C in an oil bath for varied duration (2 or 4 minutes) using a hot plate and a magnetic stirrer at 300 rpm. The hydrophobic phase was heated till all solids were dissolved, which was indicated by clarity of the solution. The hydrophobic phase was then rapidly injected using a hypodermic needle (21 g, 50 mm) into the vortex of stirring (300 rpm) aqueous phase (20 mL) consisted of 0.3 mg/mL surfactant solution in DI water at ambient temperature and placed in a two-necked RBF (50 mL). The surfactants tested were DBiB-*p*(OEGMA$_{10}$-*co*-EGDMA$_{0.6}$), Tween 80 or SBL either on their own or in combination with each other. The final concentration (total solids) of the resultant HDL-SLNs dispersions was 0.15-1 mg/mL, and DRV concentration of 0.53 mg/mL for drug loaded formulations, for dual drug-loaded formulations the DRV/RTV mass ratio was kept at 8:1. The SLNs dispersions were left to stir for 3-15 minutes to ensure full mixing of both phases. The dispersion was then freeze-dried to remove the IPA and deionised water.

3.3.2.5 Freeze-drying of HDL-SLNs

SLNs dispersions were freeze dried in the same day of preparation to remove IPA and deionised water to get stable solidified SLNs. 1 mL of the HDL-SLNs dispersions were place in 4-mL vials and were frozen using liquid nitrogen. The freeze-drying process was carried out using a condenser temperature of -100 °C, and vacuum of <40 μbar for 4 days using a VirTis BenchTop K freeze dryer (SP Scientific, Ipswich, UK).

3.3.2.6 Characterisation of the size of HDL-SLNs by DLS

Dynamic light scattering (DLS) was the main analytical method used to determine the size of HDL-SLNs. The setting of measurements was the same as described in Chapter 2, except for concentration of the measured sample, which was 0.15-1 mg/mL.

3.4 Results and discussion

3.4.1 Characterisation of the synthesised DBIB initiator

To obtain branched copolymers with amphiphilic characters, the use of hydrophobic initiator in the ATRP reaction was essential. The key role of the initiator was the determination of the number of growing polymer chains.[255] The number of the growing polymer chains will be constant and equal to the added amount of the initiator (if the initiation step is rapid enough and the termination rate can be neglected). A dodecyl α-bromoisobutyrate (DBiB) initiator was synthesised (see Scheme 3.2) by an esterification reaction between the hydroxyl groups of 1-dedcanol and α-bromoisobutyryl bromide using a well-established procedure.[256] The esterification reaction was catalysed by TEA at 0 °C, where $Et_3NH^+Br^-$ salt was formed upon the addition of α-bromoisobutyryl bromide. After stirring for 24 hours the formed salt was filtered and the purified product was characterised by ^{1}H NMR, ^{13}C NMR CI-MS and elemental analysis.

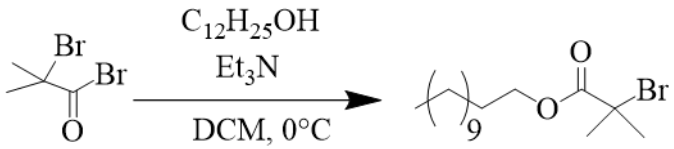

Scheme 3.2 Synthesis of dodecyl α-bromoisobutyrate (DBiB) by esterification reaction.

The successful synthesis reaction of the DBiB was shown in the ^{1}H NMR spectrum of the purified product as seen in Figure 3.3.A, where a singlet peak attributing to two CH_3 groups with the label (e) was shown at 1.9 ppm. If a residual starting material (α-bromoisobutyryl bromide) was still present, a secondary singlet peak would have appeared up field. ^{13}C NMR (Figure 3.3.B) further proved the purity of the initiator. CI-MS (Figure 3.4) agreed with the desired product, where DBiB exact mass = 335 and the CI-MS experimentally determined $[M+NH_4]^+$ m/z = 352.

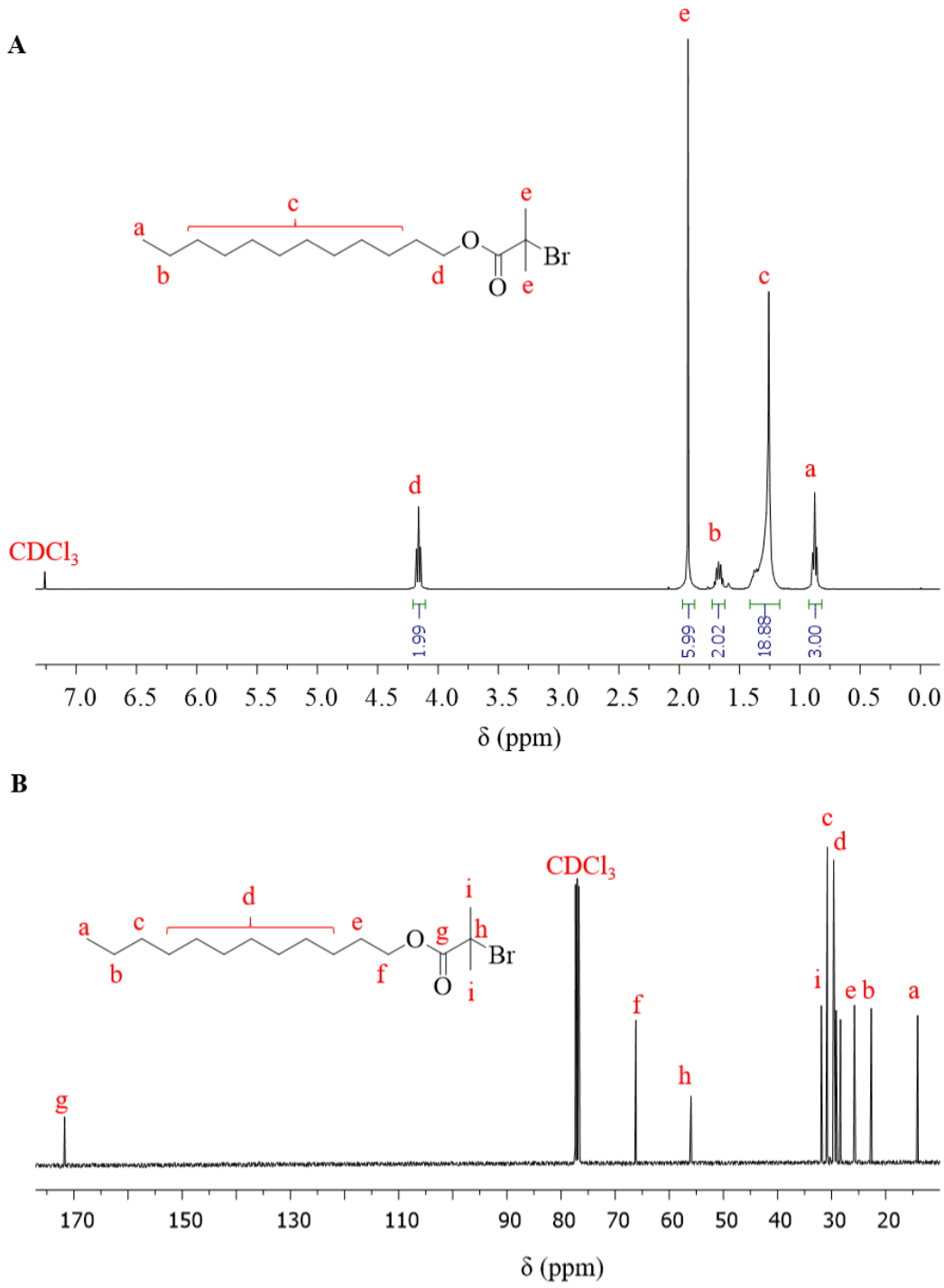

Figure 3.3 Nuclear magnetic resonance spectra of dodecyl α-bromoisobutyrate (DBiB) A) ^{1}H NMR spectra (CDCl3, 400 MHz) and B) ^{13}C NMR spectra (CDCl3, 100 MHz).

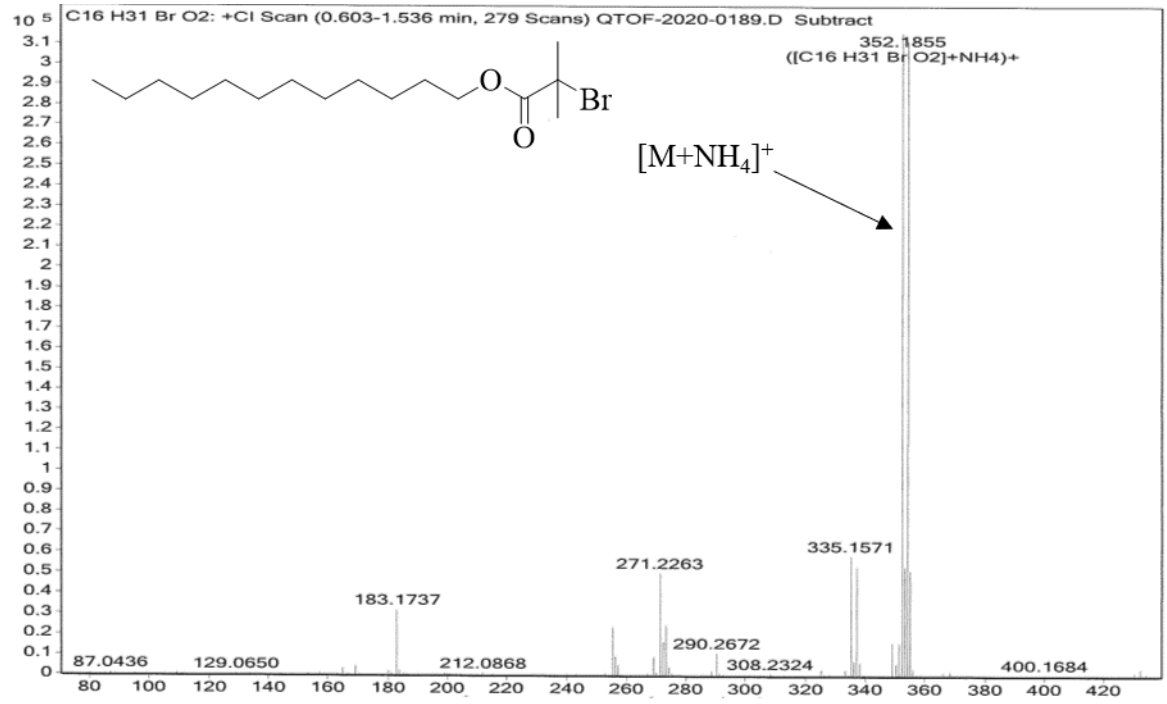

Figure 3.4 CI-MS (NH_3) analysis of DBiB

.

3.4.2 Characterisation of the synthesised branched copolymers

In the synthesis of DBiB-*p*(OEGMA$_{10}$-*co*-EGDMA$_{0.6}$) as the amphiphilic branched copolymer, the hydrophilic OEGMA (number average degree of polymerisation (DP_n) = 4-5 ethylene glycol units, M_n = 300 g.mol^{-1}) was used as a monomer along with divinyl monomer (EGDMA). Divinyl and vinyl were statistically added, in a ratio of less than one branching point per each primary chain, to avoid *in situ* cross-linking and gelation.[257] EGDMA as a brancher was added at EGDMA/initiator ratio of 0.6/1 and the reaction was left for 24 hours for complete polymerisation and maximum branching. The polymerisation was carried out under aqueous conditions, as reported in previous studies,[258–261] where water accelerate the polymerisation of OEGMA. The polymerisation was conducted at 40 ^{o}C using CuCl:bpy as a catalyst, and isopropyl alcohol/water (IPA:H_2O, 92.5:7.5 v/v) at 55 % w/v (monomer:solvent) as the solvent mixture, as shown in Scheme 3.3.

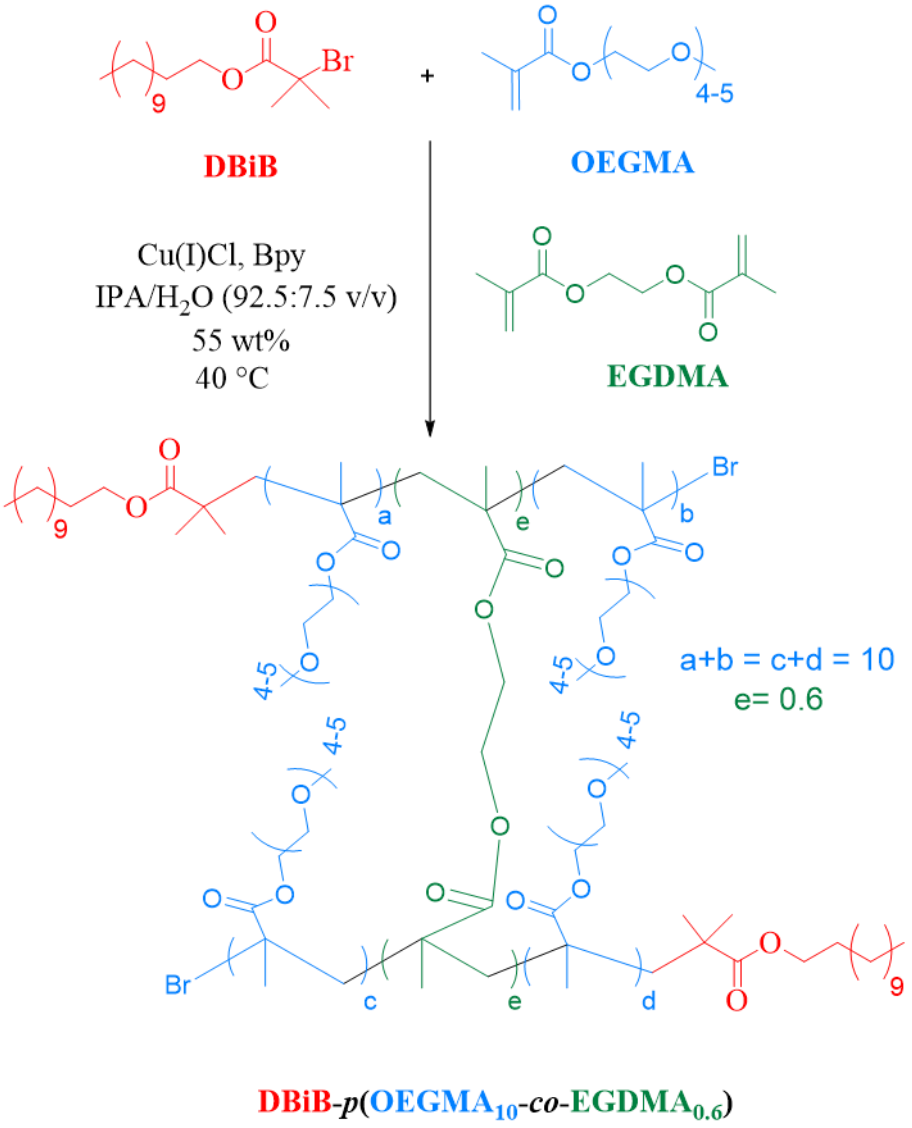

Scheme 3.3 Synthesis of amphiphilic DBiB-p(OEGMA$_{10}$-co-EGDMA$_{0.6}$) using hydrophilic monomer, oligo (ethylene glycol) methacrylate (OEGMA) and branching unit, ethylene glycol dimethacrylate (EGDMA) and the hydrophobic initiator DBiB.

A relatively low degree of polymerisation (DP_n) was targeted, DP_{10}, for the ATRP of OEGMA. Targeting small DP_n meant that the hydrophobic chain represented a considerable percentage of the overall molecular mass of the polymer, which was selected to give the polymer amphiphilic character to allow the polymer to act as a successful surfactant for SLNs. ^{1}H NMR was used to monitor the polymerisation reaction, and to determine the conversion. A high conversion was targeted (> 99%) which was important in the synthesis of branched polymers. Conversion was determined by the disappearance of the vinyl monomer peaks *via* ^{1}H NMR, see Figure 3.5. A neutral alumina column was used for the removal of the catalysts and the produced copolymer was purified by precipitation into petroleum ether (40/60).

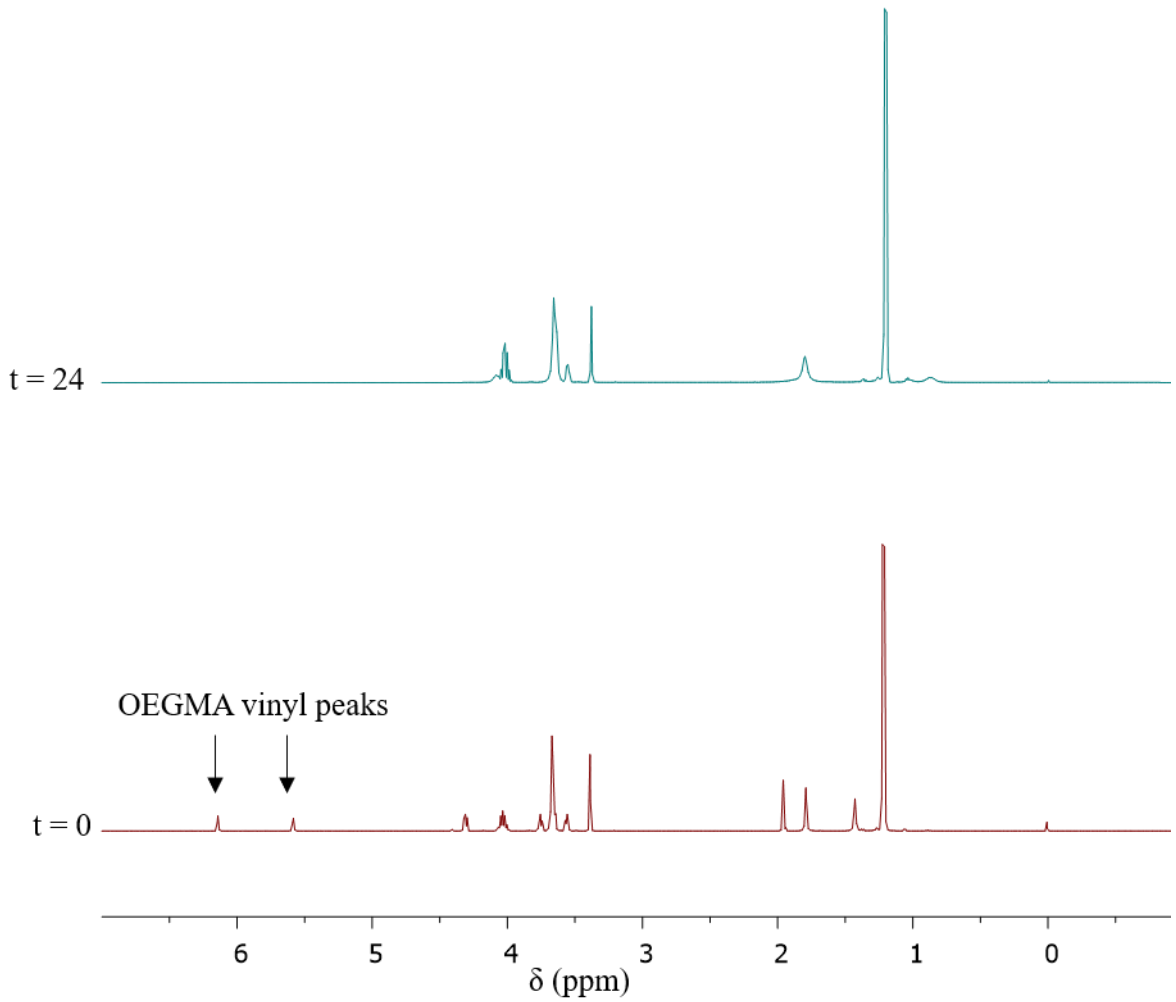

Figure 3.5 ^{1}H NMR spectra (CDCl3, 400 MHz) for DBiB-p(OEGMA$_{10}$-co-EGDMA$_{0.6}$) sampled at the beginning of the polymerisation (t=0 hours) and at the end of the polymerisation (t = 24 hours) which was indicated by the absence of monomer OEGMA vinyl peaks at 5.5 and 6.1 ppm.

^{1}H NMR and Gel permeation chromatography (GPC) were used to characterise the produced branched copolymer as shown in Table 3.1. $[M]_0 / [I]_0$ was calculated by ^{1}H NMR at T_0 by assigning the signal of vinyl protons of the monomer 1H δ = 5.6 and 6.1 ppm, and the of protons of the DBiB initiator, 3H δ = 0.88 ppm.

Table 3.1 ^{1}H NMR (CDCl3, 400 MHz) and GPC (DMF/0.01 M LiBr Eluent 60 ^{o} C) data for branched p(OEGMA). $[B]_0$, $[I]_0$ and $[M]_0$ are the concentrations of the brancher, initiator and monomer at t_0.

Target Polymer	^{1}H NMR			GPC		
	$[B]_0 / [I]_0$	$[M]_0 / [I]_0$	Conversion (%)	M_w (g mol^{-1})	M_n (g mol^{-1})	Đ (M_w/ M_n)
DBiB-*p*(OEGMA$_{10}$-*co*-EGDMA$_{0.6}$)	0.60	10	>99	32,167	10,809	2.98

Figure 3.6 compares the refractive index (RI) and the right-angle light scattering (RALS) chromatograms of DBiB-*p*(OEGMA$_{10}$-*co*-EGDMA$_{0.6}$). Branched polymers have a higher weight average molecular weight (M_w) and usually are eluted at lower retention volumes when compared to the linear polymers. For branched polymers, a broad distribution of molecular weights is quite common using both detectors, RI and RALS. For the RALS detector, it is more sensitive to higher molecular weight polymer such as the branched polymer formed with the brancher (EGDMA) and therefore the scattering of light is usually dominated by small number of high molecular weight polymers. On the other hand, the RI detector focuses on the concentration of individual separated portions of the polymer solution. From Figure 3.6, we can conclude that branched polymers of high molecular weight existed as confirmed by the low elution volume in the RALS chromatograms, which was in correlation with the RI chromatogram, which showed low concentration of high molecular weight polymers at the same retention volume.

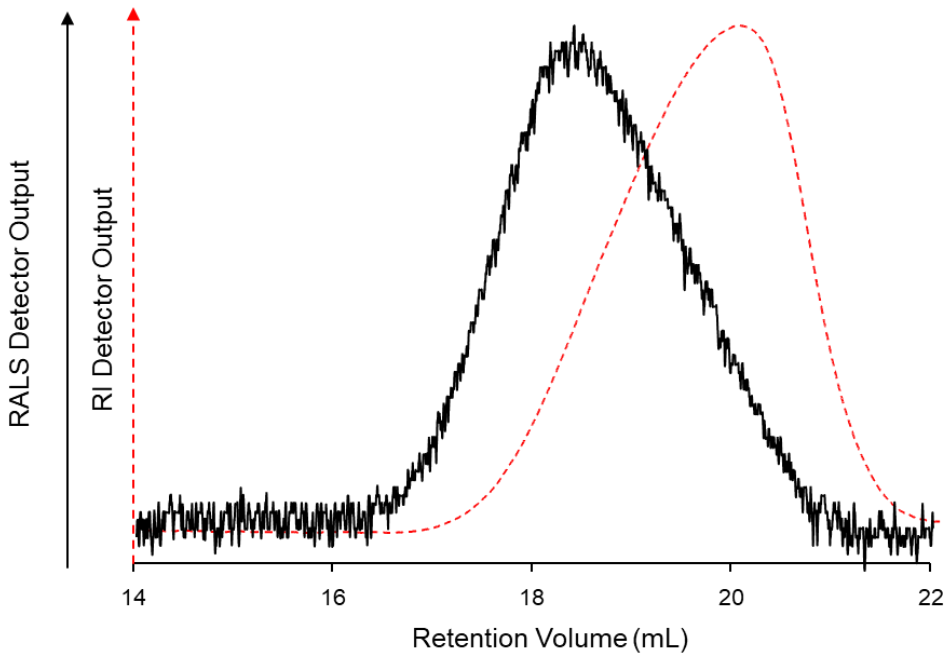

f

Figure 3.6 Overlay of Triple detector size exclusion chromatography (TD-SEC) chromatograms of DBiB-p(OEGMA$_{10}$-co-EGDMA$_{0.6}$) comparing RI detector output (red, dashed line) and RALS detector output (black, solid line)

.

3.4.3 Optimisation of the synthetic parameters of HDL-SLNs by solvent injection

Solvent injection was used as the synthesis technique of HDL-SLNs in this study. DBiB-*p*(OEGMA$_{10}$-*co*-EGDMA$_{0.6}$) has previously been investigated as potential stabilisers for HDL-SLNs, it was found to be the optimum polymer (in terms of SLNs stability, sustained release, and high drug loading) for the stabilisation of SLNs loaded with Maraviroc in a study by M. Omir *et al.*[254] In this study, the solvent injection method was optimised for the use of DBiB-DBiB-*p*(OEGMA$_{10}$-*co*-EGDMA$_{0.6}$) as the stabiliser for SLNs loaded with DRV/RTV (8:1), see Figure 3.7. Among the synthetic parameters tested were the heating temperature of the hydrophobic phase, the stirring time of both the hydrophobic and hydrophilic phases, type of solid lipid and the type of surfactant and surfactant combination.

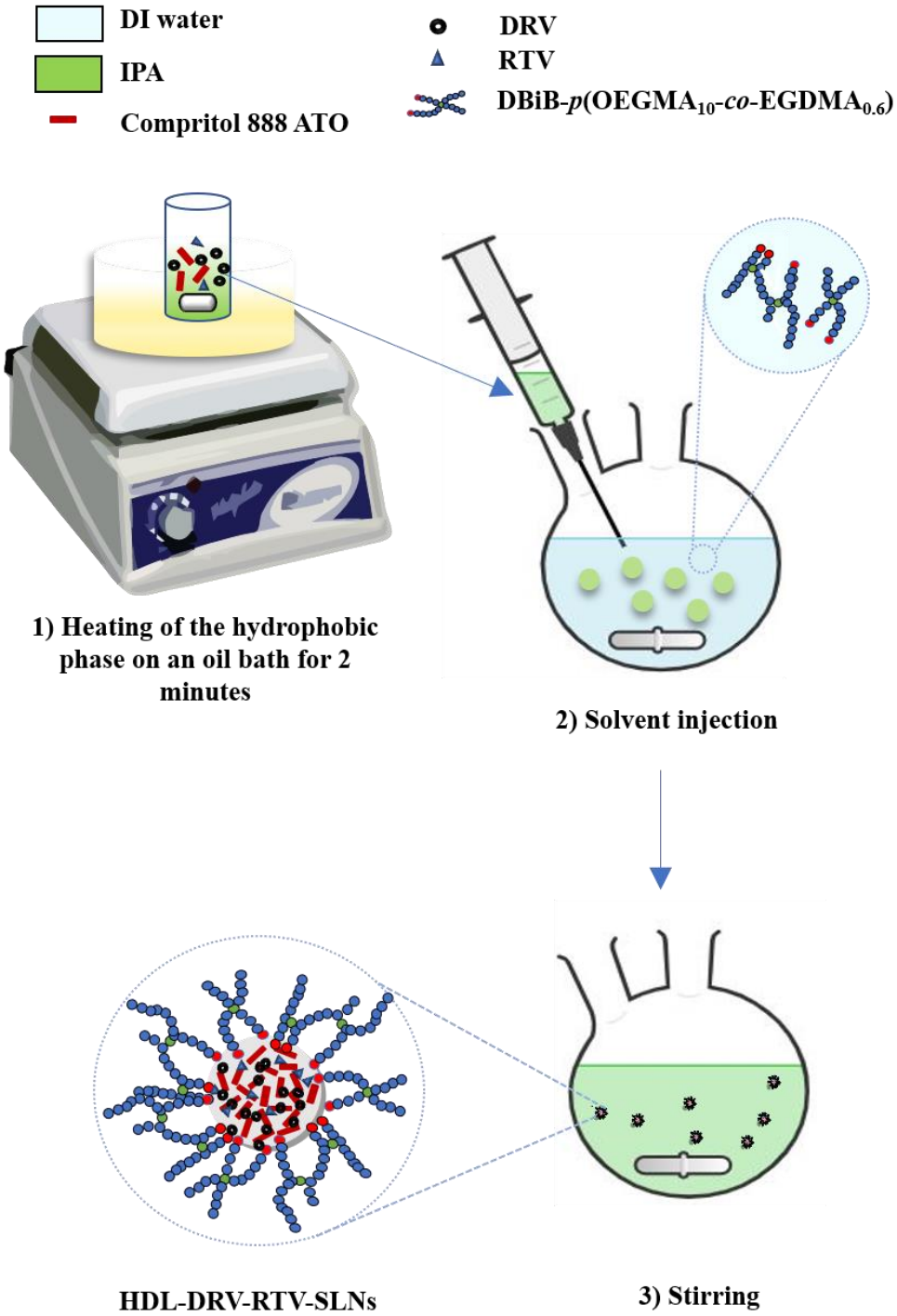

Figure 3.7 Different steps of the synthesis of HDL-DRV-RTV-SLNs by optimised solvent injection method. Step 1: heating the hydrophobic phase at 80 °C for 2 minutes and stirring at 300 rpm. Step 2: rapid injection of the hydrophobic phase into the stirring (300 rpm) hydrophilic phase made of 0.3 mg/mL aqueous solution of DBiB-p(OEGMA$_{10}$-co-EGDMA$_{0.6}$) at room temperature using a hypodermic needle. Step 3: stirring the formed HDL-SLNs suspension for 3 minutes at 300 rpm.

In addition to the dual drug-loaded HDL-DRV-RTV-SLNs, other formulations were synthesised as controls including blank-SLNs and HDL-DRV-SLNs which contained no drug

and single drug-loaded respectively, see Figure 3.8. Both types of HDL-SLNs dispersions had the same concentration of DRV (0.53 mg/mL), the only difference was that HDL-DRV-RTV-SLNs dispersions also included RTV, with keeping DRV/RTV at 8:1 mass ratio.

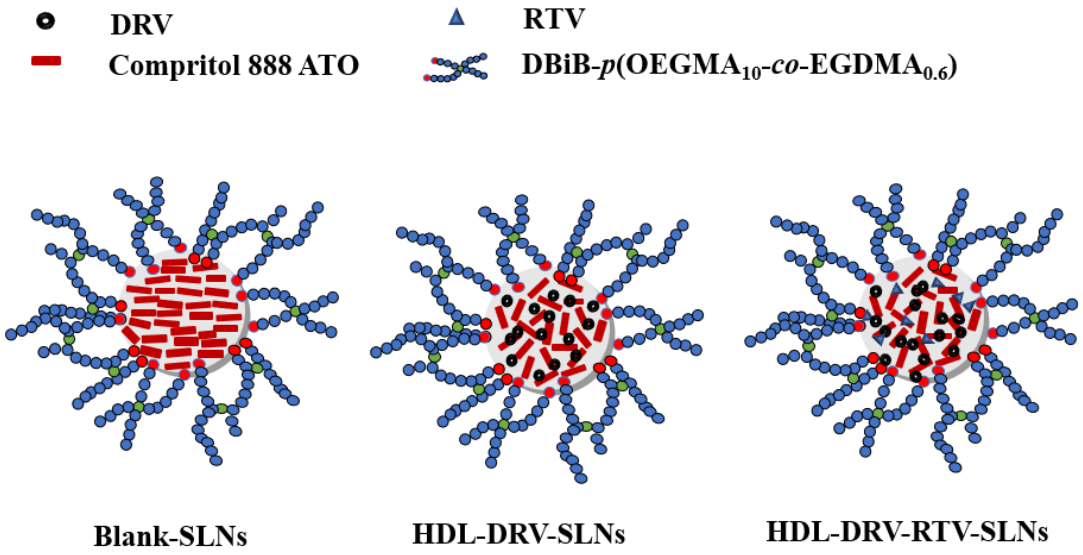

Figure 3.8 Different SLNs types synthesised by solvent injection and stabilised by DBiB-p(OEGMA$_{10}$-co-EGDMA$_{0.6}$)

.

3.4.3.1 The effect of varying the heating temperature of the hydrophobic phase on the DLS data of blank-SLNs and HDL-SLNs dispersions.

Heating of the hydrophobic phase is very important in the solvent injection method to ensure complete dissolution of the high melting point solid lipids and the hydrophobic drugs in the water miscible organic solvent. IPA was chosen as a water miscible solvent for the hydrophobic phase as it has boiling point of 82.6 °C which is suitable for dissolving the used lipid which was Compritol 888 ATO® that has a melting point of ~70 °C.[113] Two different temperatures were tested: 70 °C and 80 °C, both temperatures were below the boiling points of IPA.

According to DLS data in Figure 3.9, it was obvious that increasing the heating temperature of the hydrophobic phase from 70 °C to 80 °C led to a decrease of both the Z-average diameter and PDI of blank-SLNs and HDL-SLNs. Where the Z-average diameter for blank-SLNs, HDL-DRV-SLNs and HDL-DRV-RTV-SLNs were 499, 600 and 641 nm, respectively at 70 °C. On the other hand, when the hydrophobic phase was heated to 80 °C, the Z-average diameter decreased to 152, 224 and 290 nm, respectively. This could be explained by the decrease of

viscosity of the hydrophobic phase when heated to a higher temperature (80 °C), which in turn might lead to a decrease in the droplet size of the hydrophobic phase when leaving the needle and entering the aqueous phase as explained in chapter 2. Also, the decrease in the viscosity would lead to increasing of diffusion rate of the lipid phase when injected in the aqueous phase, leading to smaller particles with lower PDI as the particles would not be in a close proximity to each other, limiting aggregation.[179] It was noted that the drug composition of HDL-SLNs played a role in determining the size of the produced particles. The Z-average diameter of produced SLNs at both heating temperatures was ascending as follows: blank-SLNs< HDL-DRV-SLNs< HDL-DRV-RTV-SLNs, where the blank-SLNs had the smallest particle size, and drug loading led to particle size increase. In conclusion, formulations synthesised with heating the hydrophobic phase at 80 °C showed smaller Z-average and PDI than those prepared by heating the hydrophobic phase at 70 °C. Therefore, heating the hydrophobic phase to 80 °C was the preferred temperature for the solvent injection method and was used for all other experiments in this study.

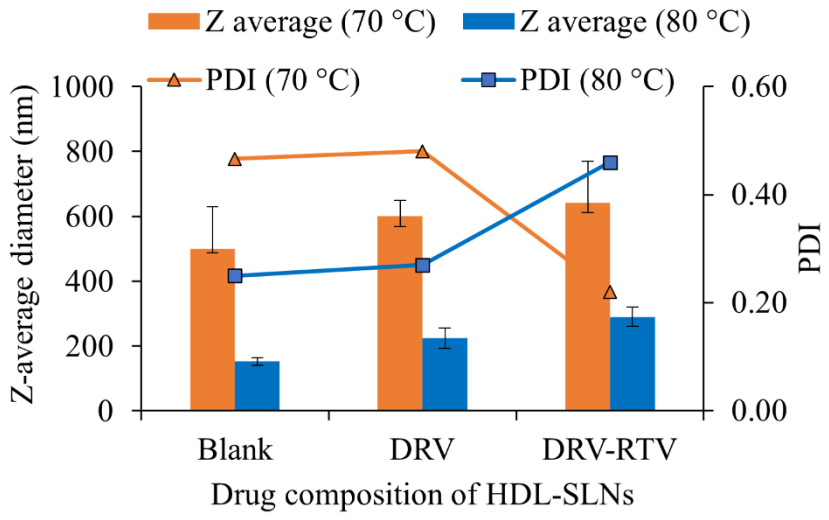

Figure 3.9 The effect of varying the heating temperature of the hydrophobic phase: 70 °C or 80 °C on the DLS data (Z-average diameter and PDI) of blank-SLNs and HDL-SLNs dispersions on day 1. The heating duration (2 minutes) and stirring time of SLNs-dispersions (3 minutes) were kept fixed for both sets of data. DRV mass was kept fixed in both types of HDL-SLNs, while HDL-DRV-RTV-SLNs had an additional RTV. Data was represented as mean ± SD (n =3), where SD is the standard deviation and n is the number of samples measured.

3.4.3.2 The effect of varying the heating time of the hydrophobic phase on the DLS data of blank-SLNs and HDL-SLNs

Herein we discuss heating the hydrophobic phase at 80 °C for a longer duration (4 minutes compared to 2 minutes) to investigate the effect of the heating time of the hydrophobic phase on the DLS data of the produced blank-SLNs and HDL-SLNs. The order of particle size increase was the same as the prior experiments: blank-SLNs< HDL-DRV-SLNs< HDL-DRV-RTV-SLNs. From the DLS data shown in Figure 3.10, we can conclude that doubling the heating time of the hydrophobic phase resulted in particles with higher Z-average diameter, while the PDI almost remained unaffected. This could likely be due to the evaporation of some of the IPA when the hydrophobic phase was heated for longer time. Solvent evaporation will increase the concentration of the lipid and/or drug in the hydrophobic phase and leading to their precipitation in the hydrophobic phase's vial. In turn, this could lead to different amounts of lipid and/or drug being injected into the hydrophilic phase each time and would explain the high standard deviation noted by the big error bars.

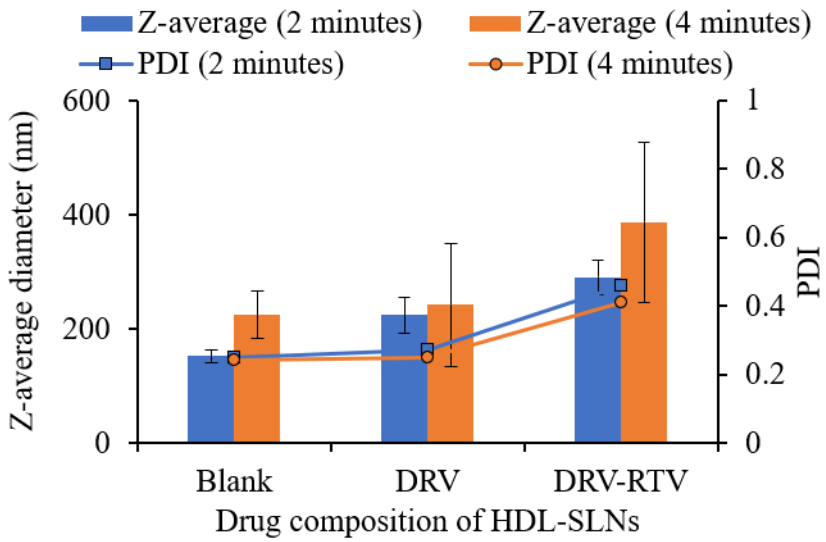

Figure 3.10 The effect of varying the heating duration of the hydrophobic phase (2 or 4 minutes) on the DLS data (Z-average diameter and PDI) of the blank-SLNs and HDL-SLNs dispersions on day 1. The heating temperature (80 °C) and stirring time of HDL-dispersions (3 minutes) were kept fixed for both sets of data. DRV mass was kept fixed in both types of HDL-SLNs, while HDL-DRV-RTV-SLNs had an additional RTV. Data was represented as mean ± SD (n =3), where SD is the standard deviation and n is the number of samples measured.

3.4.3.3 Varying the stirring time of the blank-SLNs and HDL-SLNs dispersions after the solvent injection

After the solvent injection of the hydrophobic phase into the hydrophilic phase, the SLNs dispersions were formed. The SLNs dispersions were stirred for varied times; 3 minutes or 15 minutes prior to freeze-drying. The DLS data in Figure 3.11 showed that increasing the stirring time of blank-SLNs and HDL-SLNs dispersions from 3 minutes to 15 minutes, led to an increase of the Z-average diameter and PDI. This could be explained by the presence of IPA in the nanodispersions, would increase the solubility of hydrophobic phases in the continuous phase which would allow faster Ostwald ripening. Increasing the stirring time provided a longer duration of Ostwald ripening to occur, resulting in the gradual dissolution of the smaller particles, and the growth of the larger particles causing an increase in the final Z-average diameter of the nanodispersions.[262] It was clear that the presence of the drug(s) increased this behaviour, this is likely due to the drugs being more soluble in the continuous phase of IPA and water than the lipid, therefore Ostwald ripening was able to occur more quickly with drug(s) present in the sample. Therefore, the quick removal of IPA by freeze-drying and shortening the stirring time will help maintain small particle size of the produced SLNs

.

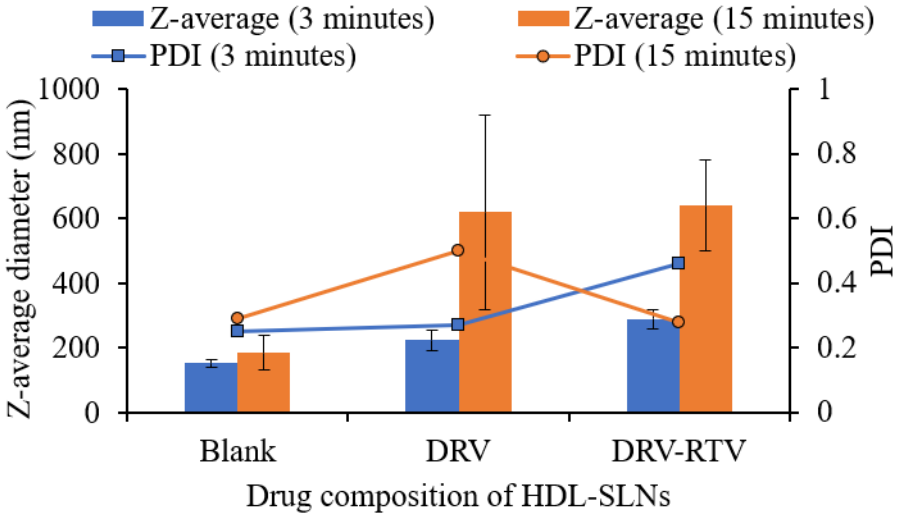

Figure 3.11 The effect of varying the stirring time of the produced SLNs dispersions (3 or 15 minutes) on the DLS data (Z-average diameter and PDI) of the blank-SLNs and HDL-SLNs dispersions on day 1. The heating temperature (80 °C) and heating time of the hydrophobic phase (2 minutes) were kept fixed for both sets of data. DRV mass was kept fixed in both types of HDL-SLNs, while HDL-DRV-RTV-SLNs had an additional RTV. Data was represented as mean ± SD (n =3), where SD is the standard deviation and n is the number of samples measured.

3.4.3.4 The effect of varying the type of solid lipid on the DLS data of blank-SLNs and HDL-SLNs

The type of the solid lipid determines the colloidal stability of SLNs.[263] The lipid used as a core for the synthesis of SLNs in the previous experiments was Compritol 888 ATO® , which is a solid lipid of melting point of 70 °C.[113] It is also known as glyceryl behenate and it is composed of a mixture composed of mono-, di- and tribehenate.[114] Compritol 888 ATO® has been extensively used as a lipid core in SLNs, It is safe and considered to be superior to other lipids in terms of drug entrapment ability.[30,84,91,95] Herein we investigate the effect of the molecular weight of the solid lipid on the DLS data of SLNs. It was hypothesised in the literature, that the lipids with lower molecular weight lead to the formation of SLNs with smaller particle size.[263] A different solid lipid for SLNs; glyceryl monostearate (GMS) was investigated. GMS has a molecular weight of 358 $g.mol^{-1}$, which is much lower than that of Compritol 888 ATO®, which has a molecular weight of 1059 $g.mol^{-1}$. The DLS data in Figure 3.12 showed that the Z-average diameter of blank-SLNs and HDL-SLNs were much smaller when Compritol 888 ATO® was used as a solid lipid compared to those prepared using GMS. The trend of the particle size was slightly different from the previous experiments; blank-SLNs< HDL-DRV-RTV-SLNs< HDL-DRV-SLNs, however the difference in size between the drug loaded formulations was very small and can be negligible. The molecular weight theory of the solid lipid reported by Li *et al.* did not explain our results.[263] Where they reported that higher the molecular weight, the bigger the particle size of the produced SLNs.[263] However our data showed an opposite trend to that theory. The most likely explanation was that Compritol 888 ATO® which is more lipophilic, nucleate better than GMS upon solvent injection in the aqueous phase.[238] That was based on the assumption in the literature that lipids that have amphiphilic characteristics e.g. GMS (HLB = 3) results in SLNs with a bigger particle size and PDI.[238] The interaction between the amphiphilic lipid and water affects nucleation causing the swelling of the lipids and therefore increase the particles size of SLNs.[238] Therefore Compritol 888 ATO® was used as the solid lipid in the upcoming experiments.

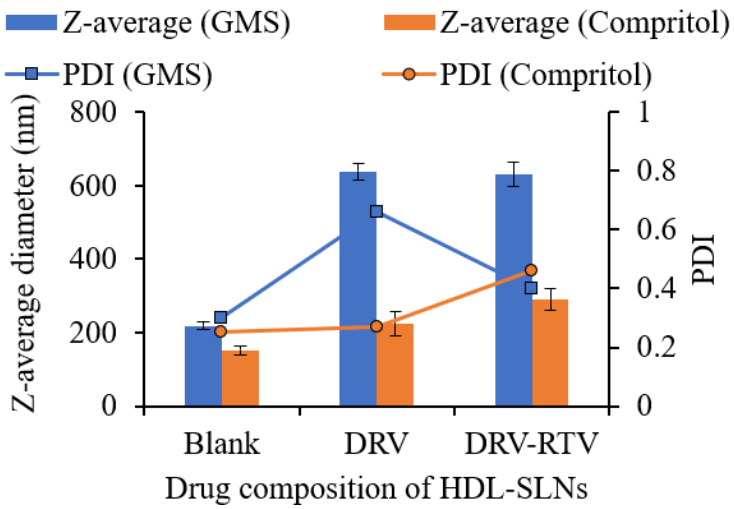

Figure 3.12 The effect of varying the type of the solid lipid; Compritol 888 ATO® or GMS on the DLS data (Z-average diameter and PDI) of the HDL-SLNs dispersions on day 1. The heating temperature (80 °C), heating time of the hydrophobic phase (2 minutes) and the stirring time of the SLNs dispersions (3 minutes) were kept fixed for both sets of data. The DLS data regarding Compritol 888 ATO® set of data has been reported before in the section 3.4.3.1. DRV mass was kept fixed in both types of HDL-SLNs, while HDL-DRV-RTV-SLNs had an additional RTV. Data was represented as mean ± SD (n =3), where SD is the standard deviation and n is the number of samples measured.

3.4.3.5 The effect of using mixture of surfactants on the DLS data of blank-SLNs and HDL-SLNs

The type of surfactant or mixtures of surfactants determine the particle size of the produced SLNs. SBL is a phospholipid which acts as an electrostatic stabiliser and Tween 80 is a non-ionic surfactant derived from polyethoxylated sorbitan and act as a bulk stabiliser. The effect of either of these stabilisers on their own or in combination with DBiB-*p*(OEGMA$_{10}$-*co*-EGDMA$_{0.6}$) on the DLS data of blank-SLNs and HDL-SLNs was investigated. Varied weight percentages of SBL or Tween 80/total surfactant (100, 70, 30 and 0% w/w) was studied. The weight of the total surfactant referred to the weight of either SBL or Tween 90 plus the weight of DBiB-*p*(OEGMA$_{10}$-*co*-EGDMA$_{0.6}$). A weight percentage of 100% w/w referred to using only SBL or Tween 80, while 0% w/w referred to using only DBiB-*p*(OEGMA$_{10}$-*co*-EGDMA$_{0.6}$) as a surfactant for blank-SLNs and HDL-SLNs.

The DLS data in Figure 3.13 showed that using that DBiB-*p*(OEGMA$_{10}$-*co*-EGDMA$_{0.6}$) as a sole stabiliser produced SLNs with smaller Z-average diameter than those stabilised with either stabilised with SBL or Tween 80. This could be due to the ability of the branched *P*(OEGMA) surfactant to attach to the lipid cores of the SLNs in contrary to Tween 80 or SBL. The use of

SBL either alone or in combination with DBiB-*p*(OEGMA$_{10}$-*co*-EGDMA$_{0.6}$) as surfactant (Figure 3.13.A) produced blank-SLNs and HDL-SLNs with bigger Z-average diameter compared to those produced by Tween 80 either alone or in combination with DBiB-*p*(OEGMA$_{10}$-*co*-EGDMA$_{0.6}$), see Figure 3.13.B. the reason for this behaviour remained unknown. The high Z-average diameter of HDL-DRV-SLNs compared to the other SLNs formulations in Figure 3.13.A possibly meant that SBL was not a compatible surfactant for DRV at such high drug loading, unlike other surfactants like Tween 80 and DBiB-*p*(OEGMA$_{10}$-*co*-EGDMA$_{0.6}$). In conclusion DBiB-*p*(OEGMA$_{10}$-*co*-EGDMA$_{0.6}$) was a better surfactant for blank-SLNs and HDL-SLNs compared to the commercially available surfactants i.e., Tween 80 and SBL, and therefore was used for further studies.

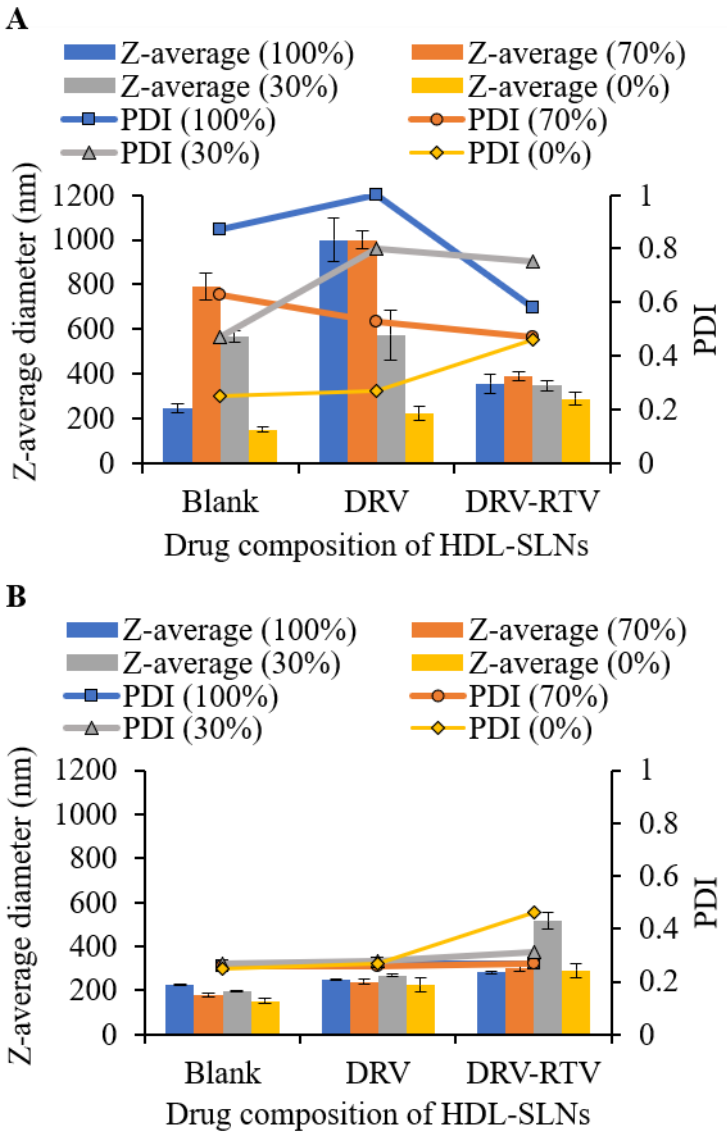

Figure 3.13 The effect of varying the type of surfactant and surfactant combination on the DLS data (Z-average diameter and PDI) of the blank-SLNs and HDL-SLNs dispersions on day 1: (A) SBL and (B) Tween 80. Both surfactants were used on their own and/or in combination with DBiB-p(OEGMA$_{10}$-co-EGDMA$_{0.6}$) with varied weight percentages of SBL or Tween 80/ total surfactant (100, 70, 30 and 0% w/w). The heating temperature (80 °C), heating time of the hydrophobic phase (2 minutes) and the stirring time of the hydrophilic phase (3 minutes) were kept fixed for both sets of data. Data was represented as mean ± SD (n =3), where SD is the standard deviation and n is the number of samples measured.

3.4.4 Freeze-drying of blank-SLNs and HDL-SLNs dispersions

To remove the IPA and DI water from the blank-SLNs and HDL-SLNs dispersions to get SLNs in a powder form, the SLNs dispersions were freeze-dried for 4 days. However, the freeze-drying led to the aggregation of the SLNs formulations in form of sticky materials, that could not be re-dispersed. Therefore, freeze drying would be thoroughly investigated in chapter 4, where varied cryoprotectant types were investigated.

3.5 Conclusion

DBiB initiator was successfully synthesised and characterised, which was used in the synthesis of amphiphilic branched copolymer DBiB-*p*(OEGMA$_{10}$-*co*-EGDMA$_{0.6}$). Solvent injection method was used for the synthesis of Blank-SLNs and HDL-SLNs with DRV loading of 50% w/w using DBiB-*p*(OEGMA$_{10}$-*co*-EGDMA$_{0.6}$) as a surfactant, and several synthetic parameters were investigated. We concluded that heating temperature of the hydrophobic phase to 80 °C for a stirring time of 2 minutes were the optimum conditions for the hydrophobic phase. 3 minutes was the optimum duration for stirring the SLNs dispersions prior to freeze drying compared to 15 minutes. For the choice of the SLNs ingredients, Compritol 888 ATO® was the solid lipid of choice as it formed SLNs with smaller Z-average diameter and PDI in comparison with GMS. DBiB-*p*(OEGMA$_{10}$-*co*-EGDMA$_{0.6}$) on its own was found to a better surfactant than Tween 80 or SBL. The optimum synthesis conditions produced blank-SLNs, HDL-DRV-SLNs and HDL-DRV-RTV-SLNs with the Z-average diameter of 152, 224 and 290 nm, respectively. Freeze-drying led to aggregation of the SLNs formulations and required further investigation as will be discussed in chapter 4.

Chapter 4

Optimisation of the Freeze-Drying Parameters of High Drug-Loaded SLNs Using Cryoprotectants

4.1 Introduction

In chapter 3, high drug-loaded SLNs (HDL-SLNs) were prepared as aqueous colloidal dispersions using solvent injection method, where high molecular weight branched polymer DBiB-*p*(OEGMA$_{10}$-*co*-EGDMA$_{0.6}$) was used as a stabiliser. "HDL-SLNs" term was used as a general term to refer to both DRV loaded and DRV/RTV (8:1) loaded. The produced HDL-SLNs dispersions had a good quality DLS data in term of the size (~200 nm) which is suitable for intestinal absorption. The Z-average diameter was 224 nm for HDL-DRV-SLNs and 290 nm for HDL-DRV-RTV-SLNs with a monomodal size distribution graphs. However, the water-miscible organic solvent used in the synthesis for HDL-SLNs was still present in the dispersion media, which in this case was isopropanol (IPA). The removal of IPA was challenging as it does not evaporate at room temperature even with stirring for few days, and it forms azeotropic mixtures with water by hydrogen bond formation. The presence of the HDL-SLNs in a liquid dispersion media, in addition to presence of the IPA initiated the instability of HDL-SLNs as they aggregated overnight. Another concern was that presence of IPA initiated drug leaching as it is a good solvent for both DRV and RTV, leading to a decrease in the drug loading overtime. This is in addition to the toxic effects of the presence of organic solvent in pharmaceutical preparations.[264] So in this study the removal of both water and IPA by freeze-drying was investigated as a possible technique for maintaining the stability and high drug loading of HDL-SLNs.

Freeze-drying is usually reported as a step in the manufacturing process, not many details are given about the properties and concentrations of both the particles and the cryoprotectants, nor the set-up of the freeze-drying process, and it must be tailored per the formulation. Cryoprotectants are very crucial for the freeze-drying process. The use of the cryoprotectants leads to the ease of the reconstitution of the SLNs dispersions after freeze drying, as the SLNs are embedded in a water soluble matrix.[112] Two main groups of cryoprotectants were studied in the literature: sugar and polymeric cryoprotectants. Among many sugar cryoprotectants, disaccharides were found to have a better cryoprotectant effect compared to other saccharides. For example, maltose is an example of a disaccharides and it was considered a more efficient cryoprotectant than monosaccharides such as glucose.[205] This effect was closely related to glass transition temperature (T_g) of each sugar. T_g of maltose and glucose are -29.5 °C and -45 °C, respectively. Since the glassy matrix that prevent particles aggregation is more stable at a

higher T_g, maltose proved to have a better performance.[205] On the other hand polymers are generally known to be better cryoprotectants compared to sugars; requiring less mass to provide good cryoprotection for nanoformulations.

In this chapter, the freeze-drying and conditions and parameters are optimised for a novel type of SLNs which is HDL-SLNs stabilised by branched polymers. The high drug concentration in the final SLNs suspension after rehydration at reduced volumes is critical for the in *vitro* studies.

4.2 Chapter objectives

Removal of both water and IPA from HDL-SLNs dispersions using freeze-drying as a dehydration technique to maintain the colloidal stability of the formulations was the main objective of this chapter. The aim was to obtain HDL-SLNs in form of dry powder that easily re-dispersed in DI water, PBS and simulated gastric fluid (SGF) as examples for physiological solutions, while maintaining the size and size distribution of HDL-SLNs during the rehydration process. For that purpose, the freeze-drying parameters were investigated which included: The duration of freezing drying and storage conditions of the freeze-dried products. Determining the type of cryoprotectants, and the optimum concentration of the freeze-drying mixture which was made of HDL-SLNs, cryoprotectant and DI water and cryoprotectant/HDL-SLNs weight ratio that maintained the DLS data of HDL-SLNs dispersions before freeze-drying. Studying the morphology of the freeze-dried formulations by scanning electron microscopy (SEM). Scale-down of the synthesis of radiolabelled HDL-SLNs by solvent injection to limit radioactive waste. The scale-up of the freeze-drying of the optimised formulations to have a drug concentration suitable for measurements of drug release using radiolabelled analogues and drug accumulation and permeability through *in vitro* triple culture model. Different studied variables and characterisations were summarised in Figure 4.1.

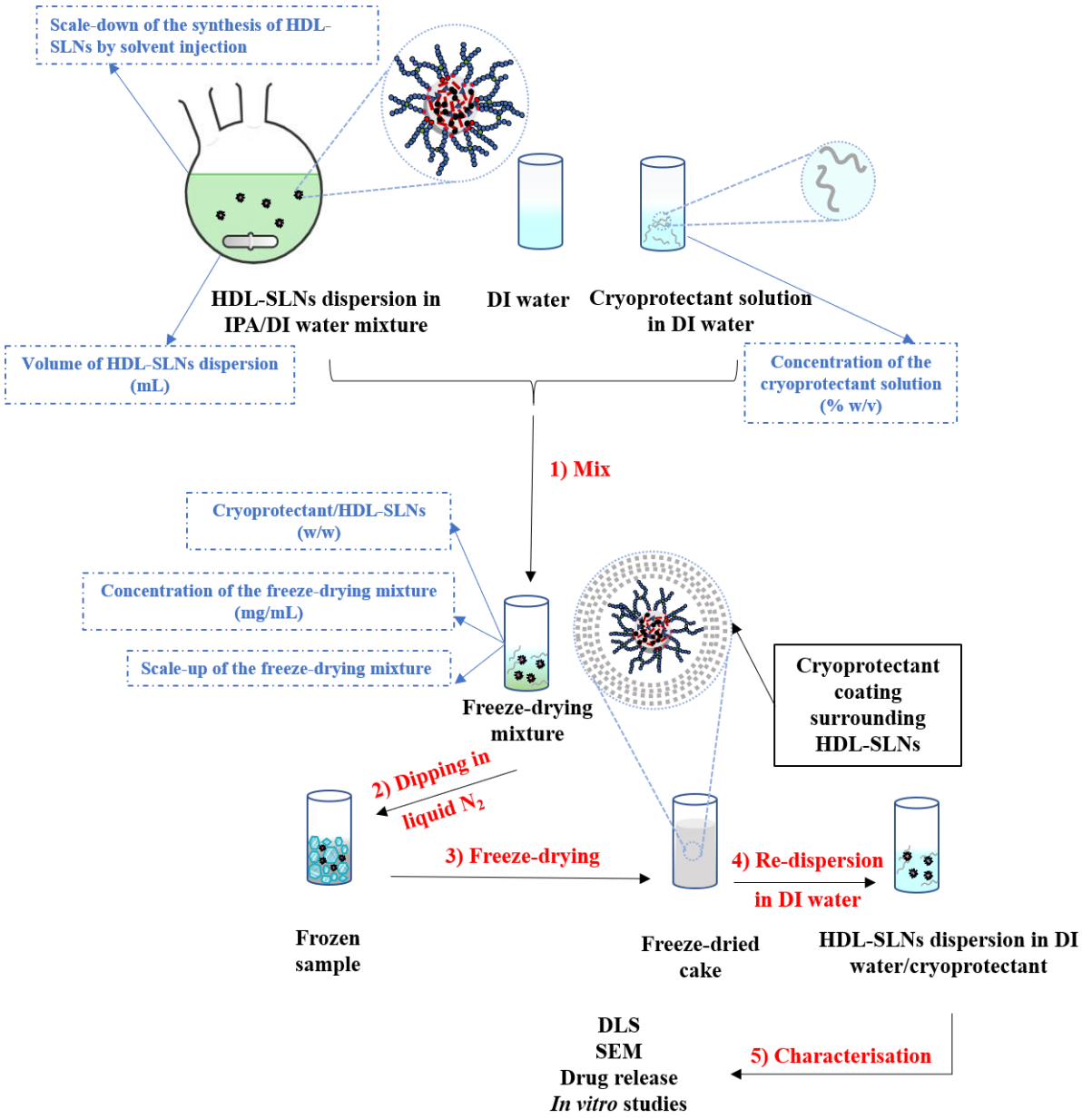

Figure 4.1 Diagram shows the steps of the freeze-drying process, re-dispersion, and characterisation of HDL-SLNs (written in red), and different measured variables and parameters (written in blue).

4.3 Materials and Methodology

4.3.1 Materials

Glycerol dibehenate (Compritol ATO 888) was a generous gift from Gattefossé, France. Isopropanol (IPA, HPLC grade) (Thermo Fischer Scientific, Leicestershire, UK.), DRV (≥98% (HPLC) and RTV (≥98% (HPLC), PEG (Mn 2050 g mol^{-1}), D-Mannitol (≥98%), dextran, maltodextrin, sucrose (≥99%), trehalose (≥99%), PBS tablets, hydrochloric acid (HCl, ≥99%), sodium chloride (NaCl, ≥99%) dimethyl sulfoxide (DMSO, 99%), hydrogen peroxide, (4-(2-hydroxyethyl)-1-piperazineethanesulfonic acid (HEPES), bovine serum albumin (BSA, ≥98%), Hank's balanced salt solution (HBSS), Dulbecco's Modified Eagle's Medium (DMEM), RPMI and trypsin-EDTA were all purchased from Sigma–Aldrich, Irvine, UK. Amicon Ultra-0.5 Centrifugal Filter Unit (Merck). Caco-2 and HT-29-MTX cells were maintained in DMEM supplemented with 15% fetal bovine serum (FBS) (Gibco, UK), 2 mM L-glutamine and 1% non-essential amino acids (Sigma–Aldrich, Irvine, UK). Raji B cells were maintained in RPMI supplemented with 10% FBS, 2 mM L-glutamine and 1% non-essential amino acids (Sigma–Aldrich, Irvine, UK). [^{3}H]-DRV was purchased from RC Tritec and [14C]-mannitol was purchased from American Radiolabelled Chemicals (US). Ultima Gold and ProSafe + liquid scintillation fluid was purchased from Meridian biotechnologies (UK). Transwells with a 3 μM pore size were purchased from Corning (US). Caco-2, HT-29-MTX and Raji B cells were purchased from American Type Culture Collection (US). All reagents were used without further purification. DBiB-*P*(OEGMA$_{10}$)-*co*-(EGDMA$_{0.60}$) was synthesised by ATRP as explained in chapter 3.

4.3.2 Methodology

4.3.2.1 Synthesis of HDL-SLNs by solvent injection

After testing different synthesis variables in chapter 3, the optimised solvent injection method was used here in the production of HDL-SLNs. Briefly, a hydrophobic phase placed in a 14-mL vial (type 1B neutral glass, Thermo Fischer Scientific, Leicestershire, UK) consisting of 3.6 mg Compritol 888 ATO®, 12.8 mg DRV and/or 1.6 mg RTV dissolved in 4 mL IPA was heated in an oil bath at 80 °C for 2 minutes using a hot plate and magnetic stirrer at 300 rpm. The hydrophobic phase was heated till all solids were dissolved, which was indicated by clarity of the solution. The hydrophobic phase was then rapidly injected using a hypodermic needle (21 g, 50 mm) into the vortex of stirring (300 rpm) aqueous phase (20 mL) consisted of 0.3

mg/mL of DBiB-*p*(OEGMA$_{10}$-*co*-EGDMA$_{0.6}$) in DI water at ambient temperature and placed in a 50 mL two-necked round bottom flask (RBF), to give a final concentration of HDL-SLNs of 0.15-1 mg/mL, and DRV concentration of 0.53 mg/mL. The SLNs dispersion was left to stir for 3 minutes to ensure full mixing. The dispersion was then freeze-dried to remove the IPA and deionised water using a wide range of cryoprotectants.

4.3.2.2 Synthesis of radiolabelled HDL-SLNs by solvent injection (scale-down)

Radiolabelled DRV containing HDL-SLNs (analogous to those described in section 4.3.2.1) were formulated to measure the drug release and test the particles behaviour in cell work studies. As only 2 mL of each HDL-SLNs formulation was required to carry out both the drug release and cell work studies, the synthesis of solvent injection was scaled-down to 3 mL instead of 24 mL to avoid unnecessary wasting of radiolabelled materials. The hydrophobic phase consisted of 0.45 mg Compritol 888 ATO®, with the addition of 1.6 mg tritiated [^{3}H]-DRV with a specific activity 25 μCi/mg and/or 0.2 mg RTV dissolved in 0.5 mL IPA. The hydrophobic phase was placed in a 1 mL glass vial and was heated to 80 °C in an oil bath for 2 minutes using a hot plate and magnetic stirrer at 300 rpm till all solids were dissolved. The hydrophobic phase was then rapidly injected using a hypodermic needle (21 g, 50 mm) into 2.5 mL of stirring (200 rpm) aqueous phase consisted of 0.3 mg/mL DBiB-*p*(OEGMA$_{10}$-*co*-EGDMA$_{0.6}$) in DI water at ambient temperature and placed in a 4 mL glass vial. The SLNs dispersions were left to stir for 3 minutes to ensure full mixing of both phases. The dispersion was then freeze-dried.

4.3.2.3 Freeze-drying and re-dispersion of HDL-SLNs

The HDL-SLNs suspended in aqueous carbohydrate, or aqueous PEG solutions at different concentrations were frozen using liquid nitrogen at –196 °C in glass vials. The freeze-drying settings was as follows: the temperature of the condenser of the was kept at -100 °C, and a vacuum of <40 μbar using a VirTis BenchTop K freeze dryer (SP Scientific, Ipswich, UK), (see Figure 1.16 in chapter 1). The samples were kept in the freeze dryer for 2 or 4 days. Scale-up of the freezing drying was investigated using increasing volumes of the freeze-drying mixture. The volumes of the samples tested were 2, 5 and 10 mL which were placed in 4-, 14- and 40-mL glass vials (type 1B neutral glass, Thermo Fischer Scientific, Leicestershire, UK),

respectively. Freeze-dried HDL-SLNs were reconstituted in 1 mL of deionised water under manual shaking. The vials were tightly closed after taking out from the freeze dryer to avoid the collapse of the freeze-dried cake.

4.3.2.4 Freeze-drying and re-dispersion of radiolabelled HDL-SLNs

Radiolabelled HDL-DRV-SLNs and HDL-DRV-RTV-SLNs synthesised by scaled-down solvent injection (see section 4.3.2.2) were freeze-dried using PEG as a cryoprotectant with a PEG/HDL-SLNs weight ratio of 38/1. 10 mL of the freeze-drying mixture consisting of 5 mL of 0.5% w/v PEG solution, 1 mL radiolabelled HDL-SLNs, and 4 mL DI water were placed in 40 mL vials and freeze-dried for 4 days under the same conditions mentioned in section 4.3.2.3. For each type of formulation, the freeze-dried contents of two 40 mL vials were combined and reconstituted in 1 mL DI water, to give a final [^{3}H]-DRV concentration of ~1 mg/mL and was tested for drug release and cell culture studies.

4.3.2.5 Characterisation of the size and morphology of HDL-SLNs by DLS and scanning electron microscope (SEM)

DLS was the main analytical method used to determine the size of HDL-SLNs. SEM was also used for characterisation of the morphology and size of selected samples. DLS settings was the same as detailed in chapter 2, with the exception for the concentration of the samples. The concentration of HDL-SLNs dispersions before freeze-drying was 0.15-1 mg/mL, while the concentration of freeze-dried HDL-SLNs dispersions after reconstitution with DI water, PBS solution (pH 7.4) or simulated gastric fluid (SGF) (pH 1.2) was 7 mg/mL, that concentration included the mass of the cryoprotectant. PBS solution was prepared by dissolving 1 PBS tablet in 100 mL deionised water, while SGF was prepared by dissolving 2 g of NaCl and 7 mL concentrated HCl per 1000 mL deionized water.

For SEM imaging, two samples were tested; HDL-DRV-SLNs and HDL-DRV-RTV-SLNs freeze-dried using PEG as a cryoprotectant with a PEG/HDL-SLNs weight ratio of 38/1, the volume of the freeze-drying mixture was 10 mL which was placed in 40 mL vials. The samples were prepared by pipetting the re-dispersed freeze-dried HDL-SLNs dispersions 1 mg/mL onto glass coverslips with 10 mm diameter which were attached to a carbon adhesive disc on top of an aluminium SEM specimen stub (12.5 mm diameter). The samples were left to dry overnight,

this was followed by coating with gold (EMITECH K550X) with a deposition current of 25 mA for 100 s before imaging. The size and the morphology of HDL-SLNs were then determined using a Hitachi S-4800 FE-SEM at 3 kV.

4.3.2.6 Measurement of drug release using radiometric analysis

For drug release studies, 1 mL of reconstituted freeze-dried radiolabelled HDL-DRV-SLNs and HDL-DRV-RTV-SLNs with [^{3}H]-DRV concentration of ~1 mg/mL were used. The synthesis by solvent injection and freeze-drying of these two formulations were described in sections 4.3.2.2 and 4.3.2.4, respectively. A dialysis method was used to quantify drug release behaviour from both types of HDL-SLNs. Reconstituted HDL-SLNs dispersions (1 mL) were placed within a double-sided bio-dialyzer fitted with membranes of 3.5 kDa MWCO. DRV release was monitored at set time points of 0.5, 1, 2, 3, 4, 5, 6, 7 and 8 hours. The details of the release experiment were the same as described in chapter 2.

4.3.2.7 Cellular accumulation and transcellular permeability of DRV across Caco-2 cells and triple culture model respectively

Reconstituted, freeze-dried radiolabelled HDL-DRV-SLNs and HDL-DRV-RTV-SLNs with [^{3}H]-DRV were tested for DRV cellular accumulation and transcellular permeability across Caco-2 cells and triple culture models, respectively. Pre-clinical preparations of unformulated DRV and/or RTV served as controls.

4.3.2.7.1 Cell culture and maintenance

Caco-2 and HT-29-MTX cells were maintained using Dulbecco's Modified Eagle Medium supplemented with 15% Foetal Bovine Serum, 1% non-essential amino acids and 2 mM L-glutamine, hereafter referred to as sDMEM, at 37^{o}C, 5% CO_2. Cell numbers and viability were determined using a NucleoCounter NC-200.

4.3.2.7.2 Cellular Accumulation

An accumulation study was conducted using Caco-2 cells to assess DRV accumulation over time. A Caco-2 cell suspension was adjusted to 1.5 x 10^6 cells per well and added to each well of the 12-well plates. The plates were incubated overnight at 37°C, 5% CO_2 to allow the cells to adhere. Following incubation, the sDMEM was aspirated and each well was washed twice

with pre-warmed transport buffer (Hanks Balanced Salt Solution (HBSS) containing 25 mM 4-(2-hydroxyethyl)-1-piperazineethanesulfonic acid (HEPES), pH 7.4). Subsequently, 1 ml transport buffer containing each 10 µM DRV and/or RTV treatment was added to the plates and incubated at 37 °C, 5% CO_2 for either 1 or 4 hours. Four treatments were prepared: unformulated DRV, HDL-DRV-SLNs, unformulated DRV/RTV (8:1) and HDL-DRV-RTV-SLNs. Following incubation, 100 µl of the extracellular buffer was sampled and placed into a 5 ml scintillation vial. The remaining buffer was removed, and the wells were washed twice with ice-cold HBSS. Scintillation fluid (500 µL) was added to each well and incubated at room temperature for 30 minutes. Subsequently, 100 µl of cell lysate from each well was placed into a 5 ml scintillation vial and 4 ml of Ultima Gold liquid scintillation fluid was added to each vial. Radiometric analysis was performed using a Perkin Elmer 3100TS scintillation counter before the data was transformed forming the cellular accumulation ratio (CAR), see Equation 4.1.

$$CAR = \left(\frac{((\sum[DRV]A>B)/4)}{((\sum[DRV]B>A)/4)}\right)$$

Equation 4.1 Calculation of cellular accumulation ratio (CAR), where (A>B) referred to DRV transport from apical-to-basolateral direction, while (B>A) referred to DRV transport from basolateral-to-apical direction.

4.3.2.7.3 Transcellular Permeability

The permeability of the HDL-DRV-SLNs and HDL-DRV-RTV-SLNs formulations was assessed across an *in vitro* intestinal triple culture model. Transwells were seeded apically with Caco-2 and HT-29-MTX cells in a 7:3 ratio with 1.4 x 10^5 cells per well, respectively, and propagated over 21-days at 37°C, 5% CO_2. Following 16-days of co-culture, 1.4 x 10^5 Raji-B cells were added to the basolateral compartment of each well and the triple culture model propagated for a further 5-days at 37°C, 5% CO_2. Following propagation, the sDMEM was removed from both compartments of each well and washed twice with HBSS. Four treatments were prepared: unformulated DRV, HDL-DRV-SLNs, unformulated DRV/RTV (8:1) and HDL-DRV-RTV-SLNs. The treatments were prepared at 10 µM DRV in the transport buffer and each treatment was added either apically (250 µl) or basolaterally (600 µl) to the donor compartment of each well. Transport buffer was added apically (250 µl), or basolaterally (600 µl) to the acceptor compartment of each well and the plates were incubated at 37°C, 5%

CO_2. At each 1-hour timepoint over a 4-hour period, 100 µl of each acceptor well contents were sampled and placed into a 5 ml scintillation vial. Following the 4-hour incubation, the buffer from each well was removed, and the wells were washed twice with HBSS. Subsequently, 100 µl mannitol solution (50 µM mannitol at 1.35 µCi/ml) was added to the apical donor compartment wells, and 600 µl buffer to the corresponding basolateral compartment. The plates were incubated for 1-hour at 37°C, 5% CO_2 and 100 µl of each basolateral content was sampled and placed into 5 ml scintillation vials. Ultima Gold liquid scintillation fluid (4 ml) was added to all scintillation vials. Radiometric analysis was performed using a Perkin Elmer 3100TS scintillation counter. Apparent permeability (P_{app}) was subsequently calculated using Equation 4.2.

$$\text{Apparent permeability } (P_{app}) = \frac{(d\,Q/d\,t)\ X\ v}{A\ X\ C0}$$

Equation 4.2 Calculation of the apparent permeability (P_{app}), where dQ/dt is the drug transportation rate (nM min^{-1}), v is the volume of the accepting compartment (ml), A is the membrane surface (cm^2) and C_0 is the initial donor concentration (nM).[265]

Subsequently, apparent oral absorption was calculated using Equation 4.3.

$$\text{Apparent oral absorption} = \frac{((\sum \text{PappA>B})/)}{((\sum \text{PappB>A})/)}$$

Equation 4.3 Calculation of the apparent oral absorption, where P_{app} A>B referred to DRV apparent permeability from apical-to-basolateral direction, while P_{app} B>A referred to DRV apparent permeability from basolateral-to-apical direction.

4.3.2.7.4 Statistical analysis

Statistical analysis was performed using GraphPad Prism v.8.2 (US). Data normality was assessed using a Shapiro-Wilk test and subsequently unpaired, two-tailed t-test were applied to the datasets. Differences were considered statistically significant at *, P<0.05; **, P < 0.01; ***, P < 0.001; ****, P < 0.0001. Samples tested were: HDL-DRV-SLNs and HDL-DRV-RTV-SLNs. The controls were unformulated DRV and unformulated DRV/RTV (8:1). Unformulated DRV referred to [^{3}H]-DRV/DRV (<1 % DMSO) aqueous preparation, whether on its own or in combination with RTV.

4.4 Results and Discussion

Freeze-drying is a way to enhance the stability of the lipid formulations, as the presence of water can cause the hydrolysis of various types of lipids and polymers of the nanoparticles.[266] The main goal of this study was to obtain HDL-SLNs in a solid powder state, that is easily re-dispersed in DI water, PBS and SGF while maintaining the original size and size distribution of HDL-SLNs before freeze-drying. For that purpose, optimisation of the freeze-drying was carried out in stages, firstly the freeze-drying conditions was optimised and that included the duration of the freeze-drying and the storage of the freeze-dried HDL-SLNs. The effect of the type of the cryoprotectant whether sugar or polymeric on the DLS data of the re-dispersed HDL-SLNs was then investigated. The chemical structure of all the used cryoprotectants in this study can be seen in Figure 4.2. Low concentrations of cryoprotectants were targeted in order to obtain a mass-efficient formulation. To determine the optimum amount required from a certain cryoprotectant to provide stabilisation of a certain volume of HDL-SLNs dispersion, several parameters were determined: the cryoprotectant/HDL-SLNs weight ratio (w/w) and concentration of the freeze-drying mixture (mg/mL). The cryoprotectant/HDL-SLNs weight ratio was calculated by dividing the mass of the cryoprotectant by the mass of the HDL-SLNs, while the concentration of the freeze-dried mixture (mg/mL) was calculated by the summation of the masses of both the cryoprotectant and the HDL-SLNs per the volume of liquid they are both dissolved or suspended in, respectively. To allow direct comparison with other studies from the literature, the relationship between the cryoprotectant and the HDL-SLNs dispersions was represented in an additional way, where the concentration of the cryoprotectant solution (% w/v) required for the stabilisation of a certain volume of HDL-SLNs dispersion (mL) was determined. Once the relationship between the cryoprotectant and the HDL-SLNs dispersion has been established, a scale-up of the freeze-drying was targeted, to speed up the freeze-drying process and use the least number of vials during the freeze-drying process. The optimised formulations were further studied, where the morphology, drug release and behaviour in cell culture models were investigated.

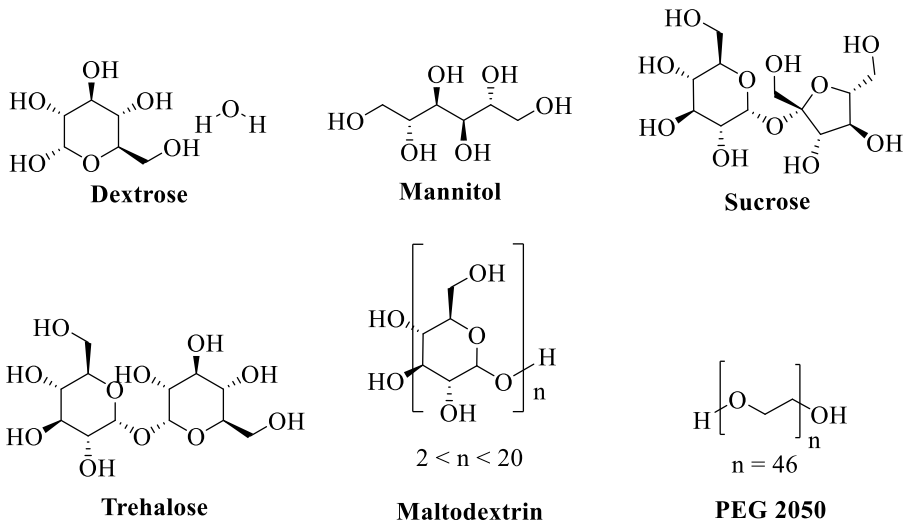

Figure 4.2 Chemical structures of different cryoprotectants used in this study.

4.4.1 Optimisation of freeze-drying conditions

Herein we discuss the optimisation of the freeze-drying conditions in terms of the duration of the freeze-drying process and the storage conditions. The optimisation was carried out for single-drug-loaded formulation: HDL-DRV-SLNs.

4.4.1.1 Duration of freeze-drying

To determine the optimal freeze-drying duration, HDL-DRV-SLNs were freeze-dried for two different durations: 2 and 4 days. The optimum freeze-drying duration was the shortest duration that ensured complete drying of the frozen samples and the removal of all ice crystals. From Figure 4.3.A, we can see that when freeze-drying was carried out for only 2 days, that duration was not sufficient for the complete removal of the water content, and the ice crystals were still visible. In Figure 4.3.B, after freeze-drying was carried out for 4 days, ice crystals were not visible and fluffy dried cake was formed which could mean proper drying of the sample. Therefore, 4 days was chosen as the optimum freeze-drying duration of HDL-SLNs.

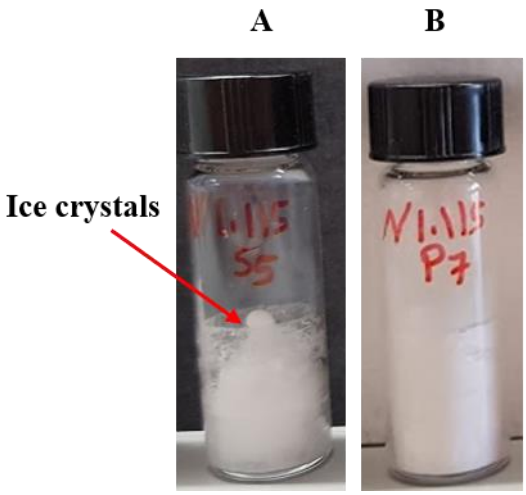

Figure 4.3 Effect of freeze-drying duration on the freeze-dried cakes of HDL-DRV-SLNs; (A) Samples left in the freeze dryer for 2 days and ice crystals can be seen (B) Samples left in the freeze dryer for 4 days, dry fluffy cake can be seen. 1 mL of 5% w/v sucrose and 0.5% w/v PEG were used as cryoprotectants, respectively for 0.2 mL HDL-DRV-SLNs dispersion.

4.4.1.2 Storage of the freeze-dried HDL-SLNs

Cryoprotectants whether carbohydrate or polymeric are hygroscopic in nature.[112,267] This meant it was important to quickly store the freeze-dried SLNs in a tightly closed vials, otherwise atmospheric moisture would eventually lead to the collapse of the freeze-dried cakes and aggregation of the particles would take place. Freeze-dried cakes of HDL-DRV-SLNs obtained using 5% w/v sucrose as a cryoprotectant remained intact when the vials were tightly closed right after synthesis (Figure 4.4.A) and resulted in a clear solution upon re-dispersion in 1 mL DI water (Figure 4.4.B). On the other hand, the freeze-dried cakes collapsed when the vials were left open for few hours (Figure 4.4.C), the reconstituted solution was turbid suggesting particle aggregation (Figure 4.4.D). Zillies *et al*. mentioned that to prevent the aggregation of nanoparticles they must be separated in the dried cake during storage.[191]

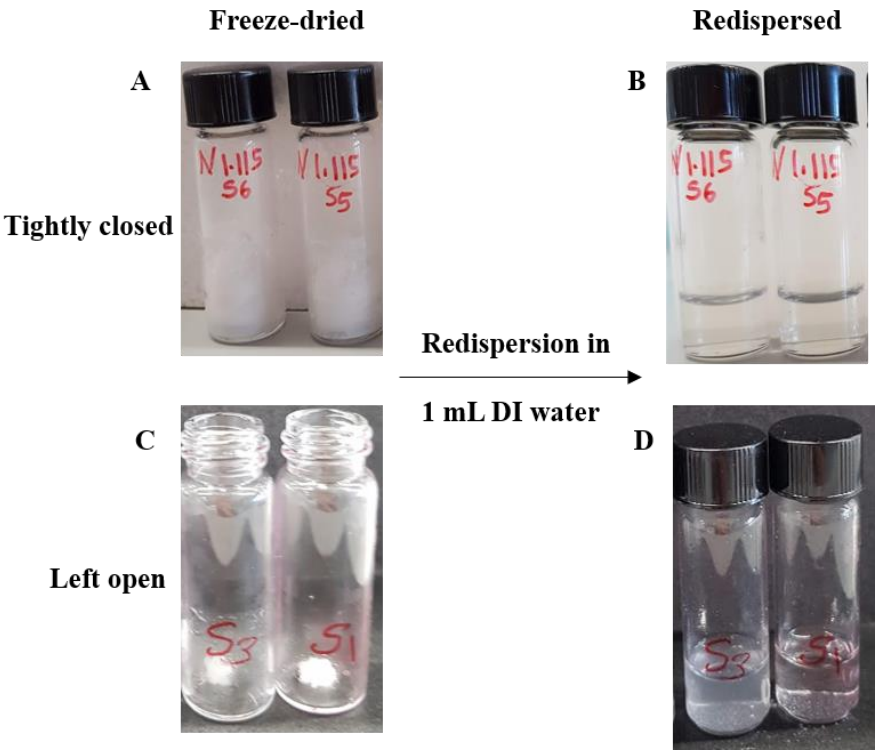

Figure 4.4 Effect of the storage conditions on the freeze-dried cakes of HDL-DRV-SLNs. (A) Image for the vials that were tightly closed right after taking off from the freeze dryer keeping the freeze-dried cake intact and fluffy days later. (B) Image of the vials that were tightly closed after re-dispersion in DI water, showing clear solutions. (C) Image for the vials that were left open for few hours after taking off from the freeze dryer leading to the collapse of the freeze-dried cake. (D) Image for the vials that were left open showing turbid solutions after re-dispersion in DI water suggesting aggregation. 5% w/v sucrose was used as a cryoprotectant for both samples.

4.4.2 The effect of varying freeze-drying parameters on the DLS data of HDL-SLNs

Ideally in the synthesis of drug delivery systems, to maximise the therapeutic efficacy of these formulations, the goal is to have the lowest excipient/drug mass ratio. However, the results in chapter 3 showed that when no cryoprotectants were used, HDL-SLNs formed a sticky material that was difficult to re-disperse in DI water. This finding was in line with the results reported in other studies.[192,207] This is due to ice formation during the freezing step, which exerts a physical stress on the HDL-SLNs located in the liquid unfrozen phase which becomes more concentrated. This in turn leads to interparticle interactions which results in irreversible aggregation of the particles.[5] The ability of the different cryoprotectants to maintain the particle size and polydispersity after freeze-drying and reconstitution in water is summarised in the following sections (4.4.2.1 and 4.4.2.2).

4.4.2.1 Influence of different sugar cryoprotectants on the DLS data of HDL-DRV-SLNs

The most widely used cryoprotectants in the literature are sugars, also referred to as carbohydrate cryoprotectants.[201] The effectiveness of sugars as cryoprotectants usually depends on their concentrations and the concentrations of the nanoformulations.[197,201] For carbohydrate cryoprotectants, the tested weight ratio range of cryoprotectant/HDL-SLNs was 8/1- 1504/1 while the tested concentrations range of the freeze-dried mixtures was 3-100 mg/mL. DI water was used to keep the volume of all the freeze-dried samples fixed at 2 mL. A total of 15 samples for each sugar cryoprotectant was tested. Different categories of sugar cryoprotectants were used; dextrose is a monosaccharide, mannitol is a sugar alcohol, sucrose and trehalose are both disaccharides, while maltodextrin is an example for polysaccharides.

4.4.2.1.1 The effect of using dextrose, mannitol, and maltodextrin as cryoprotectants on the size properties of re-dispersed HDL-DRV-SLNs

Upon dispersion of the HDL-DRV-SLNs formulations which were freeze-dried using dextrose, mannitol, and maltodextrin, the visual aggregates could be observed by eye after reconstitution with DI water and these samples were therefore not measured by DLS. This behaviour was regardless of the cryoprotectant/HDL-DRV-SLNs weight ratio and the concentration of the freeze-dried sample. Although the three carbohydrate cryoprotectants failed to maintain the size and the physical characteristics of HDL-DRV-SLNs, but there could be different reasons to explain that failure as explained in the following paragraphs.

For dextrose and maltodextrin which are examples for monosaccharides and polysaccharides, respectively, both are classified as reducing sugars which can exist in both open and ring forms (Figure 4.5).[208] They form internal hydrogen bonds, so there were less OH groups available to form hydrogen bonds with nanoparticles, therefore their cryoprotection ability were reduced. The cryoprotection effect of a certain cryoprotectant is dependent on its ability to form hydrogen bonds.[208] The hydrogen bond between the cryoprotectant and nanoparticles help maintain the pseudo-hydrated state during the dehydration, thus provide protection during the dehydration and rehydration steps.[192]

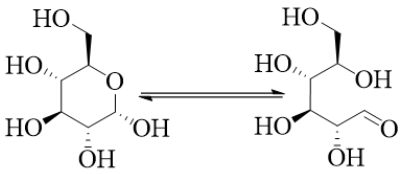

Ring form **Acyclic aldehyde form**

Figure 4.5 Different chemical forms of Dextrose.

There are some suggestions that the failure of some cryoprotectants could be related to the collapsed freeze-dried cake, and that fluffy cakes usually provide better re-dispersion of nanoparticles. Some cryoprotectants form better freeze-dried cakes than others, Figure 4.6 showed that maltodextrin formed fluffy freeze-dried cakes when using 0.2 mL of HDL-DRV-SLNs dispersions at varied concentrations of maltodextrin solutions (2.5-20% w/v). On the other hand, dextrose only formed a proper cake at a higher concentration (20% w/v), collapsing of the freeze-dried cake of monosaccharides has been reported before.[208] This might suggest that polysaccharides form better freeze-dried cakes than monosaccharides, however in both cases the re-dispersed HDL-SLNs aggregated.

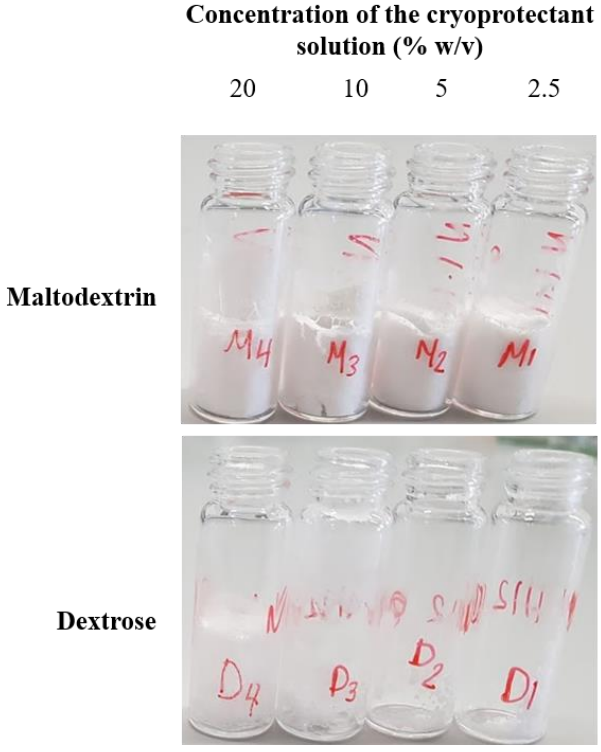

Figure 4.6 Shape of the freeze-dried cake right after removal from the freeze dryer at varied cryoprotectant solution concentrations (2.5-20% w/v) using maltodextrin and dextrose as cryoprotectants, while keeping the volume of HDL-DRV-SLNs dispersions fixed at 0.2 mL for all formulations.

Mannitol, a sugar alcohol with low molecular weight (182.172 g.mol^{-1}), was also a poor cryoprotectant even at high concentrations, when there should have been enough cryoprotectant to cover the HDL-DRV-SLNs. The reason for this behaviour was likely due to the crystallisation of mannitol. The crystal growth of mannitol might lead to a mechanical stress (Figure 4.7), caused by the ice crystals growth, which initiates SLNs aggregation. The growth of the crystals resulted in less free space available for SLNs in this highly concentrated nanoparticle environment.[192]

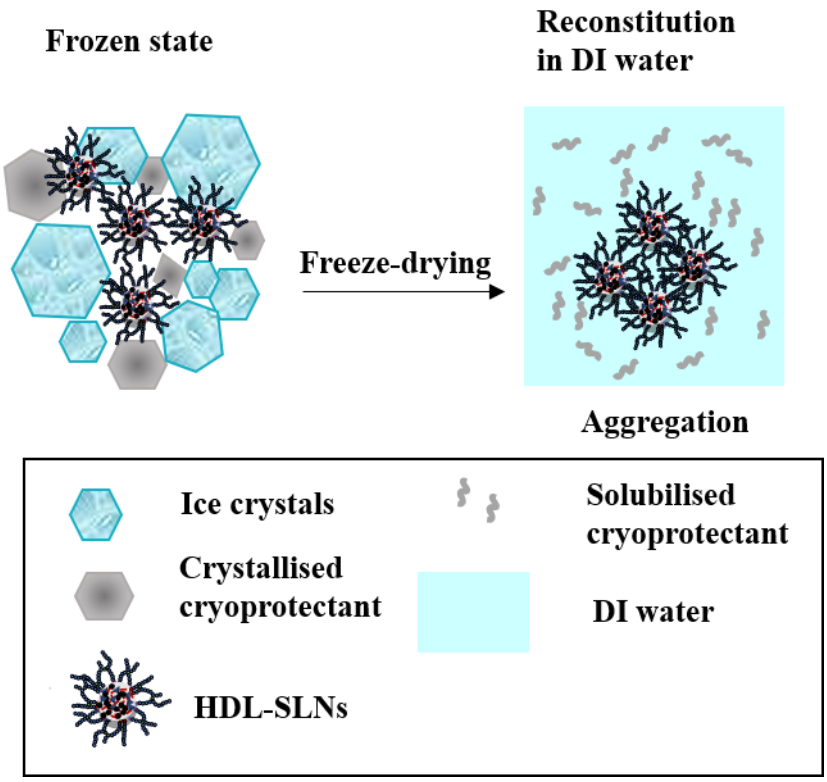

Figure 4.7 Diagram showing mechanism of how mannitol as a cryoprotectant causes aggregation of HDL-SLNs. Mannitol crystalises out causing additional mechanical stress to HDL-SLNs.

In conclusion, the use of these three cryoprotectants led to the ineffective cryoprotection of the HDL-SLNs during the freeze-drying process, and further cryoprotectants were investigated.

4.4.2.1.2 The effect of using trehalose and sucrose as cryoprotectants on the DLS data of re-dispersed HDL-DRV-SLNs

The use of trehalose and sucrose as examples of disaccharide cryoprotectants on the other hand, proved to be more promising than other carbohydrate cryoprotectants mentioned previously.

Optimising the weight ratio of cryoprotectant/nanoparticles was crucial in determining the stabilisation effect of the cryoprotectant after freeze-drying.[197] Although the majority of the studied weight ratios of cryoprotectant/HDL-DRV-SLNs and concentration of the freeze-dried sample led to particle aggregation upon reconstitution with water (see Table 4.1) There were four formulations with varied cryoprotectant/HDL-DRV-SLNs weight ratios and concentrations of the freeze-dried sample that managed to produce a re-dispersible HDL-DRV-SLNs formulations. The lowest successful weight ratio was cryoprotectant/HDL-DRV-SLNs of 188/1 at a concentration of the freeze-dried mixture (combined mass of SLNs, excipients and cryoprotectant in 2ml) of 13 mg/mL. Further increases in the weight ratio of cryoprotectant/HDL-DRV-SLNs and freeze-dried mixture concentration that also produced re-dispersible freeze-dried formulations were: 376/1 w/w at 25 mg/mL, 752/1 w/w at 50 mg/mL and 1504/1 w/w at 100 mg/mL.

From the observations in Table 4.1 , it was clear that re-dispersibility of the freeze-dried SLNs depends on a fine balance between the weight ratio of cryoprotectant/HDL-DRV-SLNs and the concentration of the freeze-dried mixture. One of these two variables cannot solely determine the re-dispersibility of the freeze-dried formulation. For example, the freeze-dried SLNs at weight ratio of 188/1 which proved successful at a concentration of 13 mg/mL, aggregated when the concentration was increased to 25 mg/mL. Also, by keeping the concentration fixed at 13 mg/mL but with decreasing the cryoprotectant/HDL-DRV-SLNs weight ratio to 47/1, 63/1 and 94/1, particle aggregation was observed. The freeze-drying parameters of the four optimised formulation were presented in Figure 4.8.

Table 4.1 Visual observation of freeze-dried HDL-DRV-SLNs after reconstitution with 1 mL DI water. Trehalose and sucrose were used as cryoprotectants during the freeze-drying process at different cryoprotectant/HDL-DRV-SLNs weight ratio and varied concentrations of the freeze-drying mixture (mg/mL). Successful re-dispersible formulations were highlighted. The term "Aggregated" refers to visual aggregation of the particles.

Cryoprotectant/HDL-DRV-SLNs weight ratio	Concentration of the freeze-drying mixture (mg/mL)	Trehalose	Sucrose
8/1	3	Aggregated	Aggregated
38/1	3	Aggregated	Aggregated
47/1	13	Aggregated	Aggregated
63/1	13	Aggregated	Aggregated
75/1	25	Aggregated	Aggregated
94/1	13	Aggregated	Aggregated
94/1	25	Aggregated	Aggregated
125/1	25	Aggregated	Aggregated
150/1	50	Aggregated	Aggregated
188/1	13	Re-dispersed	Re-dispersed
188/1	25	Aggregated	Aggregated
301/1	100	Aggregated	Aggregated
376/1	25	Re-dispersed	Re-dispersed
752/1	50	Re-dispersed	Re-dispersed
1504/1	100	Re-dispersed	Re-dispersed

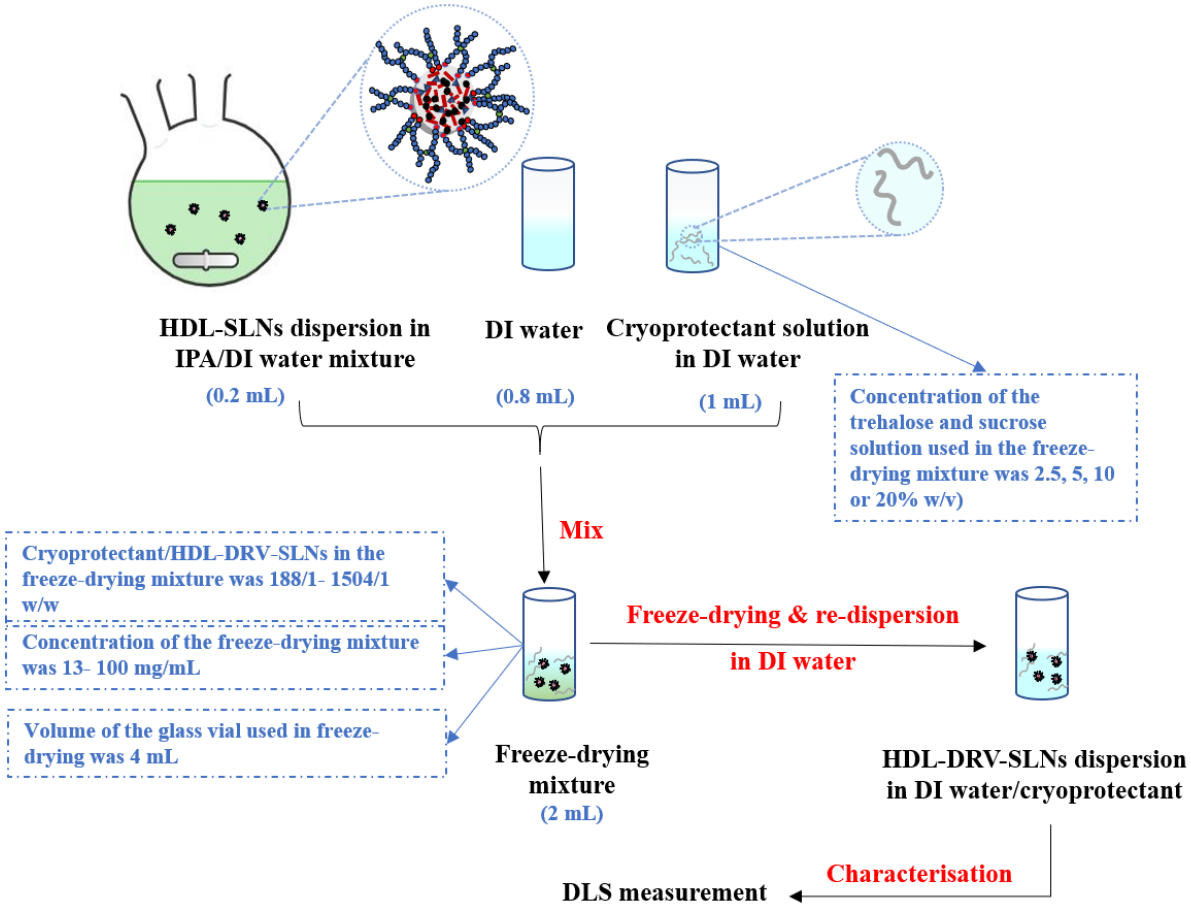

Figure 4.8 Optimum freeze-drying parameters required to produce re-dispersible HDL-DRV-SLNs using trehalose and sucrose as cryoprotectants. The formulations were characterised by DLS. Steps of freeze drying, and characterisation were written in red, while the freeze-drying variables were written in blue.

To determine the effect of increasing cryoprotectant/HDL-DRV-SLNs weight ratio on the Z-average diameter and PDI of the HDL-SLNs, the four re-dispersible formulations were tested by DLS (see Figure 4.9). In addition of presenting the data as the effect of cryoprotectant/HDL-DRV-SLNs weight ratio on the Z-average diameter and PDI of HDL-SLNs, the concentration of both trehalose and sucrose solutions was also presented to allow direct comparison with literature; Abdelwahed *et al.* stated that the cryoprotectant concentration was crucial in determining the level of stabilisation for nanoparticles.[197] From the data shown in Figure 4.9, it was evident that sucrose was more effective as a cryoprotectant than trehalose. This conclusion was because lower concentration of sucrose (2.5% w/v) was needed to keep the original diameter (~200 nm) of HDL-DRV-SLNs compared to trehalose, where the minimum concentration required was 5% w/v. Those concentrations were equivalent to cryoprotectant/HDL-DRV-SLNs of 188/1 and 376/1 w/w for sucrose and trehalose,

respectively. Above those concentrations of the cryoprotectants, the Z-average diameters increased to ~400 nm. That increase in the Z-average diameter could be due to the concentration of sample of the freeze-dried mixture was too high, forcing particles in near proximity to each other, which in turn lead to particle collision and increase in the final particle diameter. Increasing cryoprotectant concentration above a certain limit can destabilise nanoparticles, as in the case of silica nanoparticles which aggregated at a high glucose concentration.[197] This was also in agreement with the results of Varshosaz *et al.*, who showed that increasing the concentration of sucrose led to the increase in the size of NLCs.[209] They explained that each cryoprotectant system has to be optimised individually depending on the type of the nanoparticles, solvent and specific crystallisation behaviour of the cryoprotectant. Their results also showed that particles lyophilised with sucrose were smaller in size than those lyophilised using dextrose.[209]

Below 5% w/v trehalose, the Z-average diameter was also around ~400 nm, where at low concentration of the cryoprotectant, it was likely that the vitreous structure of the cryoprotectants was insufficient to cover the nanoparticles and thus particles aggregation happened as the nanoparticles were subjected to the mechanical stress of the ice crystals.[208]

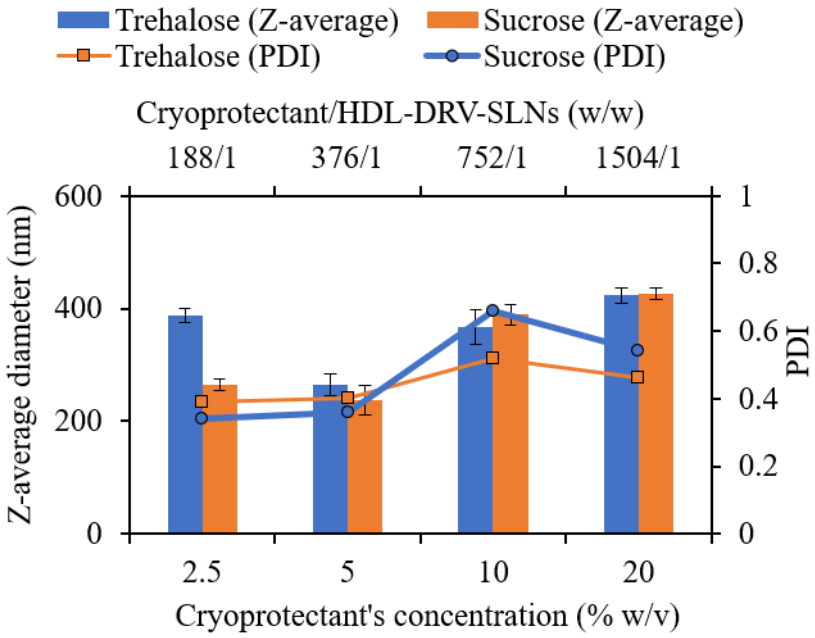

Figure 4.9 DLS data (Z-average diameter and PDI on the Y-axis left and right respectively) of freeze-dried HDL-DRV-SLNs after reconstitution in 1 mL DI water. The concentrations: 2.5, 5, 10 and 20% w/v of both trehalose and sucrose that were used during the freeze-drying process for 0.2 mL HDL-DRV-SLNs dispersions. The concentrations of the cryoprotectants were represented at the primary X-axis. While the cryoprotectant/HDL-DRV-SLNs weight ratio was represented on the secondary upper X-axis. Data were represented as mean ± SD (n =3), where SD is the standard deviation and n is the number of samples measured.

The cryoprotectant/HDL-SLNs weight ratio and concentration of the freeze-drying mixture (mg/mL) both influence the aggregation of HDL-SLNs dispersions. When no cryoprotectant was used during the freeze-drying process, as shown in Figure 4.10.A, the HDL-SLNs were subjected to mechanical stress caused by the formation of ice crystals during the freezing step, causing irreversible particle aggregation. If the amount of cryoprotectant was not sufficient to provide a thick layer around the HDL-SLNs (i.e., at low cryoprotectant/HDL-SLNs weight ratio), this would also result in irreversible particle aggregation (Figure 4.10.B). Increasing of the cryoprotectant/HDL-SLNs weight ratio would lead to re-dispersible particles (Figure 4.10.C), as the HDL-SLNs were coated with a thick layer of cryoprotectant which prevented SLNs collision during the freezing step and prevented aggregation. However, very high cryoprotectant/HDL-SLNs weight ratio should be avoided, although a thick layer of the cryoprotectant covered the HDL-SLNs during the freezing step, however the concentration of the freeze-dried mixture increased significantly, which would lead to particles collision in this limited space and eventually aggregation would take place (Figure 4.10.D).

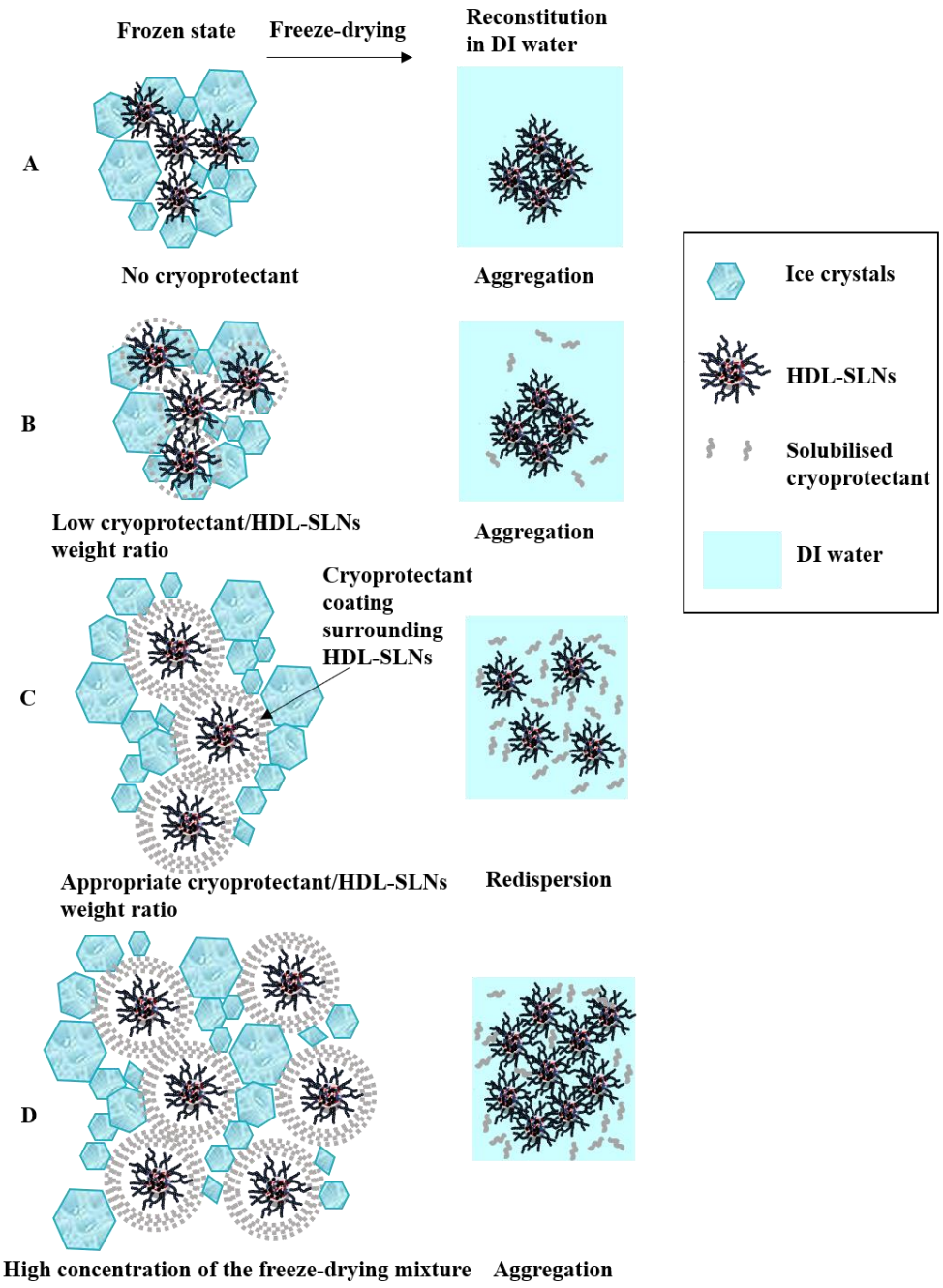

Figure 4.10 Diagram showing the effect of the cryoprotectant/HDL-SLNs weight ratio and concentration of the freeze-drying mixture (mg/mL) on the re-dispersion of freeze-dried HDL-SLNs. (A) No cryoprotectant was used. (B) Low cryoprotectant/HDL-SLNs weight ratio was used. (C) Appropriate cryoprotectant/HDL-SLNs weight ratio was used. (D) Very high concentration of the freeze-dried mixture. In all cases HDL-SLNs aggregated after re-dispersion in DI water except for (C).

The size distributions of the formulations were obtained by DLS (see Figure 4.11). The size distribution of the freeze-dried HDL-DRV-SLNs after reconstitution that most closely resembled that of the HDL-DRV-SLNs dispersion before freeze-drying was that of 5% w/v trehalose (Figure 4.11.A) and that of 2.5% w/v sucrose (Figure 4.11.B). At trehalose concentration above 5% w/v, a bimodal distribution of size can be seen, which suggested particle aggregation. For sucrose all the concentrations above 2.5% w/v showed slightly shifted or broader size distributions also suggesting particle aggregation.

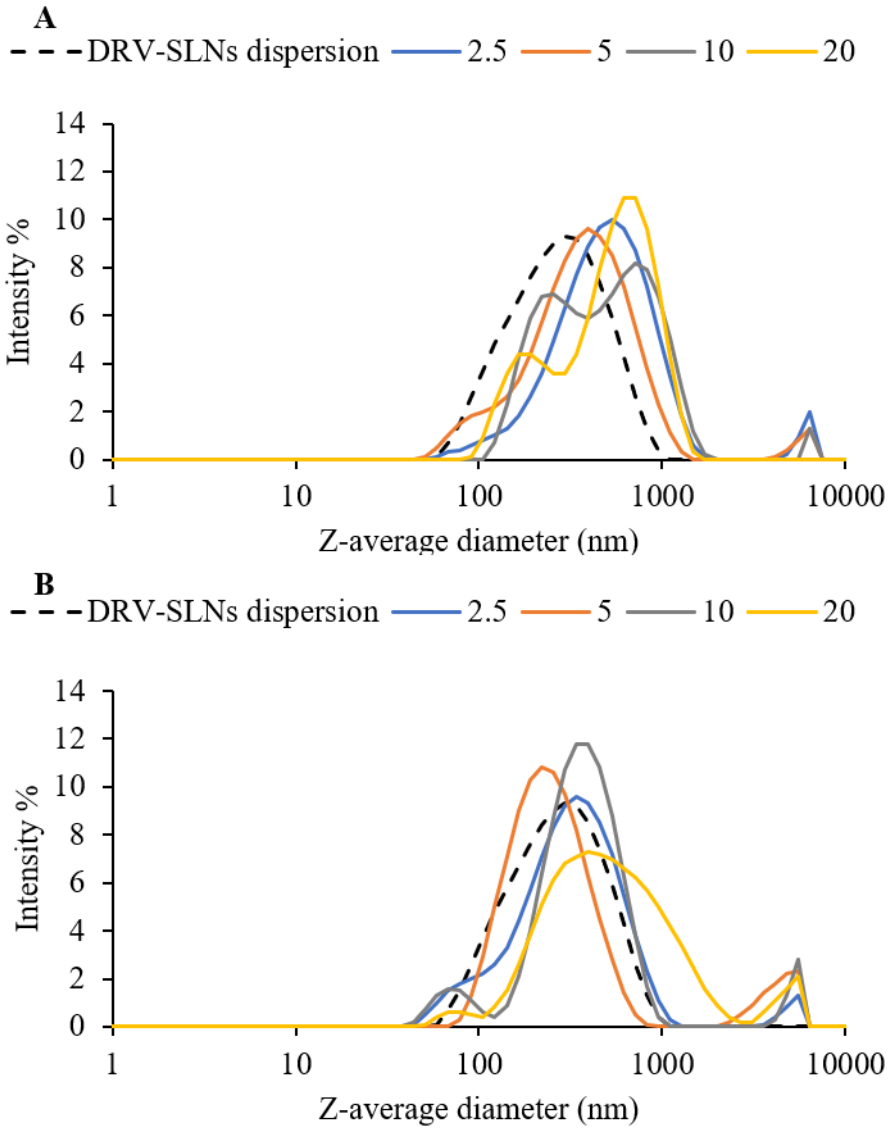

Figure 4.11 Size distribution obtained by DLS for HDL-DRV-SLNs disperion before freeze-drying and freeze-dried HDL-DRV-SLNs after reconstitution with 1 mL DI water. The concentrations: 2.5, 5, 10 and 20% w/v were for A) trehalose and B) sucrose as cryoprotectants used during the freeze-drying process for 0.2 mL HDL-DRV-SLNs dispersions.

Figure 4.12 shows pictures for the vials of the freeze-dried cakes of the two optimised formulations using 1 mL of 2.5% w/v sucrose or 5% w/v trehalose as cryoprotectants respectively, after removal from the freeze dryer and after re-dispersion in 1 mL DI water. Each formulation showed transparent solutions, which suggested particles did not aggregate.

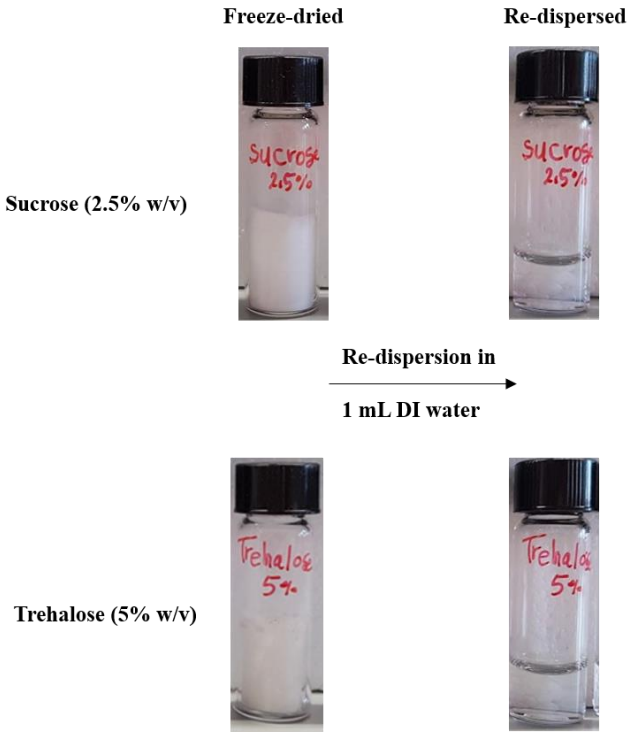

Figure 4.12 Images of vials showing how the optimised HDL-DRV-SLNs look like as freeze-dried cakes and after reconstitution in DI water. On the left-hand side, pictures of vials containing cakes of the optimised freeze-dried HDL-DRV-SLNs using 1 mL of 2.5% w/v sucrose or 5% w/v trehalose as cryoprotectants. The right-hand side showed pictures of the same vials after re-dispersion of the freeze-dried cakes in 1 mL DI water showing clear solutions. 0.2 mL of HDL-DRV-SLNs dispersions was used in both formulations.

The superior capability of sucrose and trehalose as cryoprotectants has been reported in the literature. Trehalose was considered as the most commonly used cryoprotectant in the freeze-drying of pharmaceuticals and biomaterials,[191] and the most effective.[201] Rodriguez *et al.* showed that the freeze-drying of SLNs with trehalose at concentrations of 5 and 10% w/v could lead to the formation of stable SLNs for up to six months.[210] In a different study by Date *et al.*, trehalose (a disaccharide) proved to be a better cryoprotectant than fructose (a monosaccharide) at an equivalent concentration.[208] On the other hand sucrose has been found more efficient than dextran and polyvinylpyrrolidone (PVP) as examples of polysaccharide and polymeric cryoprotectants, respectively for the stabilisation of nanosuspensions even at low concentration.[193] While Lim *et al.* showed that the freeze-drying of SLNs using sucrose as a cryoprotectant enhanced the stability of SLNs without significant increase in the particle

size.[207] There are four factors that contributed to trehalose and sucrose being better cryoprotectants compared to dextrose, mannitol, and maltodextrin:

1) Particle isolation hypothesis, where disaccharides have the ability to keep individual SLNs separated.[197] In this case vitrification is not essential for cryoprotection and spatial separation is enough to limit particle aggregation.[197]

2) The cryoprotective effect of disaccharides might also arise from the ability sugars to form a glassy shell surrounding SLNs when they are frozen below their glass transition temperatures,[206] which is considered one of the most important properties of semi-crystalline and amorphous materials.[199] Carbohydrates help maintaining the nanoparticles static in amorphous glass phase, and that would in turn limit particle aggregation. The higher the T_g of a sugar, the better its cryoprotectant ability and the better its vitrification ability.[197] Since trehalose has the highest T_g of all saccharides, that is why it has superior cryoprotectant abilities compared to other saccharides. This can be contrasted to monosaccharides where they form cakes that are liable to collapse.[208] For more detailed discussion on this behaviour, see section 1.5.2.4.2 in chapter 1.

3) Trehalose and sucrose have a better capping ability for SLNs as they are both examples of non-reducing disaccharides.[210] They only exist as closed ring form. The absence of internal hydrogen bonds in both compounds, allow more hydrogen bond formation between OH of the disaccharides and OH groups on the surface of the nanoparticles. Unlike, reducing sugars which can exist on both open and ring forms like dextrose and maltodextrin form internal hydrogen bonds, so there are less OH groups available to form hydrogen bonds with nanoparticles.[208]

4) Other factors are related to the amorphous properties of trehalose at the dried state, unlike mannitol for example which crystalises.[197] Trehalose is also less hygroscopic than other sugar cryoprotectants.[192]

In conclusion, except for sucrose and trehalose, all the other carbohydrates failed to act as effective cryoprotectants for the HDL-DRV-SLNs at different concentrations for various reasons. In our study, we were able to optimise the freeze-drying formulation and reached much lower concentration of the cryoprotectants: 2.5% w/v for sucrose and 5% w/v for trehalose, which in turn meant overall higher drug loading. This is in a significant decrease in the concentrations compared to those reported in the literature, where usually high concentration of cryoprotectants (10-30%) is required to provide stabilisation of the particles during freeze drying.[205] Abdelwahed *et al.* also stated that at least 15% w/v trehalose solution was required

to cryoprotect SLNs.[197] The lowest cryoprotectant/HDL-DRV-SLNs weight ratio that could be achieved were 188/1 and 376/1 for sucrose and trehalose, respectively. Although these weight ratios proved successful, we aimed to have lower weight ratios to have formulations with higher drug loading. Therefore, a different cryoprotectant category, which is polymeric cryoprotectant was investigated to determine the ability of having lower cryoprotectant/HDL-SLNs weight ratios.

4.4.2.2 Influence of PEG as a polymeric cryoprotectant on the re-dispersion of HDL-SLNs

Water soluble polymers can be used as cryoprotectants. PEG has been used as a coating agent for nanoparticles and proteins during freeze drying.[205] In this section PEG (Mn 2050) was studied as a possible cryoprotectant for HDL-SLNs. The optimum freeze-dried formula would have the lowest PEG concentration and the highest volume of SLNs as this would yield the highest drug loading. For polymeric cryoprotectants, the tested weight ratio range of cryoprotectant/HDL-SLNs was 4/1- 752/1, while the tested concentrations range of the freeze-drying mixtures was 1-50 mg/mL.

4.4.2.2.1 The effect of PEG/HDL-SLNs weight ratio and the concentration of the freeze-drying mixture on the DLS data of HDL-SLNs

In this study a wide range of PEG concentrations was investigated (0.125- 10% w/v), 1 mL of each PEG concentration was added to three volumes of HDR-DRV-SLNs dispersions (0.2, 0.4 and 0.5 mL) with of a concentration HDL-SLNs dispersions of 1 mg/mL. The total volume of the freeze-drying mixture was kept fixed at 2 mL by the addition of DI water. Higher concentration of PEG, above 10% w/v were not tested, because a previous study by Lee *et al.* showed that PEG concentration of 15% w/v act as a promotor for aggregation.[268] Different parameters tested for the freeze-drying using PEG 2050 as a cryoprotectant were presented in Figure 4.13.

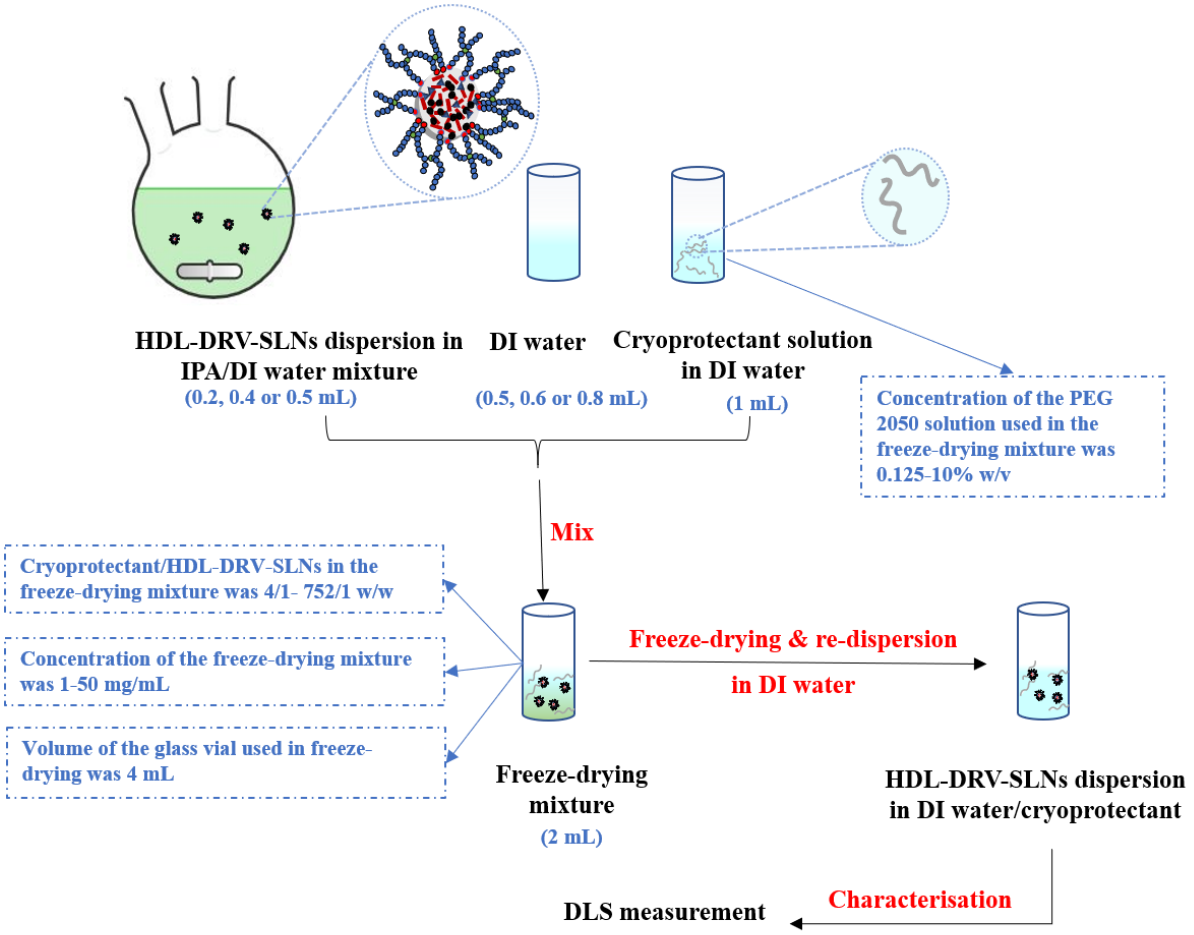

Figure 4.13 Optimisation of the freeze-drying parameters required to produce re-dispersible HDL-DRV-SLNs using PEG 2050 as cryoprotectant. The formulations were characterised by DLS.

Since all the freeze-dried formulations were re-dispersed in DI-water with no aggregation, they were all measured by DLS (Figure 4.14). From the DLS data we can conclude that a concentration dependent cryoprotection was observed when PEG was used as a cryoprotectant in the freeze-drying of HDL-SLNs, where a significant increase in the Z-average diameter was observed at low PEG concentrations (<0.5% w/v). The lowest PEG concentration that provided proper cryoprotection and prevented particle size increase, was 0.5% w/v at HDL-SLNs dispersion volume of 0.2 mL. Unlike the sugar cryoprotectants, where minimum concentrations of 2.5% w/v for sucrose and 5% w/v for trehalose were required to provide cryoprotection, PEG allowed the use of a much lower concentrations (0.5-10% w/v) and at different HDL-SLNs volumes. However, to maintain a particle size around 200 nm, it seemed that 0.2 mL of HDL-SLNs dispersion was the optimum volume, regardless to the concentration of PEG. At only PEG concentrations of 2.5 and 5% w/v, and at all HDL-DRV-SLNs volumes, the re-

dispersed freeze-dried particles maintained the original size of ~200 nm. It was also noticed that the particle size of some formulations was slightly reduced after rehydration, as compared to the particle size before freeze-drying. In Figure 4.14, the data was represented as concentrations of PEG and volumes of SLNs dispersions due to complications of representing such huge number of data as PEG/HDL-SLNs (w/w) and concentration of the freeze-dried sample, however the optimised data was represented as PEG/HDL-SLNs w/w at a fixed concentration (Figure 4.17).

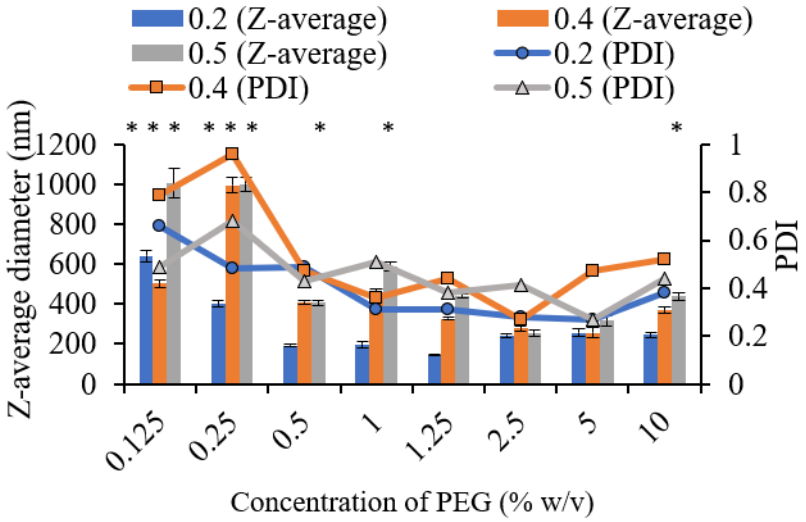

Figure 4.14 DLS measurements (Z-average diameter and PDI) for the effect of the increasing the concentration of PEG (0.125-10 % w/v) at different volume of HDL-DRV-SLNs (0.2, 0.4, 0.5 mL). The asterisk (*) refers to poor quality DLS data. Data were represented as mean ± SD (n =3), where SD is the standard deviation and n is the number of samples measured.

The size distribution graphs obtained by DLS can be seen in Figure 4.15 further confirmed the Z-average diameter and PDI data shown in Figure 4.14. The lowest concentration of PEG that provided the size distribution graph that most closely resembled that of HDL-DRV-SLNs dispersion before freeze-drying and showed a monomodal size distribution was that of 0.5% w/v PEG (Figure 4.15.A). Although the graphs of higher PEG concentrations (2.5-10% w/v) showed closer overlap with the size distribution graph of HDL-DRV-SLNs dispersions prior to freeze-drying (Figure 4.15.B), using such high concentration would mean compromising drug loading. So, the decision was made to use 0.5% w/v PEG for further studies to have overall higher drug loading and it also maintained good quality DLS data.

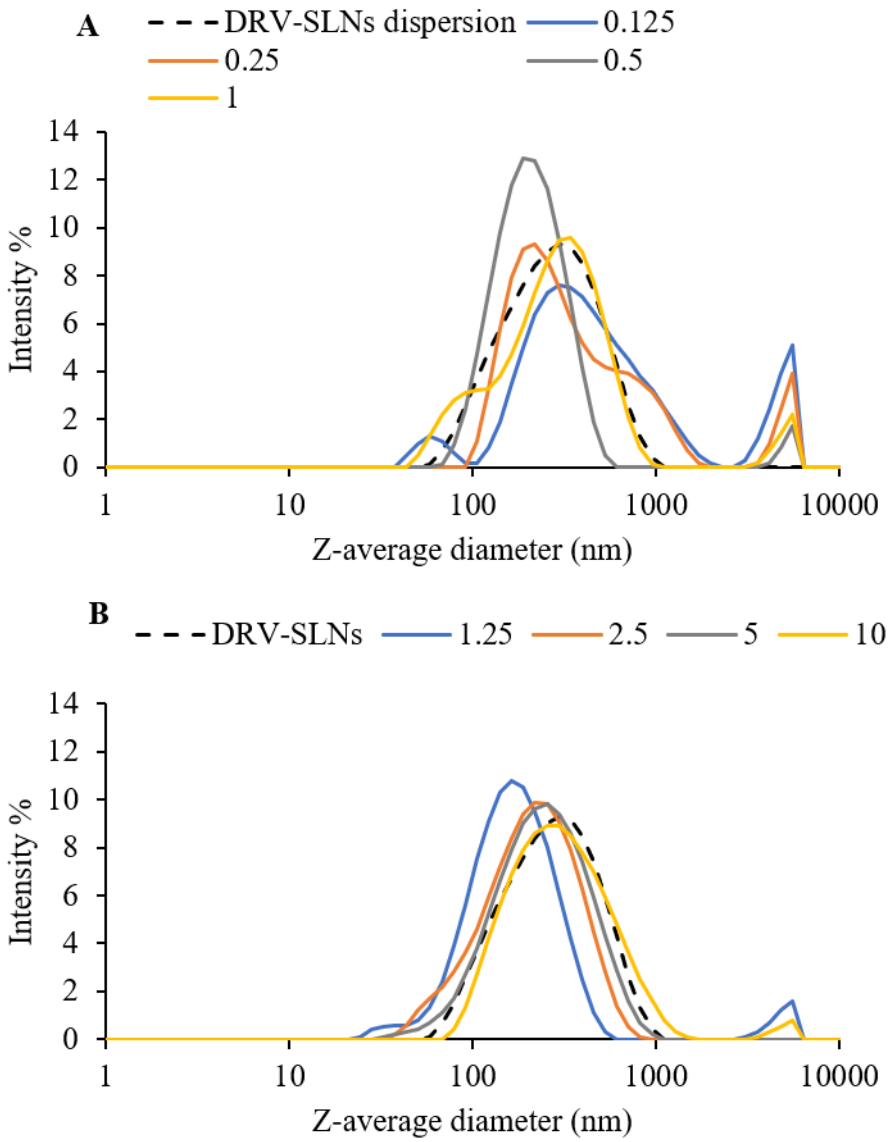

Figure 4.15 Size distribution graphs obtained by DLS for HDL-DRV-SLNs disperion before freeze-drying and freeze-dried HDL-DRV-SLNs after reconstitution with 1 mL DI water. The used concentrations of PEG as a cryoprotectant were A) 0.125-1% w/v B) 1.25-10% w/v, 0.2 mL HDL-DRV-SLNs dispersions were used in all formulations.

Since 0.5% w/v of PEG was the lowest concentration that provided efficient cryoprotection for HDL-DRV-SLNs. That concentration of PEG was more thoroughly studied, using a wider range of HDL-SLNs dispersion volume (0.2-1 mL), and was also used as a cryoprotectant for HDL-DRV-RTV-SLNs that has the combination of the two drugs: DRV/RTV (8:1). HDL-SLNs dispersion volume referred to the volume of SLNs dispersion before freeze-drying that was added to the freeze-drying mixture. Optimisation of the freeze-drying parameters required to produce re-dispersible HDL- SLNs using 0.5% w/v PEG 2050 as cryoprotectant were shown in Figure 4.16.

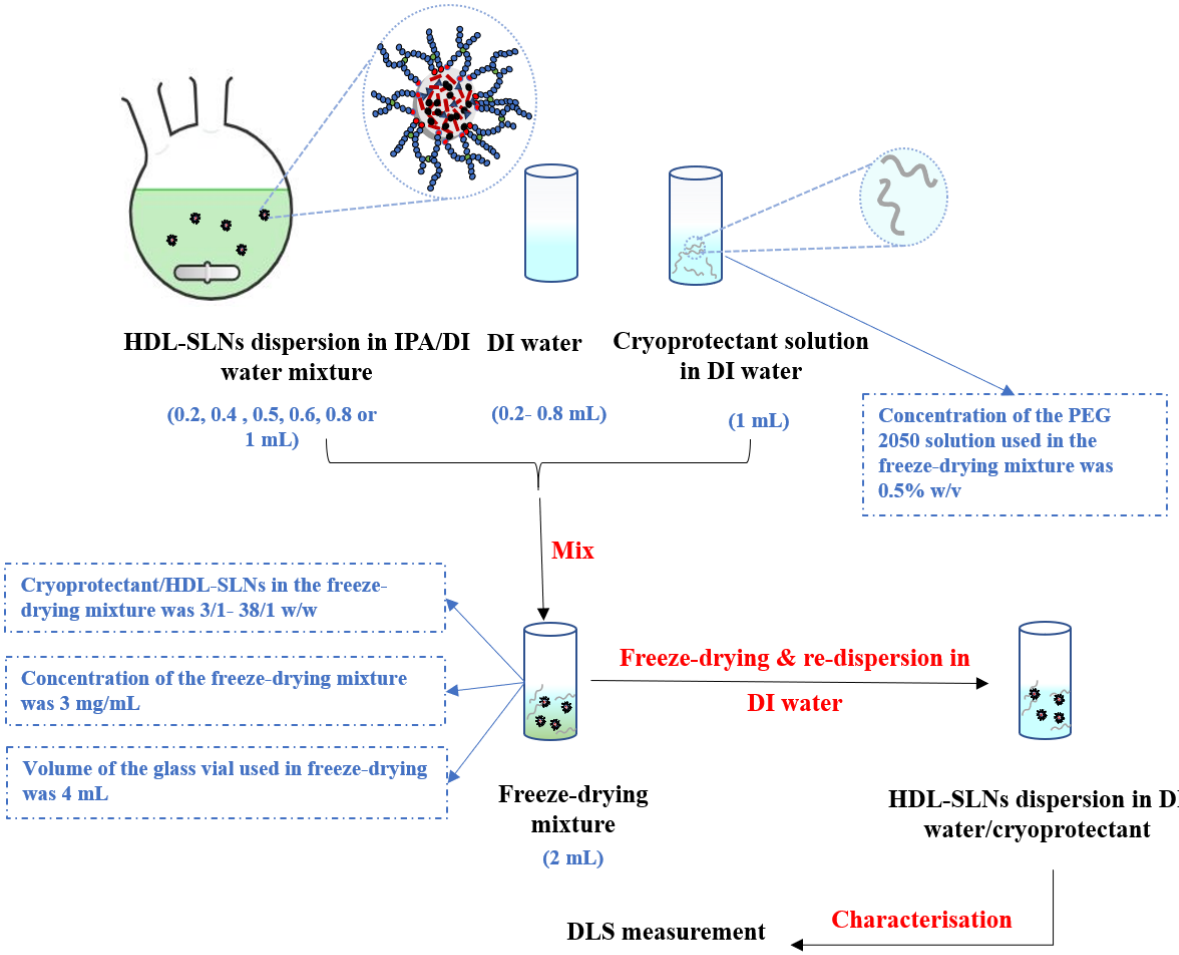

Figure 4.16 Optimisation of the freeze-drying parameters required to produce re-dispersible HDL-SLNs using 0.5% w/v PEG 2050 as cryoprotectant. The formulations were characterised by DLS.

The DLS data of the produced formulations was represented in Figure 4.17 in two ways to allow better understanding of the findings: 1) PEG/HDL-SLNs weight ratio, which was plotted on the lower X-axis, at fixed freeze-drying mixture concentration of 3% w/v. 2) HDL-SLNs dispersion volume (0.2-1 mL) at a fixed concentration of PEG (0.5% w/v), which was plotted on the upper X-axis. From the DLS data shown in Figure 4.17, we can conclude that at a fixed PEG concentration of 0.5% w/v, when a single drug or drug combination were used, both sets of formulations behaved similarly. The highest HDL-SLNs dispersion volume that could be used and maintained a size of 200 nm was 0.2 mL. Above this volume the particle size and PDI increased and completely deteriorated at 0.6 mL and above. This observation is closely related to the PEG/HDL-SLNs weight ratio. At 0.2 mL SLNs, this formulation would have the highest PEG/HDL-SLNs weight ratio (38/1 w/w) which provided the best cryoprotection effect. At 1

mL HDL-SLNs dispersion, this formulation would have the lowest the PEG/HDL-SLNs weight ratio of 3/1, and that proved insufficient to provide cryoprotection.

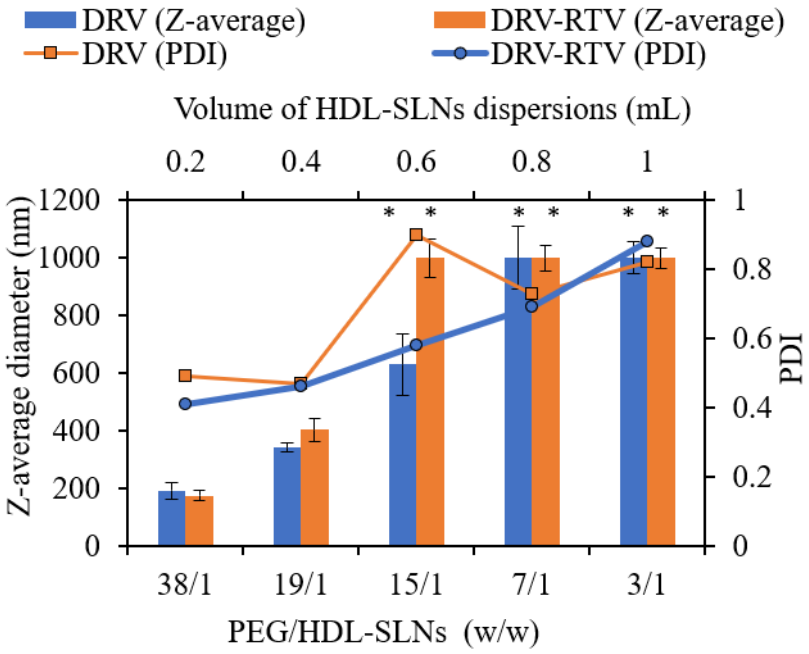

Figure 4.17 DLS data (Z-average diameter and PDI) of freeze-dried HDL-DRV-SLNs and HDL-DRV-RTV-SLNs after reconstitution with 1 mL of DI water. 1 mL of 0.5% w/v PEG was used as a cryoprotectant during the freeze-drying process for 0.2- 1 mL HDL-SLNs dispersions. The data was also plotted as PEG/-HDL-SLNs (3/1- 38/1 w/w). Data are represented as mean ± SD (n =3), where SD is the standard deviation and n is the number of samples measured.

The size distribution obtained by DLS (see Figure 4.18) further confirmed the Z-average diameter and PDI data shown in (Figure 4.17). It was found that when 0.2 mL of HDL-SLNs was used, equivalent to PEG/HDL-SLNs weight ratio of 38/1 for both HDL-SLNs sets of formulations, displayed a monomodal size distribution (Figure 4.18.A) for HDL-DRV-SLNs and Figure 4.18.B for HDL-DRV-RTV-SLNs after re-dispersion with DI water. These formulations displayed size distributions after reconstitution with DI water that was most similar to the formulation prior freeze drying. While formulations which were freeze-dried using a volume of the HDL-SLNs dispersions above 0.2 mL, their size distributions tended to become multimodal which showed a considerable change in the particle properties compared to the formulation prior to freeze-drying.

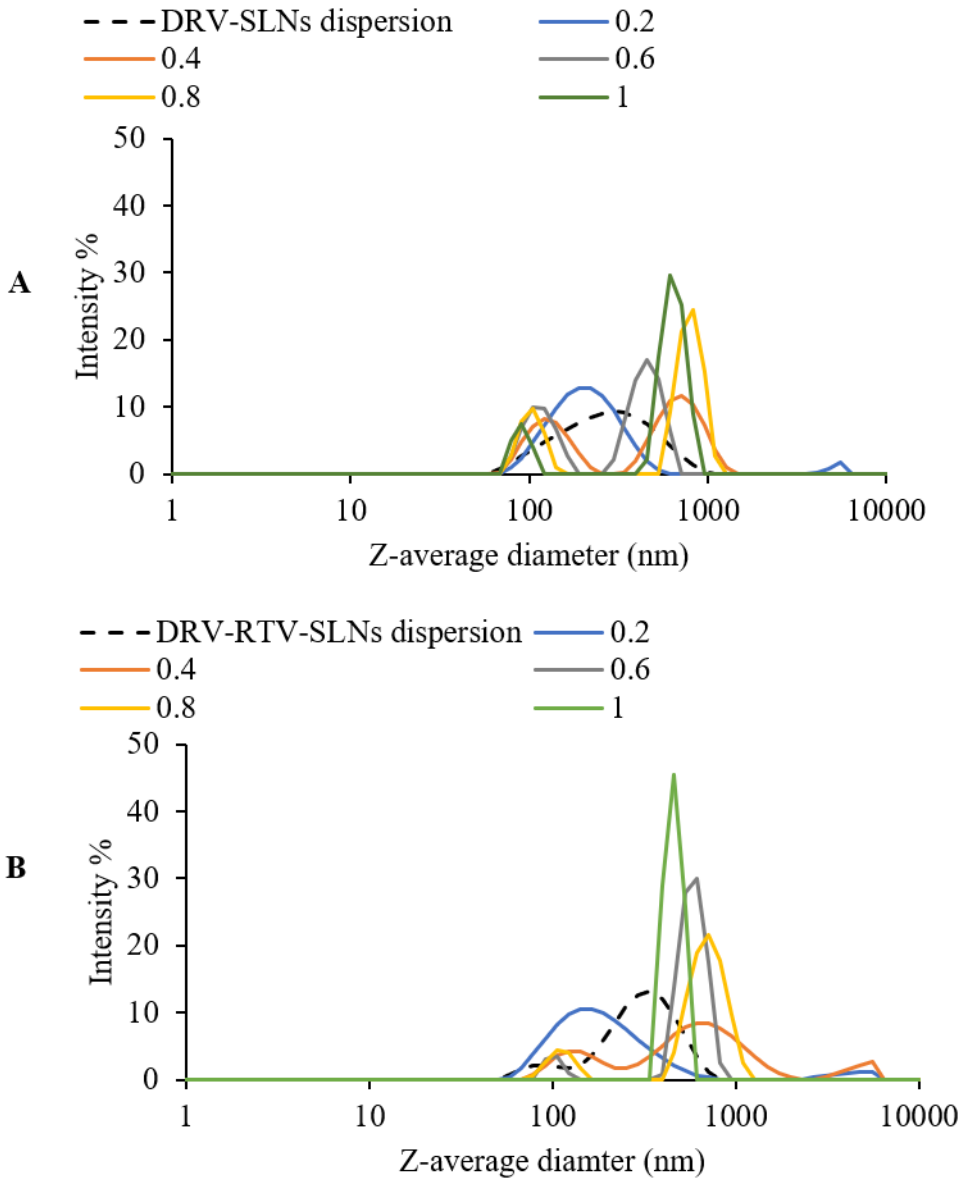

Figure 4.18. Size distribution obtained by DLS for A) Re-dispersed HDL-DRV-SLNs and B) Re-dispersed HDL-DRV-RTV-SLNs after reconstitution with 1 mL DI water. The used volume of HDL-SLNs dispersion were 0.2-1 mL. The size distribution of HDL-SLNs dispersions before freeze-drying of each formulation were plotted as controls.

In conclusion, in our study we were able to use low concentration of PEG (0.5% w/v) for 0.2 mL HDL-SLNs dispersion to provide stability, prevent aggregation and enhance re-dispersion in water of the HDL-SLNs after freeze drying. This was achieved using a single drug loaded or dual drug loaded formulations. In contrast, the sugar cryoprotectants were much less effective; a concentration of 2.5% w/v was required for sucrose and 5% w/v was required for trehalose to provide re-dispersible formulations when a volume of HDL-SLNs 0.2 mL was used. Regarding to the cryoprotectant/HDL-SLNs weight ratio, a 38/1 w/w for PEG, in oppose to 188/1 for sucrose and 376/1 for trehalose. Obtaining re-dispersible freeze-dried formulations

at a PEG concentration of 0.5% w/v is considered a progress compared to previous studies which required a PEG concentration of at least 1% w/v to provide cryoprotection.[192] In a study by Umerska *et al*., PEG concentration of 0.5% w/v at varied molecular weights was not sufficient to provide cryoprotection to polyelectrolyte nanoparticles.[192] They also found that PEG was found to more efficient as a cryoprotectant compared to trehalose.[192]

4.4.2.2.2 Scale up of the freeze-drying of HDL-SLNs using PEG as a cryoprotectant

The volume of the freeze-drying container plays an important role of the freeze-drying process. The rate of freezing inside the vial will depend on the surface area that is in contact with liquid N_2. Additionally, the rate of sublimation is also influenced by vial shape; at a fixed volume, maximum sublimation happens with large surface area, therefore wider containers are preferred.[199] In this section we discuss the scale up of the freeze-drying of HDL-SLNs and its effect on the final Z-average diameter, PDI and size distribution of the freeze-dried HDL-SLNs, using freeze-drying vials of varied sizes filled with different volumes of the freeze-drying mixture. In the previous experiment, the optimised freeze-drying mixture had a total volume of 2 mL, which was made of 1 mL of the 0.5% w/v PEG solution, 0.2 mL HDL-SLNs dispersions and 0.8 mL DI water, which made the volume ratio between three constituents of the freeze-drying mixture. This was the volume ratio that allowed the use of the least amount of cryoprotectant while keeping the size original size of HDL-SLNs after freeze drying and was also equivalent to PEG/HDL-SLNs weight ratio of 38/1. In this study, we aimed to increase the total volume of the used freeze-drying mixture above 2 mL. For that purpose, in addition to the 2 mL freeze-drying mixture, 5 and 10 mL of that mixture was also freeze-dried in 4-, 14- and 40-mL glass vials respectively for four days, with keeping the composition fixed. Two sets of samples were tested: HDL-DRV-SLNs and HDL-DRV-RTV-SLNs, the optimisation of the scale-up parameters is shown in Figure 4.19.

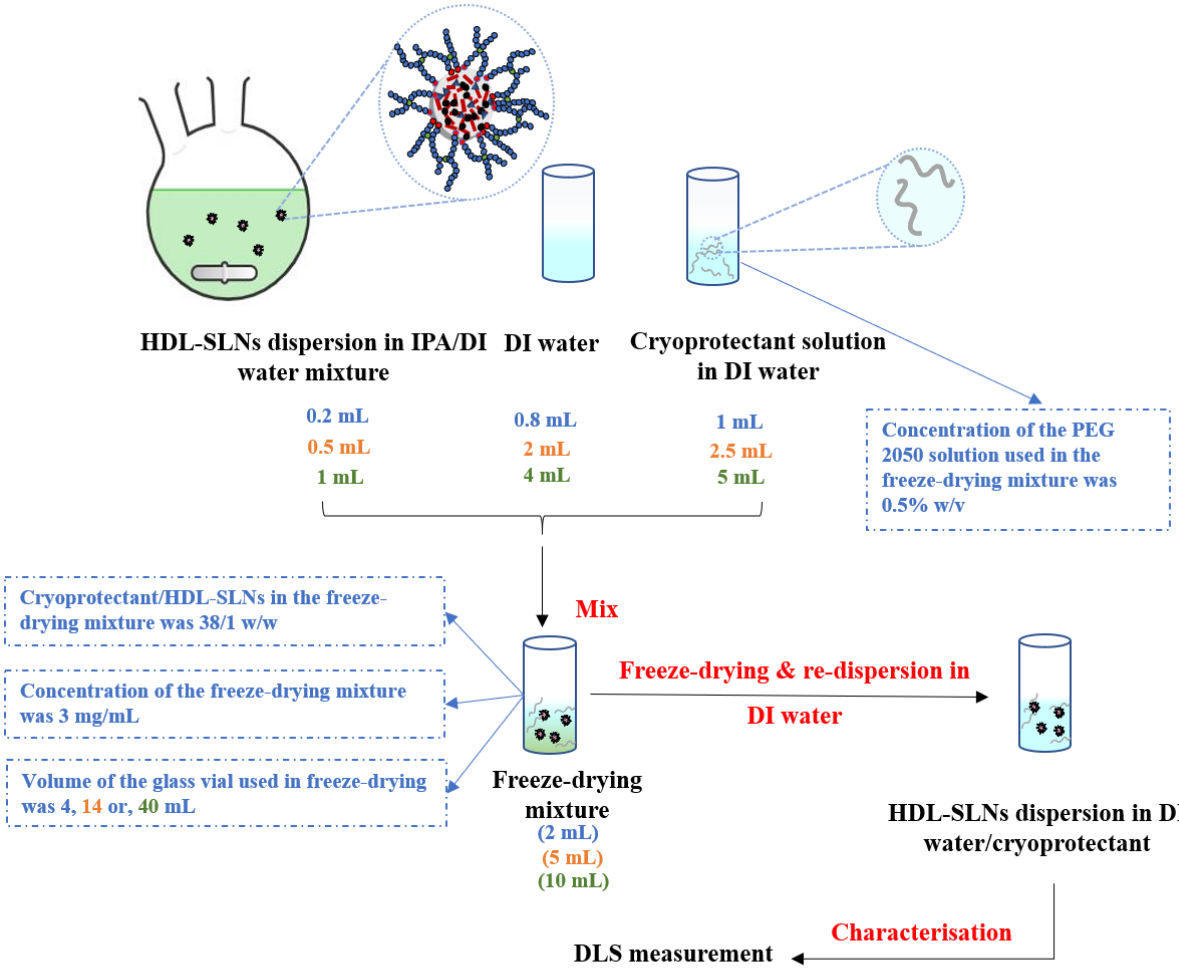

Figure 4.19 Optimisation of the parameters required for scale-up of freeze-drying to produce re-dispersible HDL-SLNs using 0.5% w/v PEG 2050 as cryoprotectant. The formulations were characterised by DLS. Volumes (mL) written in blue, orange or green, represents the volume of constituents required to produce a freeze-drying mixture of 2, 5 or 10 mL, that were placed in glass vials with a volume of 4, 14, or 40 mL, respectively.

From DLS data in Figure 4.20, it was observed that the Z-average diameter for all samples were below 200 nm at the different scale-up levels, except for the Z-average diameter of HDL-DRV-RTV-SLNs which has a size of ~ 250 nm when 10 mL of the freeze-drying mixture was used. However, that size was acceptable, as the original Z-average diameter was ~290 nm.

When the volume of the freeze-drying mixture was further increased to up to 15 or 20 mL, but with keeping the volume of the vial fixed at 40 mL, the samples did not fully dry out and remained in the frozen state even when the freezing-drying time was increased to one week instead of 4 days. This could be explained by the larger surface area/volume ratio, which led to thinner frozen layers in case of using 10 mL of the freeze-drying mixture which occupied

only 25% the volume of the 40 mL vials. Thinner frozen layers would in turn lead to a decrease the duration of drying, less aggregation of particles during freezing, and decrease the heterogeneity of the produced solidified particles.[269] On the contrary, drying was affected when 15 or 20 mL of the freeze-drying mixture were used which occupied 38% and 50%, respectively of the volume of the 40 mL vials. During primary drying, heat is transferred to the frozen solution from the shelf through the vial. Ice sublimes into water vapour which then passes through the dried segment of the sample and to the sublimation front. At the end of this stage a porous mass is formed, the porous spaces represents the ice crystals that have sublimed.[197] In conclusion the optimum set up for the freeze-drying scale-up was using 10 mL of the freeze-drying mixture in a 40 mL vial, for a duration of 4 days, as it did not affect the size of the re-dispersed freeze-dried HDL-SLNs.

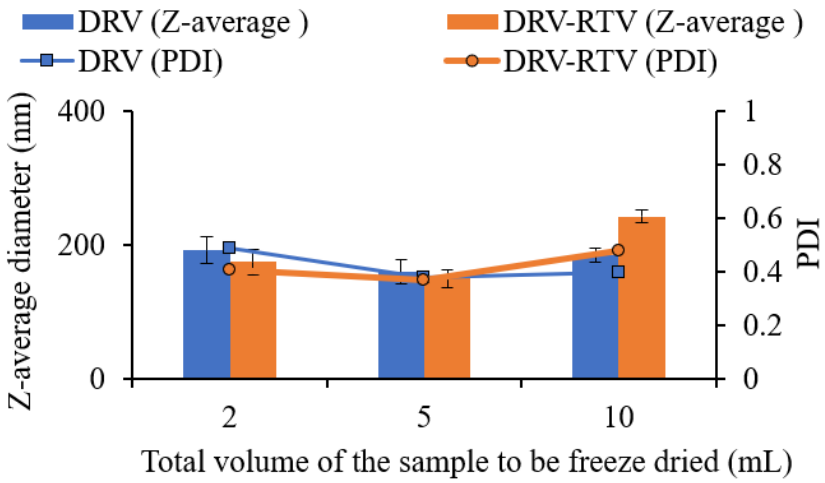

Figure 4.20 DLS data (Z-average diameter and PDI) of freeze-dried HDL-DRV-SLNs and HDL-DRV-RTV-SLNs after reconstitution with 1 mL DI water. 2, 5 and 10 mL of the freeze-drying mixture were placed in 4, 14 and 40 mL respectively, and freeze-dried for 4 days. Data are represented as mean ± SD (n =3), where SD is the standard deviation and n is the number of samples measured.

The size distributions obtained by DLS shown in Figure 4.21 agreed with the Z-average diameter and PDI data Figure 4.20. All tested samples had size distributions that resembled that of HDL-SLNs dispersion before freeze-drying, some had slightly shifted peaks, but all showed a monomodal size distribution. Only HDL-DRV-RTV-SLNs showed a slightly broader peak when 10 mL of the freeze-drying mixture was used.

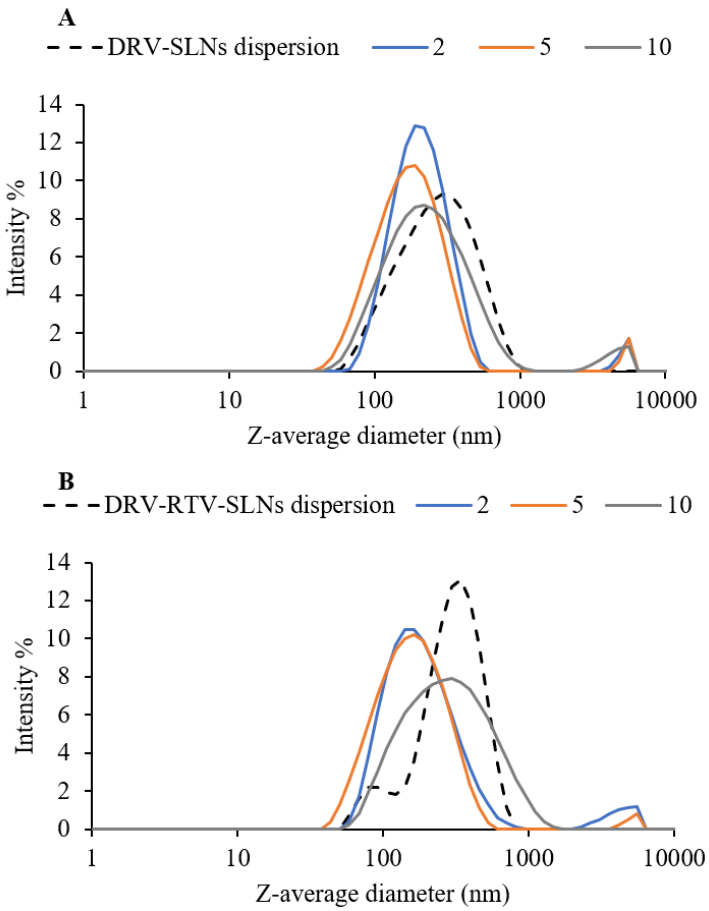

Figure 4.21 Size distributions obtained by DLS for A) Re-dspiersed HDL-DRV-SLNs and B) Re-dspiersed HDL-DRV-RTV-SLNs after reconstitution with 1 mL DI water using 2, 5 and 10 mL of the freeze-drying mixture were placed in 4, 14 and 40 mL respectively freeze-dried for 4 days. The size distribution of HDL-SLNs dispersions of each formulation before freeze-drying was plotted as a control.

4.4.2.2.3 Testing of colloidal stability of freeze-dried HDL-SLNs by reconstitution in PBS and SGF

The colloidal stability of freeze-dried HDL-SLNs was assessed via measurement of the Z-average diameter and PDI of the reconstituted formulations upon exposure to physiological ionic strength. The freeze-dried HDL-SLNs were stable when was re-dispersed in 1 mL of PBS solution at pH 7.4, see Table 4.2. The Z-average diameter and PDI were 250 nm and 0.32 for HDL-DRV-SLNs and 300 nm and 0.45 for HDL-DRV-RTV-SLNs, respectively. These DLS results were very similar to the DLS data of the same formulations when re-dispersed in DI water. On the other hand, both formulations aggregated instantly upon re-dispersion in simulated gastric fluid at pH 1.2, the aggregated particles could be seen by the naked eye. which suggest poor colloidal stability in acidic conditions. To overcome the instability problem, the freeze-dried materials can be coated with excipients resistant to stomach acidity, an example of

such excipient is Cruciferin.[270] To understand the reason of particles aggregation more investigation are required, which might include testing surfactants from different groups and study the relationship between the surfactant structure and the stability in acidic conditions.

Table 4.2 DLS data (Z-average diameter and PDI) of freeze-dried HDL-DRV-SLNs and HDL-DRV-RTV-SLNs after reconstitution with 1 mL PBS. Data are represented as mean ± SD (n =3), where SD is the standard deviation and n is the number of samples measured.

Formulation	Z-average diameter (nm)	PDI
HDL-DRV-SLNs	250 ± 11	0.32 ± 0.03
HDL-DRV-RTV-SLNs	300 ± 20	0.45 ± 0.07

4.4.3 Morphology and size analysis of the freeze-dried HDL-SLNs by SEM

The size and morphology of HDL-SLNs were investigated using SEM. Images produced by SEM analysis showed spherical particles with smooth surface for HDL-DRV-SLNs (Figure 4.22.A) and HDL-DRV-RTV-SLNs (Figure 4.22.B). The particles appeared to be coated with a film that was probably due to the presence of PEG. The particles had a Z-average diameter of ~ 200 nm with a narrow size distribution (Figure 4.22.C).

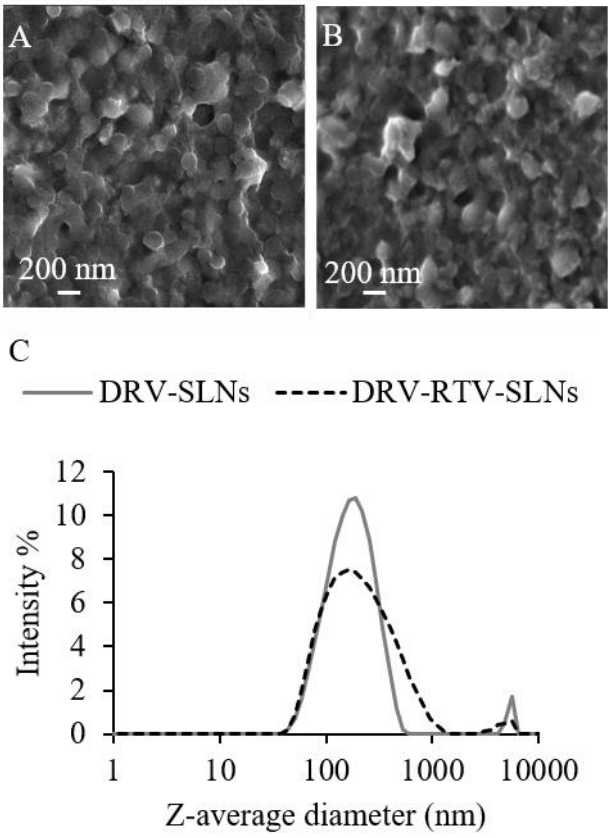

Figure 4.22 Particle characterisation of HDL-SLNs that were freeze-dried using PEG/ HDL-SLNs of 38:1 w/w, for formulations with different drug composition; (A) SEM image of HDL-DRV-SLNs. (B) SEM image HDL-DRV-RTV-SLNs. (C) Size distribution graphs obtained by DLS for the same 2 formulations, the graph shows narrow distribution of size for HDL-DRV-SLNs and slightly broader size distribution for HDL-DRV-RTV-SLNs with Z-average diameters around 200 nm.

4.4.4 Scale-down of the synthesis of HDL-SLNs by solvent injection

After establishing all the parameters that affect the freeze-drying of HDL-SLNs, the optimised freeze-dried formulations were further tested for drug release and cell work using radiometric analysis. The initial solvent injection technique produced 24 mL of HDL-SLNs dispersions, however for drug release and cell work only 3 mL of each radiolabelled formulation was required. Therefore, a scale-down of the synthesis of HDL-SLNs was carried out to limit the radioactive waste and compile with guidelines on ‘as low as reasonably practicable’. The size properties of the produced HDL-SLNs before freeze-drying were tested by DLS, the Z-average diameter and PDI of HDL-DRV-SLNs and HDL-DRV-RTV-SLNs were 266 nm, 0.29 and 312 nm, 0.40, respectively. The size distributions are shown in Figure 4.23 revealing a monomodal

distribution of nanoparticles indicating the successful synthesis of the HDL-SLNs by the scaled-down technique.

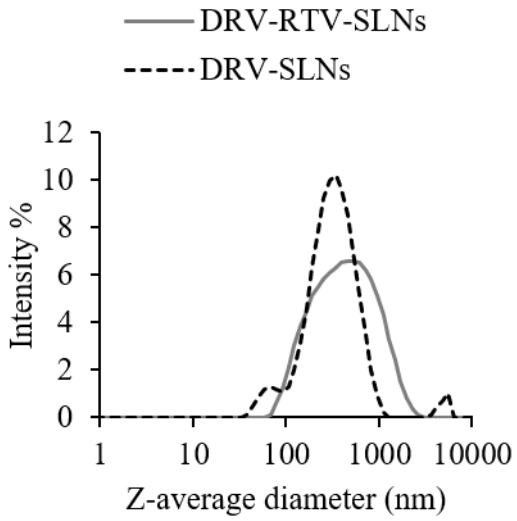

Figure 4.23 Size distributions obtained by DLS for HDL-DRV-SLNs and HDL-DRV-RTV-SLNs dispersions before freeze-drying synthesised using small scale solvent injection method.

4.4.5 Release studies

Radiometric dialysis experiments were used to quantify the drug release behaviour from HDL-SLNs. The drug released quantified using radiolabelled [^{3}H]-DRV. DRV is slightly soluble in water (0.15 mg/mL, as listed on the FDA datasheet), therefore DRV concentration was kept below this limit during the release study. The two formulations used in this study were freeze-dried HDL-DRV-SLNs and HDL-DRV-RTV-SLNs, using PEG as a cryoprotectant for both formulations. The freeze-dried formulations were re-dispersed in DI water prior drug release measurement. Both samples had [^{3}H]-DRV concentration of 1 mg/mL and both formulations showed little burst release (measured at the first time point of 0.5 hours) of 8%, which might be due to adsorbed drug on the surface of the particles that was unencapsulated within the SLNs. Both samples had very similar drug release behaviour with over 85% of the drug being released in the first 8 hours (Figure 4.24). The freeze-drying might cause burst drug release, due to the drug leakage through fragile structure of nanoparticles, which may not resist the harsh freeze-drying conditions.[206] According to ANOVA test there was no significant difference in the accumulative DRV release between HDL-DRV-SLNs and HDL-DRV-RTV-SLNs, as $P = 0.287$ (i.e., $P > 0.05$).

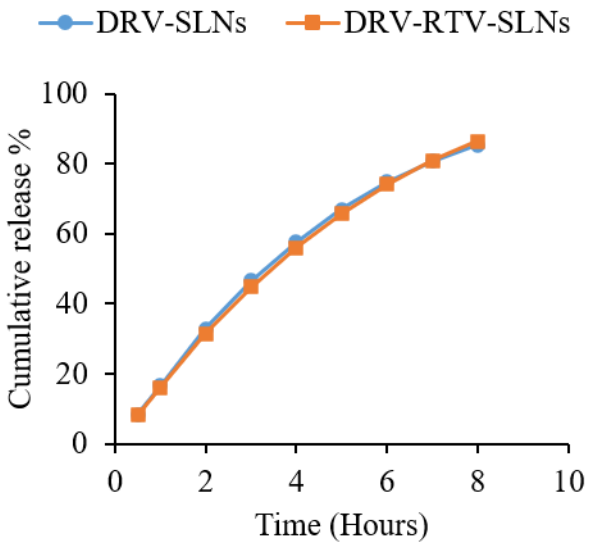

Figure 4.24 Drug release of HDL-SLNs that were freeze-dried using PEG/ HDL-SLNs of 38:1 w/w, for formulations with different drug composition; HDL-DRV-SLNs and HDL-DRV-RTV-SLNs. Samples were re-dispersed in 1 mL DI water prior to drug release measurements

4.4.6 The behaviour of freeze-dried HDL-SLNs and the absorption of DRV across Caco-2 and triple culture model

An *in vitro* experiment was conducted to establish the apparent permeability of DRV for both single and dual drug loaded formulations. In order in investigate if freeze-dried HDL-SLNs can facilitate an increase in bioavailability of orally administered drugs. A cellular accumulation study was also undertaken to assess the pharmacokinetics of both HDL-DRV-SLNs and HDL-DRV-RTV-SLNs.[271] A triple culture transwell model (Caco-2, HT-29-MTX and Raji-B cells) was used to mimic some of the physiology of the small intestine.[272] The triple culture transwell model was used to determine if the formulations modified the rate of permeation of DRV across the biological barriers, which were represented in the form of intestinal epithelium model. As with the drug release experiments, the DRV was radiolabelled with ^{3}H which allowed drug absorption to be measured.[273]

4.4.6.1 Cellular Accumulation

The cellular accumulation of both types of HDL-SLNs formulations were significantly greater than the unformulated DRV and/or RTV: The CARs of HDL-DRV-SLNs and HDL-DRV-RTV-SLNs, displaying higher accumulation at both post 1-hour incubation and post 4-hour

incubation times (Figure 4.25). It is likely that the HDL-SLNs facilitated greater drug uptake as lipophilicity is a fundamental factor in passive diffusion across cellular membranes.[274] Calculation of CAR was carried out according to Equation 4.1 in section 4.3.2.7.2.

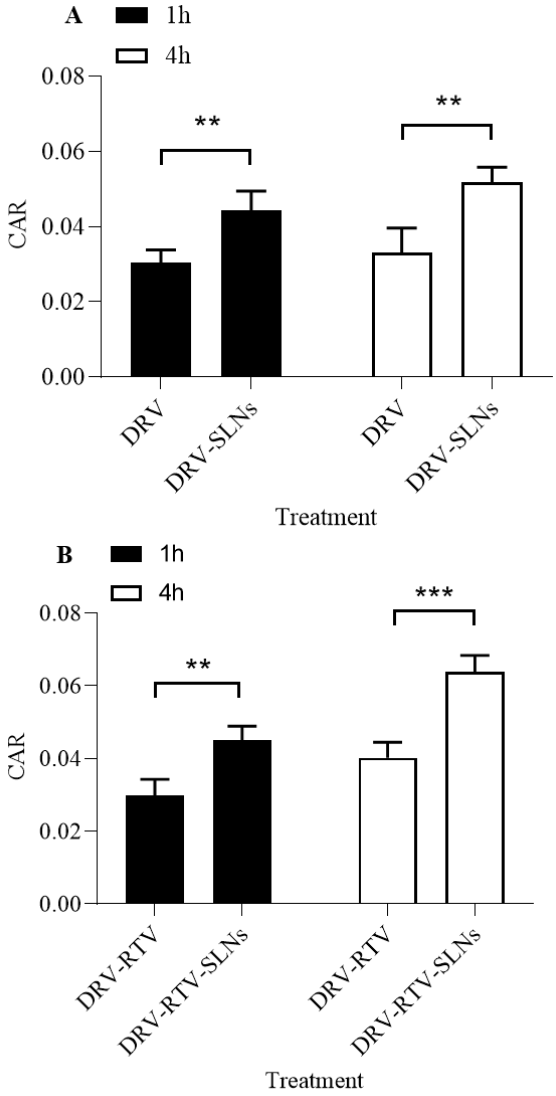

*Figure 4.25. Cellular accumulation of formulations studied after 1-hour and 4-hour incubations: Mean (n=4 ± standard deviation) Cellular Accumulation Ratio (CAR) of four 10 µM samples: (A) Unformulated DRV and HDL-DRV-SLNs (B) Unformulated DRV/RTV (8:1) and HDL-DRV-RTV-SLNs. following 1-hour and 4-hour incubations (37 °C, 5%, CO_2) in Caco-2 cells. Differences between the treatments were considered statistically significant at *, P<0.05; **, P < 0.01; ***, P < 0.001; ****, P < 0.0001.*

4.4.6.2 Transcellular Permeability

In the literature, transwell studies have demonstrated that nanoformulations may also be transported via enterocytes and clathrin-mediated endocytosis methods,[275] showing further nanoformulation uptake opportunities. Moreover, William, *et al.* found that microfold cells (M-

cells), identified in such models, have the ability to uptake macromolecules (e.g.) liposomes sized between 0.2 nm-5 µm.[275] As the nanoformulations used were ~250 nm, it can be speculated that M-cells can uptake these nanoformulations due to their size compatibility. Therefore, the triple culture membrane model was used as a physiologically relevant approach to study the drug delivery behaviour for these orally administered therapies. Figure 4.26 demonstrated that as cell exposure to both HDL-DRV-SLNs and HDL-DRV-RTV-SLNs increased, the apparent permeability (P_{app}) increased. The triple culture membrane model is asymmetrical in its structure, the 'A' side of the transwell represents the apical side (inside of the gut) while the 'B' side is the basolateral side and represents the blood side of the gut. Unformulated DRV had greater P_{app} bidirectionally than HDL-DRV-SLNs at all four timepoints (Figure 4.26.A). For example, on average (mean across all timepoints) unformulated DRV had a 1.13-fold greater P_{app} value than HDL-DRV-SLNs A>B and a 1.32-fold greater P_{app} value B>A. The unformulated DRV/RTV (8:1) had lower P_{app} bidirectionally than HDL-DRV-RTV-SLNs (Figure 4.26.B). On average across all timepoints, HDL-DRV-RTV-SLNs had a 1.64-fold greater P_{app} value than unformulated DRV/RTV (8:1) A>B and a 1.51-fold greater P_{app} value B>A. This data shows that the combination of the DRV and RTV into the nanoparticles (HDL-DRV-RTV-SLNs) resulted in increased permeability across the model for the gut compared to the single drug-loaded SLNs (HDL-DRV-SLNs). The presence of lipids is known to modify the behaviour of CYP3A4, the enzyme responsible for DRV metabolism.[276] RTV is also used to inhibit CYP3A4 to improve the bioavailability of DRV. The data shown in Figure 4.26.A suggests that the lipid content from the nanoformulations may upregulated CYP3A4 transcription,[277] thus DRV metabolism occurs. Further support is presented in (Figure 4.26.B) where by the same method, the increased metabolic capacity of CYP3A4 would have been ineffective due to RTV's inhibition of CYP3A4,[278] reducing DRV metabolism.

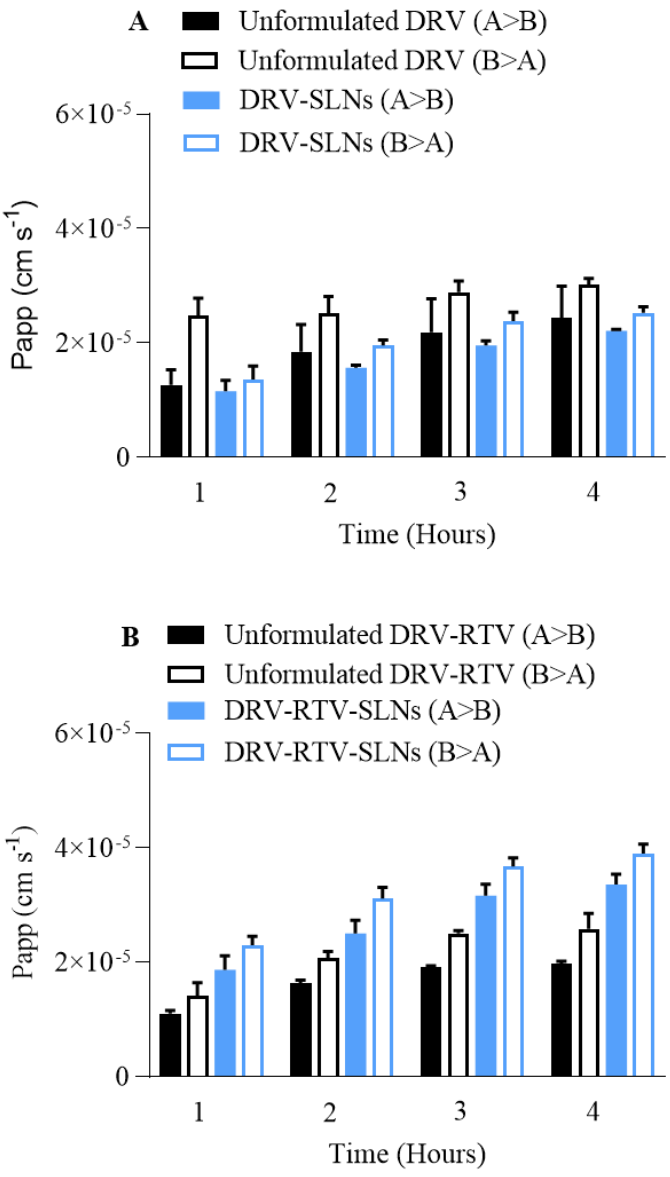

Figure 4.26 Permeability of triple culture membrane model to formulations over a 4-hour period: Mean (n=4 ± standard deviation) bidirectional apparent permeabilities (Papp cm s-1) four 10 µM samples: (A) Unformulated DRV and HDL-DRV-SLNs (B) Unformulated DRV/RTV (8:1) and HDL-DRV-RTV-SLNs across a triple culture membrane model (10: 7: 3 of Raji-B, Caco-2 and HT-29-MXT cells) following incubation (37 °C, 5%, CO2) at 1-hour timepoints over a 4 hour period.

The apparent oral absorption can be estimated by the transport of A>B/B>A to give the P_{app} ratio. Figure 4.27 depicts apparent oral absorption (P_{app} ratio) of the four samples over a 4-hour period. Figure 4.27A shows single drug delivery; unformulated DRV and HDL-DRV-SLNs. Figure 4.27B shows the dual drug delivery; unformulated DRV/RTV (8:1) and HDL-DRV-RTV-SLNs. The P_{app} ratio of unformulated DRV increased with each consecutive timepoint whereas the P_{app} ratio of HDL-DRV-SLNs fluctuated over time. No formulation demonstrated an average net influx greater than average net efflux (i.e.) a P_{app} ratio greater than 1; no

significance ($p>0.05$) was found between formulations at any timepoint (Figure 4.27A and B). Throughout the study, the triple culture model (Figure 4.26 and Figure 4.27) maintained good integrity and barrier properties as demonstrated with a P_{app} value less than 1.0×10^{-6}, validating the results collected.[265] Due to the narrow range of P_{app} ratios, and the similarity in results across both unformulated DRV/RTV (8:1) and HDL-DRV-RTV-SLNs data, this might suggest that formulation of DRV/RTV (8:1) into SLNs did not affect the uptake through cells (Figure 4.27.B).

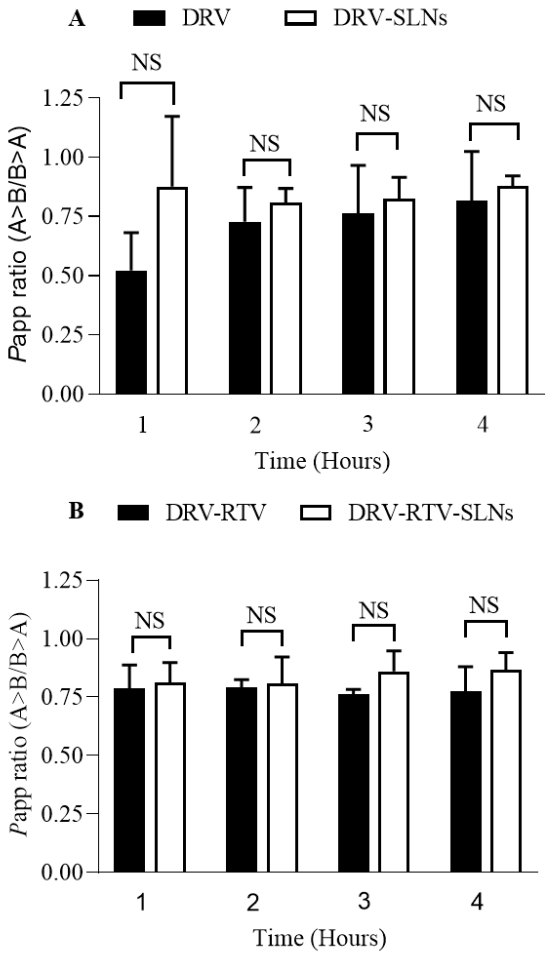

Figure 4.27 Apparent oral absorption of formulations over a 4-hour period: Mean (n=4 ± standard deviation) apparent oral absorption (Papp ratio) of) four 10 µM samples: (A) Unformulated DRV and HDL-DRV-SLNs (B) Unformulated DRV/RTV (8:1) and HDL-DRV-RTV-SLNs across a triple culture transwell membrane model (10: 7: 3 of Raji B, Caco-2 and HT-29-MXT cells) following incubation (37 °C, 5% CO2) at 1- hour timepoints over a 4 hour period.

In order to further confirm that the nanoformulations did not impact the barrier properties of the gut model, the low permeability marker mannitol was used as a control to measure the membrane integrity of the triple culture model following the 4-hour incubation.[265] The apparent permeability of mannitol was <0.953 x 10^{-6} cm s^{-1} for all treatments, demonstrating the triple culture model remained intact following incubation (Figure 4.28).

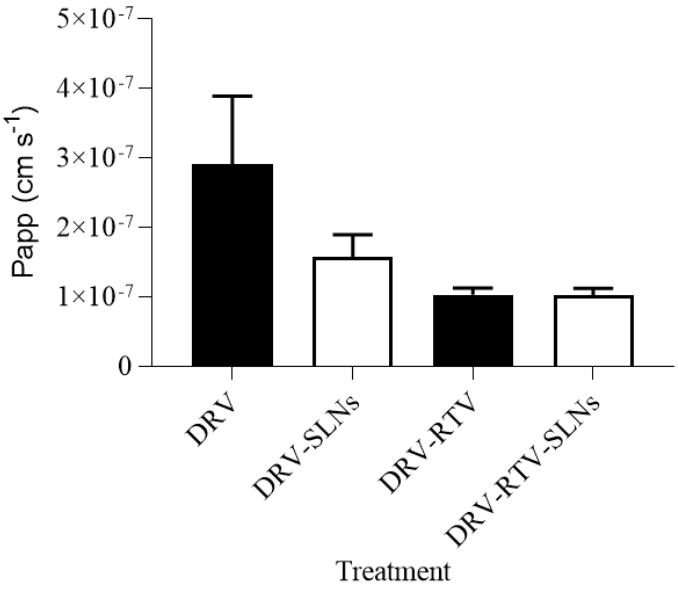

Figure 4.28 Mannitol apparent permeability (P_{app} cm s^{-1}), post treatment with unformulated DRV, HDL-DRV-SLNs, unformulated DRV/RTV (8:1) and HDL-DRV-RTV-SLNs, following 1 h incubation at 37°C, 5% CO_2. NS, P > 0.05 (unpaired, two-tailed t-test) (n=4).

4.5 Conclusion

In this chapter, successful freeze-drying of HDL-SLNs was carried out to remove both water and IPA and obtain HDL-SLNs in a dry powdered form, that was easily re-dispersed in DI water and maintained the original size parameters of HDL-SLNs before freeze drying. This has been achieved by varying some of the freeze-drying conditions: duration and storage of freeze drying and investigating several types of cryoprotectants: sugar cryoprotectants such as dextrose, mannitol, trehalose, sucrose, and maltodextrin and polymeric cryoprotectant such as PEG 2050. For the cryoprotectant parameter, the effect of several variables on the re-dispersion and the DLS data of both HDL-DRV-SLNs and HDL-DRV-RTV-SLNs were studied after freeze-drying and re-dispersion in DI water. These variables were: the weight ratio of cryoprotectant/HDL-SLNs (w/w) and the concentration of the freeze-drying mixture (mg/mL), these two variables were also represented in a different way in the form of the relationship between the concentration of the cryoprotectant (% w/v) and the volume of HDL-SLNs

dispersion (mL). Our results showed that 4 days was minimum duration required for the complete drying of the frozen samples, and the samples had to be tightly closed after removal from the freeze dryer to avoid the collapse of the freeze-dried cake, and subsequently particles aggregation.

For the sugar cryoprotectants our results showed varied cryoprotection and re-dispersion properties depending on the type of the cryoprotectant and its concentration. Dextrose, mannitol, and maltodextrin all failed to produce re-dispersible freeze-dried cakes and they all aggregated when re-dispersed in DI water. The disaccharides sucrose and trehalose were the only successful sugar cryoprotectants used in this study, with a minimum concentration of 2.5 and 5% w/v respectively. The results meant that sucrose was more efficient as a cryoprotectant for our system, with cryoprotectant/HDL-SLNs and the concentration of the freeze-drying mixture of 188/1 w/w at 13 mg/mL for sucrose and 376/1 at 25 mg/mL for trehalose respectively, with keeping a Z-average diameter of ~200 nm for both cryoprotectants. On the other hand, using PEG as a cryoprotectant showed excellent cryoprotection and re-dispersion at a minimum PEG concentration of 0.5% w/v, and cryoprotectant/HDL-SLNs and the concentration of the freeze-drying mixture of 38/1 w/w and 3 mg/mL respectively, with a Z-average diameter below 200 nm for both types of HDL-SLNs. Therefore, PEG was used as the cryoprotectant for all the other studies. The freeze-drying was successfully scaled-up to 5 folds (10 mL freeze-drying mixture in 40 mL vial) The morphology was studied using SEM showing spherical particles with narrow size distribution. Release studies showed a burst release and 80% of the drug was released in 8 hours duration.

The formulation of DRV and the DRV/RTV combination into HDL-SLNs resulted in increased cellular accumulation. A triple culture transwell model was used to investigate the potential oral delivery behaviour of the SLNs. The HDL-DRV-RTV-SLNs showed increased permeability both A > B ‘gut-to-blood’ and B > A ‘blood-to-gut’, than the unformulated combination of DRV and RTV. Unfortunately, there was no increase in the apparent oral absorption seen for the SLNs. Further mechanistic studies into the nanoparticle uptake and transport behaviour would be useful in order to try to improve the drug delivery behaviour.

Therefore, we can conclude that freeze-drying using cryoprotectants of HDL-SLNs was shown to be a robust and convenient and was able to provide proper stabilisation. The reconstitution of the freeze-dried HDL-SLNs in 1 mL of DI water, provided concentrated formulation for in

vitro testing. The HDL-SLNs demonstrated promise in increasing bioavailability of DRV and/or RTV. However, due to the potential limitations of the results, further studies must be conducted to establish the extent of this promise and whether these nanoformulations translate to improved oral bioavailability *in vivo* (e.g.) pre-clinical animal models. Looking forward, nanoformulations are showing early promise in longer-acting treatments, a hugely beneficial step in combating HIV.

Chapter 5

Optimisation of the Synthetic Parameters of Lipid Polymer Hybrid Nanoparticles Dual Loaded with Darunavir and Ritonavir for the Treatment of HIV[a]

[a] This chapter contains work adapted from following published paper: Elkateb, H. *et al.* Optimisation of the synthetic parameters of lipid polymer hybrid nanoparticles dual loaded with darunavir and ritonavir for the treatment of HIV. *Int. J. Pharm.* **588**, 119794 (2020).

5.1 Introduction

Lipid based formulations have the potential to be selectively taken up by the lymphatic route following oral administration.[79,97] In the previous chapters, we investigated several types of lipid based nanocarriers like SLNs, NLCs and NEs as potential drug delivery systems for DRV/RTV (8:1) drug mixture. These types of carriers are characterised by the presence of the lipid in the core. In this chapter, we investigate LPHNs as a potential nanocarrier for the same drug mixture, where the lipid in this system is in form of a monolayer coating the polymeric cores, PLGA is a commonly used polymer.[158,165,279]

LPHNs are usually stabilised by two types of stabilisers: bulk stabiliser and electrostatic stabiliser. The bulk stabiliser is usually in the form of a lipid-polyethylene glycol (PEG) shell and is typically a part of the LPHNs composition. Brij 78 (C_{18}, PEG_{20}), a saturated polyethylene glycol octadecyl ether, is a stabiliser that is widely used in lipid-based formulations.[280] Brij 78 has previously been used as surfactant in the synthesis of many formulations: liposomes,[280–282] micelles,[233] solid lipid nanoparticles,[283] active targeted nanoparticles,[284] and nisomes,[285] and it has been used as a replacement of 1,2-distearoyl-*sn*-glycerol-3-phosphatidylethanolamine-*N*-[methoxy(polyethylene glycol)-2000] known as (DSPE-PEG_{2000}) in the synthesis of liposomes.[286] However, to the best of our knowledge Brij 78 has not been investigated as a stabiliser for LPHNs. The phospholipid soybean lecithin (SBL) is a compound that has previously been used in the literature to form the lipid layer around the polymeric core, it is low cost, has good biocompatibility and is highly accepted in both food and pharmaceutical industry.[162] Additionally, SBL can act as both an absorption enhancer which increase the bioavailability of poorly soluble drugs as it bio-mimics natural lecithin in the cell wall,[161–164] and a non-irritant electrolytic stabiliser that prevent particles aggregation.[145]

Drug delivery *via* oral administration can be modelled using an *in vitro* intestinal triple culture model containing Caco-2 cells, microfold cells (M cells) and HT-29-MTX mucus secreting goblet cells. Caco-2 cells are human intestinal adenocarcinoma cells (enterocytes) that offer morphological and physiological similarity to the human intestinal epithelium.[272] Transwells can be used to support Caco-2 monolayers as the cells polarise, differentiate and form tight junctions. The polarised monolayer resembles the functional lining of the small intestine offering an *in vitro* model for absorption across the gut. The apical surface of the cells models is the surface exposed inside the gut whilst the basolateral surface models the interface with

the blood. The Caco-2 model provides exploratory data and is widely used to screen for absorption potential.[265,287,288] Despite these important features, one cell type cannot fully reflect the physiology of the intestine. An *in vitro* triple culture model comprising Caco-2 cells, HT-29-MTX mucus secreting goblet cells and Raji B lymphocytes can be used to stimulate the differentiation of Caco-2 cells into microfold cells (M cells) to study the absorption of nanocarriers. It has been suggested that goblet cells and M cells play a significant role in the uptake and permeation of nanoparticles in the intestine and inclusion of these cells provides a more representative *in vitro* model to assess and compare such materials.[289–291] Specifically, goblet cells continuously secrete mucus often limiting the ability of particles to permeate and gain access to the underlying epithelium.[292,293] M cells located in the epithelium and overlaying the Peyer's patches are responsible for the uptake of exogenous materials (*e.g.* bacteria) and delivering them to the lymphoid follicles.[272,294] Some studies suggest that nanoparticles enter the intestinal epithelium predominantly *via* the M cell route.[294,295] Although the mechanisms that underpin particle permeation across the intestinal epithelium are not clearly understood, various processes have been described and these have been reviewed elsewhere.[291,296–298]

A considerable challenge in the clinical use of nanoparticles for drug delivery is the ability to obtain a formulation that offers long-term storage stability.[299] This is particularly important given the supply chain challenges associated with administering therapies in low- and middle-income countries, where the capacity for temperature-controlled storage is limited. One possible solution is the ability to prepare dry formulations that can be formulated into capsules or redispersed upon administration.

5.2 Chapter objective

In this work, the synthetic parameters of LPHNs prepared by solvent injection loaded with both DRV and RTV designed for the treatment of HIV were investigated. Several parameters that affect the formulation of LPHNs using the solvent injection method were studied: mass percentage of the total stabiliser to the polymer core, the mass percentage of two different stabilisers (Brij 78 and SBL) and drug loading. The morphology of the particles was studied using scanning electron microscope (SEM) and transmission electron microscope (TEM). Freeze-drying of drug loaded LPHNs dispersions into dispersible powders using PEG as a cryoprotectant was investigated. The encapsulation efficiency and drug release were also quantified. Finally, the composition of the surfactant mixture and the colloidal stability in

physiological solutions were investigated and the drug delivery behaviour in an *in vitro* intestinal triple culture model for intestinal permeability was assessed.

5.3 Materials and Methodology

5.3.1 Materials

HPLC grade acetone (Thermo Fischer Scientific, Leicestershire, UK), ethanol (EtOH, Fisher Scientific, UK), soybean lecithin (SBL, 90%) were purchased from Alfa Aesar, Lancashire, UK. DRV (≥98% (HPLC) and RTV (≥98% (HPLC), PEG (Mn 2050 g mol^{-1}), Brij 78, resomer® RG 503 H, PLGA, PBS tablets, hydrochloric acid (HCl), sodium chloride (NaCl, ≥99%) dimethyl sulfoxide (DMSO, 99%), hydrogen peroxide, (4-(2-hydroxyethyl)-1-piperazineethanesulfonic acid (HEPES), bovine serum albumin (BSA, ≥98%), Hank's balanced salt solution (HBSS), Dulbecco's Modified Eagle's Medium (DMEM), RPMI and trypsin-EDTA were all purchased from Sigma–Aldrich, Irvine, UK. Amicon Ultra-0.5 Centrifugal Filter Unit (Merck). Caco-2 and HT-29-MTX cells were maintained in DMEM supplemented with 15 % fetal bovine serum (FBS) (Gibco, UK), 2 mM L-glutamine and 1 % non-essential amino acids (Sigma–Aldrich, Irvine, UK). Raji B cells were maintained in RPMI supplemented with 10 % FBS, 2 mM L-glutamine and 1 % non-essential amino acids (Sigma–Aldrich, Irvine, UK). [^{3}H]-DRV was purchased from RC Tritec and [^{14}C]-mannitol was purchased from American Radiolabeled Chemicals (US). Ultima Gold and ProSafe+ liquid scintillation fluid was purchased from Meridian biotechnologies (UK). Transwells with a 3 µM pore size were purchased from Corning (US). Caco-2, HT-29-MTX and Raji B cells were purchased from American Type Culture Collection (US). All reagents were used without further purification.

5.3.2 Methodology

5.3.2.1 Synthesis of LPHNs

LPHNs were prepared by a one-step optimised solvent injection method, where the formation of the polymeric cores and the assembly of the lipid around them happens simultaneously. The procedure used in this study was based on the modified solvent injection method reported by H. Fang *et al.*[300] and Pramual *et al.*[301] Briefly, 2.5 mg PLGA was dissolved in 1.5 mL acetone to form an organic solvent polymeric solution. In the case of drug loaded LPHNs different amounts of DRV or DRV/RTV (8:1) were added to the organic solvent phase with varied drug/polymer mass percentage (5-80% w/w). For blank, unloaded LPHNs no drugs were

added. The aqueous phase was prepared by dissolving different amounts of stabilisers, SBL and/or Brij 78, in 4% v/v ethanolic aqueous solution (2.5 mL). In LPHNs where only one stabiliser was used, a total SBL or Brij 78 mass percentage of (3.75- 20% w/w) with respect to the PLGA core was used. When mixtures of SBL and Brij 78 were used, the total stabiliser/PLGA mass percentage was kept constant at 20% w/w and the Brij 78/total stabiliser mass percentage was 10-90% w/w. The aqueous phase was heated to 60 °C for 3 minutes to ensure that the SBL molecules do not self-assemble to form vesicular structure prior the addition of the PLGA solution, this temperature is above the gel-to-liquid transition temperature of SBL, which ensure the obtaining of a homogenously dispersed liquid crystalline phase, so the phospholipids molecules are not close enough to each other to self-assemble into vesicular structure.[302] The polymer solution was then injected dropwise into the heated stirring lipid aqueous phase to form the LPHNs dispersion, which were then vortexed for 3 minutes and left to stir overnight, allowing for evaporation of acetone. The LPHNs were maintained as dispersions (4 mL) by addition of deionized water.

5.3.2.2 Freeze-drying

To obtain stable particles in solid form, the LPHNs dispersions were freeze dried using a VirTis Freeze Dryer. Samples were prepared for freeze-drying by the addition of a cryoprotectant, 0.5% w/v PEG aqueous solution. Diluted LPHNs dispersions were used to limit particles aggregation, with PEG/LPHNs of 38/1 w/w. The LPHNs/cryoprotectant mixtures (2 mL) were placed in 14-mL vials and snap-frozen in liquid nitrogen, the solid mixture was then placed in the freeze-drier for 4 days resulting in a solid monolith in the form of white fluffy powder.

5.3.2.3 Characterisation of the size and morphology of LPHNs

The predominant analytical method used to determine the size of LPHNs was dynamic light scattering (DLS). Scanning electron microscopy (SEM) and transmission electron microscopy (TEM) were also used for characterisation of the morphology and size of selected samples. The setting of the DLS measurements was the same as described in Chapter 2, except for concentration of the measured sample. The concentration range of the LPHNs dispersions analysed was 0.65- 1 mg/mL, when these samples were measured in PBS solution (pH 7.4) or simulated gastric fluid (SGF) (pH 1.2), the above-mentioned concentration range was halved, as 0.5 mL of the LPHNs dispersions was diluted with either 0.5 mL of PBS solution or SGF. The concentration of the re-dispersed freeze-dried formulations was 1 mg/mL. The measurements recorded at room temperature (25 °C). The measurements were carried out in

triplicate to obtain the size average (Z-average) diameter and polydispersity index (PDI). PBS solution was prepared by dissolving 1 PBS tablet in 100 mL deionized water, while SGF was prepared by dissolving 2 g of NaCl and 7 mL concentrated HCl per 1000 mL deionized water. Samples were prepared for SEM imaging by pipetting the LPHNs dispersions (0.75- 0.9 mg/mL) onto glass coverslips with 10 mm diameter which were attached to a carbon adhesive disc on top of an aluminum SEM specimen stub (12.5 mm diameter). The samples were left to dry overnight, this was followed by coating with gold (EMITECH K550X) with a deposition current of 25 mA for 100 seconds before imaging. The size and the morphology of LPHNs were then determined using a Hitachi S-4800 FE-SEM at 3 kV. For TEM imaging, the sample was incubated on a 200-mesh copper formvar/carbon grid for 15 minutes. Excess sample was wicked off with filter paper before incubating the grid on 2% aqueous uranyl acetate (UA) for 1 minute. Excess UA was wicked off, grids left to dry for 10 minutes and then viewed at 120 kV in a Tecnai T12 bioTwin electron microscope with Gatan RIO16 camera.

5.3.2.4 Measurement of entrapment efficiency and drug release using radiometric analysis

Radiolabelled DRV containing LPHNs (analogous to those described in section 5.3.2.1) were formulated with the addition of tritiated [^{3}H]-DRV (specific activity 25 µCi/mg) to the organic solvent phase. Drug loading within LPHNs were determined *via* liquid scintillation counting (LSC) analysis, the details of the measurement are the same as mentioned in chapter 2, with the exception for the concentration of the measured sample, where 0.4 mL of a dispersion of the LPHNs (0.9 mg/mL) was added to a centrifugal unit.

Drug release behaviour from the LPHNs was quantified by use of a dialysis method using LSC analysis, the details of the experiment are the same as mentioned in chapter 2, with the exception for the measured sample. LPHNs dispersions (1 mL, 0.9 mg/mL) were placed within a double-sided bio-dialyzer fitted with 3.5 kDa MWCO membranes. DRV release was monitored at set time points of 0.5, 1, 2, 3, 4, 5, 6, 7 and 8 hours.

5.3.2.5 Transcellular permeability of Darunavir across a triple culture model

5.3.2.5.1 Cell culture and maintenance

Cells were incubated at 37 °C, 5 % CO_2. Adherent cells were sub-cultured once ca. 85 % confluent and Raji B cells were sub-cultured every 3 days. Cell numbers and viability were assessed using a NucleoCounter NC-200 (Denmark).

The permeability of DRV and DRV loaded LPHNs was assessed across an *in vitro* intestinal triple culture model using a method adapted from Schimpel *et al.*[272] Briefly, transwells were seeded apically with Caco-2 and HT-29-MTX cells in a 7:3 ratio with 1.4 x 10^5 cells per well, respectively, and propagated over 21-days at 37 °C, 5 % CO_2. Following 16-days of co-culture, 1.4 x 10^5 Raji B cells were added to the basolateral compartment of each well and the triple culture model propagated for a further 5-days at 37 °C, 5 % CO_2. During the initial 16-days of propagation, the entire volume of media was aspirated from both apical and basolateral compartments and replaced with an equal volume of fresh pre-warmed media every other day. Following addition of the Raji B cells, 25 % of the media was aspirated and replaced from the basolateral compartment every other day whilst the entire volume was changed apically as previously described. Transepithelial electrical resistance (TEER) values of >800 Ω were observed for all cultured wells. After 21-days of culture, all the media was aspirated, wells washed twice with pre-warmed HBSS and replaced with either DMSO dissolved [^{3}H]-DRV (<1 % total DMSO volume per well) or [^{3}H]-DRV LPHN suspensions spiked into transport buffer to a final concentration of 10 µM DRV. Each suspension was added to either apical or basolateral compartments and transport buffer was added to the opposing chamber. DRV transport from apical-to-basolateral (A>B) and basolateral-to-apical (B>A) directions was assessed. The transwell plates were incubated at 37 °C, 5 % CO_2 for the duration of the experiment and 0.1 mL was sampled hourly from the acceptor chamber over 4 hours and replaced with an equal volume of fresh pre-warmed transport buffer. Samples were placed into empty 5 mL scintillation vials before mixing with 4 mL of liquid scintillation fluid. Apparent permeability (P_{app}) and apparent oral absorption ((P_{app} (A>B) / Papp (B>A)) equations were used to calculate the rate of DRV permeation as previously described.[288] The integrity of the triple culture models were assessed following the 4 h incubation with each test condition. Transport buffer was aspirated, and the wells washed twice with pre-warmed HBSS.

Subsequently, 0.1 mL of transport buffer containing [^{14}C]-mannitol (50 µM, 2 µCi/mL) was added to the apical compartment of each well and 0.6 mL of transport buffer was added to the basolateral compartments. The transwells were incubated for 1 h at 37 °C, 5 % CO_2 and 0.1 mL of the basolateral contents were sampled and placed into a 5 mL scintillation vial before mixing with 4 mL scintillation fluid for radiometric analysis as described above.

5.3.2.6 Statistical analysis

One-way ANOVA was adopted as a statistical analysis tool for testing different LPHNs formulations in both EE% and drug release experiments using Microsoft Excel spreadsheet software, version 2105. The data difference was considered to be statistically significant when the p-value was less than 0.05. Number of samples (n) was 3. Different LPHNs formulations were compared to each other whether as LPHNs suspensions or redispersed LPHNs after freeze drying, that is why ANOVA was used. On the other hand, for transcellular permeability studies, two-tailed t-test were applied to the datasets, as only two samples were tested, each formulation was compared to unformulated drug solution which was [^{3}H]-DRV/DRV (<1 % DMSO) aqueous preparation either on its own or in combination with RTV (8:1). Statistical analysis was performed using GraphPad Prism v.8.2 (US). Data normality was assessed using a Shapiro-Wilk test and subsequently unpaired, Differences were considered statistically significant at *, $P<0.05$; **, $P < 0.01$; ***, $P < 0.001$; ****, $P < 0.0001$.

5.4 Results and discussion

5.4.1 Optimisation of the synthesis of LPHNs

To optimise the formulation of LPHNs, blank (without drug) and DRV loaded LPHNs were prepared *via* solvent injection (Figure 5.1). The aim of this optimisation was to prepare nanoparticles that had the highest possible drug loading and possessed colloidal stability under physiological ionic strength. Three variables were tested: the effect of varying the mass percentage of the total stabiliser to the PLGA polymer core, the mass percentage of Brij 78 to total stabiliser and the drug loading. The first two variables were optimised using blank nanoparticles, then the drug loading was investigated once drug was incorporated. DLS was used to measure the Z-average diameter, the size distribution, and the polydispersity index of the particles in all formulations. The colloidal stability of the formulations was assessed *via* measurement of the diameter of the particles upon exposure to physiological ionic strength (in PBS) at pH 7.4. Poor colloidal stability would result in aggregation of the particles which would be observed as an increase in diameter and polydispersity.

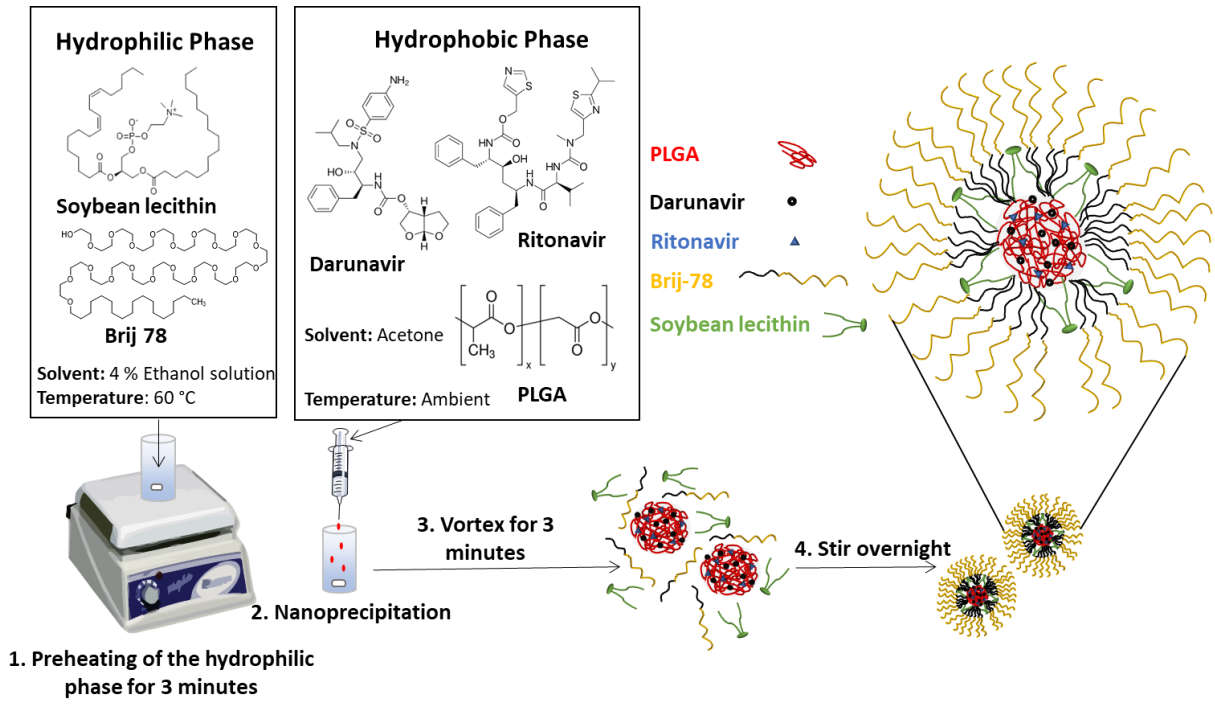

Figure 5.1 Schematic representation of the synthetic steps of formulating drug loaded LPHNs by solvent injection. DRV, RTV and PLGA were dissolved in acetone and added to an aqueous phase, under moderate magnetic stirring, containing SBL and Brij 78. Acetone evaporation at ambient temperature overnight allowed an aqueous suspension of LPHNs to be obtained. The LPHNs were composed of a core of PLGA containing the drugs and a shell of SBL and Brij 78.

5.4.1.1 The effect of varying the mass percentage of total stabiliser to the polymer core

The repulsive interactions between nanoparticles that are provided by the stabilisers (surfactants) used in the formulation of LPHNs are integral to their colloidal stability. The mass percentage of the stabiliser to the PLGA polymer core is a key variable as it must provide enough repulsion between particles to obtain colloidal stability. Initially, the effect of each stabiliser on the colloidal stability of the particles was studied. The two stabilisers SBL and Brij 78 were used as sole stabilisers to form blank nanoparticles at different stabiliser/PLGA mass percentage (3.75- 20% w/w), keeping the amount of PLGA constant. Control nanoparticles made of PLGA cores only with no stabiliser were synthesised, these particles had a Z-average diameter of 66 nm and a PDI of 0.46, however they aggregated immediately upon dispersion in PBS.

5.4.1.1.1 Soybean lecithin as a stabiliser for LPHNs

When SBL was used on its own as a stabiliser (Table 5.1) for LPHNs, and the particles were dispersed in water, mean diameters of 70-79 nm were observed. Smaller particles formed when higher amounts of SBL were used relative to the polymer core. If the particles were added to PBS at physiological ionic strength the particles aggregated at all SBL/PLGA mass percentages (0.375 – 20% w/w). This was likely due to the electrostatic stabilisation mechanism provided by SBL; electrostatic repulsion is greatly reduced in the presence of high ionic strength due to the electrostatic screening effect of the dissolved ions. The same behaviour was reported for a different phospholipid by Chan *et al.*,[165] their results showed that using phosphatidylcholine as a stabiliser for docetaxel LPHNs led to particle aggregation even at lipid/polymer mass percentage up to 20% w/w. The zeta potential of the particles stabilised by SBL ranged from -54 to -67 mV when dispersed in water (Table 5.1), upon dispersion of the particles in PBS, there was a decrease in the zeta potential value of the LPHNs (-29 to -35 mV) which affects the colloidal stability. It has been suggested by Hu *et al.* [303] that to obtain a full electrostatic stabilisation, a zeta potential more than ±30 mV and ideally more than ±60 mV is required. It was therefore concluded SBL as a lone stabiliser was not able to provide enough stabilisation under physiological conditions.

Table 5.1. Summary of DLS data (Z-average diameter, PDI and Zeta potential) of blank LPHNs dispersions synthesised with different mass percentages of SBL/PLGA dispersed in deionized water or PBS. The term "Aggregated" refers to particle aggregation that can be seen by naked eye that is accompanied by Z-average diameter above 1000 nm. Data are represented as mean ± SD (n =3), where SD is the standard deviation and n is the number of samples measured.

SBL/PLGA % w/w	Deionized water			PBS	
	Z-average diameter (nm)	PDI	Zeta potential (mv)	Z-average diameter (nm)	Zeta potential (mv)
3.75	79 ± 6	0.35 ± 0.09	-54 ± 8	Aggregated	-30 ± 6
7.5	79 ± 4	0.38 ± 0.05	-60 ± 10	Aggregated	-35 ± 8
15	71 ± 5	0.42 ± 0.07	-67 ± 5	Aggregated	-29 ± 3
20	70 ± 3	0.40 ± 0.03	-59 ± 9	Aggregated	-31 ± 9

5.4.1.1.2 Brij 78 as a stabiliser for LPHNs

Brij 78 was used in a varying ratio to PLGA mass percentage, resultant LPHNs had a mean Z-average diameter of 62-85 nm with low PDIs (0.20-0.35). An increase in the Brij 78/PLGA mass percentage above 3.75% w/w resulted in a slight decrease in the Z-average of the particles (Figure 5.2). The particles had mean Z-average of 48-70 nm and PDI of 0.23-0.25 when dispersed in PBS. Unlike SBL, the steric stabilisation provided by Brij 78 allowed colloidal stability in PBS when > 7.5% w/w of the mass percentage of Brij 78/PLGA was used. Below this, at a Brij 78/PLGA mass percentage of 3.75 %, aggregation of the particles occurred in PBS as the amount of surfactant was insufficient to give full steric coverage of the PLGA cores. Brij 78/PLGA ratio of 20% w/w was chosen for further studies, as it provided the particles with the smallest Z-average diameter following dispersion in PBS.

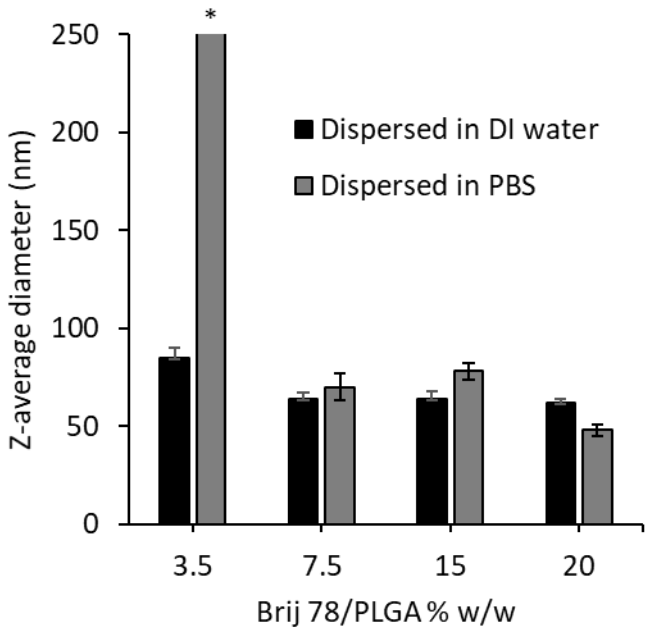

Figure 5.2 Comparison of Z-average diameter of blank LPHNs dispersions synthesised using Brij 78 as a stabiliser at different Brij 78/PLGA% w/w. LPHNs were dispersed in two different media; DI water or PBS. (Asterisks (*) indicates poor quality DLS data meaning that the measurements were unreliable likely due to particle aggregation). Data are represented as mean ± SD (n =3).

5.4.1.2 Using a combination of Brij 78 and soybean lecithin as stabilisers for LPHNs

To obtain LPHNs that offer the combination of enhanced pharmacokinetic behaviour from a lipid shell with the colloidal stability under physiological ionic strength, the effect of varying the Brij 78 and SBL mass percentages were investigated. The mass percentage of the surfactant relative to the PLGA polymer core was kept fixed at 20% w/w as this was the percentage that showed the lowest Z-average for LPHNs dispersions when dispersed in water and PBS for SBL (Table 5.1) and Brij 78 (Figure 5.2), respectively.

LPHNs with different mass percentages of Brij 78 with respect to the total mass of surfactants (SBL and Brij 78) ranging from 10-90 % were investigated (Figure 5.3). The aim was to determine the optimum mass percentage that would allow LPHNs to maintain stability in PBS, with the highest amount of SBL that might enhance the biological behaviour of the particles. Previously SBL has been shown to enhance the bioavailability of hydrophobic drugs such as curcumin in a mixed polymeric micellar system.[163] In water, all samples showed very similar mean diameters regardless of the composition, indicating that both stabilisers were equally effective surfactants. However, in PBS the effect of surfactant composition was much more

pronounced, when the total mass of stabiliser contained less than 30% Brij 78 then aggregation was observed. An increase in Brij 78/total stabiliser to greater than 50% w/w showed effective stability in PBS. The samples with Brij 78 content of either 70 or 90% w/w were selected for further optimisation of drug loading due to their small diameters. These results showed that the formulation requirements for LPHNs in terms of the ratio between Brij 78 and phospholipids mixture (7:3 and 9:1) compares closely to the work of Chan et al. who used a lipid-PEG conjugate to lipid at a 7.2: 2.5 ratio.[165]

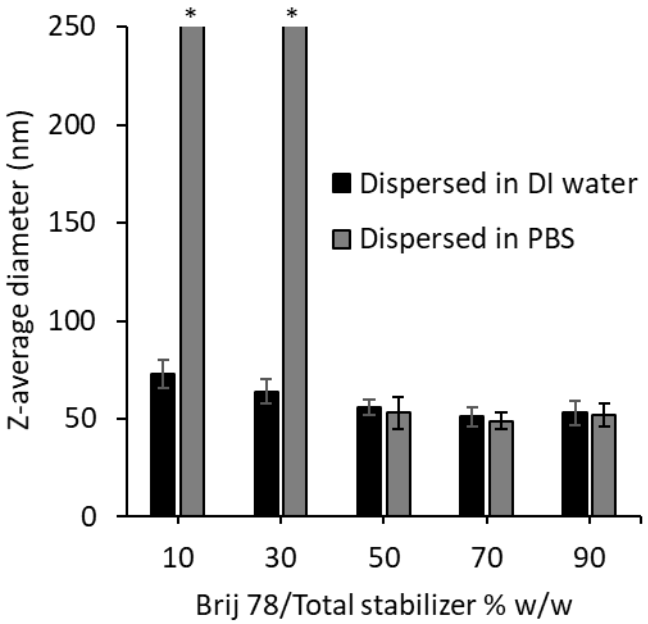

Figure 5.3 Comparison of Z-average diameter of blank LPHNs synthesised using a mixture of Brij 78 and SBL with different Brij 78/Total stabiliser % w/w, (total stabiliser refers to the mass of both of (SBL and Brij 78). The measurements were carried out on the LPHNs dispersed in different media; DI water and PBS. (Asterisks (*) indicates poor quality DLS data, meaning that the measurements were unreliable likely due to particle aggregation). Data are represented as mean ± SD (n =3).

5.4.1.3 Effect of drug/PLGA mass percentage on particle properties and formation of dispersible formulation

As the role of each surfactant has been established in stabilising blank LPHNs, drug loaded LPHNs were prepared to determine the highest possible drug loading. The Brij 78/total stabiliser percentage chosen for these studies were 70 and 90% w/w, and a 100% Brij 78 was used as a control. The drug mixture was composed of a mixture of DRV and RTV with a ratio 8:1 w/w as this is the clinically used ratio. Given the benefits that would be offered by a dispersible formulation, the effect of freeze-drying was also investigated on the particle

properties. Drug-loaded LPHNs (DRV-RTV-LPHNs) with a range of different DRV/PLGA mass percentages were studied (5-80% w/w). The DLS data in Table 5.2 showed that before freeze drying, the samples had similar Z-average diameters even with the increase of DRV/PLGA mass percentage from 5 to 40% w/w, at the three different Brij 78/total stabiliser mass percentage used (70, 90 and 100 % w/w). The Z-average diameter range was 45-109 nm and the PDI was 0.16-0.37 for LPHNs dispersed in DI water (Table 5.2). Upon dispersion in PBS, the Z-average diameter of LPHNs ranged from 50-98 nm and the PDI was 0.13-0.24 (Table 5.3). Increasing DRV/PLGA mass percentage above 20% w/w led to particle aggregation upon dispersion in PBS with poor quality DLS data (data not shown). This showed that LPHNs with high drug loading of up to 20% w/w could be formed with a range of stabiliser compositions.

The effect of freeze-drying on the formulations was investigated using a cryoprotectant, 0.5% w/v PEG, which is a significantly lower concentration of the cryoprotectant compared to that reported by Nidhi *et al.*[304] Lower concentration of excipients as cryoprotectants was targeted as it meant a relative higher concentration of drug-loaded LPHNs can be achieved. After re-dispersion, the effect of increasing the DRV/PLGA mass percentage on particles properties became apparent; increasing the DRV/PLGA mass percentage above 20% w/w led to particle aggregation. For LPHNs with DRV/PLGA mass percentage of 5-20% w/w, the Z-average for freeze-dried LPHNs dispersed in DI water ranged between 125-255 nm (Table 5.2), while upon dispersion in PBS (Table 5.3), the Z-average diameter of freeze-dried LPHNs became larger ranging between 185-374 nm. After freeze-drying all samples, independent of dispersion media, increased in diameter. Such increases in particle size have previously been shown to be due to the aggregation of particles in the freezing step.[305] For drug-loaded LPHNs (DRV-RTV-LPHNs), it was possible to incorporate relatively high amount of the drug into the polymeric cores (up to 20% w/w of DRV/PLGA, the DRV/RTV ratio was kept at 8:1) whilst maintaining a mean diameter below <330 nm. Varying the Brij 78/total stabiliser mass percentage between 70-100 % w/w did not show a significant difference on particle properties.

From the parameters tested (Table 5.3), it was apparent that 20% w/w DRV/PLGA mass percentage is the highest value that can be achieved among the studied mass percentages while maintaining good quality DLS data, while dispersed in PBS.

The optimum DRV-RTV-LPHNs formulas selected for further studies were referred to as LPHN70, LPHN90 and LPHN100, which refers to Brij 78/total stabiliser of 70, 90 and 100% w/w, respectively. In all three formulations, the mass percentage of total stabiliser/PLGA was 20% w/w and DRV/PLGA was also 20% w/w.

Table 5.2 Summary of DLS data (Z-average diameter and PDI) of DRV-RTV-LPHNs synthesised with different DRV/PLGA mass percentage (before and after freeze drying). The DRV/RTV ratio was kept at (8:1). All samples were suspended in DI water. The term "Aggregated" refers to particle aggregation that can be seen by naked eye that is accompanied by Z-average diameter above 1000 nm. Data are represented as mean ± SD (n =3), where SD is the standard deviation and n is the number of samples measured.

Brij 78/Total lipid% w/w	DRV/PLGA% w/w	Before freeze drying		Freeze-dried	
		Z-average diameter (nm)	PDI	Z-average diameter (nm)	PDI
70	5	73 ± 3	0.16 ± 0.04	158 ± 18	0.26 ± 0.09
90	5	106 ± 10	0.22 ± 0.05	155 ± 11	0.23 ± 0.06
100	5	86 ± 5	0.23 ± 0.01	125 ± 9	0.26 ± 0.03
70	10	56 ± 8	0.23 ± 0.03	176 ± 17	0.30 ± 0.08
90	10	109 ± 12	0.25 ± 0.06	154 ± 13	0.26 ± 0.04
100	10	77 ± 5	0.23 ± 0.04	182 ± 10	0.28 ± 0.02
70	20	66 ± 9	0.16 ± 0.08	255 ± 20	0.37 ± 0.1
90	20	75 ± 6	0.20 ± 0.02	161 ± 10	0.27 ± 0.08
100	20	83 ± 4	0.21 ± 0.03	186 ± 12	0.32 ± 0.05
70	40	53 ± 7	0.22 ± 0.01	Aggregated	
90	40	47 ± 3	0.25 ± 0.03	Aggregated	
100	40	45 ± 6	0.37 ± 0.02	Aggregated	

Table 5.3 Summary of DLS data (Z-average diameter and PDI) of DRV-RTV-LPHNs synthesised with different DRV/PLGA mass percentage (before and after freeze drying). The DRV/RTV ratio was kept at (8:1). All samples were dispersed in PBS. Data are represented as mean ± SD (n =3), where SD is the standard deviation and n is the number of samples measured.

Brij 78/Total lipid% w/w	DRV/PLGA% w/w	Before freeze drying		Freeze-dried	
		Z-average diameter (nm)	PDI	Z-average diameter (nm)	PDI
70	5	66 ± 4	0.14 ± 0.07	199 ± 21	0.20 ± 0.05
90	5	95 ± 6	0.21 ± 0.10	185 ± 13	0.30 ± 0.02
100	5	76 ± 7	0.23 ± 0.04	440 ± 35	0.54 ± 0.04
70	10	51 ± 10	0.17 ± 0.02	374 ± 39	0.33 ± 0.07
90	10	98 ± 17	0.24 ± 0.09	199 ± 17	0.19 ± 0.02
100	10	70 ± 5	0.23 ± 0.06	199 ± 25	0.37 ± 0.05
70	20	61 ± 7	0.13 ± 0.05	247 ± 19	0.44 ± 0.04
90	20	69 ± 5	0.19 ± 0.03	333 ± 30	0.41 ± 0.06
100	20	76 ± 4	0.21 ± 0.07	254 ± 15	0.53 ± 0.08

The stability of LPHN70, LPHN90 and LPHN100 in SGF was tested, DLS data in Table 5.4 showed that all three formulations were stable in SGF as LPHNs dispersions (before freeze drying). The LPHNs had a mean Z-average diameter of 129- 138 nm and the PDI was 0.31-0.34. However, the freeze-dried formulations all aggregated once re-dispersed in SGF, the cause for this aggregation is unclear.

Table 5.4 Summary of DLS data (Z-average diameter and PDI) of DRV-RTV-LPHNs synthesised with DRV/PLGA 20% w/w before freeze drying. The DRV/RTV ratio was kept at (8:1). All samples were suspended in SGF. Data are represented as mean ± SD (n =3), where SD is the standard deviation and n is the number of samples measured.

Brij 78/Total lipid% w/w	Before freeze drying	
	Z-average diameter (nm)	PDI
70	138 ± 7	0.32 ± 0.05
90	133 ± 11	0.31 ± 0.09
100	129 ± 8	0.34 ± 0.04

5.4.2 Analysis of the morphology and size of the LPHNs by SEM and TEM

SEM and TEM were used to explore the structure and morphology of DRV-RTV-LPHNs with either SBL as the sole stabiliser or with a combination of the surfactants Brij 78 (70% w/w) and SBL (30% w/w) (Figure 5.4). SEM analysis provided images of spherical particles with smooth surfaces (Figure 5.4.A and B). TEM analysis was used to give an insight into the structure of the nanoparticles (Figure 5.4.C and D), both samples had a dark ring surrounding the cores of the particles. These dark rings represent the lipid shell of the particles which were stained with uranyl acetate to increase the electron density in this peripheral region as was reported by Mandal *et al*.[306] It was apparent that the use of mixture of Brij 78 and SBL result in a LPHN structure with a polymer core and a shell containing the lipid. An average diameter of approximately 50 nm with narrow size distributions was determined, concordant with the DLS size distribution data shown in Figure 5.4.E.

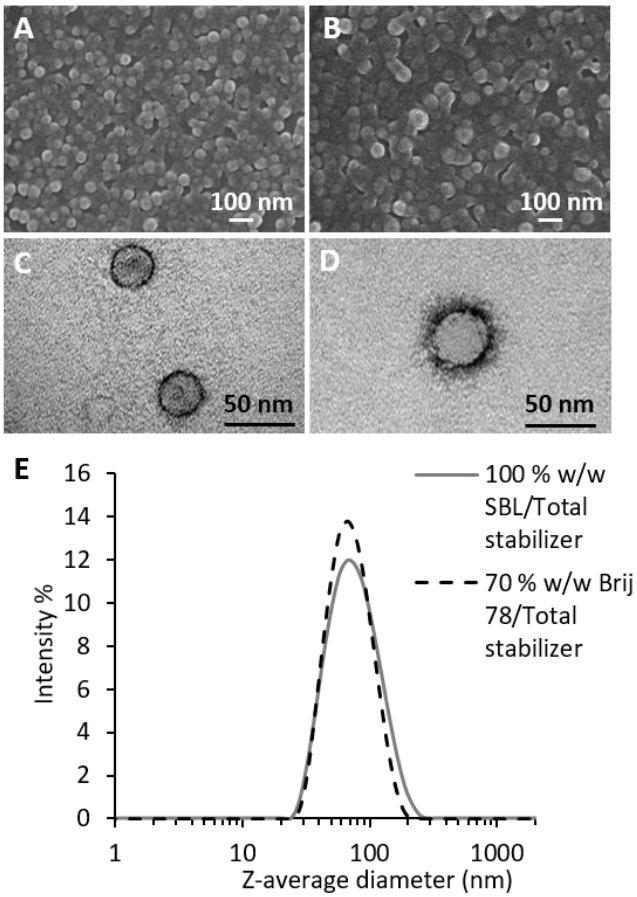

Figure 5.4 Particle characterisation of DRV-RTV-LPHNs with 20% w/w DRV/PLGA and 20% w/w total stabiliser/PLGA using different stabilisers; (A) SEM image of LPHNs stabilised by SBL only. (B) SEM image for LPHNs with Brij 78/Total stabiliser of 70% w/w. (C) TEM image for LPHNs stabilised by SBL only. (D) TEM image for LPHNs with Brij/Total stabiliser of 70% w/w. (E) Size distribution graphs obtained by DLS for the same 2 formulations, the graph shows monomodal distribution of size with Z-average diameters below 100 nm. The dispersion media of these samples was DI water.

5.4.3 Encapsulation efficiency and drug release

To assess the effect of surfactant composition on drug encapsulation and drug release behaviour, three different LPHNs formulations were tested: LPHN70, LPHN90 and LPHN100. These formulations all contained DRV/PLGA at 20% w/w using both [^{3}H]-DRV/DRV and unlabelled RTV in an 8:1 ratio. Firstly, the encapsulation efficiency of the formulations was investigated using a spin filter method to separate the free drug from the encapsulated drug. The analysis of this showed that the DRV encapsulation efficiency of the three formulations was similar (62, 68.1 and 68.5% w/w) for formulations LPHN70, LPHN90 and LPHN100 respectively, with a slight increase in encapsulation efficiency noticed with increasing Brij 78 content. The difference in the EE% between the three formulations was significantly different according to the ANOVA testing, ($P < 0.05$).

The effect of freeze-drying and drug combination on the drug encapsulation efficiency of LPHN70 was also studied. The encapsulation efficiency of freeze-dried LPHN70 loaded with DRV/RTV (8:1) or DRV on its own was 90.8 and 95.7% w/w, respectively. There was a significant difference between the EE% between the single and dual drug loaded LPHN70, ($P < 0.05$). We can conclude that freeze-drying increased the DRV encapsulation efficiency of LPHN70 from 62 to 90.8 %. This increase in the encapsulation efficiency may be caused by the cryogenic freezing of the samples resulting in the formation of solid drug nanoparticles from the non-encapsulated drug. Indeed, freezing and freeze-drying in the presence of surfactants are key steps used in the process of some solid drug nanoparticles formulations.[307,308] These solid drug nanoparticles would have been unable to penetrate the dialysis membrane and would therefore be measured as encapsulated drug. The formation of such nanoparticles would be difficult to detect by DLS as this technique provides a limited ability to resolve separate nanoparticle populations unless the size differences are approximately 4 fold.[309] Unfortunately, it was not possible to carry out useful SEM analysis on these samples after freeze-drying to investigate the potential presence of solid drug nanoparticles, this was due to the film forming behaviour of the PEG cryoprotectant which meant that it was not possible to resolve individual nanoparticles. It was also found that the incorporation of RTV led to an increase in the total drug content which caused a decrease in the encapsulation efficiency from 95.7 to 90.8% w/w. Due to the role of RTV as a booster for DRV, the encapsulation efficiency of RTV in the formulations was not investigated in this study.

The drug release behaviour from LPHNs was investigated using radiometric dialysis and the drug released quantified using radiolabelled [^{3}H]-DRV (Figure 5.5.A). DRV is slightly soluble in water (0.15 mg/mL as listed on the FDA datasheet) and the concentration of DRV used in the release study was below this limit. The three formulations showed little burst release (measured at the first time point of 30 minutes) of less than 14% which can be contributed to drug not encapsulated within the particles which may be adsorbed onto the surface of the particles. This value for burst release was lower than expected given that the encapsulation efficiency studies suggested that at least 30% of the drug was not trapped within the particles. However, this discrepancy might be due to harsher separation conditions that occurred during the spin-filter separation. With regards to the drug release profile of the three formulations, they were relatively similar with over 75% of the drug being released in the first 8 hours (Figure 5.5.A). The sample containing the most SBL (30%) and least Brij 78 (70%) showed the fastest

release. Increasing the Brij 78/total stabiliser mass from 70 to 100% w/w led to slower release. This may be attributed to the PEG corona surrounding the PLGA cores derived from the Brij 78, as this corona layer becomes denser, it retards drug release from the cores, leading to slower release and higher encapsulation efficiency. Zhang and Chen showed that pegylated lipid nanoparticles displayed slower and sustained drug release compared to the non-pegylated ones.[310] All three formulations tested showed low burst release and were selected for further biological studies to assess how the composition of the surfactant might influence the biological behaviour. According to the ANOVA test, the accumulative drug release of the three LPHNs formulations was significantly different ($P < 0.05$). Interestingly, LPHNs post-freeze-drying (Figure 5.5.B) showed that freeze-drying did not influence the release behaviour of the particles. There was a significant difference between the accumulative drug release between the single and dual drug loaded freeze-dried LPHN70, ($P < 0.05$).

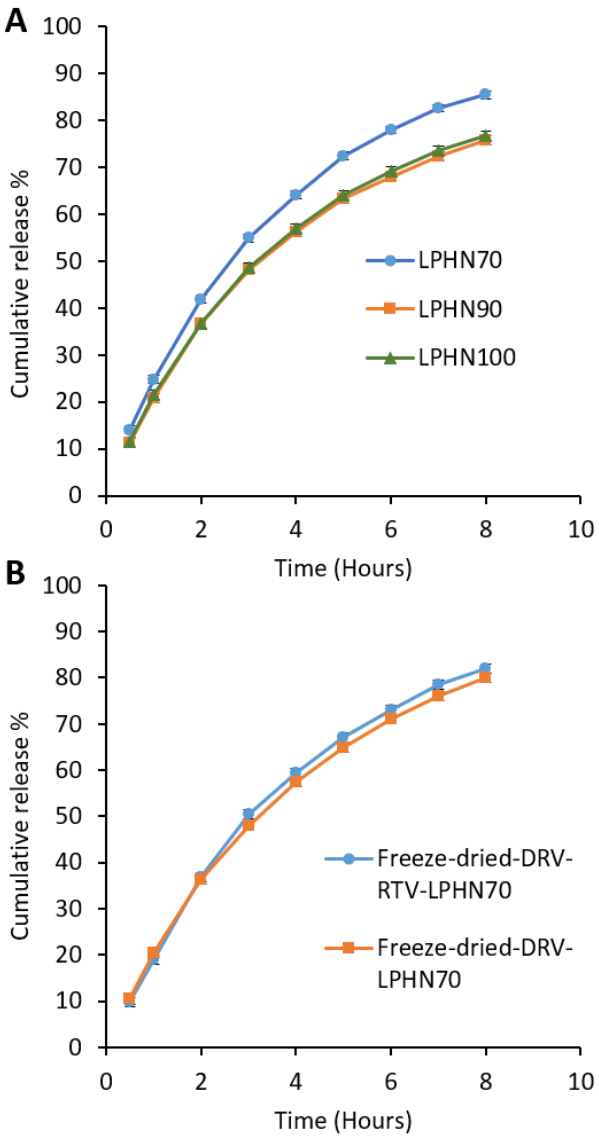

Figure 5.5 Drug release graphs of LPHNs containing [^{3}H]-DRV at 20% w/w with respect to PLGA. (A) DRV-RTV-LPHNs (not freeze-dried) stabilised with varied Brij 78/total stabiliser mass percentage (70, 90 or 100% w/w). (B) Freeze dried DRV- LPHNs and DRV-RTV-LPHNs stabilised with 70 % w/w Brij 78/total stabiliser. Error bars represent 3 times LSC background.

5.4.4 The effect of LPHNs surfactant composition on the absorption of DRV across a triple culture model

The three LPHNs formulations, namely LPHN70, LPHN90 and LPHN100 were investigated for their potential to deliver DRV in a model for the human intestinal epithelium. These formulations all contained DRV/PLGA at 20% w/w using both [^{3}H]-DRV/DRV and unlabelled RTV in an 8:1 ratio both before and after freeze drying. Radiolabelling was used to permit a quantitative assessment of DRV transcellular permeation and enabled a comparison to a conventional [^{3}H]-DRV/DRV (<1 % DMSO) aqueous preparation. An *in vitro* triple culture

model comprising; Caco-2 cells, HT-29-MTX mucus secreting goblet cells and Raji B lymphocytes which stimulate the differentiation of Caco-2 cells into microfold cells (M cells) were utilized to study the absorption of [^{3}H]-DRV/DRV loaded LPHNs. This *in vitro* model has been shown to be a useful predictive model for intestinal permeability of small molecules[311] while also providing a more physiologically accurate representation of the permeability of nanoparticles compared to Caco-2 monolayers alone.[272]

The permeation of DRV in both apical-to-basolateral and basolateral-to-apical directions was assessed. The results in Figure 5.6.A showed that LPHN70 displayed a significant increase in the P_{app} ratio of DRV equivalent to a 15 %, 84 % and 156 % increase following a 2-, 3- and 4-hours incubation respectively. Lower DRV apparent oral absorption at all time-points when formulated into LPHN90 (Figure 5.6.B) and LPHN100 (Figure 5.6.C) compared to the equivalent aqueous preparation was noted. The observed increase in P_{app} ratio for LPHN70 appears to be facilitated by an increase in A>B permeation. Conversely, the reduced P_{app} ratio for LPHN90 and LPHN100 appears to be primarily driven by an increased B>A permeation (efflux) (Figure 5.7). Previous studies have demonstrated enhancements in the oral bioavailability of poorly water-soluble drugs when co-formulated with lipids.[312–314] It is possible that the greater mass percentage of SBL used in LPHN70 formulation permitted greater solubility enhancement and subsequent permeation of DRV in the triple culture model. However, the effect of reducing Brij 78 in LPHN70 composition and increased P_{app} ratio cannot be excluded and warrants further investigation. Due to the similar mean diameter (61-76 nm) and polydispersity index (0.13-0.21) for all three formulations, these particle properties can be excluded as the causation factor driving the differences in biological behaviour. Integrity of the triple culture models were assessed using the low permeability marker [^{14}C]-mannitol following incubation with each treatment. The integrity was assessed post-incubation to identify any potential cumulative damage over the 4 hours. The results in Figure 5.6.D and Figure 5.8.B indicate mannitol P_{app} values less than 0.953×10^{-6} cm s^{-1} and suggest that the triple culture model remains intact following each treatment.[265] Therefore, the differences in the permeability of the different formulations was derived from the different surfactant compositions used in the formulations. The development of a LPHNs with 70% Brij 78 and 30% SBL as the surfactant provided excellent colloidal stability while also displaying enhanced apparent oral absorption in the triple culture model.

Subsequently, the biological behaviour of freeze-dried LPHN70 was investigated using the triple culture model. The DRV P_{app} ratio was markedly different compared to the non-freeze-dried preparation with increased P_{app} ratio at 1- and 2-hours incubation but lower P_{app} ratio at

3- and 4-hours incubation (Figure 5.8). No statistically significant differences in P_{app} between the unformulated DRV and LPHN70 formulated DRV were observed over the 4 hours which contrasts with the results observed for the non-freeze-dried preparation. It is difficult to be certain of the mechanism responsible for the marked difference in P_{app} due to freeze-drying the formulation, however, the presence of the PEG cryoprotectant may have coated the LPHNs and inhibited their interaction with the cells. Additionally, the freeze-drying processed resulted in an increased mean diameter (61 vs. 247 nm) and increased polydispersity (0.13 vs. 0.44) which may have influenced the interaction of the particles with the cells. Our formulations met the key parameters in developing pharmaceutical formulations, which include using excipients that are safe, biodegradable and approved by the regulatory authorities, i.e., FDA. In the case of the LPHNs, PLGA, Brij 78 and SBL were used as excipients and are all approved by the FDA and have been well reported in the literature in the synthesis of pharmaceutical preparations.[315] The drug loading of these DRV-RTV-LPHNs at 20% w/w was much higher than those reported in the literature. For example, Dalmoro *et al.*[167] reported a drug loading of 10% for indomethacin-loaded LPHNs synthesised using chitosan as a polymer. In another study, the drug loading of bupivacaine-LPHNs was found to be 8.6 % also prepared by a nanoprecipitation method. [316]

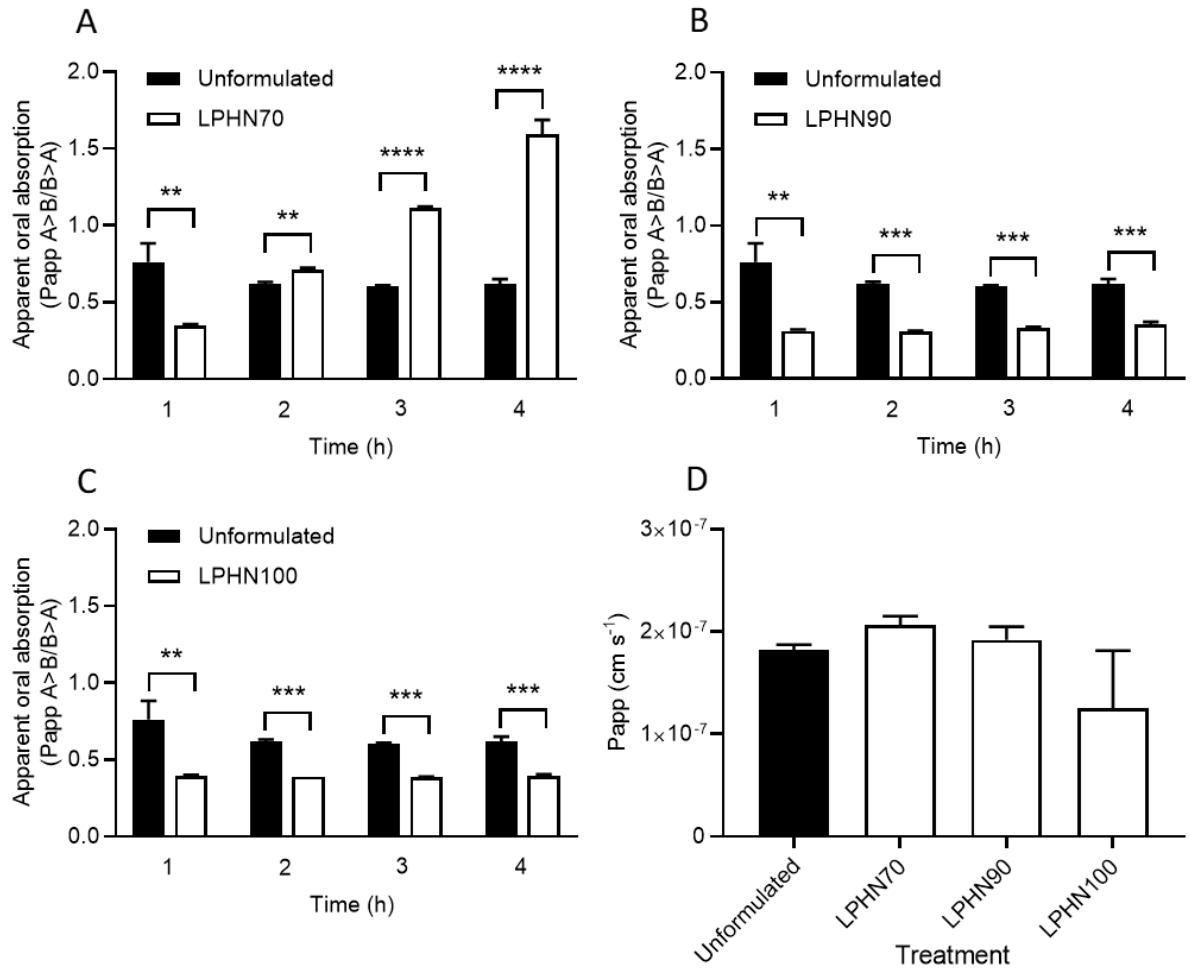

*Figure 5.6 Biological assessment of the effect of surfactant formulation on permeability. (A-C) Apparent oral absorption (Papp ratio) of conventional [3H]-DRV/DRV (<1 % DMSO) and three [3H]-DRV-LPHN preparations across a triple culture permeability model over a 4 h incubation at 37 °C, 5% CO2. (D) Mannitol apparent permeability (P_{app} cm s^{-1}), post DRV treatment, following 1 h incubation at 37 °C, 5% CO2. **, P < 0.01; ***, P < 0.001; ****, P < 0.0001 (unpaired, two-tailed t-test) (n=4).*

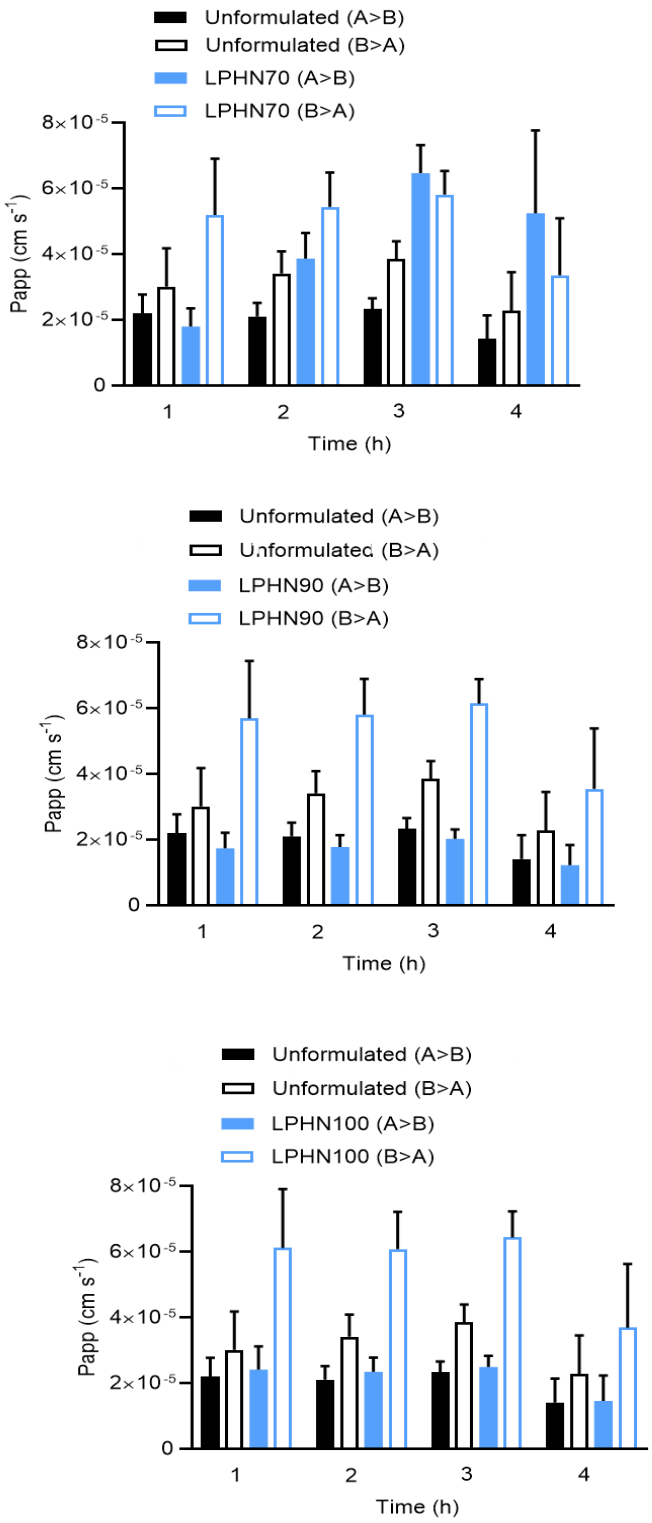

Figure 5.7 The apparent permeability (Papp) of conventional [3H]-DRV (<1% DMSO) and three [3H]-DRV-LPHN preparations across a triple culture permeability model over a 4 h incubation at 37oC, 5% CO2 (n=4).

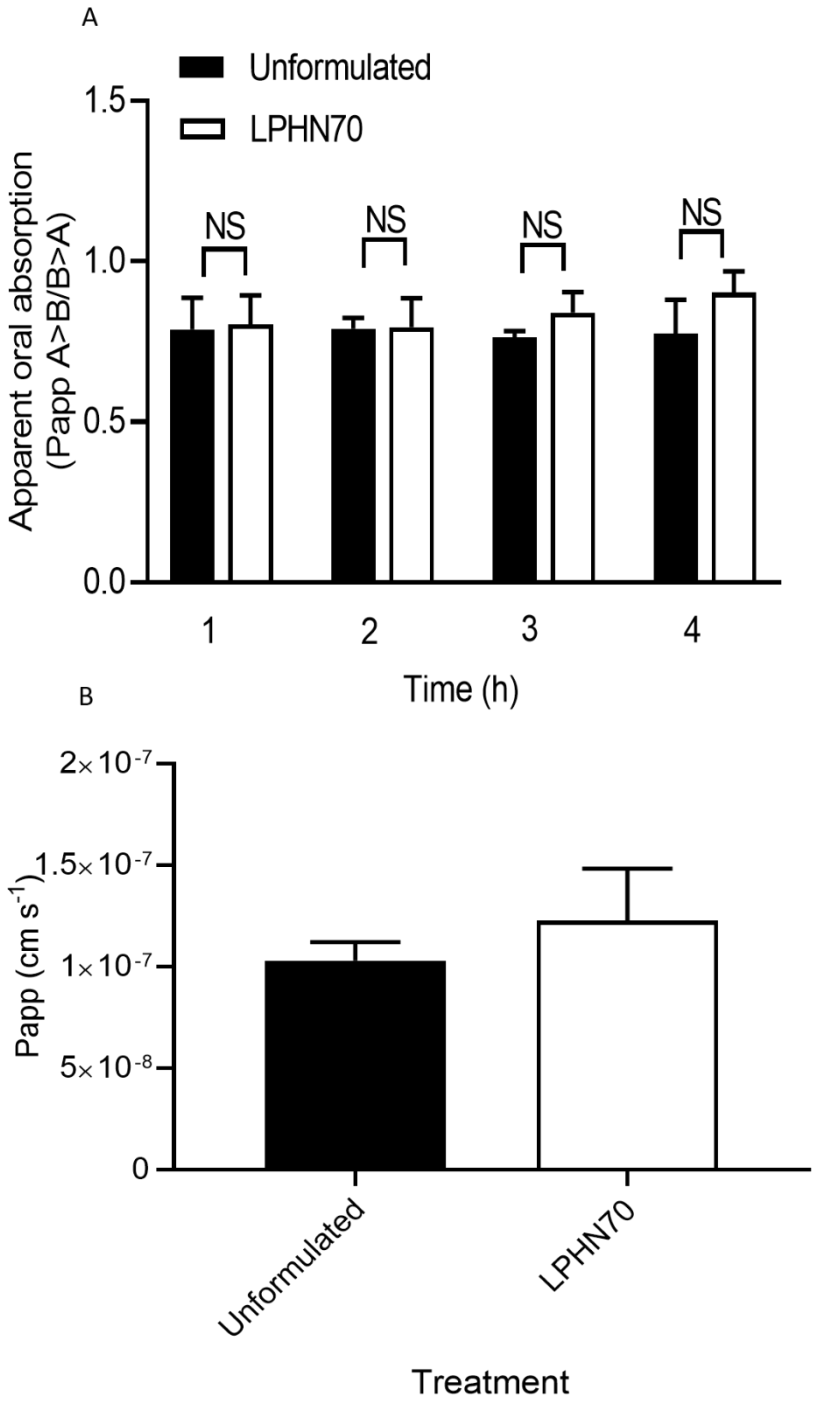

Figure 5.8 (A) Apparent oral absorption (P_{app} ratio) of conventional [^{3}H]-DRV (<1% DMSO) and freeze-dried [^{3}H]-DRV-LPHN70 across a triple culture permeability model over a 4 h incubation at 37^{o}C, 5% CO_2. (B) Mannitol apparent permeability (P_{app} cm s^{-1}), post DRV treatment, following 1 h incubation at 37^{o}C, 5% CO_2. NS, P > 0.05 (unpaired, two-tailed t-test) (n=4).

5.5 Conclusion

This work showed that LPHNs can be prepared with high drug loadings of DRV/PLGA (20% w/w) without negatively impacting the particle properties. The particles encapsulate the clinically used antiretrovirals (DRV/RTV) and the surfactant composition was tuned to combine colloidal stability under physiological conditions with sufficient lipid (in the form of SBL) to offer enhanced permeability. From the formulation ranges tested, our findings suggest that the optimum stabiliser to polymer mass percentage was 20% w/w. Brij 78 was crucial in providing stability in biologically relevant media. We have shown that these LPHNs dispersions can be freeze-dried to obtain solid formulations, addressing many of the stability issues that are faced for the storage of liquid nanomedicine formulations. These solids can then be re-dispersed at the time of need, which is currently a considerable challenge in nanomedicine. However, for this formulation, the freeze-drying process reduced the permeation behaviour in a triple culture model. The cause for this reduction in biological performance will need further research to understand the factors controlling this behaviour. Our work showed that SBL plays an important role in the permeation of drug loaded particles across the intestinal epithelium. Formulations of DRV/RTV in LPHNs may offer improved drug delivery for the treatment of HIV.

Chapter 6

Conclusions and Future Work

6.1 Conclusions

The target of this research discussed in this thesis was to synthesise and characterise lipid nanoformulations as potential oral drug delivery systems of a mixture of two hydrophobic antiretrovirals for the treatment of HIV. The chosen antiretroviral drug mixture was made of darunavir (DRV) and ritonavir (RTV). DRV is a protease inhibitor and used as a first line antiretroviral agent. The main limitation of DRV is its low oral bioavailability, which could be due to its low water solubility, high lipophilicity and it is also subjected to first pass metabolism. RTV is another protease inhibitor that acts as a booster for DRV and increasing the oral bioavailability of DRV from 37 % to 82 %. The ratio of DRV/RTV was kept at 8:1, as the clinical dose of DRV is 800 mg with 100 mg RTV once daily. Lipid nanoformulations were chosen as the drug carriers for this project as they have a good potential of incorporating lipophilic drug substances, they have good biocompatibility, offer improved physical stability, enhanced bioavailability, and controlled release for the drug molecules. These advantages make lipid nanocarriers good candidates for oral drug delivery. Lipid nanoformulations have a special advantage for targeting HIV reservoir sites in the gut, as they are selectively up taken by the lymphatics avoiding first pass metabolism. Among many lipid nanocarriers, solid lipid nanoparticles (SLNs), nanostructured lipid carriers (NLCs), nanoemulsions (NEs) and lipid polymer hybrid nanoparticles (LPHNs) have been selected for this study due to the availability of their excipients, low cost, simple production techniques at a large scale. Solvent injection technique was used as the synthesis technique for the formulations in this thesis as it is a simple and fast method. A key aim within this thesis was to investigate the different parameters affecting the synthesis of these different lipid nanoformulations by solvent injection, and to understand how these different formulations affect the morphology, entrapment efficiency, release, and bioavailability of DRV/RTV (8:1) drug mixture. Another aim was to have dry formulations in a powder form, so freeze-drying was investigated as a dehydration technique that aimed at maintaining the stability and particle size characteristics of the original nanoparticles' dispersions.

Initially, a comparison between the three formulations: SLNs, NLCs, and NEs was carried out. Although for the three nanocarriers, the cores were made of lipids, however they differ in the composition, physical state, and stability. This comparative study used the same synthesis method, the solvent injection method, for all three types of different lipid formulations, which has not been used before in a comparative study for such formulations. The synthesis of SLNs,

NLCs, and NEs was carried out using hot and cold solvent injection method, in which the hydrophobic was heated or kept at room temperature, respectively. Heating of the hydrophobic phase was essential when high melting point lipids were used, e.g., Compritol 888 ATO®. After varying several synthesis parameters, it was concluded that both methods enabled the successful synthesis of the three formulations. The following findings were common for both methods: 1) Increasing the lipid concentration in the hydrophobic phase led to a subsequent increase in the particle size on both day 1 and day 3. This trend could be attributed to the increase of viscosity of the hydrophobic phase, or the lipid cores were not sufficiently covered with the surfactants. The optimum lipid concentration of the lipid in the hydrophobic phase was 4 mg/mL. 2) The SLNs had the biggest particle sizes followed by NLCs and finally NEs, which showed the smallest particle size. The size of different NLCs depended on the S/L ratio, the higher the S/L ratio the bigger the diameter of the particles. 3) The investigation of the morphology of the synthesised formulations using CryoSEM showed spherical particles with smooth surface. 4) For the DSC crystallinity studies, the formation of lipid nanoparticles was confirmed by the disappearance or the shifting of the melting peaks for the solid lipid and the shifted melting peaks of the surfactants. For the hot solvent injection, the optimum concentration of Tween 80 was 1% w/v, above this concentration the Z-average diameter increased for both SLNs and NEs. On the other hand, the main drawback of the hot solvent injection was of the presence of residual ethanol in the dispersion media as it was not completely removed after it was left stirring for 48 hours. The cold solvent injection method addressed the problem of residual solvent, where THF was used as instead of ethanol, as it was volatile over the 48 hours period. In the cold solvent injection study, Brij 78 proved to a better surfactant compared to Tween 80 in terms of keeping small Z-average diameter (~ 200 nm) and PDI, especially with formulations with high solid lipid content: SLNs and NLCs (9:1). However. both surfactants were equally good for formulations with higher content of liquid lipid: NLCs (7:3) and (5:5), and NEs. Imwitor® 900 K was chosen as the solid lipid in the cold solvent injection study as, as it produced particles with smaller Z-average diameter and PDI. From the drug loading experiments using cold solvent injection method, it was concluded that the 10% DRV/total lipid was the highest weight percentage that can be used for SLNs without causing particle aggregation, while for the other lipid nanoformulations, that weight percentage was increased to 20% DRV/total lipid. Within these weight percentages of DRV/total lipid, all the drug-loaded formulations synthesised using Brij 78 were stable for a week, as determined by the DLS studies. The EE% range was 92.5- 95.8%, where drug-loaded SLNs showed the

highest drug loading, while NEs showed the lowest. Among all the tested formulations, NLCs (5:5) showed the most controlled drug release (52% drug release over 24 hours duration).

An alternative approach to address the residual solvent issue of hot solvent injection was to freeze-dry the dispersions of the lipid nanoformulations to remove both water and the water-miscible organic solvent. This study focused on SLNs as it was the most unstable among the three lipid nanoformulations as it suffers from polymorphism. A main aim of this study was to obtain high drug-loaded SLNs (HDL-SLNs), with targeted DRV loading of 50% w/w, with keeping the DRV/RTV ratio fixed at 8:1. For that purpose, a poly-oligo (ethylene glycol) methacrylates (*p*(OEGMA)) based branched polymer was synthesised by ATRP and tested as a potential surfactant for HDL-SLNs. The branched copolymer might provide better stabilisation for the high drug-loaded SLNs. The ATRP initiator (DBiB) was successfully synthesised using esterification reaction which was then incorporated in the synthesis of the branched copolymer DBiB-*p*(OEGMA$_{10}$-*co*-EGDMA$_{0.6}$) as a stabiliser for HDL-SLNs. As this was a novel surfactant for a novel type of SLNs, the solvent injection method had to be optimised. The optimum solvent injection setup can be summarised as follows: 1) The heating temperature of the hydrophobic phase was 80 °C for a stirring time of 2 minutes. 2) The optimum duration for stirring the HDL-SLNs dispersions before freeze-drying was 3 minutes. 3) Compritol 888 ATO® was the preferred solid lipid compared to glyceryl monostearate (GMS), as it formed HDL-SLNs with smaller Z-average diameter and PDI. 4) For the stabilisers, DBiB-*p*(OEGMA$_{10}$-*co*-EGDMA$_{0.6}$) proved to a better choice compared to commercially available surfactants: Tween 80 or soybean lecithin (SBL). However, the freeze-drying of the optimised HDL-SLNs without the use of cryoprotectants, led to their aggregation, which required further investigation.

As the freeze-drying of the HDL-SLNs dispersions led to their aggregation, several cryoprotectants were investigated, as an approach to limit aggregation and preserve original particles size. Dextrose, mannitol, and maltodextrin as sugar cryoprotectants all failed to provide cryoprotection and their use let to particles aggregation upon re-dispersion in DI water. On the other hand, the disaccharides sucrose and trehalose, provided proper cryoprotection for the HDL-SLNs with keeping a Z-average diameter of ~200 nm for both cryoprotectants, at a cryoprotectant concentration of 2.5 and 5% w/v respectively. As lower sucrose concentration was required, that meant that sucrose was more efficient as a cryoprotectant for our system compared to trehalose. Those concentrations of the disaccharide cryoprotectant were

equivalent to cryoprotectant/HDL-SLNs and the concentration of the freeze-drying mixture of 188/1 w/w and 13 mg/mL for sucrose and 376/1 w/w at 25 mg/mL for trehalose, respectively. On the other hand, PEG 2050 as an example for polymeric cryoprotectant proved to be more efficient than all the different types of sugar cryoprotectants. The minimum concentration required form PEG 2050 was 0.5% w/v, which was equivalent to a cryoprotectant/HDL-SLNs and the concentration of the freeze-drying mixture of 38/1 w/w and 3 mg/mL, respectively. Therefore PEG 2050 was the cryoprotectant of choice for all other studies at a scale of 10 mL freeze-drying mixture in 40 mL vial. The freeze-dried cakes of PEG 2050 were re-dispersed in PBS keeping their original size of ~200 nm, however they aggregated upon re-dispersion in simulated gastric fluid. The SEM morphology studies showed spherical particles with narrow size distribution, with a film coating the particles which could be due to the use of PEG as a cryoprotectant. 80% of DRV was released over 8 hours period, which was accompanied by initial burst release. The formulation of HDL-SLNs resulted in increased cellular uptake of DRV. The DRV-RTV-HDL-SLNs showed increased permeability both A > B 'gut-to-blood' and B > A 'blood-to-gut', more than the unformulated combination of DRV and RTV. However, there was no increase in the apparent oral absorption observed for the HDL-SLNs, which could be due to the use of the hydrophilic PEG 2050 which alters the lipophilic nature of SLNs.

After investigating various lipid nanoformulations where the lipid was located in the core, a different type of lipid nanoformulations was examined, in which the lipid forms a layer that coat the polymeric core. The type of formulation is called lipid polymer hybrid nanoparticles (LPHNs). Our work showed that LPHNs can be successfully prepared using solvent injection method, where a mixture of surfactants was used, soybean lecithin as an electrostatic stabiliser which offered enhanced permeability and Brij 78 as a bulk stabiliser, which help the stabilisation of LPHNs under physiological conditions. The optimum stabiliser to polymer mass percentage was found to be 20% w/w. The LPHNs was loaded with DRV/RTV (8:1) at a high drug loading of DRV/PLGA (20% w/w) without adversely affecting the particle properties. Although the LPHNs dispersions showed enhanced apparent oral absorption, however upon freeze-drying using PEG 2050 as a cryoprotectant, the permeation across triple culture model was greatly reduced. Also, the freeze-dried formulations, were redispersed in DI water and PBS, however they aggregated once re-dispersed in simulated gastric fluid which is the same behaviour of freeze-dried HDL-SLNs. The reduction in biological performance and the instability of the freeze-dried materials in SGF should be further investigated.

Overall, this thesis showed the value of formulating the drug mixture of DRV/RTV (8:1) into the lipid nanoformulations: SLNs, NLCs, NEs and LPHNs. Those lipid nanoformulations with high drug loading, provided enhanced physicochemical characteristics and biological behaviour compared to the unformulated drugs. Moreover, the freeze-drying enhanced the physical stability of both HDL-SLNs and LPHNs. To the best of the author knowledge, this is the first time a comparative study SLNs, NLCs and NEs using solvent injection has been carried out. It is also the first attempt to use DBiB-*p*(OEGMA$_{10}$-*co*-EGDMA$_{0.6}$) as stabiliser for SLNs with over 50% drug loading. It was also the first time to use LPHNs as a drug carrier for HIV treatment. All the unfreeze-dried lipid nanoformulations and LPHNs dispersions prepared in this thesis were stable in both PBS (pH 7.4) and SGF (pH 1.2), therefore overcome the challenge of the GIT pH. The transcellular permeability studies showed that unfreeze-dried LPHNs provided enhanced permeability compared to the unformulated DRV solution, which meant that LPHNs increased the bioavailability of the hydrophobic DRV and addressed the GIT mucus barrier issue. In addition to that, our formulations met the pharmacopeial requirements in developing pharmaceutical formulations, which include using excipients that are safe, biodegradable and approved by the regulatory authorities, i.e., FDA. The pharmacological benefits of the synthesised formulations, in addition to the ease of preparation using solvent injection method, offers the potential of the industrial scale-up and future use in the market.

6.2 Future work

Further investigations would be of value in terms of understanding the cause of reduced oral bioavailability the freeze-dried HDL-SLNs and LPHNs using the hydrophilic cryoprotectant PEG 2050. In a study by Schimpel, C. *et al.,* the *in vivo* data correlates with our data collected using triple culture models demonstrating that such models effectively simulate the intestinal environment.[272] However, since publication of such studies, major limitations of the model have become apparent (e.g.) suboptimal physiological relevance; the tumour-like behaviour of cell cultures cannot represent true intestinal physiology.[317] Moreover, as Caco-2 cells under-express influx transporters including organic anion transporters,[318] key in DRV uptake,[319] the data collected do not replicate physiological behaviour. Therefore, future experiments regarding intestinal uptake could utilise 3D organoid models to more accurately represent *in vivo* activity, thus providing more representative pre-clinical data.[317]

Also, more experiments to be carried out to provide enhanced stabilisation of those freeze-dried materials in the simulated gastric fluids. Possibly the freeze-dried materials can be further coated with different excipients resistant to stomach acidity. The coating could be a polymer from natural source like Cruciferin. Cruciferin is a major canola protein, that has been used by Akbari and Wu as a successful coating for chitosan nanoparticles, to protect them from the harsh conditions of the GIT, as Cruciferin is resistant to gastric digestion.[270] Synthetic polymers like Eudragit, which is a polyacrylate polymer can be investigated. Eudragit also has a resistance to the harsh conditions of the GIT. It has been used to coat anti-inflammatory drugs like diclofenac, limiting the ulcerogenic side effects and enhancing its poor bioavailability.[320]

Another area for investigation, is to keep the optimised lipid nanoformulations, while exploring newer antiretroviral drugs instead of the DRV/RTV combination. A good candidate could be dolutegravir (DTG), which is sold under the brand name Tivicay. It is an integrase inhibitor that was approved by the FDA in 2013, and it is considered by the WHO as a first line treatment. It is given in combination therapy along with abacavir (reverse transcriptase inhibitor), and lamivudine (nucleoside analogue reverse transcriptase inhibitor).[320]

An investigation of the *in vivo* pharmacokinetics (PK) would be very useful in the future because it is critical to understand the relationship between particle properties for the nanoformulations and their PK profiles. Unfortunately, it was not possible to obtain nanoformulations with a sufficiently high concentration of DRV to be suited to oral dosing. Therefore, a key future aim is to increase the DRV concentration to fit the limit required for *in vivo* as it gives a better idea on how these formulations would behave inside the body. Currently the concentration of DRV in DI water required for the *in vivo* testing is 7 mg/mL. To obtain higher drug loading, a wider range of lipids, solvents and surfactants must be screened to reach a dose suitable for oral dosing in mice.

A wide range of polymers with varied architecture in terms of HLB, chain length and degree of branching can be synthesised and tailored for the use of different nanoformulations. In this thesis only one polymer was synthesised and used as a stabiliser for HDL-SLNs. Future work could involve, synthesising a library of polymers with a systemic change of its structure to test how would these variables affect the size and stability of the produced lipid nanoformulations.

Wider application of these findings may contribute towards the development of improved HIV therapy of different drugs. Presently in clinical development, nanoformulations are being utilised to design long-acting HIV therapies such as cabotegravir and rilpivirine. Although currently administered via intramuscular injection, the frequency of administration is significantly reduced compared to current daily-dosing, with monthly/quarterly injections.[321] However, intramuscular injections raise concerns due to safe disposal and healthcare requirements implicated with, as such administration remains impractical for large-scale HIV therapy because two-thirds of all HIV patients are situated in Sub-Saharan Africa, an area with limited health-related facilities.[322] The potential to achieve long-acting oral dosing is therefore very exciting. An attractive consequence of drug reformulation also includes a potential reduction in dosage, reducing dose-dependent side-effects so greatly benefitting HIV patients.[274] Ultimately, McCrudden *et al*. proposes that a reduced frequency of administration facilitated by nanoformulated drugs could diminish compliance issues associated with daily drug administration, thus increasing the effectiveness of HIV treatment globally.[323]

References

1. Panel on Antiretroviral Therapy and Medical Management of HIV-Infected Children. *Guidelines For The Use Of Antiretroviral Agents In HIV-1-Infected Adults And Adolescents Developed By The HHS Panel On Antiretroviral Guidelines For*. **October**. 2012;
2. World Health Organisation (WHO). *HIV/AIDS/Fact Sheets* [Https://www.who.int/news-room/fact-sheets/detail/hiv-aids]. 2019.
3. Mahajan SD, Aalinkeel R, Law WC, Reynolds JL, Nair BB, Sykes DE, Yong KT, Roy I, Prasad PN, Schwartz SA. *Anti-HIV-1 Nanotherapeutics: Promises And Challenges For The Future*. **International Journal Of Nanomedicine**. 2012;7:5301–14.
4. Cooray S, Howe SJ, Thrasher AJ. *Retrovirus And Lentivirus Vector Design And Methods Of Cell Conditioning*. In: Methods in Enzymology. 1st ed. Elsevier Inc.; 2012. p. 29–57.
5. Seitz R. *Human Immunodeficiency Virus (HIV)*. **Transfusion Medicine And Hemotherapy**. 2016;43(3):203–22.
6. Services USD of H& H. *HIV Life Cycle | AIDSinfo* [Https://aidsinfo.nih.gov/understanding-hiv-aids/infographics/7/hiv-life-cycle]. 2016.
7. Flynn JK, Ellenberg P, Duncan R, Ellett A, Zhou J, Sterjovski J, Cashin K, Borm K, Gray LR, Lewis M, Jubb B, Westby M, Lee B, Lewin SR, Churchill M, Roche M, Gorry PR. *Analysis Of Clinical HIV-1 Strains With Resistance To Maraviroc Reveals Strain-Specific Resistance Mutations, Variable Degrees Of Resistance, And Minimal Cross-Resistance To Other CCR5 Antagonists*. **AIDS Research And Human Retroviruses**. 2017;33(12):1220–35.
8. Malik T, Chauhan G, Rath G, Murthy RSR, Goyal AK. *"Fusion And Binding Inhibition" Key Target For HIV-1 Treatment And Pre-Exposure Prophylaxis: Targets, Drug Delivery And Nanotechnology Approaches*. **Drug Delivery**. 2017;24(1):608–21.
9. Song L, Ding S, Ge Z, Zhu X, Qiu C, Wang Y, Lai E, Yang W, Sun Y, Chow SA, Yu L. *Nucleoside/Nucleotide Reverse Transcriptase Inhibitors Attenuate Angiogenesis And Lymphangiogenesis By Impairing Receptor Tyrosine Kinases Signalling In Endothelial Cells*. **British Journal Of Pharmacology**. 2018;175(8):1241–59.
10. Azeem SM, Muwonge AN, Thakkar N, Lam KW, Frey KM. *Structure-Based Methods To Predict Mutational Resistance To Diarylpyrimidine Non-Nucleoside Reverse Transcriptase Inhibitors*. **Journal Of Molecular Graphics And Modelling**. 2018;79:133–9.

11. Lisziewicz J, Toke ER. *Nanomedicine Applications Towards The Cure Of HIV*. **Nanomedicine: Nanotechnology, Biology, And Medicine**. 2013;9(1):28–38.
12. Kommavarapu P, Maruthapillai A, Palanisamy K. *Preparation, Characterization And Evaluation Of Elvitegravir-Loaded Solid Lipid Nanoparticles For Enhanced Solubility And Dissolution Rate*. **Tropical Journal Of Pharmaceutical Research**. 2015;14(9):1549–56.
13. Gupta U, Jain NK. *Non-Polymeric Nano-Carriers In HIV/AIDS Drug Delivery And Targeting*. **Advanced Drug Delivery Reviews**. 2010;62(4–5):478–90.
14. Lv Z, Chu Y, Wang Y. *HIV Protease Inhibitors: A Review Of Molecular Selectivity And Toxicity*. **HIV/AIDS (Auckland, NZ)**. 2015;7:95–104.
15. Kumar L, Verma S, Prasad DN, Bhardwaj A, Vaidya B, Jain AK. *Nanotechnology: A Magic Bullet For HIV AIDS Treatment*. **Artificial Cells, Nanomedicine, And Biotechnology**. 2015;43(2):71–86.
16. Sarmento B, Gomes MJ, das Neves J. *Nanoparticle-Based Drug Delivery To Improve The Efficacy Of Antiretroviral Therapy In The Central Nervous System*. **International Journal Of Nanomedicine**. 2014;9(1):1757.
17. Borgmann K, Rao KS, Labhasetwar V, Ghorpade A. *Efficacy Of Tat-Conjugated Ritonavir-Loaded Nanoparticles In Reducing HIV-1 Replication In Monocyte-Derived Macrophages And Cytocompatibility With Macrophages And Human Neurons*. **AIDS Research And Human Retroviruses**. 2011;27(8):853–62.
18. Lascar R. *Role Of Darunavir In The Management Of HIV Infection*. **HIV/AIDS - Research And Palliative Care**. 2009;1(1):31.
19. Wagner C, Zhao P, Arya V, Mullick C, Struble K, Au S. *Physiologically Based Pharmacokinetic Modeling For Predicting The Effect Of Intrinsic And Extrinsic Factors On Darunavir Or Lopinavir Exposure Coadministered With Ritonavir*. **The Journal Of Clinical Pharmacology**. 2017;57(10):1295–304.
20. Parboosing R, Maguire GEM, Govender P, Kruger HG. *Nanotechnology And The Treatment Of HIV Infection*. **Viruses**. 2012;4(12):488–520.
21. Adesina SK, Akala EO. *Nanotechnology Approaches For The Delivery Of Exogenous SiRNA For HIV Therapy*. **Molecular Pharmaceutics**. 2015;12(12):4175–87.
22. Swartz JE, Vandekerckhove L, Ammerlaan H, De Vries AC, Begovac J, Bierman WFW, Boucher CAB, Van Der Ende ME, Grossman Z, Kaiser R, Levy I, Mudrikova T, Paredes R, Perez-Bercoff D, Pronk M, Richter C, Schmit JC, Vercauteren J, Zazzi M, Židovec Lepej S, De Luca A, Wensing AMJ. *Efficacy Of Tenofovir And Efavirenz In*

Combination With Lamivudine Or Emtricitabine In Antiretroviral-Naive Patients In Europe. **Journal Of Antimicrobial Chemotherapy**. 2014;70(6):1850–7.

23. Nelson AG, Zhang X, Ganapathi U, Szekely Z, Flexner CW, Owen A, Sinko PJ. *Drug Delivery Strategies And Systems For HIV/AIDS Pre-Exposure Prophylaxis And Treatment*. **Journal Of Controlled Release**. 2015;219(2015):669–80.
24. Aji Alex MR, Chacko AJ, Jose S, Souto EB. *Lopinavir Loaded Solid Lipid Nanoparticles (SLN) For Intestinal Lymphatic Targeting*. **European Journal Of Pharmaceutical Sciences**. 2011;42(1–2):11–8.
25. Vedha Hari BN, Lu CL, Narayanan N, Wang RR, Zheng YT. *Engineered Polymeric Nanoparticles Of Efavirenz: Dissolution Enhancement Through Particle Size Reduction*. **Chemical Engineering Science**. 2016;155:366–75.
26. Antoniou T, Szadkowski L, Walmsley S, Cooper C, Burchell AN, Bayoumi AM, Montaner JSG, Loutfy M, Klein MB, Machouf N, Tsoukas C, Wong A, Hogg RS, Raboud J. *Comparison Of Atazanavir/Ritonavir And Darunavir/Ritonavir Based Antiretroviral Therapy For Antiretroviral Naïve Patients*. **BMC Infectious Diseases**. 2017;17(1):266.
27. Adkins JC, Faulds D. *Amprenavir*. **Adis New Drug Profile**. 1998;55(6):837–42.
28. Desai J, Thakkar H. *Darunavir-Loaded Lipid Nanoparticles For Targeting To HIV Reservoirs*. **AAPS PharmSciTech**. 2018;19(2):648–60.
29. Bhalekar MR, Upadhaya PG, Madgulkar AR, Kshirsagar SJ, Dube A, Bartakke US. In-Vivo *Bioavailability And Lymphatic Uptake Evaluation Of Lipid Nanoparticulates Of Darunavir*. **Drug Delivery**. 2015;7544(September):1–6.
30. Bhalekar M, Upadhaya P, Madgulkar A. *Formulation And Characterization Of Solid Lipid Nanoparticles For An Anti-Retroviral Drug Darunavir*. **Applied Nanoscience**. 2017;7(1–2):47–57.
31. Desai J, Thakkar H. *Effect Of Particle Size On Oral Bioavailability Of Darunavir-Loaded Solid Lipid Nanoparticles*. **Journal Of Microencapsulation**. 2016;33(7):669–78.
32. Capetti AF, Cossu MV, Orofino G, Sterrantino G, Cenderello G, De Socio G V., Cattelan AM, Soria A, Rusconi S, Riccardi N, Baldin GM, Niero FP, Barbarini G, Rizzardini G. *A Dual Regimen Of Ritonavir/Darunavir Plus Dolutegravir For Rescue Or Simplification Of Rescue Therapy: 48 weeks' Observational Data*. **BMC Infectious Diseases**. 2017;17(1):658.
33. Naahidi S, Jafari M, Edalat F, Raymond K, Khademhosseini A, Chen P.

Biocompatibility Of Engineered Nanoparticles For Drug Delivery. **Journal Of Controlled Release**. 2013;166(2):182–94.

34. Sörensen J, Velikyan I, Sandberg D, Wennborg A, Feldwisch J, Tolmachev V, Orlova A, Sandström M, Lubberink M, Olofsson H, Carlsson J, Lindman H. *Measuring HER2-Receptor Expression In Metastatic Breast Cancer Using [68Ga]ABY-025 Affibody PET/CT*. **Theranostics**. 2016;6(2):262–71.
35. Jain NK, Srivastava R, Naidu V. *Niclosamide Loaded Cationic Solid Lipid Nanoparticles For Treatment Of Cancer*. In: 2016 IEEE 16th International Conference on Nanotechnology (IEEE-NANO). IEEE; 2016. p. 245–8.
36. Amini Y, Moradi B, Fasihi-Ramandi M. *Aluminum Hydroxide Nanoparticles Show Strong Activity To Stimulate Th-1 Immune Response Against Tuberculosis*. **Artificial Cells, Nanomedicine And Biotechnology**. 2017;45(7):1331–5.
37. Nguyen DN, Clasen C, Van den Mooter G. *Encapsulating Darunavir Nanocrystals Within Eudragit L100 Using Coaxial Electrospraying*. **European Journal Of Pharmaceutics And Biopharmaceutics**. 2017;113:50–9.
38. Garinot M, Fiévez V, Pourcelle V, Stoffelbach F, Plapied L, Theate I, Freichels H, Jérôme C, Marchand-brynaert J, Schneider Y, Préat V. *PEGylated PLGA-Based Nanoparticles Targeting M Cells For Oral Vaccination*. 2007;120:195–204.
39. Crucho CIC, Barros MT. *Polymeric Nanoparticles: A Study On The Preparation Variables And Characterization Methods*. **Materials Science And Engineering C**. 2017;80:771–84.
40. Sosnik A, Augustine R. *Challenges In Oral Drug Delivery Of Antiretrovirals And The Innovative Strategies To Overcome Them ☆*. **Advanced Drug Delivery Reviews**. 2016;103:105–20.
41. Khalil NM, Carraro E, Cótica LF, Mainardes RM. *Potential Of Polymeric Nanoparticles In AIDS Treatment And Prevention*. **Expert Opinion On Drug Delivery**. 2011;8(1):95–112.
42. Shibata A, Mcmullen E, Pham A, Belshan M, Sanford B. *Polymeric Nanoparticles Containing Combination Antiretroviral Drugs For HIV Type 1 Treatment Annemarie*. **AIDS Research And Human Retroviruses**. 2013;29(5):746–54.
43. Hillaireau H, Le Doan T, Appel M, Couvreur P. *Hybrid Polymer Nanocapsules Enhance In Vitro Delivery Of Azidothymidine-Triphosphate To Macrophages*. **Journal Of Controlled Release**. 2006;116(3):346–52.

44. Shah LK, Amiji MM. *Intracellular Delivery Of Saquinavir In Biodegradable Polymeric Nanoparticles For HIV / AIDS*. **Pharmaceutical Research**. 2006;23(11):2638–45.
45. Hume DA. *The Mononuclear Phagocyte System*. **Current Opinion In Immunology**. 2006;18(1):49–53.
46. Tomoda K, Yabuki N, Terada H, Makino K. *Colloids And Surfaces A : Physicochemical And Engineering Aspects Surfactant Free Preparation Of PLGA Nanoparticles : The Combination Of Antisolvent Diffusion With Preferential Solvation*. **Colloids And Surfaces A: Physicochemical And Engineering Aspects**. 2014;457:88–93.
47. Mu L, Feng S. *PLGA/TPGS Nanoparticles For Controlled Release Of Paclitaxel: Effects Of The Emulsifier And Drug Loading Ratio*. **Pharmaceutical Research**. 2003;20(11):1864–72.
48. Bhardwaj V, Ankola DD, Gupta SC, Schneider M, Lehr C-M, Kumar MNVR. *PLGA Nanoparticles Stabilized With Cationic Surfactant: Safety Studies And Application In Oral Delivery Of Paclitaxel To Treat Chemical-Induced Breast Cancer In Rat*. **Pharmaceutical Research**. 2009;26(11):2495–503.
49. Fay F, Quinn DJ, Gilmore BF, McCarron PA, Scott CJ. *Gene Delivery Using Dimethyldidodecylammonium Bromide-Coated PLGA Nanoparticles*. **Biomaterials**. 2010;31(14):4214–22.
50. Wohlfart S, Khalansky AS, Gelperina S, Maksimenko O, Bernreuther C, Glatzel M, Kreuter J. *Efficient Chemotherapy Of Rat Glioblastoma Using Doxorubicin-Loaded PLGA Nanoparticles With Different Stabilizers*. Castro MG, editor. **PLoS ONE**. 2011;6(5):19121.
51. Santander-Ortega MJ, Jódar-Reyes AB, Csaba N, Bastos-González D, Ortega-Vinuesa JL. *Colloidal Stability Of Pluronic F68-Coated PLGA Nanoparticles: A Variety Of Stabilisation Mechanisms*. **Journal Of Colloid And Interface Science**. 2006;302(2):522–9.
52. Scott CJ, Marouf WM, Quinn DJ, Buick RJ, Orr SJ, Donnelly RF, McCarron P a. *Immunocolloidal Targeting Of The Endocytotic Siglec-7 Receptor Using Peripheral Attachment Of Siglec-7 Antibodies To Poly(Lactide-Co-Glycolide) Nanoparticles*. **Pharmaceutical Research**. 2008;25(1):135–46.
53. McCarron P a., Marouf WM, Donnelly RF, Scott C. *Enhanced Surface Attachment Of Protein-Type Targeting Ligands To Poly(Lactide-Co-Glycolide) Nanoparticles Using Variable Expression Of Polymeric Acid Functionality*. **Journal Of Biomedical Materials Research - Part A**. 2008;87(4):873–84.

54. Italia JL, Yahya MM, Singh D, Ravi Kumar MN V. *Biodegradable Nanoparticles Improve Oral Bioavailability Of Amphotericin B And Show Reduced Nephrotoxicity Compared To Intravenous Fungizone.* **Pharmaceutical Research**. 2009;26(6):1324–31.

55. Schwarz C, Mehnert W, Lucks JS, Müller RH. *Solid Lipid Nanoparticles (SLN) For Controlled Drug Delivery. I. Production, Characterization And Sterilization*. **Journal Of Controlled Release**. 1994;30(1):83–96.

56. Das S, Chaudhury A. *Recent Advances In Lipid Nanoparticle Formulations With Solid Matrix For Oral Drug Delivery*. **AAPS PharmSciTech**. 2011;12(1):62–76.

57. Saupe A, Gordon KC, Rades T. *Structural Investigations On Nanoemulsions, Solid Lipid Nanoparticles And Nanostructured Lipid Carriers By Cryo-Field Emission Scanning Electron Microscopy And Raman Spectroscopy*. **International Journal Of Pharmaceutics**. 2006;314(1):56–62.

58. Shinde PB, Gunvantrao DS, Meghraj S. *Lipid Based Nanoparticles: SLN / NLCS – Formulation Techniques , Its Evaluation And Applications*. **International Journal Of Creative And Innovative Research In All Studies**. 2019;1(April):20–31.

59. Kriegel C, Amiji M. *Oral TNF Gene Silencing Using A Polymeric Microsphere-Based Delivery System For The Treatment Of Inflammatory Bowel Disease*. **Journal Of Controlled Release**. 2011;150(1):77–86.

60. El-Say KM, El-Sawy HS. *Polymeric Nanoparticles: Promising Platform For Drug Delivery*. **International Journal Of Pharmaceutics**. 2017;528(1–2):675–91.

61. Boisgard AS, Lamrayah M, Dzikowski M, Salmon D, Kirilov P, Primard C, Pirot F, Fromy B, Verrier B. *Innovative Drug Vehicle For Local Treatment Of Inflammatory Skin Diseases: Ex Vivo And In Vivo Screening Of Five Topical Formulations Containing Poly(Lactic Acid) (PLA) Nanoparticles*. **European Journal Of Pharmaceutics And Biopharmaceutics**. 2017;116:51–60.

62. Nilsson JS, Broos S, Akagi T, Akashi M, Hermansson A, Cayé-Thomasen P, Lindstedt M, Greiff L. *Amphiphilic γ-PGA Nanoparticles Administered On Rat Middle Ear Mucosa Produce Adjuvant-Like Immunostimulation* In Vivo. **Acta Oto-Laryngologica**. 2014;134(10):1034–41.

63. Brenza TM, Ghaisas S, Ramirez JEV, Harischandra D, Anantharam V, Kalyanaraman B, Kanthasamy AG, Narasimhan B. *Neuronal Protection Against Oxidative Insult By Polyanhydride Nanoparticle-Based Mitochondria-Targeted Antioxidant Therapy*. **Nanomedicine: Nanotechnology, Biology, And Medicine**. 2017;13(3):809–20.

64. Du BX, Xu H, Li J, Li Z. *Space Charge Behaviors Of PP/POE/ZnO Nanocomposites For HVDC Cables*. **IEEE Transactions On Dielectrics And Electrical Insulation**. 2016;23(5):3165–74.

65. Al-Amin M, Cao J, Naeem M, Banna H, Kim M, Jung Y, Chung HY, Moon HR, Yoo J-W. *Increased Therapeutic Efficacy Of A Newly Synthesized Tyrosinase Inhibitor By Solid Lipid Nanoparticles In The Topical Treatment Of Hyperpigmentation*. **Drug Design, Development And Therapy**. 2016;10:3947–57.

66. Badri W, Miladi K, Nazari QA, Fessi H, Elaissari A. *Effect Of Process And Formulation Parameters On Polycaprolactone Nanoparticles Prepared By Solvent Displacement*. **Colloids And Surfaces A: Physicochemical And Engineering Aspects**. 2017;516:238–44.

67. Lanz-Landaźuri A, Portilla-Arias J, De Ilarduya AM, Garciá-Alvarez M, Holler E, Ljubimova J, M͡noz-Guerra S. *Nanoparticles Of Esterified Polymalic Acid For Controlled Anticancer Drug Release*. **Macromolecular Bioscience**. 2014;14(9):1325–36.

68. Bonyani M, Mirzaei A, Leonardi SG, Neri G. *Silver Nanoparticles/Polymethacrylic Acid (AgNPs/PMA) Hybrid Nanocomposites-Modified Electrodes For The Electrochemical Detection Of Nitrate Ions*. **Measurement: Journal Of The International Measurement Confederation**. 2016;84:83–90.

69. Seo Y, Oshikawa N, Miyake T, Sakoda T, Anjiki T. *Characteristics Of Hydrophobicity Loss On Silicone Rubber Surface During A Dynamic Drop Test With Direct Current Voltage Application*. **Nanoscale Research Letters**. 2012;7(1):4.

70. Bhardwaj V, Ankola DD, Gupta SC, Schneider M, Lehr C-M, Kumar MNVR. *PLGA Nanoparticles Stabilized With Cationic Surfactant: Safety Studies And Application In Oral Delivery Of Paclitaxel To Treat Chemical-Induced Breast Cancer In Rat*. **Pharmaceutical Research**. 2009;26(11):2495–503.

71. Batist G, Barton J, Chaikin P, Swenson C, Welles L. *Myocet (Liposome-Encapsulated Doxorubicin Citrate): A New Approach In Breast Cancer Therapy*. **Expert Opinion On Pharmacotherapy**. 2002;3(12):1739–51.

72. Amaral AC, Bocca AL, Ribeiro AM, Nunes J, Peixoto DLG, Simioni AR, Primo FL, Lacava ZGM, Bentes R, Titze-de-Almeida R, Tedesco AC, Morais PC, Felipe MSS. *Amphotericin B In Poly(Lactic-Co-Glycolic Acid) (PLGA) And Dimercaptosuccinic Acid (DMSA) Nanoparticles Against Paracoccidioidomycosis*. **The Journal Of Antimicrobial Chemotherapy**. 2009;63(3):526–33.

73. Kouchakzadeh H, Abbas S, Tahmasebi F, Shokri F. *Optimization Of An Anti-HER2 Monoclonal Antibody Targeted Delivery System Using PEGylated Human Serum Albumin Nanoparticles*. **International Journal Of Pharmaceutics**. 2013;447(1–2):62–9.

74. Rahimian S, Fransen MF, Kleinovink JW, Christensen JR, Amidi M, Hennink WE, Ossendorp F. *Polymeric Nanoparticles For Co-Delivery Of Synthetic Long Peptide Antigen And Poly IC As Therapeutic Cancer Vaccine Formulation*. **Journal Of Controlled Release**. 2015;203:16–22.

75. Duan Y, Dhar A, Patel C, Khimani M, Neogi S, Sharma P, Siva Kumar N, Vekariya RL. *A Brief Review On Solid Lipid Nanoparticles: Part And Parcel Of Contemporary Drug Delivery Systems*. **RSC Advances**. 2020;10(45):26777–91.

76. Medina SH, El-Sayed MEH. *Dendrimers As Carriers For Delivery Of Chemotherapeutic Agents*. **Chemical Reviews**. 2009;109(7):3141–57.

77. Nahar M, Mishra D, Dubey V, Jain NK. *Development Of Amphotericin B Loaded PLGA Nanoparticles For Effective Treatment Of Visceral Leishmaniasis*. In: 13th International Conference on Biomedical Engineering. 2009. p. 1241–3.

78. Cheng Y, Zhao L, Li Y, Xu T. *Design Of Biocompatible Dendrimers For Cancer Diagnosis And Therapy: Current Status And Future Perspectives*. **Chemical Society Reviews**. 2011;40(5):2673.

79. Zhu X, Anquillare ELB, Farokhzad OC, Shi J. *Polymer- And Protein-Based Nanotechnologies For Cancer Theranostics*. Cancer Theranostics. Elsevier Inc.; 2014. 419–436 p.

80. Mandal A, Bisht R, Rupenthal ID, Mitra AK. *Polymeric Micelles For Ocular Drug Delivery: From Structural Frameworks To Recent Preclinical Studies*. **Journal Of Controlled Release**. 2017;248:96–116.

81. Li S-D, Huang L. *Nanoparticles Evading The Reticuloendothelial System: Role Of The Supported Bilayer*. **Biochimica Et Biophysica Acta (BBA) - Biomembranes**. 2009;1788(10):2259–66.

82. Tang X, Dai J, Xie J, Zhu Y, Zhu M, Wang Z, Xie C, Yao A, Liu T, Wang X, Chen L, Jiang Q, Wang S, Liang Y, Xu C. *Enhanced Antifungal Activity By Ab-Modified Amphotericin B-Loaded Nanoparticles Using A PH-Responsive Block Copolymer*. **Nanoscale Research Letters**. 2015;10(1):256.

83. Goldberg M, Langer R, Jia X. *Nanostructured Materials For Applications In Drug Delivery And Tissue Engineering.* **J Biomat Sci, Polym Ed**. 2007;18:241–68.

84. Khan AA, Mudassir J, Mohtar N, Darwis Y. *Advanced Drug Delivery To The Lymphatic System: Lipid-Based Nanoformulations*. **International Journal Of Nanomedicine**. 2013;8:2733–44.

85. Chiappetta DA, Hocht C, Taira C, Sosnik A. *Oral Pharmacokinetics Of The Anti-HIV Efavirenz Encapsulated Within Polymeric Micelles*. **Biomaterials**. 2011;32(9):2379–87.

86. Khandare J, Minko T. *Polymer-Drug Conjugates: Progress In Polymeric Prodrugs*. **Progress In Polymer Science (Oxford)**. 2006;31(4):359–97.

87. Yin S, Huai J, Chen X, Yang Y, Zhang X, Gan Y, Wang G, Gu X, Li J. *Intracellular Delivery And Antitumor Effects Of A Redox-Responsive Polymeric Paclitaxel Conjugate Based On Hyaluronic Acid*. **Acta Biomaterialia**. 2015;26:274–85.

88. Eldar-Boock A, Blau R, Ryppa C, Baabur-Cohen H, Many A, Vicent MJ, Kratz F, Sanchis J, Satchi-Fainaro R. *Integrin-Targeted Nano-Sized Polymeric Systems For Paclitaxel Conjugation: A Comparative Study*. **Journal Of Drug Targeting**. 2017;25(9–10):829–44.

89. Giammona G, Cavallaro G, Fontana G, Pitarresi G, Carlisi B. *Coupling Of The Antiviral Agent Zidovudine To Polyaspartamide And In Vitro Drug Release Studies*. **Journal Of Controlled Release**. 1998;54(3):321–31.

90. Shukla T, Upmanyu N, Prakash Pandey S, Gosh D. *Lipid Nanocarriers*. Lipid Nanocarriers for Drug Targeting. Elsevier Inc.; 2018. 1–47 p.

91. Makwana V, Jain R, Patel K, Nivsarkar M, Joshi A. *Solid Lipid Nanoparticles (SLN) Of Efavirenz As Lymph Targeting Drug Delivery System: Elucidation Of Mechanism Of Uptake Using Chylomicron Flow Blocking Approach*. **International Journal Of Pharmaceutics**. 2015;495(1):439–46.

92. Prajapati JB, Katariya H, Patel R. *Peyer'e Patch Targeting Of Isradipine Loaded Solid Lipid Nanoparticles: It's Cellular Uptake Study*. **Journal Of Drug Delivery Science And Technology**. 2018;43:318–26.

93. Paliwal R, Rai S, Vaidya B, Khatri K, Goyal AK, Mishra N, Mehta A, Vyas SP. *Effect Of Lipid Core Material On Characteristics Of Solid Lipid Nanoparticles Designed For Oral Lymphatic Delivery*. **Nanomedicine: Nanotechnology, Biology, And Medicine**. 2009;5(2):184–91.

94. Mishra A, Vuddanda PR, Singh S. *Intestinal Lymphatic Delivery Of Praziquantel By Solid Lipid Nanoparticles: Formulation Design, In Vitro And In Vivo Studies*. **Journal Of Nanotechnology**. 2014;2014.

95. Hu L, Tang X, Cui F. *Solid Lipid Nanoparticles (SLNs) To Improve Oral Bioavailability Of Poorly Soluble Drugs*. **Journal Of Pharmacy And Pharmacology**. 2004;56(12):1527–35.
96. Desai J, Thakkar H. *Colloids And Surfaces B : Biointerfaces Enhanced Oral Bioavailability And Brain Uptake Of Darunavir Using Lipid Nanoemulsion Formulation*. **Colloids And Surfaces B: Biointerfaces**. 2019;175:143–9.
97. Neves J, Gomes MJ, das Neves J, Sarmento B. *Nanoparticle-Based Drug Delivery To Improve The Efficacy Of Antiretroviral Therapy In The Central Nervous System*. **International Journal Of Nanomedicine**. 2014;9(1):1757–69.
98. Hiroshi Y, Shozo M, Chiharu K, Hitoshi S. *Bifunctional Delivery System For Selective Transfer Of Bleomycin Into Lymphatics Via Enteral Route*. **International Journal Of Pharmaceutics**. 1981;8(4):291–302.
99. Plapied L, Duhem N, des Rieux A, Préat V. *Fate Of Polymeric Nanocarriers For Oral Drug Delivery*. **Current Opinion In Colloid And Interface Science**. 2011;16(3):228–37.
100. Clares B, Calpena AC, Parra A, Abrego G, Alvarado H, Fangueiro JF, Souto EB. *Nanoemulsions (NEs), Liposomes (LPs) And Solid Lipid Nanoparticles (SLNs) For Retinyl Palmitate : Effect On Skin Permeation*. **International Journal Of Pharmaceutics**. 2014;473(1–2):591–8.
101. Bunjes H. *Lipid Nanoparticles For The Delivery Of Poorly Water-Soluble Drugs*. **Journal Of Pharmacy And Pharmacology**. 2010;62(11):1637–45.
102. Khatak S, Pradesh U. *Solid Lipid Nanoparticles- A Review*. **International Journal Of Applied Pharmaceutics**. 2013;5(2):8–18.
103. Javan F, Vatanara A, Azadmanesh K, Nabi-Meibodi M, shakouri M. *Encapsulation Of Ritonavir In Solid Lipid Nanoparticles: In-Vitro Anti-HIV-1 Activity Using Lentiviral Particles*. **Journal Of Pharmacy And Pharmacology**. 2017;69(8):1002–9.
104. Zununi Vahed S, Salehi R, Davaran S, Sharifi S. *Liposome-Based Drug Co-Delivery Systems In Cancer Cells*. **Materials Science And Engineering C**. 2017;71:1327–41.
105. Alavi M, Karimi N, Safaei M. *Application Of Various Types Of Liposomes In Drug Delivery Systems*. **Advanced Pharmaceutical Bulletin**. 2017;7(1):3–9.
106. Kaur CD, Nahar M, Jain NK. *Lymphatic Targeting Of Zidovudine Using Surface-Engineered Liposomes*. **Journal Of Drug Targeting**. 2008;16(10):798–805.
107. Jin SX, Bi DZ, Wang J, Wang YZ, Hu HG, Deng YH. *Pharmacokinetics And Tissue Distribution Of Zidovudine In Rats Following Intravenous Administration Of*

Zidovudine Myristate Loaded Liposomes. **Pharmazie**. 2005;60(11):840–3.

108. Tapeinos C, Battaglini M, Ciofani G. *Advances In The Design Of Solid Lipid Nanoparticles And Nanostructured Lipid Carriers For Targeting Brain Diseases*. **Journal Of Controlled Release**. 2017;264(August):306–32.
109. Bahari LAS, Hamishehkar H. *The Impact Of Variables On Particle Size Of Solid Lipid Nanoparticles And Nanostructured Lipid Carriers; A Comparative Literature Review*. **Advanced Pharmaceutical Bulletin**. 2016;6(2):143–51.
110. Ganesan P, Narayanasamy D. *Lipid Nanoparticles: Different Preparation Techniques, Characterization, Hurdles, And Strategies For The Production Of Solid Lipid Nanoparticles And Nanostructured Lipid Carriers For Oral Drug Delivery*. **Sustainable Chemistry And Pharmacy**. 2017;6(May):37–56.
111. Mehnert W, Mäder K. *Solid Lipid Nanoparticles: Production, Characterization And Applications*. **Advanced Drug Delivery Reviews**. 2012;64:83–101.
112. Shahgaldian P, Gualbert J, Aïssa K, Coleman AW. *A Study Of The Freeze-Drying Conditions Of Calixarene Based Solid Lipid Nanoparticles*. **European Journal Of Pharmaceutics And Biopharmaceutics**. 2003;55(2):181–4.
113. Souto EB, Mehnert W, Müller RH. *Polymorphic Behaviour Of Compritol??888 ATO As Bulk Lipid And As SLN And NLC*. **Journal Of Microencapsulation**. 2006;23(4):417–33.
114. Aburahma MH, Badr-Eldin SM. *Compritol 888 ATO: A Multifunctional Lipid Excipient In Drug Delivery Systems And Nanopharmaceuticals*. **Expert Opinion On Drug Delivery**. 2014;11(12):1865–83.
115. Almeida AJ, Runge S. *Intemational Journal Of Pharmaceutics Peptide-Loaded Solid Lipid Nanoparticles (SLN): Influence Of Production Parameters*. 1997;149:255–65.
116. Pathak K, Raghuvanshi S. *Oral Bioavailability: Issues And Solutions Via Nanoformulations*. **Clinical Pharmacokinetics**. 2015;54(4):325–57.
117. Kumar S, Dilbaghi N, Saharan R, Bhanjana G. *Nanotechnology As Emerging Tool For Enhancing Solubility Of Poorly Water-Soluble Drugs*. **BioNanoScience**. 2012;2(4):227–50.
118. Mu RH, Runge SA, Ravelli V, Thu AF. *Cyclosporine-Loaded Solid Lipid Nanoparticles (SLN Ò): Drug – Lipid Physicochemical Interactions And Characterization Of Drug Incorporation*. 2008;68:535–44.
119. Chen YC, Liu DZ, Liu JJ, Chang TW, Ho HO, Sheu MT. *Development Of Terbinafine Solid Lipid Nanoparticles As A Topical Delivery System*. **International Journal Of**

Nanomedicine. 2012;7:4409–18.

120. Bondì ML, Craparo EF, Giammona G, Drago F. *Brain-Targeted Solid Lipid Nanoparticles Containing Riluzole: Preparation, Characterization And Biodistribution*. **Nanomedicine**. 2010;5(1):25–32.
121. Bhalekar MR, Upadhaya PG, Madgulkar AR, Kshirsagar SJ, Dube A, Bartakke US. *In-Vivo Bioavailability And Lymphatic Uptake Evaluation Of Lipid Nanoparticulates Of Darunavir*. **Drug Delivery**. 2016;23(7):2581–6.
122. Kumar R, Singh A, Sharma K, Dhasmana D, Garg N, Siril PF. *Preparation, Characterization And In Vitro Cytotoxicity Of Fenofibrate And Nabumetone Loaded Solid Lipid Nanoparticles*. **Materials Science And Engineering: C**. 2020;106:110–84.
123. Nair R, Kumar KSA, Vishnu K, Badivaddin T, Sevukarajan M. *Preparation And Characterization Of Rizatriptan Loaded Solid Lipid Nanoparticles*. **Biomedical Science And Research**. 2011;3(2):392–6.
124. Heiati H, Tawashi R, Phillips NC. *Solid Lipid Nanoparticles As Drug Carriers. II. Plasma Stability And Biodistribution Of Solid Lipid Nanoparticles Containing The Lipophilic Prodrug 3'-Azido-3'-Deoxythymidine Palmitate In Mice*. **International Journal Of Pharmaceutics**. 1998;174(1–2):71–80.
125. Negi JS, Chattopadhyay P, Sharma AK, Ram V. *Development And Evaluation Of Glyceryl Behenate Based Solid Lipid Nanoparticles (SLNs) Using Hot Self-Nanoemulsification (SNE) Technique*. **Archives Of Pharmacal Research**. 2014;37(3):361–70.
126. Chattopadhyay N, Zastre J, Wong HL, Wu XY, Bendayan R. *Solid Lipid Nanoparticles Enhance The Delivery Of The HIV Protease Inhibitor, Atazanavir, By A Human Brain Endothelial Cell Line*. **Pharmaceutical Research**. 2008;25(10):2262–71.
127. Ansari H, Singh P. *Formulation And In-Vivo Evaluation Of Novel Topical Gel Of Lopinavir For Targeting HIV*. **Current HIV Research**. 2018;16(4):270–9.
128. Desai J, Thakkar H. *Darunavir-Loaded Lipid Nanoparticles For Targeting To HIV Reservoirs*. **AAPS PharmSciTech**. 2018;19(2):648–60.
129. Bhalekar M, Upadhaya P, Madgulkar A. *Formulation And Characterization Of Solid Lipid Nanoparticles For An Anti-Retroviral Drug Darunavir*. **Applied Nanoscience (Switzerland)**. 2017;7(1–2):47–57.
130. Ravi PR, Vats R, Dalal V, Murthy AN. *A Hybrid Design To Optimize Preparation Of Lopinavir Loaded Solid Lipid Nanoparticles And Comparative Pharmacokinetic Evaluation With Marketed Lopinavir/Ritonavir Coformulation*. **Journal Of Pharmacy**

And Pharmacology. 2014;66(7):912–26.

131. Savardekar P, Bajaj A. *Nanoemulsions- A Review*. **International Journal Of Research In Pharmacy And Chemistry**. 2016;6(2):312–22.
132. Chaudhari MB, Desai PP, Patel PA, Patravale VB. *Solid Lipid Nanoparticles Of Amphotericin B (AmbiOnp): In Vitro And In Vivo Assessment Towards Safe And Effective Oral Treatment Module*. **Drug Delivery And Translational Research**. 2016;6(4):354–64.
133. Madhav PB and S. *A Detailed Review On Nanoemulsion Drug Delivery System*. **International Journal Of Pharmaceutical Sciences And Research**. 2011;2(10):2482–9.
134. Donsì F, Annunziata M, Vincensi M, Ferrari G. *Design Of Nanoemulsion-Based Delivery Systems Of Natural Antimicrobials : Effect Of The Emulsifier*. **Journal Of Biotechnology**. 2012;159(4):342–50.
135. Guttoff M, Saberi AH, McClements DJ. *Formation Of Vitamin D Nanoemulsion-Based Delivery Systems By Spontaneous Emulsification: Factors Affecting Particle Size And Stability*. **Food Chemistry**. 2015;171:117–22.
136. Saberi AH, Fang Y, Mcclements DJ. *Journal Of Colloid And Interface Science Fabrication Of Vitamin E-Enriched Nanoemulsions : Factors Affecting Particle Size Using Spontaneous Emulsification*. **Journal Of Colloid And Interface Science**. 2013;391:95–102.
137. Mou D, Chen H, Du D, Mao C, Wan J, Xu H, Yang X. *Hydrogel-Thickened Nanoemulsion System For Topical Delivery Of Lipophilic Drugs*. **International Journal Of Pharmaceutics**. 2008;353(1–2):270–6.
138. Majeed H, Antoniou J, Hategekimana J, Sharif HR, Haider J, Liu F, Ali B, Rong L, Ma J, Zhong F. *Influence Of Carrier Oil Type, Particle Size On In Vitro Lipid Digestion And Eugenol Release In Emulsion And Nanoemulsions*. **Food Hydrocolloids**. 2016;52:415–22.
139. Hsu J, Nacu A. *Behavior Of Soybean Oil-In-Water Emulsion Stabilized By Nonionic Surfactant*. **Journal Of Colloid And Interface Science**. 2003;259(2):374–81.
140. Adamczak M, Para G, Simon C, Warszyński P. *Natural Oil Nanoemulsions As Cores For Layer-By-Layer Encapsulation*. **Journal Of Microencapsulation**. 2013;30(5):479–89.
141. faheim samar, Gardouh A, Nouh A, Ghorab M. *Review Article On Nanoemulsions And Nanostructured Lipid Carriers*. **Records Of Pharmaceutical And Biomedical**

Sciences. 2018;2(2):23–31.

142. Kumar M, Bishnoi RS, Shukla AK, Jain CP. *Techniques For Formulation Of Nanoemulsion Drug Delivery System: A Review*. **Preventive Nutrition And Food Science**. 2019;24(3):225–34.
143. Vyas TK, Shahiwala A, Amiji MM. *Improved Oral Bioavailability And Brain Transport Of Saquinavir Upon Administration In Novel Nanoemulsion Formulations*. **International Journal Of Pharmaceutics**. 2008;347(1–2):93–101.
144. Singh G, Pai RS. *Optimized Self-Nanoemulsifying Drug Delivery System Of Atazanavir With Enhanced Oral Bioavailability: In Vitro/In Vivo Characterization*. **Expert Opinion On Drug Delivery**. 2014;11(7):1023–32.
145. Zhang J, Fan Y, Smith E. *Experimental Design For The Optimization Of Lipid Nanoparticles*. **Journal Of Pharmaceutical Sciences**. 2009;98(5):1813–9.
146. Anantaworasakul P, Chaiyana W, Michniak-Kohn BB, Rungseevijitprapa W, Ampasavate C. *Enhanced Transdermal Delivery Of Concentrated Capsaicin From Chili Extract-Loaded Lipid Nanoparticles With Reduced Skin Irritation*. **Pharmaceutics**. 2020;12(5):463.
147. Mitrea E, Ott C, Meghea A, Biofarm SA. *New Approaches On The Synthesis Of Effective Nanostructured Lipid Carriers*. **Revista De Chimie**. 2014;65(1):50–5.
148. Kasongo KW, Müller RH, Walker RB. *The Use Of Hot And Cold High Pressure homogenisation To Enhance The Loading Capacity And Encapsulation Efficiency Of Nanostructured Lipid Carriers For The Hydrophilic Antiretroviral Drug, Didanosine For Potential Administration To Paediatric Patients*. **Pharmaceutical Development And Technology**. 2012;17(3):353–62.
149. Hu F, Jiang S, Du Y, Yuan H, Ye Y, Zeng S. *Preparation And Characterization Of Stearic Acid Nanostructured Lipid Carriers By Solvent Diffusion Method In An Aqueous System*. **Colloids And Surfaces B: Biointerfaces**. 2005;45(3–4):167–73.
150. Kumbhar DD, Pokharkar VB. *Engineering Of A Nanostructured Lipid Carrier For The Poorly Water-Soluble Drug, Bicalutamide: Physicochemical Investigations*. **Colloids And Surfaces A: Physicochemical And Engineering Aspects**. 2013;416(1):32–42.
151. Poonia N, Kaur J, Lather V, Beg S, Sharma T. *Colloids And Surfaces B : Biointerfaces Resveratrol Loaded Functionalized Nanostructured Lipid Carriers For Breast Cancer Targeting : Systematic Development , Characterization And Pharmacokinetic Evaluation*. **Colloids And Surfaces B: Biointerfaces**. 2019;181(June):756–66.
152. Khurana S, Bedi PMS, Jain NK. *Development Of Nanostructured Lipid Carriers For*

Controlled Delivery Of Mefenamic Acid. **International Journal Of Biomedical Nanoscience And Nanotechnology**. 2012;2(3–4):232–50.

153. Kaithwas V, Parkash C, Kushwah V, Jain S. *Colloids And Surfaces B : Biointerfaces Nanostructured Lipid Carriers Of Olmesartan Medoxomil With Enhanced Oral Bioavailability*. **Colloids And Surfaces B: Biointerfaces**. 2017;154:10–20.
154. Garg B, Beg S, Kumar R, Katare OP, Singh B. *Nanostructured Lipidic Carriers Of Lopinavir For Effective Management Of HIV-Associated Neurocognitive Disorder*. **Journal Of Drug Delivery Science And Technology**. 2019;53(April):101–220.
155. Walimbe CA, More SS, Walawalkar RU, Shah RR, Ghodake D. *Optimisation Of Nanostructured Lipid Carriers Of Ritonavir*. **Inventi Rapid: NDDS**. 2012;(4):4–11.
156. Hadinoto K, Sundaresan A, Cheow WS. *European Journal Of Pharmaceutics And Biopharmaceutics Lipid – Polymer Hybrid Nanoparticles As A New Generation Therapeutic Delivery Platform : A Review*. **European Journal Of Pharmaceutics And Biopharmaceutics**. 2013;85(3):427–43.
157. Mandal B, Bhattacharjee H, Mittal N, Sah H, Balabathula P, Thoma LA, Wood GC. *Core – Shell-Type Lipid – Polymer Hybrid Nanoparticles As A Drug Delivery Platform*. **Nanomedicine: Nanotechnology, Biology, And Medicine**. 2013;9(4):474–91.
158. Yu F, Ao M, Zheng X, Li N, Xia J, Li Y, Li D, Hou Z, Qi Z, Chen XD. *PEG–Lipid–PLGA Hybrid Nanoparticles Loaded With Berberine–Phospholipid Complex To Facilitate The Oral Delivery Efficiency*. **Drug Delivery**. 2017;24(1):825–33.
159. Li Q, Cai T, Huang Y, Xia X, Cole S, Cai Y. *A Review Of The Structure, Preparation, And Application Of NLCs, PNPs, And PLNs*. **Nanomaterials**. 2017;7(6):122.
160. Zhang L, Chan JM, Gu FX, Rhee J, Wang AZ, Radovic-Moreno AF, Alexis F, Langer R, Farokhzad OC. *Self-Assembled Lipid−Polymer Hybrid Nanoparticles: A Robust Drug Delivery Platform*. **ACS Nano**. 2008;2(8):1696–702.
161. Jin X, Zhang ZH, Sun E, Tan X Bin, Zhu FX, Li SL, Jia X Bin. *Preparation Of Icariside II-Phospholipid Complex And Its Absorption Across Caco-2 Cell Monolayers*. **Pharmazie**. 2012;67(4):293–8.
162. Su C, Liu J, Ho Y, Huang Y, Chang VH, Liu D-Z, Chen L-C, Ho H-O, Sheu M-T. *Development And Characterization Of Docetaxel-Loaded Lecithin-Stabilized Micellar Drug Delivery System (L Sb MDDs) For Improving The Therapeutic Efficacy And Reducing Systemic Toxicity*. **European Journal Of Pharmaceutics And Biopharmaceutics**. 2018;123(November 2017):9–19.
163. Chen LC, Chen YC, Su CY, Wong WP, Sheu MT, Ho HO. *Development And*

Characterization Of Lecithin-Based Self-Assembling Mixed Polymeric Micellar (SaMPMs) Drug Delivery Systems For Curcumin. **Scientific Reports**. 2016;6(1):37122.

164. Li J, Wang X, Zhang T, Wang C, Huang Z, Luo X, Deng Y. *A Review On Phospholipids And Their Main Applications In Drug Delivery Systems*. **Asian Journal Of Pharmaceutical Sciences**. 2015;10(2):81–98.
165. Chan JM, Zhang L, Yuet KP, Liao G, Rhee J, Langer R, Farokhzad OC. *Biomaterials PLGA – Lecithin – PEG Core – Shell Nanoparticles For Controlled Drug Delivery*. **Biomaterials**. 2009;30(8):1627–34.
166. Zhang L, Zhang L. *Lipid–Polymer Hybrid Nanoparticles: Synthesis, Characterization And Applications*. **Nano Life**. 2010;01(01n02):163–73.
167. Dalmoro A, Bochicchio S, Nasibullin SF, Bertoncin P, Lamberti G, Barba AA, Moustafine RI. *Polymer-Lipid Hybrid Nanoparticles As Enhanced Indomethacin Delivery Systems*. **European Journal Of Pharmaceutical Sciences**. 2018;121(December 2017):16–28.
168. Gao J, Xia Y, Chen H, Yu Y, Song J, Li W, Qian W, Wang H, Dai J, Guo Y. *Polymer–Lipid Hybrid Nanoparticles Conjugated With Anti-EGF Receptor Antibody For Targeted Drug Delivery To Hepatocellular Carcinoma*. **Nanomedicine**. 2014;9(2):279–93.
169. Jadon RS, Sharma M. *Journal Of Drug Delivery Science And Technology Docetaxel-Loaded Lipid-Polymer Hybrid Nanoparticles For Breast Cancer Therapeutics*. **Journal Of Drug Delivery Science And Technology**. 2019;51(March):475–84.
170. Cheow WS, Hadinoto K. *Colloids And Surfaces B : Biointerfaces Factors Affecting Drug Encapsulation And Stability Of Lipid – Polymer Hybrid Nanoparticles*. **Colloids And Surfaces B: Biointerfaces**. 2011;85(2):214–20.
171. Gajra B, Dalwadi C, Patel R. *Formulation And Optimization Of Itraconazole Polymeric Lipid Hybrid Nanoparticles (Lipomer) Using Box Behnken Design*. **DARU Journal Of Pharmaceutical Sciences**. 2015;23(1):1–15.
172. Hu CJ, Kaushal S, Cao HST, Aryal S, Sartor M, Esener S, Bouvet M, Zhang L. *Half-Antibody Functionalized Lipid−Polymer Hybrid Nanoparticles For Targeted Drug Delivery To Carcinoembryonic Antigen Presenting Pancreatic Cancer Cells*. **Molecular Pharmaceutics**. 2010;7(3):914–20.
173. Dong W, Wang X, Liu C, Zhang X, Zhang X, Chen X, Kou Y, Mao S. *Chitosan Based Polymer-Lipid Hybrid Nanoparticles For Oral Delivery Of Enoxaparin*. **International Journal Of Pharmaceutics**. 2018;547(1–2):499–505.

174. Yalcin TE, Ilbasmis-tamer S, Takka S. *Development And Characterization Of Gemcitabine Hydrochloride Loaded Lipid Polymer Hybrid Nanoparticles (LPHNs) Using Central Composite Design*. **International Journal Of Pharmaceutics**. 2018;548(1):255–62.

175. Leng D, Thanki K, Fattal E, Foged C, Yang M. *Engineering Of Budesonide-Loaded Lipid-Polymer Hybrid Nanoparticles Using A Quality-By-Design Approach*. **International Journal Of Pharmaceutics**. 2018;548(2):740–6.

176. Liu D, Jiang S, Shen H, Qin S, Liu J, Zhang Q, Li R, Xu Q. *Diclofenac Sodium-Loaded Solid Lipid Nanoparticles Prepared By Emulsion/Solvent Evaporation Method*. **Journal Of Nanoparticle Research**. 2011;13(6):2375–86.

177. Boonme P, Souto EB, Wuttisantikul N, Jongjit T, Pichayakorn W. *Influence Of Lipids On The Properties Of Solid Lipid Nanoparticles From Microemulsion Technique*. **European Journal Of Lipid Science And Technology**. 2013;115(7):820–4.

178. Li W, Li H, Yao H, Mu Q, Zhao G, Li Y, Hu H, Niu X. *Pharmacokinetic And Anti-Inflammatory Effects Of Sanguinarine Solid Lipid Nanoparticles*. **Inflammation**. 2014;37(2):632–8.

179. Schubert M. *Solvent Injection As A New Approach For Manufacturing Lipid Nanoparticles – Evaluation Of The Method And Process Parameters*. **European Journal Of Pharmaceutics And Biopharmaceutics**. 2003;55(1):125–31.

180. Dave V, Tak K, Sohgaura A, Gupta A, Sadhu V, Reddy KR. *Lipid-Polymer Hybrid Nanoparticles: Synthesis Strategies And Biomedical Applications*. **Journal Of Microbiological Methods**. 2019;160(January):130–42.

181. Ferreira Soares DC, Domingues SC, Viana DB, Tebaldi ML. *Polymer-Hybrid Nanoparticles: Current Advances In Biomedical Applications*. **Biomedicine & Pharmacotherapy**. 2020;131(September):110–695.

182. Kathe N, Henriksen B, Chauhan H. *Physicochemical Characterization Techniques For Solid Lipid Nanoparticles: Principles And Limitations.* **Drug Development And Industrial Pharmacy**. 2014;9045(12):1–11.

183. Martínez Rivas CJ, Tarhini M, Badri W, Miladi K, Greige-Gerges H, Nazari QA, Galindo Rodríguez SA, Román RÁ, Fessi H, Elaissari A. *Nanoprecipitation Process: From Encapsulation To Drug Delivery*. **International Journal Of Pharmaceutics**. 2017;532(1):66–81.

184. Dong Y, Ng WK, Shen S, Kim S, Tan RBH. *Solid Lipid Nanoparticles: Continuous And Potential Large-Scale Nanoprecipitation Production In Static Mixers*. **Colloids And**

Surfaces B: Biointerfaces. 2012;94:68–72.

185. Kelmann RG, Kuminek G, Teixeira HF, Koester LS. *Carbamazepine Parenteral Nanoemulsions Prepared By Spontaneous Emulsification Process*. **International Journal Of Pharmaceutics**. 2007;342(1–2):231–9.
186. Mukherjee A, Waters AK, Kalyan P, Achrol AS, Kesari S, Yenugonda VM. *Lipid–Polymer Hybrid Nanoparticles As A Next-Generation Drug Delivery Platform: State Of The Art, Emerging Technologies, And Perspectives*. **International Journal Of Nanomedicine**. 2019;Volume 14:1937–52.
187. Shah M, Pathak K. *Development And Statistical Optimization Of Solid Lipid Nanoparticles Of Simvastatin By Using 23 Full-Factorial Design*. **AAPS PharmSciTech**. 2010;11(2):489–96.
188. Agrawal U, Gupta M, Vyas SP. *Capsaicin Delivery Into The Skin With Lipidic Nanoparticles For The Treatment Of Psoriasis*. **Artificial Cells, Nanomedicine, And Biotechnology**. 2015;43(1):33–9.
189. Jain A, Mehra NK, Nahar M, Jain NK. *Topical Delivery Of Enoxaparin Using Nanostructured Lipid Carrier*. **Journal Of Microencapsulation**. 2013;30(7):709–15.
190. Elkateb H, Tatham LM, Cauldbeck H, Niezabitowska E, Owen A, Rannard S, McDonald T. *Optimization Of The Synthetic Parameters Of Lipid Polymer Hybrid Nanoparticles Dual Loaded With Darunavir And Ritonavir For The Treatment Of HIV*. **International Journal Of Pharmaceutics**. 2020;588(August):119–794.
191. Zillies JC, Zwiorek K, Hoffmann F, Vollmar A, Anchordoquy TJ, Winter G, Coester C. *Formulation Development Of Freeze-Dried Oligonucleotide-Loaded Gelatin Nanoparticles*. **European Journal Of Pharmaceutics And Biopharmaceutics**. 2008;70(2):514–21.
192. Umerska A, Paluch KJ, Santos-Martinez MJ, Corrigan OI, Medina C, Tajber L. *Freeze Drying Of Polyelectrolyte Complex Nanoparticles: Effect Of Nanoparticle Composition And Cryoprotectant Selection*. **International Journal Of Pharmaceutics**. 2018;552(1–2):27–38.
193. Beirowski J, Inghelbrecht S, Arien A, Gieseler H. *Freeze-Drying Of Nanosuspensions, 1: Freezing Rate Versus Formulation Design As Critical Factors To Preserve The Original Particle Size Distribution*. **Journal Of Pharmaceutical Sciences**. 2011;100(5):1958–68.
194. Wang L, Ma Y, Gu Y, Liu Y, Zhao J, Yan B, Wang Y. *Cryoprotectant Choice And Analyze Of Freeze-Drying Drug Suspension Of Nanoparticles With Functional*

Stabilizers. **Journal Of Microencapsulation**. 2018;2048:1–26.

195. Malamatari M, Charisi A, Malamataris S, Kachrimanis K, Nikolakakis I. *Spray Drying For The Preparation Of Nanoparticle-Based Drug Formulations As Dry Powders For Inhalation*. **Processes**. 2020;8(7):788.
196. Sosnik A, Seremeta KP. *Advantages And Challenges Of The Spray-Drying Technology For The Production Of Pure Drug Particles And Drug-Loaded Polymeric Carriers*. **Advances In Colloid And Interface Science**. 2015;223:40–54.
197. Abdelwahed W, Degobert G, Stainmesse S, Fessi H. *Freeze-Drying Of Nanoparticles: Formulation, Process And Storage Considerations*. **Advanced Drug Delivery Reviews**. 2006;58(15):1688–713.
198. Marengo E, Cavalli R, Rovero G, Gasco MR. *Scale-Up And Optimization Of An Evaporative Drying Process Applied To Aqueous Dispersions Of Solid Lipid Nanoparticles*. **Pharmaceutical Development And Technology**. 2003;8(3):299–309.
199. Franks F. *Freeze-Drying Of Bioproducts: Putting Principles Into Practice*. **European Journal Of Pharmaceutics And Biopharmaceutics**. 1998;45(3):221–9.
200. Van Den Hoven JM, Metselaar JM, Storm G, Beijnen JH, Nuijen B. *Cyclodextrin As Membrane Protectant In Spray-Drying And Freeze-Drying Of PEGylated Liposomes*. **International Journal Of Pharmaceutics**. 2012;438(1–2):209–16.
201. Varshosaz J, Eskandari S, Tabbakhian M. *Freeze-Drying Of Nanostructure Lipid Carriers By Different Carbohydrate Polymers Used As Cryoprotectants*. **Carbohydrate Polymers**. 2012;88(4):1157–63.
202. Nireesha GR, Divya L, Sowmya C, Venkateshan N, Babu MN, Lavakumar V. *Lyophilization / Freeze Drying - An Review*. **International Journal Of Novel Trends In Pharmaceutical Sciences**. 2013;3(4):87–98.
203. Scoffin K. *Designing Trouble-Free Freeze-Drying Processes*. **Pharmaceutical Technology**. 2015;39(4):78–9.
204. David M. *Lyophilization*. **Journal Of GXP Compliance**. 2010;14(4):52.
205. Moretton MA, Chiappetta DA, Sosnik A. *Cryoprotection-Lyophilization And Physical Stabilization Of Rifampicin-Loaded Flower-Like Polymeric Micelles*. **Journal Of The Royal Society Interface**. 2012;9(68):487–502.
206. Ghaffari S, Varshosaz J, Saadat A, Atyabi F. *Stability And Antimicrobial Effect Of Amikacin-Loaded Solid Lipid Nanoparticles*. **International Journal Of Nanomedicine**. 2011;6(1):35–43.
207. Lim SJ, Kim CK. *Formulation Parameters Determining The Physicochemical*

Characteristics Of Solid Lipid Nanoparticles Loaded With All-Trans Retinoic Acid. **International Journal Of Pharmaceutics**. 2002;243(1–2):135–46.

208. Date P V., Samad A, Devarajan P V. *Freeze Thaw: A Simple Approach For Prediction Of Optimal Cryoprotectant For Freeze Drying*. **AAPS PharmSciTech**. 2010;11(1):304–13.
209. Varshosaz J, Ghaffari S, Khoshayand MR, Atyabi F, Dehkordi AJ, Kobarfard F. *Optimization Of Freeze-Drying Condition Of Amikacin Solid Lipid Nanoparticles Using D-Optimal Experimental Design*. **Pharmaceutical Development And Technology**. 2012;17(2):187–94.
210. Pozo-rodríguez A, Solinís MA, Gascón AR, Pedraz JL. *European Journal Of Pharmaceutics And Biopharmaceutics Short- And Long-Term Stability Study Of Lyophilized Solid Lipid Nanoparticles For Gene Therapy*. **European Journal Of Pharmaceutics And Biopharmaceutics**. 2009;71(2):181–9.
211. Li Y, Ma Q, Huang C, Liu G. *crystallisation Of Poly (Ethylene Glycol) In Poly (Methyl Methacrylate) Networks*. **Medziagotyra**. 2013;19(2):147–51.
212. Zhao S, Yang X, Garamus VM, Handge UA, Bérengère L, Zhao L, Salamon G, Willumeit R, Zou A, Fan S. *Mixture Of Nonionic/Ionic Surfactants For The Formulation Of Nanostructured Lipid Carriers: Effects On Physical Properties*. **Langmuir**. 2014;30(23):6920–8.
213. Aditya NP, Macedo AS, Doktorovova S, Souto EB, Kim S, Chang P, Ko S. *Development And Evaluation Of Lipid Nanocarriers For Quercetin Delivery: A Comparative Study Of Solid Lipid Nanoparticles (SLN), Nanostructured Lipid Carriers (NLC), And Lipid Nanoemulsions (LNE)*. **LWT - Food Science And Technology**. 2014;59(1):115–21.
214. Gönüllü Ü, Üner M, Yener G, Karaman EF, Aydoğmuş Z. *Formulation And Characterization Of Solid Lipid Nanoparticles, Nanostructured Lipid Carriers And Nanoemulsion Of Lornoxicam For Transdermal Delivery*. **Acta Pharmaceutica**. 2015;65(1):1–13.
215. Zhang Z, Feng S. *In Vitro Investigation On Poly(Lactide)−Tween 80 Copolymer Nanoparticles Fabricated By Dialysis Method For Chemotherapy*. **Biomacromolecules**. 2006;7(4):1139–46.
216. Cauldbeck H, Le Hellaye M, Long M, Kennedy SM, Williams RL, Kearns VR, Rannard SP. *Controlling Drug Release From Non-Aqueous Environments: Moderating Delivery From Ocular Silicone Oil Drug Reservoirs To Combat Proliferative Vitreoretinopathy*. **Journal Of Controlled Release**. 2016;244:41–51.

217. Troncoso E, Aguilera JM, McClements DJ. *Development Of Nanoemulsions By An Emulsification-Evaporation Technique*. **Food Process Engineering In A Changing World Proceedings Of The 11th International Congress On Engineering And Food, May 22-26, 2011, Athens, Greece**. 2011;(January 2011):929–30.
218. Vitorino C, Carvalho FA, Almeida AJ, Sousa JJ, Pais AACC. *Colloids And Surfaces B : Biointerfaces The Size Of Solid Lipid Nanoparticles : An Interpretation From Experimental Design*. **Colloids And Surfaces B: Biointerfaces**. 2011;84(1):117–30.
219. Joseph S, Bunjes H. *Preparation Of Nanoemulsions And Solid Lipid Nanoparticles By Premix Membrane Emulsification*. **Journal Of Pharmaceutical Sciences**. 2012;101(7):2479–89.
220. Zielińska A, Ferreira NR, Feliczak-guzik A, Souto EB. *Loading , Release Profile And Accelerated Stability Assessment Of Monoterpenes-Loaded Solid Lipid Nanoparticles (SLN)*. **Pharmaceutical Development And Technology**. 2020;0(0):1–13.
221. Mehnert W, Mader K. *Solid Lipid Nanoparticles Production, Characterization And Applications*. **Advanced Drug Delivery Reviews**. 2001;47(2–3):165–96.
222. Helgason T, Awad TS, Kristbergsson K, Mcclements DJ, Weiss J. *Journal Of Colloid And Interface Science Effect Of Surfactant Surface Coverage On Formation Of Solid Lipid Nanoparticles (SLN)*. **Journal Of Colloid And Interface Science**. 2009;334(1):75–81.
223. Zimmermann E. *Electrolyte- And PH-Stabilities Of Aqueous Solid Lipid Nanoparticle (SLN^{TM}) Dispersions In Artificial Gastrointestinal Media*. **European Journal Of Pharmaceutics And Biopharmaceutics**. 2001;52(2):203–10.
224. Jores K, Haberland A, Wartewig S, Mäder K, Mehnert W. *Solid Lipid Nanoparticles (SLN) And Oil-Loaded SLN Studied By Spectrofluorometry And Raman Spectroscopy*. **Pharmaceutical Research**. 2005;22(11):1887–97.
225. Gonzalez-mira E, Egea MA, Garcia ML, Souto EB. *Colloids And Surfaces B : Biointerfaces Design And Ocular Tolerance Of Flurbiprofen Loaded Ultrasound-Engineered NLC*. **Colloids And Surfaces B: Biointerfaces**. 2010;81(2):412–21.
226. Jores K, Mehnert W, Drechsler M, Bunjes H, Johann C, Mäder K. *Investigations On The Structure Of Solid Lipid Nanoparticles (SLN) And Oil-Loaded Solid Lipid Nanoparticles By Photon Correlation Spectroscopy, Field-Flow Fractionation And Transmission Electron Microscopy*. **Journal Of Controlled Release**. 2004;95(2):217–27.
227. Muhamad II, Quin CH, Selvakumaran S. *Preparation And Evaluation Of Water-In-Soybean Oil – In-Water Emulsions By Repeated Premix Membrane Emulsification*

Method Using Cellulose Acetate Membrane. **Journal Of Food Science And Technology**. 2016;53(April):1845–55.

228. Rp T, Cr P, Gannu R, Mudragada S, Vl H, Srwhqwldo HWD, Hqwudsphqw G, Flhqf HI, Lq DQG, Guxj Y, Ehkdylru U, Das S, Kiong W, Kanaujia P, Kim S, Tan RBH, Kovacevic A, Savic S, Vuleta G, Müller RH, Keck CM, Kim B, Na K, Choi H, Vitorino C, Carvalho FA, Almeida AJ, Sousa JJ, Pais AACC. *Colloids And Surfaces B : Biointerfaces Formulation Design , Preparation And Physicochemical Characterizations Of Solid Lipid Nanoparticles Containing A Hydrophobic Drug : Effects Of Process Variables*. **Colloids And Surfaces B: Biointerfaces**. 2011;24(1):199–205.
229. Klang V, Matsko NB, Valenta C, Hofer F. *Electron Microscopy Of Nanoemulsions: An Essential Tool For Characterisation And Stability Assessment*. **Micron**. 2012;43(2–3):85–103.
230. Kong Y, Hay JN. *The Enthalpy Of Fusion And Degree Of Crystallinity Of Polymers As Measured By DSC*. **European Polymer Journal**. 2003;39(8):1721–7.
231. Hou DZ, Xie CS, Huang KJ, Zhu CH. *The Production And Characteristics Of Solid Lipid Nanoparticles (SLNs)*. **Biomaterials**. 2003;24(10):1781–5.
232. Peng Y, Lu X, Liu B, Zhu J. *Separation Of Azeotropic Mixtures (Ethanol And Water) Enhanced By Deep Eutectic Solvents*. **Fluid Phase Equilibria**. 2017;448:128–34.
233. Ribeiro MENP, Moura CL De, Vieira MGS, Gramosa N V, Chaibundit C, Mattos MC De, Attwood D, Yeates SG, Nixon SK, Ricardo NMPS. *Solubilisation Capacity Of Brij Surfactants*. **International Journal Of Pharmaceutics**. 2012;436(1–2):631–5.
234. Kovacevic A, Savic S, Vuleta G, Müller RH, Keck CM. *Polyhydroxy Surfactants For The Formulation Of Lipid Nanoparticles (SLN And NLC): Effects On Size , Physical Stability And Particle Matrix Structure*. **International Journal Of Pharmaceutics**. 2011;406(1–2):163–72.
235. Zhang JQ, Liu J, Li XL, Jasti BR. *Preparation And Characterization Of Solid Lipid Nanoparticles Containing Silibinin*. **Drug Delivery**. 2007;14(6):381–7.
236. Jenning V, Gohla S. *Comparison Of Wax And Glyceride Solid Lipid Nanoparticles (SLN®)*. **International Journal Of Pharmaceutics**. 2000;196(2):219–22.
237. Subedi RK, Kang KW, Choi H. *Preparation And Characterization Of Solid Lipid Nanoparticles Loaded With Doxorubicin*. **European Journal Of Pharmaceutical Sciences**. 2009;37(3–4):508–13.
238. Jensen LB, Magnussson E, Gunnarsson L, Vermehren C, Nielsen HM, Petersson K.

Corticosteroid Solubility And Lipid Polarity Control Release From Solid Lipid Nanoparticles. **International Journal Of Pharmaceutics**. 2010;390(1):53–60.

239. Yassin AE, Ibrahim W, Al-Omrani A. *Novel Sulpiride-Loaded Solid Lipid Nanoparticles With Enhanced Intestinal Permeability*. **International Journal Of Nanomedicine**. 2013;20:129–44.
240. Silva AC, González-mira E, García ML, Egea MA, Fonseca J, Silva R, Santos D, Souto EB, Ferreira D. *Colloids And Surfaces B : Biointerfaces Preparation , Characterization And Biocompatibility Studies On Risperidone-Loaded Solid Lipid Nanoparticles (SLN): High Pressure homogenisation Versus Ultrasound*. **Colloids And Surfaces B: Biointerfaces**. 2011;86(1):158–65.
241. Dudhipala N, Veerabrahma K. *Candesartan Cilexetil Loaded Solid Lipid Nanoparticles For Oral Delivery: Characterization, Pharmacokinetic And Pharmacodynamic Evaluation*. **Drug Delivery**. 2016;23(2):395–404.
242. Souto EB, Doktorovova S, Zielinska A, Amélia M. *Key Production Parameters For The Development Of Solid Lipid Nanoparticles By High Shear homogenisation*. **Pharmaceutical Development And Technology**. 2019;24(9):1181–5.
243. Rehman M, Madni A, Khan WS, Ihsan A, Khan MI, Mahmood MA, Ashfaq M, Bajwa SZ, Shakir I. *Solid And Liquid Lipid-Based Binary Solid Lipid Nanoparticles Of Diacerein: In Vitro Evaluation Of Sustained Release, Simultaneous Loading Of Gold Nanoparticles, And Potential Thermoresponsive Behavior*. **International Journal Of Nanomedicine**. 2015;10(4):2805–28.
244. Abdelbary G, Fahmy RH. *Diazepam-Loaded Solid Lipid Nanoparticles: Design And Characterization*. **AAPS PharmSciTech**. 2009;10(1):211–9.
245. Surender V, Deepika M. *Solid Lipid Nanoparticles : A Comprehensive Review*. **Journal Of Chemical And Pharmaceutical Research**. 2016;8(8):102–14.
246. Shah R, Eldridge D, Palombo E, Harding I. *Optimisation And Stability Assessment Of Solid Lipid Nanoparticles Using Particle Size And Zeta Potential*. **Journal Of Physical Science**. 2014;25(1):59–75.
247. Dhawan S, Kapil R, Singh B. *Formulation Development And Systematic Optimization Of Solid Lipid Nanoparticles Of Quercetin For Improved Brain Delivery*. **Journal Of Pharmacy And Pharmacology**. 2011;63(3):342–51.
248. Hatton FL, Chambon P, Savage AC, Rannard SP. *Role Of Highly Branched, High Molecular Weight Polymer Structures In Directing Uniform Polymer Particle Formation During Nanoprecipitation*. **Chemical Communications**.

2016;52(20):3915–8.

249. Ambade A V., Kumar A. *Controlling The Degree Of Branching In Vinyl polymerisation* . **Progress In Polymer Science (Oxford)**. 2000;25(8):1141–70.
250. Matyjaszewski K. *Atom Transfer Radical polymerisation (ATRP): Current Status And Future Perspectives*. **Macromolecules**. 2012;45(10):4015–39.
251. Matyjaszewski K, Xia J. *Atom Transfer Radical polymerisation* . **Chemical Reviews**. 2001;101(9):2921–90.
252. Maçon ALB, Rehman SU, Bell R V., Weaver JVM. *Reversible Assembly Of PH Responsive Branched Copolymer-Stabilised Emulsion Via Electrostatic Forces*. **Chemical Communications**. 2016;52(1):136–9.
253. Hou C, Lin S, Liu F, Hu J, Zhang G, Liu G, Tu Y, Zou H, Luo H. *Synthesis Of Poly(2-Hydroxyethyl Methacrylate) End-Capped With Asymmetric Functional Groups Via Atom Transfer Radical polymerisation* . **New Journal Of Chemistry**. 2014;38(6):2538.
254. Omir MK. *Preparation And Characterisation Of Maraviroc Loaded SLNs Stabilised With Branched Copolymers* [Https://livrepository.liverpool.ac.uk/id/eprint/3019044]. 2017.
255. Matyjaszewski K, Xia J. *Atom Transfer Radical polymerisation* . **Chemical Reviews**. 2001;101(9):2921–90.
256. Hou C, Lin S, Liu F, Hu J, Zhang G, Liu G, Tu Y, Zou H, Luo H. *Synthesis Of Poly(2-Hydroxyethyl Methacrylate) End-Capped With Asymmetric Functional Groups Via Atom Transfer Radical polymerisation* . **New Journal Of Chemistry**. 2014;38(6):2538–47.
257. Li Y, Armes SP. *Synthesis And Chemical Degradation Of Branched Vinyl Polymers Prepared Via ATRP: Use Of A Cleavable Disulfide-Based Branching Agent*. **Macromolecules**. 2005;38(20):8155–62.
258. Dwyer AB, Chambon P, Town A, He T, Owen A, Rannard SP. *Is Methanol Really A Bad Solvent For Poly(N-Butyl Methacrylate)? Low Dispersity And High Molecular Weight Polymers Of N-Butyl Methacrylate Synthesised Via ATRP In Anhydrous Methanol*. **Polym Chem**. 2014;5(11):3608–16.
259. He T, Adams DJ, Butler MF, Yeoh CT, Cooper AI, Rannard SP. *Direct Synthesis Of Anisotropic Polymer Nanoparticles*. **Angewandte Chemie International Edition**. 2007;46(48):9243–7.
260. Hobson JJ, Edwards S, Slater RA, Martin P, Owen A, Rannard SP. *Branched Copolymer-Stabilised Nanoemulsions As New Candidate Oral Drug Delivery Systems*.

RSC Advances. 2018;8(23):12984–91.

261. Shipp DA, Wang J, Matyjaszewski K. *Synthesis Of Acrylate And Methacrylate Block Copolymers Using Atom Transfer Radical polymerisation* . **Macromolecules**. 1998;31(23):8005–8.

262. Tan TB, Yussof NS, Abas F, Mirhosseini H, Nehdi IA, Tan CP. *Forming A Lutein Nanodispersion Via Solvent Displacement Method: The Effects Of Processing Parameters And Emulsifiers With Different Stabilizing Mechanisms*. **Food Chemistry**. 2016;194:416–23.

263. Li M, Zahi MR, Yuan Q, Tian F, Liang H. *Preparation And Stability Of Astaxanthin Solid Lipid Nanoparticles Based On Stearic Acid*. **European Journal Of Lipid Science And Technology**. 2016;118(4):592–602.

264. Waring WS. *Alcohols And Glycols Poisoning*. **Medicine (United Kingdom)**. 2020;48(3):185–8.

265. Elsby R, Surry DD, Smith VN, Gray AJ. *Validation And Application Of Caco-2 Assays For The In Vitro Evaluation Of Development Candidate Drugs As Substrates Or Inhibitors Of P-Glycoprotein To Support Regulatory Submissions*. **Xenobiotica**. 2008;38(7–8):1140–64.

266. Abdelwahed W, Degobert G, Stainmesse S, Fessi H. *Freeze-Drying Of Nanoparticles: Formulation, Process And Storage Considerations*. **Advanced Drug Delivery Reviews**. 2006;58(15):1688–713.

267. Varshosaz J, Eskandari S, Tabbakhian M. *Freeze-Drying Of Nanostructure Lipid Carriers By Different Carbohydrate Polymers Used As Cryoprotectants*. **Carbohydrate Polymers**. 2012;88(4):1157–63.

268. Lee MK, Kim MY, Kim S, Lee J. *Cryoprotectants For Freeze Drying Of Drug Nano-Suspensions: Effect Of Freezing Rate*. **Journal Of Pharmaceutical Sciences**. 2009;98(12):4808–17.

269. Liu J, Viverette T, Virgin M, Anderson M, Dalal P. *A Study Of The Impact Of Freezing On The Lyophilization Of A Concentrated Formulation With A High Fill Depth*. **Pharmaceutical Development And Technology**. 2005;10(2):261–72.

270. Akbari A, Wu J. *Cruciferin Coating Improves The Stability Of Chitosan Nanoparticles At Low PH*. **Journal Of Materials Chemistry B**. 2016;4(29):4988–5001.

271. Ahmad AM. *Potential Pharmacokinetic Interactions Between Antiretrovirals And Medicinal Plants Used As Complementary And African Traditional Medicines*. **Biopharmaceutics & Drug Disposition**. 2007;28(3):135–43.

272. Schimpel C, Teubl B, Absenger M, Meindl C, Fr??hlich E, Leitinger G, Zimmer A, Roblegg E. *Development Of An Advanced Intestinal In Vitro Triple Culture Permeability Model To Study Transport Of Nanoparticles*. **Molecular Pharmaceutics**. 2014;11(3):808–18.

273. Isin EM, Elmore CS, Nilsson GN, Thompson RA, Weidolf L. *Use Of Radiolabeled Compounds In Drug Metabolism And Pharmacokinetic Studies*. **Chemical Research In Toxicology**. 2012;25(3):532–42.

274. Zhou T, Su H, Dash P, Lin Z, Dyavar Shetty BL, Kocher T, Szlachetka A, Lamberty B, Fox HS, Poluektova L, Gorantla S, McMillan JE, Gautam N, Mosley RL, Alnouti Y, Edagwa B, Gendelman HE. *Creation Of A Nanoformulated Cabotegravir Prodrug With Improved Antiretroviral Profiles*. **Biomaterials**. 2018;151:53–65.

275. Williams IR, Owen RL. *M Cells: Specialized Antigen Sampling Cells In The Follicle-Associated Epithelium*. In: Mucosal Immunology. Fourth Edi. Elsevier; 2015. p. 211–29.

276. Zanger UM, Schwab M. *Cytochrome P450 Enzymes In Drug Metabolism: Regulation Of Gene Expression, Enzyme Activities, And Impact Of Genetic Variation*. **Pharmacology And Therapeutics**. 2013;138(1):103–41.

277. Fucci A, Colangelo T, Votino C, Pancione M, Sabatino L, Colantuoni V. *The Role Of Peroxisome Proliferator-Activated Receptors In The Esophageal, Gastric, And Colorectal Cancer*. **PPAR Research**. 2012;2012.

278. Roberts O, Khoo S, Owen A, Siccardi M. *Interaction Of Rifampin And Darunavir-Ritonavir Or Darunavir-Cobicistat In Vitro*. **Antimicrobial Agents And Chemotherapy**. 2017;61(5):1–11.

279. Kumar S, Lather V, Pandita D. *A Facile Green Approach To Prepare Core-Shell Hybrid PLGA Nanoparticles For Resveratrol Delivery*. **International Journal Of Biological Macromolecules**. 2016;84:380–4.

280. Tagami T, Ernsting MJ, Li S. *Optimization Of A Novel And Improved Thermosensitive Liposome Formulated With DPPC And A Brij Surfactant Using A Robust In Vitro System*. **Journal Of Controlled Release**. 2011;154(3):290–7.

281. Hsu S, A. Al-Suwayeh S, Chen C, Chi C, Fang J. *PEGylated Liposomes Incorporated With Nonionic Surfactants As An Apomorphine Delivery System Targeting The Brain: In Vitro Release And In Vivo Real-Time Imaging*. **Current Nanoscience**. 2011;7(2):191–9.

282. Tagami T, Ernsting MJ, Li S. *Ef Fi Cient Tumor Regression By A Single And Low Dose*

Treatment With A Novel And Enhanced Formulation Of Thermosensitive Liposomal Doxorubicin. **Journal Of Controlled Release**. 2011;152(2):303–9.

283. Zhang JQ, Liu J, Li XL, Jasti BR. *Preparation And Characterization Of Solid Lipid Nanoparticles Containing Silibinin*. **Drug Delivery**. 2007;14(6):381–7.
284. Oyewumi MO, Mumper RJ. *Influence Of Formulation Parameters On Gadolinium Entrapment And Tumor Cell Uptake Using Folate-Coated Nanoparticles*. **International Journal Of Pharmaceutics**. 2003;251(1–2):85–97.
285. Bayindir ZS, Yuksel N. *Characterization Of Niosomes Prepared With Various Nonionic Surfactants For Paclitaxel Oral Delivery*. **Journal Of Pharmaceutical Sciences**. 2010;99(4):2049–60.
286. Hsu S-H, A. Al-Suwayeh S, Chen C-C, Chi C-H, Fang J-Y. *PEGylated Liposomes Incorporated With Nonionic Surfactants As An Apomorphine Delivery System Targeting The Brain: In Vitro Release And In Vivo Real-Time Imaging*. **Current Nanoscience**. 2011;7(2):191–9.
287. Hatton FL, Tatham LM, Tidbury LR, Chambon P, He T, Owen A, Rannard SP. *Hyperbranched Polydendrons: A New Nanomaterials Platform With Tuneable Permeation Through Model Gut Epithelium*. **Chemical Science**. 2015;6(1):326–34.
288. Savage AC, Tatham LM, Siccardi M, Scott T, Vourvahis M, Clark A, Rannard SP, Owen A. *Improving Maraviroc Oral Bioavailability By Formation Of Solid Drug Nanoparticles*. **European Journal Of Pharmaceutics And Biopharmaceutics**. 2019;138:30–6.
289. Antunes F, Andrade F, Araújo F, Ferreira D, Sarmento B. *Establishment Of A Triple Co-Culture In Vitro Cell Models To Study Intestinal Absorption Of Peptide Drugs*. **European Journal Of Pharmaceutics And Biopharmaceutics**. 2013;83(3):427–35.
290. Beloqui A, des Rieux A, Préat V. *Mechanisms Of Transport Of Polymeric And Lipidic Nanoparticles Across The Intestinal Barrier*. **Advanced Drug Delivery Reviews**. 2016;106:242–55.
291. Tatham LM, Rannard SP, Owen A. *Nanoformulation Strategies For The Enhanced Oral Bioavailability Of Antiretroviral Therapeutics*. **Therapeutic Delivery**. 2015;6(4):115–9.
292. Beloqui A, Solinís MÁ, Rieux A Des, Préat V, Rodríguez-Gascón A. *Dextran-Protamine Coated Nanostructured Lipid Carriers As Mucus-Penetrating Nanoparticles For Lipophilic Drugs*. **International Journal Of Pharmaceutics**. 2014;468(1–2):105–11.

293. Ferraretto A, Bottani M, De Luca P, Cornaghi L, Arnaboldi F, Maggioni M, Fiorilli A, Donetti E. *Morphofunctional Properties Of A Differentiated Caco2/HT-29 Co-Culture As An In Vitro Model Of Human Intestinal Epithelium*. **Bioscience Reports**. 2018;38(2):150–70.

294. des Rieux A, Fievez V, Théate I, Mast J, Préat V, Schneider Y-J. *An Improved In Vitro Model Of Human Intestinal Follicle-Associated Epithelium To Study Nanoparticle Transport By M Cells*. **European Journal Of Pharmaceutical Sciences : Official Journal Of The European Federation For Pharmaceutical Sciences**. 2007;30(5):380–91.

295. Rieux A Des, Ragnarsson EGE, Gullberg E, Préat V, Schneider YJ, Artursson P. *Transport Of Nanoparticles Across An In Vitro Model Of The Human Intestinal Follicle Associated Epithelium*. **European Journal Of Pharmaceutical Sciences**. 2005;25(4–5):455–65.

296. Yameen B, Choi W Il, Vilos C, Swami A, Shi J, Farokhzad OC. *Insight Into Nanoparticle Cellular Uptake And Intracellular Targeting*. **Journal Of Controlled Release**. 2014;190:485–99.

297. Desai PP, Date AA, Patravale VB. *Overcoming Poor Oral Bioavailability Using Nanoparticle Formulations - Opportunities And Limitations*. **Drug Discovery Today: Technologies**. 2012;9(2):87–95.

298. Hunter a. C, Elsom J, Wibroe PP, Moghimi SM. *Polymeric Particulate Technologies For Oral Drug Delivery And Targeting: A Pathophysiological Perspective*. **Maturitas**. 2012;73(1):5–18.

299. Mukherjee A, Waters AK, Kalyan P, Achrol AS, Kesari S, Yenugonda VM. *Lipid–Polymer Hybrid Nanoparticles As A Next-Generation Drug Delivery Platform: State Of The Art, Emerging Technologies, And Perspectives*. **International Journal Of Nanomedicine**. 2019;14:1937–52.

300. Fang RH, Aryal S, Hu CJ, Zhang L. *Quick Synthesis Of Lipid−Polymer Hybrid Nanoparticles With Low Polydispersity Using A Single-Step Sonication Method*. **Langmuir**. 2010;26(22):16958–62.

301. Pramual S, Lirdprapamongkol K, Svasti J, Bergkvist M, Jouan-Hureaux V, Arnoux P, Frochot C, Barberi-Heyob M, Niamsiri N. *Polymer-Lipid-PEG Hybrid Nanoparticles As Photosensitizer Carrier For Photodynamic Therapy*. **Journal Of Photochemistry And Photobiology B: Biology**. 2017;173(January):12–22.

302. Mukherjee A, Waters AK, Kalyan P, Achrol AS, Kesari S, Yenugonda VM. *Lipid–*

Polymer Hybrid Nanoparticles As A Next-Generation Drug Delivery Platform: State Of The Art, Emerging Technologies, And Perspectives. **International Journal Of Nanomedicine**. 2019;Volume 14:1937–52.

303. Hu H, Liu D, Zhao X, Qiao M, Chen D. *Preparation, Characterization, Cellular Uptake And Evaluation In Vivo Of Solid Lipid Nanoparticles Loaded With Cucurbitacin B*. **Drug Development And Industrial Pharmacy**. 2013;39(5):770–9.
304. Nidhi K, Indrajeet S, Khushboo M, Gauri K, Sen DJ. *Hydrotropy: A Promising Tool For Solubility Enhancement: A Review*. **International Journal Of Drug Development And Research**. 2011;3(2):26–33.
305. Niu L, Panyam J. *Freeze Concentration-Induced PLGA And Polystyrene Nanoparticle Aggregation: Imaging And Rational Design Of Lyoprotection*. **Journal Of Controlled Release**. 2017;248:125–32.
306. Mandal B, Mittal NK, Balabathula P, Thoma LA, Wood GC. *European Journal Of Pharmaceutical Sciences Development And In Vitro Evaluation Of Core – Shell Type Lipid – Polymer Hybrid Nanoparticles For The Delivery Of Erlotinib In Non-Small Cell Lung Cancer*. **PHASCI**. 2016;81:162–71.
307. McDonald TO, Giardiello M, Martin P, Siccardi M, Liptrott NJ, Smith D, Roberts P, Curley P, Schipani A, Khoo SH, Long J, Foster AJ, Rannard SP, Owen A. *Antiretroviral Solid Drug Nanoparticles With Enhanced Oral Bioavailability: Production, Characterization, And In Vitro-In Vivo Correlation.* **Advanced Healthcare Materials**. 2014;3(3):400–11.
308. Giardiello M, Liptrott NJ, McDonald TO, Moss D, Siccardi M, Martin P, Smith D, Gurjar R, Rannard SP, Owen A. *Accelerated Oral Nanomedicine Discovery From Miniaturized Screening To Clinical Production Exemplified By Paediatric HIV Nanotherapies*. **Nature Communications**. 2016;7:13184.
309. Filipe V, Hawe A, Jiskoot W. *Critical Evaluation Of Nanoparticle Tracking Analysis (NTA) By NanoSight For The Measurement Of Nanoparticles And Protein Aggregates*. **Pharmaceutical Research**. 2010;27(5):796–810.
310. Wu B, Liu H, Chen G, Zhang Y, Ma Z. *Effects Of PEGylated Lipid Nanoparticles On The Oral Absorption Of One BCS II Drug: A Mechanistic Investigation*. **International Journal Of Nanomedicine**. 2014;9(1):5503–14.
311. Lozoya-Agullo I, Araújo F, González-Álvarez I, Merino-Sanjuán M, González-Álvarez M, Bermejo M, Sarmento B. *Usefulness Of Caco-2/HT29-MTX And Caco-2/HT29-MTX/Raji B Coculture Models To Predict Intestinal And Colonic Permeability*

Compared To Caco-2 Monoculture. **Molecular Pharmaceutics**. 2017;14(4):1264–70.

312. McEvoy CL, Trevaskis NL, Feeney OM, Edwards GA, Perlman ME, Ambler CM, Porter CJH. *Correlating In Vitro Solubilization And Supersaturation Profiles With In Vivo Exposure For Lipid Based Formulations Of The CETP Inhibitor CP-532,623*. **Molecular Pharmaceutics**. 2017;14(12):4525–38.
313. Mohsin K. *Design Of Lipid-Based Formulations For Oral Administration Of Poorly Water-Soluble Drug Fenofibrate: Effects Of Digestion*. **AAPS PharmSciTech**. 2012;13(2):637–46.
314. Lee M. Tatham, Alison C. Savage, Andrew Dwyer, Marco Siccardi, Trevor Scott, Manoli Vourvahis SPR& AO. *Maraviroc Solid Drug Nanoparticles With Improved Oral Pharmacokinetics*. In: Conference On Retroviruses And Opportunistic Infections (CROI) - Poster 482. Boston, USA; 2018.
315. Muchow M, Maincent P, Müller RH. *Lipid Nanoparticles With A Solid Matrix (SLN®, NLC®, LDC®) For Oral Drug Delivery*. **Drug Development And Industrial Pharmacy**. 2008;34(12):1394–405.
316. Ma P, Li T, Xing H, Wang S, Sun Y, Sheng X, Wang K. *ScienceDirect Local Anesthetic Effects Of Bupivacaine Loaded Lipid-Polymer Hybrid Nanoparticles : In Vitro And In Vivo Evaluation*. **Biomedicine Et Pharmacotherapy**. 2017;89(October 2011):689–95.
317. Noben M, Vanhove W, Arnauts K, Santo Ramalho A, Van Assche G, Vermeire S, Verfaillie C, Ferrante M. *Human Intestinal Epithelium In A Dish: Current Models For Research Into Gastrointestinal Pathophysiology*. **United European Gastroenterology Journal**. 2017;5(8):1073–81.
318. Balimane P V., Chong S. *Cell Culture-Based Models For Intestinal Permeability: A Critique*. **Drug Discovery Today**. 2005;10(5):335–43.
319. Hartkoorn RC, Kwan WS, Shallcross V, Chaikan A, Liptrott N, Egan D, Sora ES, James CE, Gibbons S, Bray PG, Back DJ, Khoo SH, Owen A. *HIV Protease Inhibitors Are Substrates For OATP1A2, OATP1B1 And OATP1B3 And Lopinavir Plasma Concentrations Are Influenced By SLCO1B1 Polymorphisms*. **Pharmacogenetics And Genomics**. 2010;20(2):112–20.
320. Sukhbir Singh, Neelam , Sandeep Arora YPS. *An Overview Of Multifaceted Significance Of Eudragit Polymers In Drug Delivery Systems*. **Asian Journal Of Pharmaceutical And Clinical Research**. 2015;8(5):1–6.
321. Owen A, Rannard S. *Strengths, Weaknesses, Opportunities And Challenges For Long Acting Injectable Therapies: Insights For Applications In HIV Therapy*. **Advanced**

Drug Delivery Reviews. 2016;103:144–56.

322. World Health Organisation (WHO). *HIV/AIDS* [Https://www.who.int/news-room/fact-sheets/detail/hiv-aids]. 2019.

323. Mc Crudden MTC, Larrañeta E, Clark A, Jarrahian C, Rein-Weston A, Lachau-Durand S, Niemeijer N, Williams P, Haeck C, McCarthy HO, Zehrung D, Donnelly RF. *Design, Formulation And Evaluation Of Novel Dissolving Microarray Patches Containing A Long-Acting Rilpivirine Nanosuspension*. **Journal Of Controlled Release**. 2018;292(July):119–29.